SITE AMPLIFICATION OF THE SELECTED AREAS OF DHAKA CITY BASED ON SHEAR WAVE VELOCITY

MOHAMMAD SALAHUDDIN RIZVI

DEPARTMENT OF CIVIL ENGINEERING
BANGLADESH UNIVERSITY OF ENGINEERING AND TECHNOLOGY
DHAKA, BANGLADESH

MARCH, 2014

SITE AMPLIFICATION OF THE SELECTED AREAS OF DHAKA CITY BASED ON SHEAR WAVE VELOCITY

A THESIS SUBMITTED BY

MOHAMMAD SALAHUDDIN RIZVI

IN PARTIAL FULFILLMENT OF THE REQUIREMENTS FOR THE DEGREE OF

MASTER OF SCIENCE IN

CIVIL AND GEOTECHNICAL ENGINEERING

DEPARTMENT OF CIVIL ENGINEERING
BANGLADESH UNIVERSITY OF ENGINEERING AND TECHNOLOGY
DHAKA, BANGLADESH

MARCH, 2014

The thesis titled **"SITE AMPLIFICATION OF THE SELECTED AREAS OF DHAKA CITY BASED ON SHEAR WAVE VELOCITY"** submitted by MOHAMMAD SALAHUDDIN RIZVI, Roll No. 040804217F, and Session: April 2008 has been accepted as satisfactory in partial fulfillment for the requirement of the degree of Master of Science in Civil and Geotechnical Engineering on **03 March 2014.**

BOARD OF EXAMINERS

Dr. Mehedi Ahmed Ansary : Chairman
Professor (Supervisor)
Department of CE, BUET, Dhaka

Dr. A.M.M. Taufiqul Anwar : Member
Professor and Head (Ex-Officio)
Department of CE, BUET, Dhaka

Dr. Abu Siddique : Member
Professor
Department of CE, BUET, Dhaka

Dr. Md. Mahmudur Rahman : Member
Professor (External)
Department of Civil Engineering
AUST, Dhaka

Declaration

Declared that, except for the contents where specific reference has been made to the work of others, the studies embodied in this thesis is the result of research work, carried by the author.

Neither the thesis nor any part thereof has been submitted or is being concurrently submitted to any other university or other educational institute for the award of any degree or diploma, except for publication.

March, 2014

_____

Author

Acknowledgement

Praise be to Allah, the beneficent, the merciful.

The author owes a debt of gratitude to his wonderful parents for their unconditioned love, affection and invaluable guidance throughout life. He would like to thank them for their never ending prayer and encouragement in every step of getting education.

The author wishes to express his indebtedness, profound gratitude and sincere appreciation to his supervisor Dr. Mehedi Ahmed Ansary, Professor, Department of Civil Engineering, BUET for his thoughtful ideas, valuable suggestions, and affectionate encouragement during all phases of this study. His careful reading of the draft, valuable comments, strong support, continuous guidance, and constructive suggestions immensely contributed to the improvement of the thesis. His fervent guidance in every aspect of this work was the most valuable achievement of the life of author and also would remain so forever.

The author wishes to express his gratefulness and sincere appreciation to his respected teachers Dr. A.M.M. Taufiqul Anwar, Professor and Head, Dr. Abu Siddique, Professor of the Dept. of Civil Engineering, BUET and Dr. Md. Mahmudur Rahman, Professor, Dept. of Civil Engineering, AUST for their valuable advice and directions in completing the thesis. The author would also like to acknowledge all the officials of Geotechnical Engineering Laboratory, BUET for their co-operation and companionship during laboratory works. Sincere gratitude of the author goes to all the experts in related fields and general people living in the study area, who provided him important information and valuable suggestion during the field works.

The author thankfully acknowledges the financial support provided by the Committee for Advanced Studies and Researches (CASR), BUET. The author would also like to thank CDMP officials for providing valuable information and discussion which makes the work fruitful.

ABSTRACT

Risk to manmade structures due to seismically induced ground deformation has been evident from past earthquakes. Influence of site effects on strong ground motions has been ascertained by many seismologists and earthquake engineers. Mechanisms related to the local soil and rock properties have the capacity to influence ground motions. Depending on the ground characteristics, the ground shaking is influenced, which may result in the amplification (causing resonance) or attenuation. Amplification mechanisms control the frequency content of ground motions. Though direct waves were used for the study of ground motion, source, path and site characterization were recognised as the prime factors that affect earthquake ground motion.

The purpose of this research is to estimate the site amplification of selected areas of Dhaka city based on shear wave velocity. For this, 10 (ten) locations has been selected in Dhaka city. In the selected locations, the depth of sand filling in areas varies from 2.0 to 6.0 m from existing ground level (EGL). The depth of clay layer varies from 4.0 m to 30.0 m. The depth of silty clay layer varies from 4.0 m to 6.0 m. The depth of clay layer varies from 4.0 m to 26.0 m**.** The depth of fine sand layer varies from 4.0 m to 20.0 m. The depth of dense sand layer varies from 4.0 m to 20.0 m from EGL. Shear wave velocities has been found out from the CPT equipment. The maximum value of shear wave velocity varies from 300 m/s to 810 m/s and minimum value of shear wave velocity varies from 50 m/s to 100 m/s. The average value of shear wave velocity varies from 164 m/s to 320 m/s.

For estimating peak ground acceleration DEEPSOIL developed by Hashash_et al. has been used. With soil layer depth, bulk density and damping as inputs, peak ground acceleration by equivalent linear analysis has been estimated. Four input motions (Gangtok data from Sikkim earthquake, Kobe data from Kobe earthquake, Northridge and Loma Prieta data) recorded in rock have been used in this analysis, which are scaled to 0.19g value. From the detailed site specific analysis, the PGA values at surface have been obtained in the range of 0.073g to 0.450g. The surface

acceleration values have been very high (>0.2g) in the areas of Gulshan, Dakhin Khan, Mirpur and Mothertek. Values of 0.1g to 0.2g are estimated in different locations like Mugda, Uttara, Asulia, Mohammadrpur, and United City. These locations are characterized by clayey sand and mixture of sand, silt and clay. Peak ground acceleration has been observed to be very low (<0.1g) in the area of Kawran Bazar. These locations have soils with layers of silty sand and silty clays. The PGA values are useful for the ground response analysis.

Amplification factors varies from 0.43 (Loma prieta) to 0.59 (Kobe) for Kawran Bazar, from 1.45 (Sikkim) to 2.18 (Kobe) for Gulshan, from 0.99 (Sikkim) to 1.24 (Kobe) for Mugda, from 1.03 (Sikkim) to 1.48 (Kobe) for Dakhin Khan, from 0.81 (Sikkim) to 1.20 (Kobe) for Uttara, from 0.34 (Loma prieta) to 0.76 (Kobe) for Asulia, from 1.12 (Loma prieta) to 1.67 (Kobe) for Mirpur, from 0.72 (Loma prieta) to 1.36 (Kobe) for Mohammadpur, from 1.85 (Sikkim) to 2.54 (Kobe) for Mothertek, from 0.53 (Loma Prieta) to 0.76 (Kobe) for United City.

Peak Spectral Acceleration (PSA) varies from 0.0029g (Northridge) to 0.35g (Kobe) for Kawran Bazar, from 0.0028g (Northridge) to 1.21g (Kobe) for Gulshan, from 0.0028g (Northridge) to 0.66g (Kobe) for Mugda, from 0.0028g (Northridge) to 0.76g (Kobe) for Dakhin Khan, from 0.0029g (Northridge) to 0.93g (Loma prieta) for Uttara, from 0.0032g (Northridge) to 0.45g (Kobe) for Asulia, from 0.0028g (Northridge) to 0.92g (Kobe) for Mirpur, from 0.0030g (Northridge) to 0.90g (Kobe) for Mohammadpur, from 0.0029g (Northridge) to 1.67g (Loma prieta) for Mothertek, from 0.0028g (Northridge) to 0.46g (Kobe) for United City. The results provided in the seismic response analysis of Dhaka city could be used as guideline for risk assessment and management of future probable event.

TABLE OF CONTENTS

Page

LIST OF FIGURES

Page

LIST OF TABLES

ABBREVIATIONS AND ACRONYMS

BNBC	Bangladesh National Building Code
BMD	Bangladesh Meteorological Department
PGA	Peak Ground Acceleration
PSA	Peak Spectral Acceleration
EGL	Existing Ground Level
NEHRP	National Earthquake hazard Reduction Programme
SSR	Standard Spectral Ratio
OCR	Over Consolidation Ratio
ΔI	Intensity increment
ΔI_{MMI}	Modified Mercalli Intensity
$\Delta IMSK$	Medvedev-Sponheuer-Karnik Intensity Scale
$\Delta\sigma$	Stress Parameter
a_{max}	Maximum ground surface acceleration
E_D	Energy dissipated in one cycle of loading
E_S	Strain energy stored in the system
G	Shear modulus
G/Gmax	Shear modulus ratio
Gmax	Maximum shear modulus
Gsec	Secant shear modulus
Gtan	Tangent shear modulus
VS	Shear wave velocity
Vs1	Shear wave velocity corrected for overburden stress
Vs30	Average shear wave velocity up to 30m
Z	Zone factor
γ	Unit weight
γ_c	Cyclic shear strain
γ_d	Dry density
γ_{sat}	Saturated density
ρ	Density of soil

Appendix A

Estimation of Shear Wave Velocity using PC-Mon at selected locations of Dhaka City

Site : Kawran Bazar

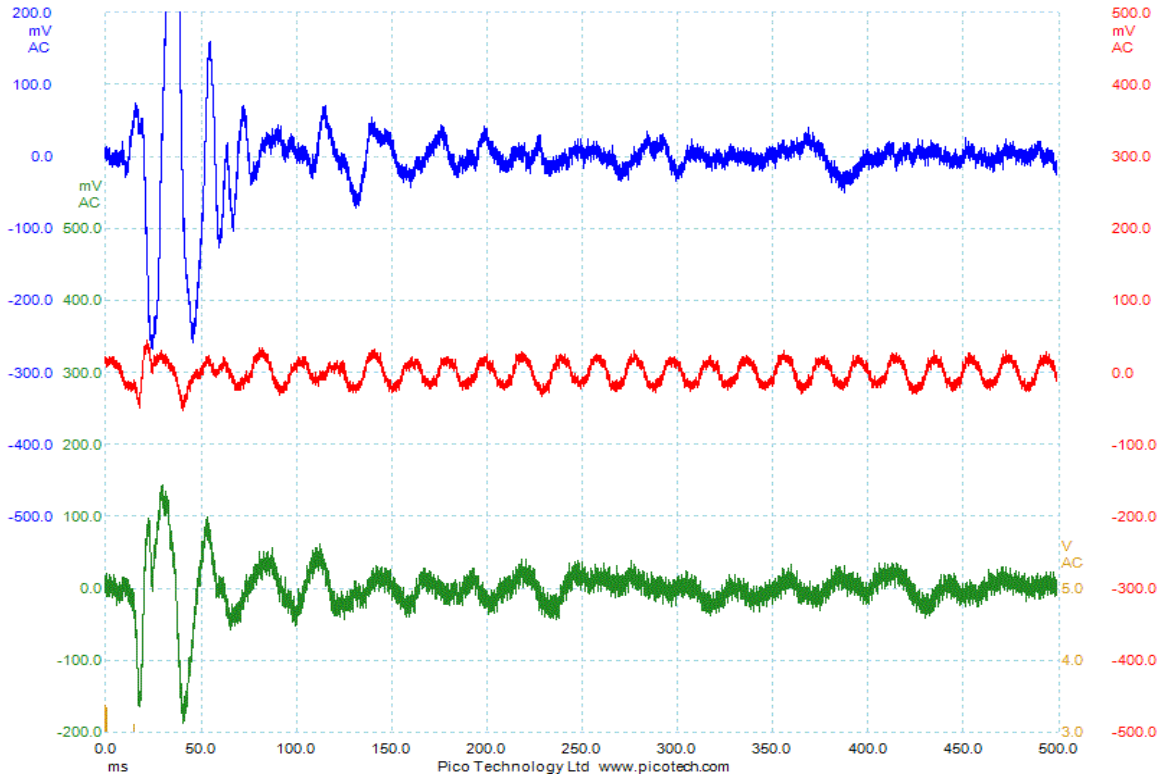

Site: Gulshan

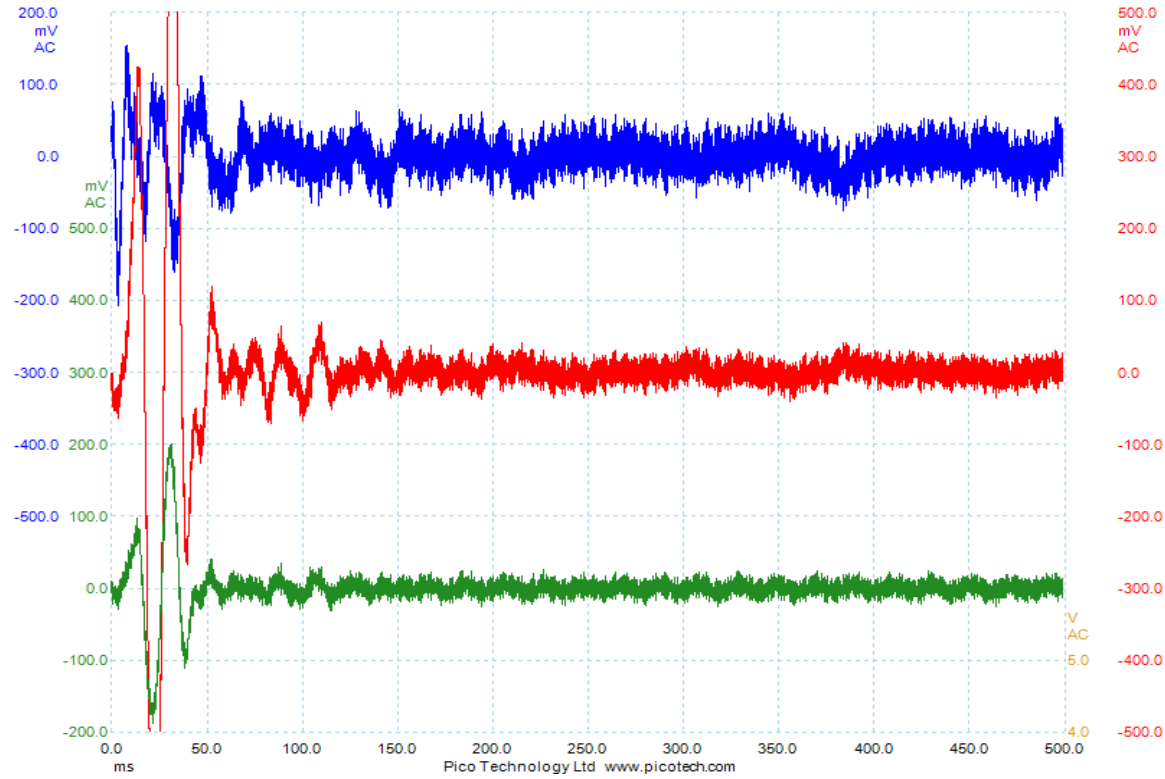

Site: Mugda

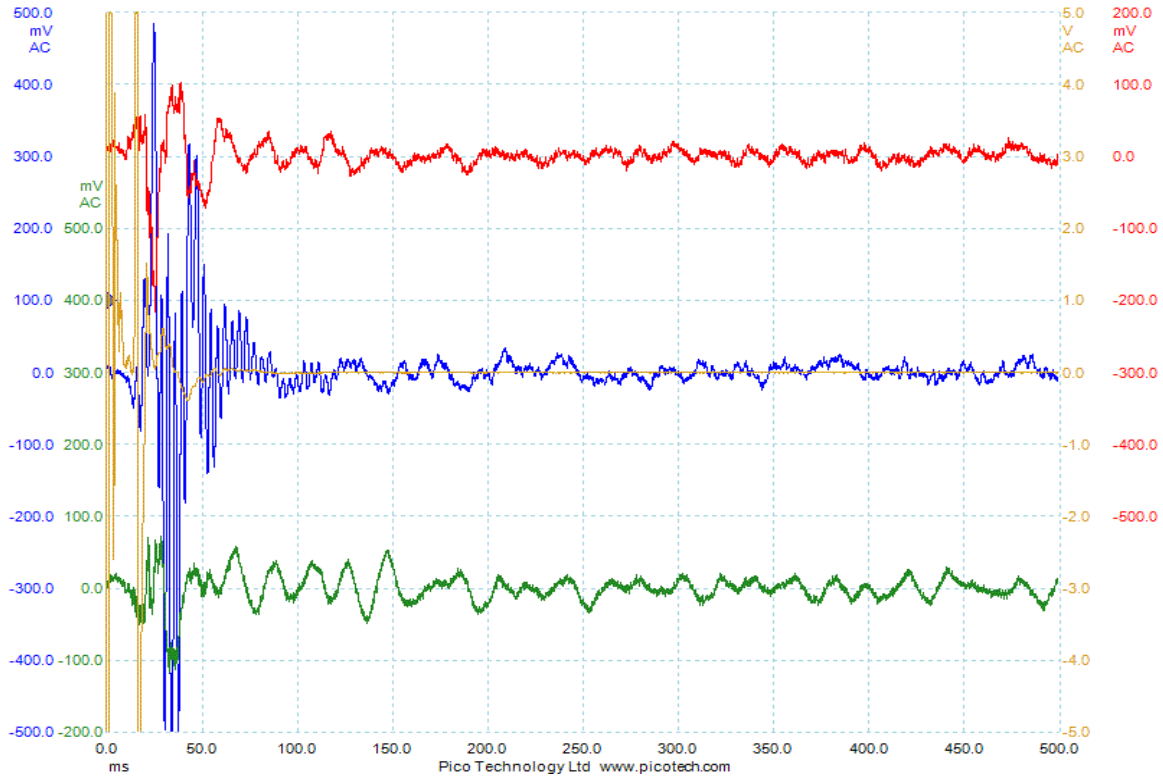

Site: Asian City

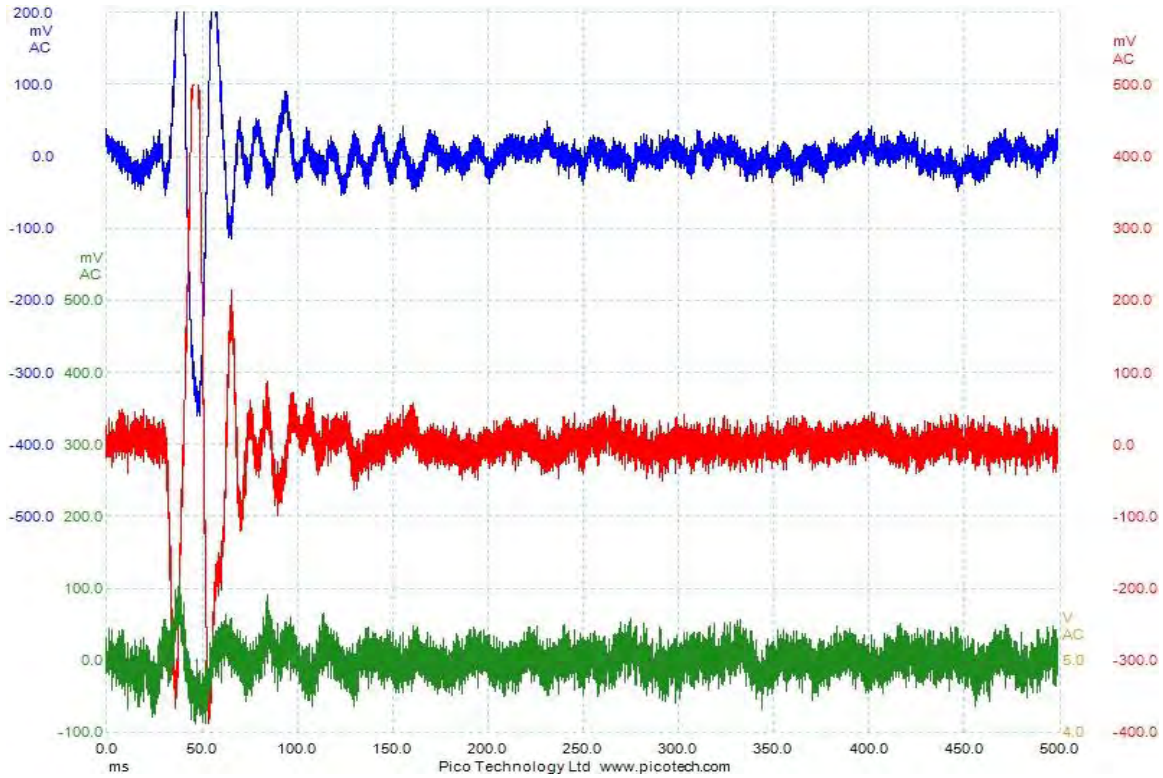

Site: Asulia

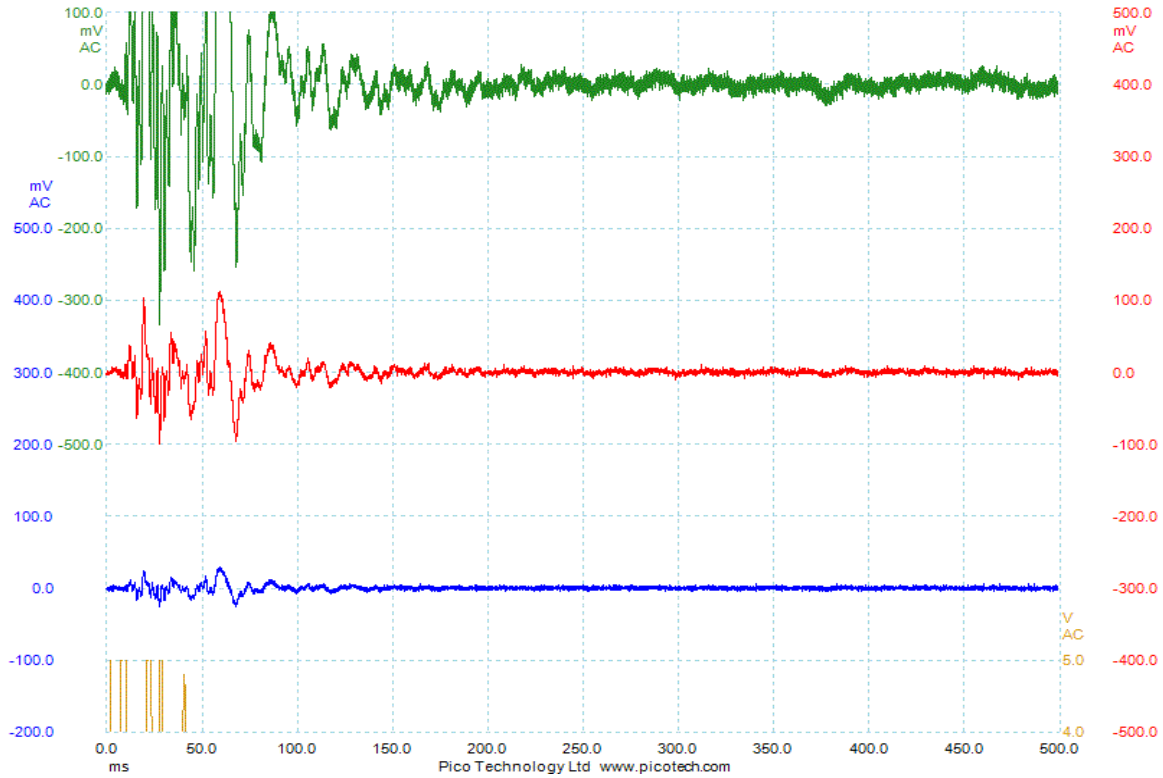

Site: Mirpur

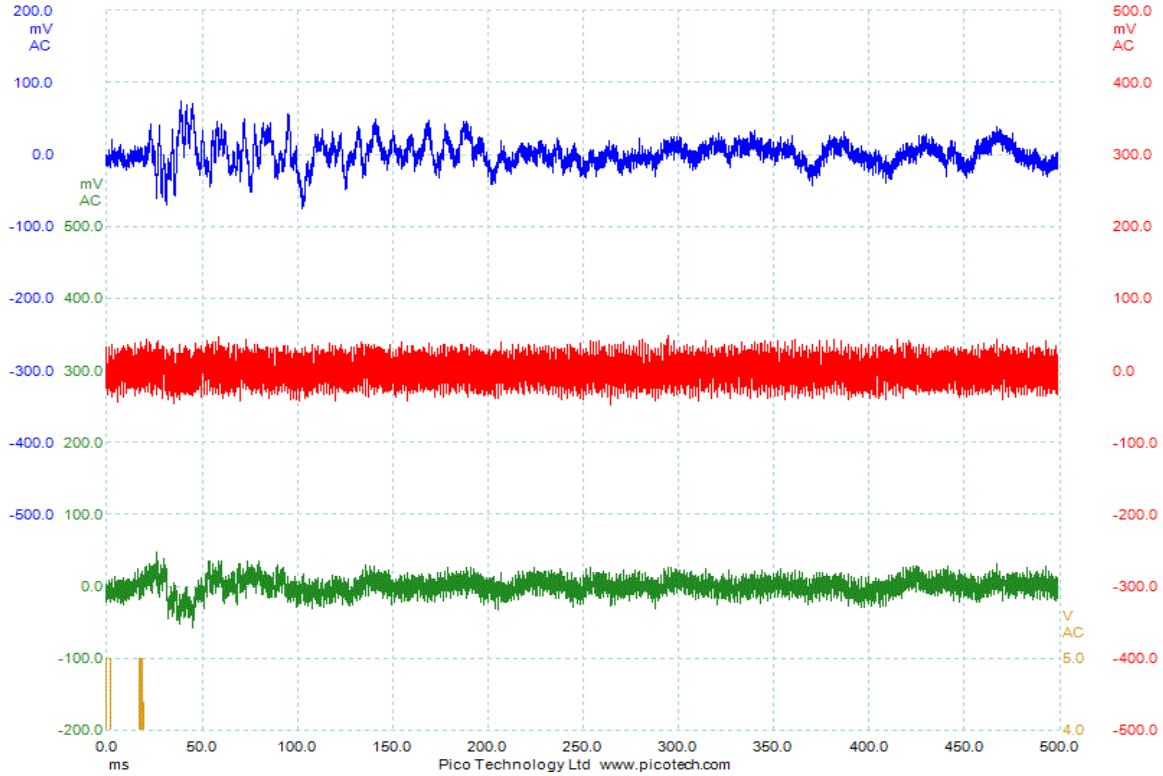

Site: Mohammadpur

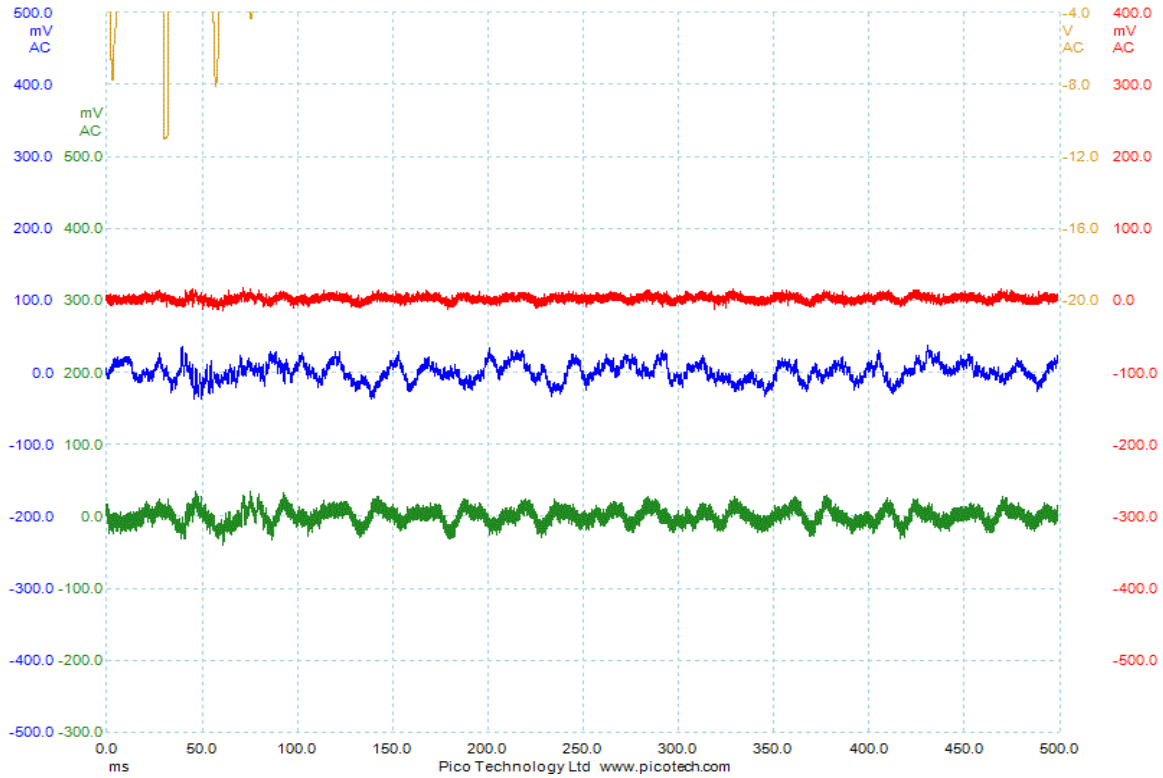

Site: Mothertek

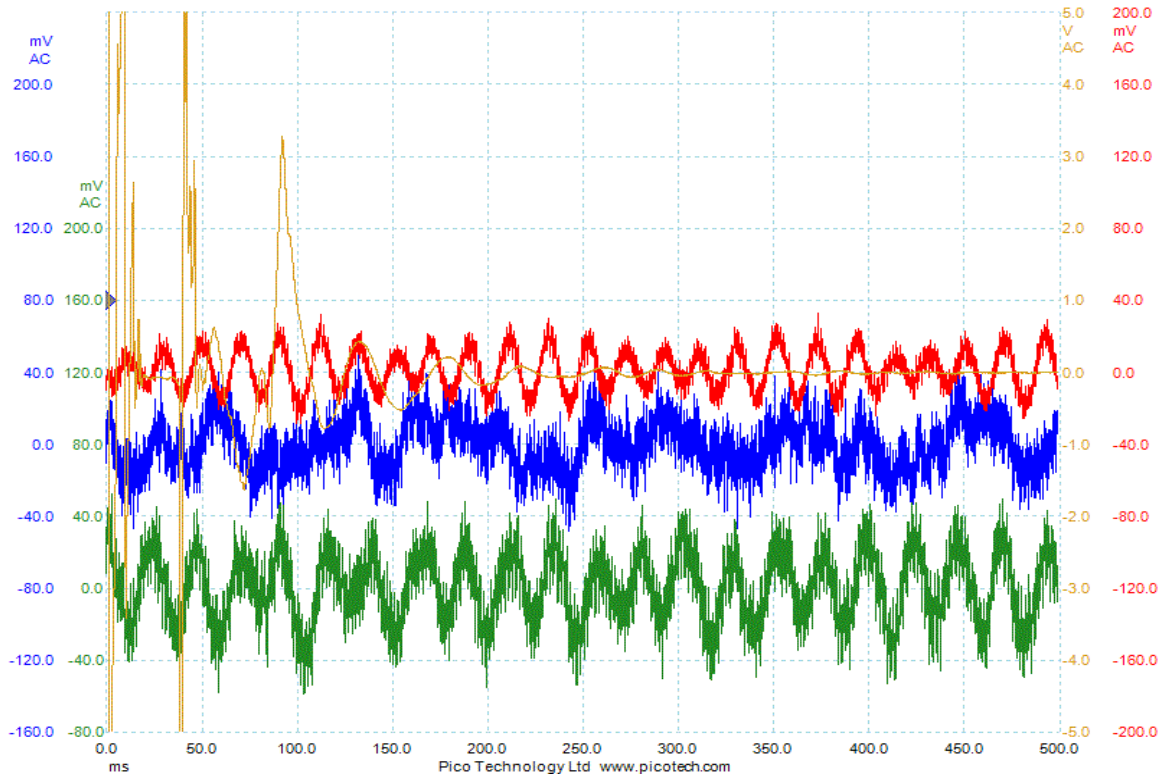

Site: Uttara

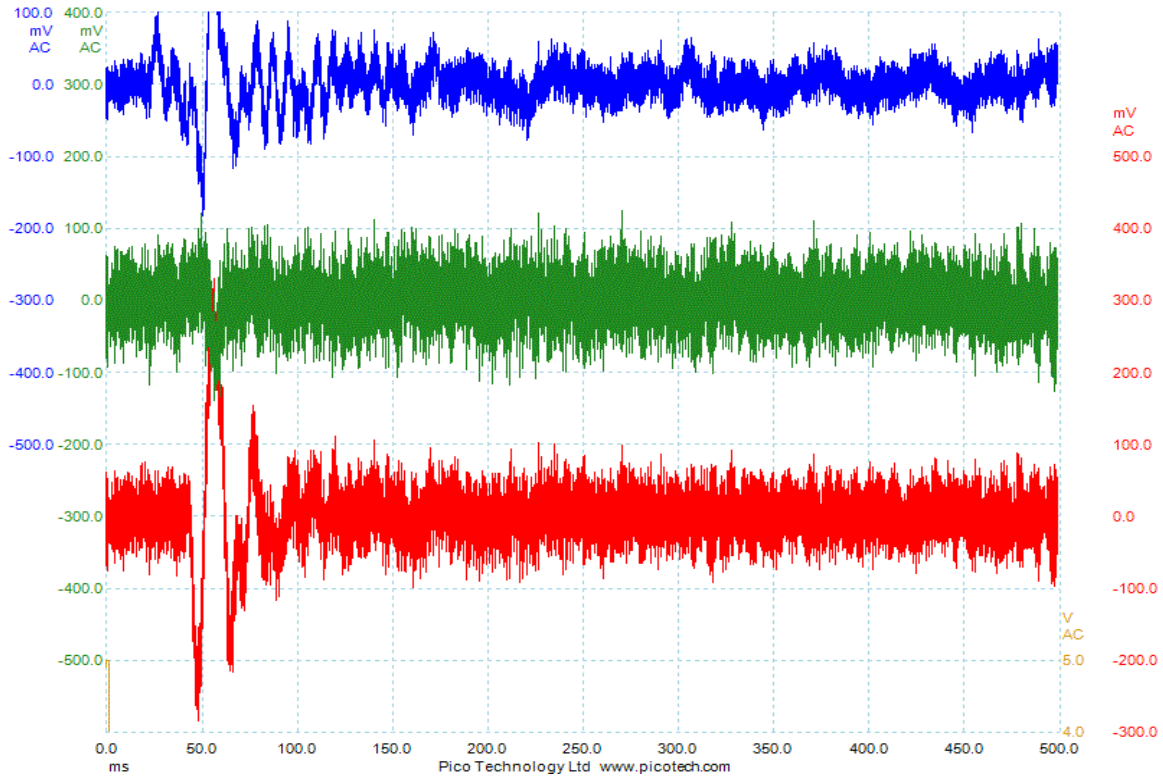

Site: United City

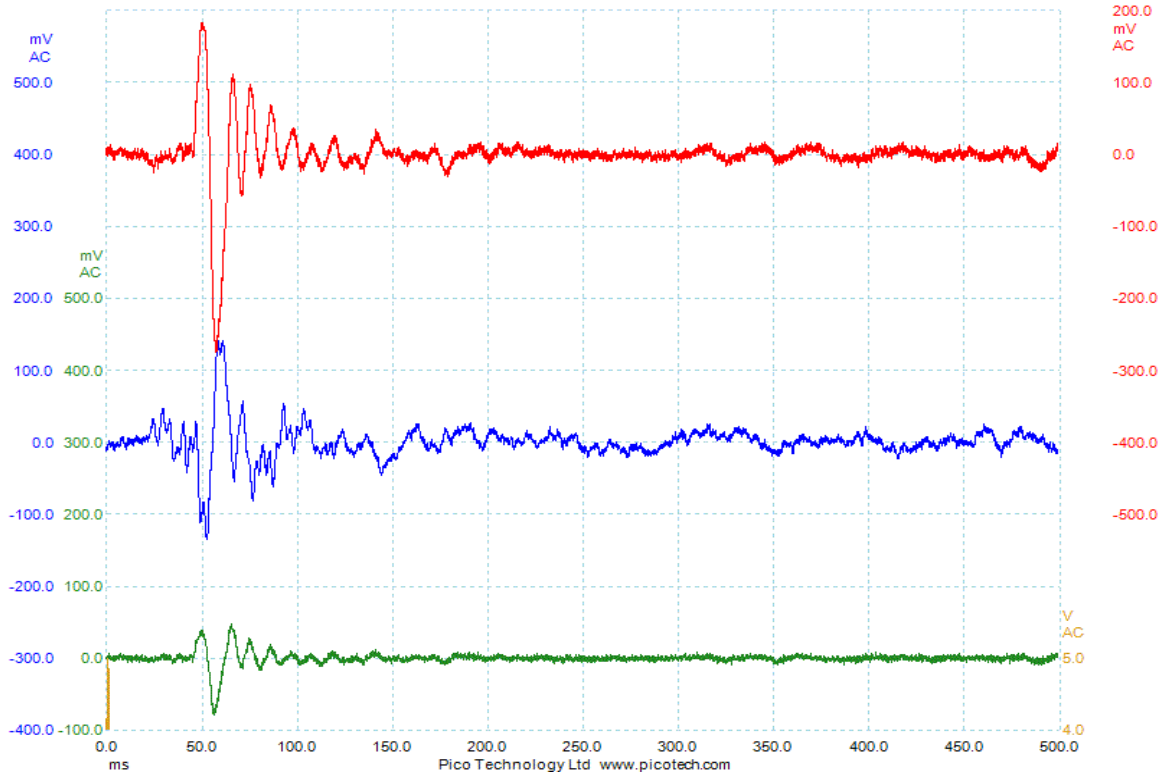

Appendix B

Test Results of CPT Equipment at selected locations of Dhaka City

SITE: KAWRAN BAZAR

DHK_01	
KARWANBAZAR (National Bank Limited)	
Depth (m)	**Shear Wave Velocity (m/sec)**
0	140
2	200
3	140
4	60
6	85
7	220
8	180
9	220
10	120
12	130
14	140
16	242
18	235
21	248
24	255
27	268
30	275

SITE: GULSHAN

DHK_02	
AARONG-GULSHAN (20 Storied Building at BRAC)	
Depth (m)	**Shear Wave Velocity (m/sec)**
0	250
1	180
2	180
3	100
4	250
5	130
6	150
7	300
8	160
9	220
10	200
11	210
12	230
13	300
14	280
15	300
16	310
18	325
20	340
21	252
24	261
27	272
30	281

SITE: MUGDA

DHK_03	
MUGDA (500 Bed Hospital)	
Depth (m)	**Shear Wave Velocity (m/sec)**
0	90
1	120
2	100
3	160
4	150
5	90
6	130
7	220
8	220
9	340
10	270
11	300
12	360
14	300
18	245
21	252
24	265
27	272
30	283

SITE: DAKHIN KHAN

DHK_04	
ASIAN CITY	
Depth (m)	**Shear Wave Velocity (m/sec)**
0	90
1	80
2	190
3	200
4	130
5	100
6	180
7	120
8	160
9	140
10	210
11	195
12	250
13	350
14	250
15	260
16	240
17	350
18	390
19	280
20	250
21	420
22	300
23	400
24	400
25	330
26	300
27	220
28	440
29	520
30	520

SITE: UTTARA

DHK_05	
UTTARA (Meher Nagar)	
Depth (m)	**Shear Wave Velocity (m/sec)**
0	80
2	85
4	80
6	100
8	150
9	390
10	410
11	250
12	260
13	410
14	420
15	230
16	300
17	380
18	310
19	370
20	450
21	400
22	320
23	300
24	280
25	370
26	490
27	500
28	500
30	500

SITE: ASULIA

DHK_06	
ASULIA (Jubak Project)	
Depth (m)	**Shear Wave Velocity (m/sec)**
0	110
1	120
2	50
3	60
4	80
5	70
6	70
7	60
8	190
9	180
10	190
11	160
12	140
13	150
14	120
15	180
16	150
17	370
18	130
19	230
20	220
21	380
22	190
23	390
24	450
25	700
26	290
27	300
28	190
29	390
30	390

SITE: MIRPUR

DHK_07	
MIRPUR-1	
Depth (m)	**Shear Wave Velocity (m/sec)**
0	190
1	280
2	390
3	420
4	750
5	810
6	430
7	560
8	420
9	300
10	290
11	310
12	390
13	250
14	220
15	390
16	300
17	290
18	280
19	300
20	250
21	380
22	280
24	285
27	274
30	300

SITE: MOHAMMADPUR

DHK_08	
MOHAMMADPUR	
Depth (m)	**Shear Wave Velocity (m/sec)**
0	160
1	50
2	180
3	390
4	200
5	90
6	180
7	210
8	250
9	210
10	180
11	180
12	210
13	350
14	300
15	200
16	190
17	290
18	200
19	250
20	210
21	220
22	180
23	260
24	320
25	390
26	150
27	210
28	300
29	300
30	450

SITE: MOTHERTEK

DHK_09	
MOTHERTEK	
Depth (m)	**Shear Wave Velocity (m/sec)**
0	100
1	70
2	100
3	230
4	220
5	300
6	480
7	320
8	250
9	320
10	460
11	440
12	450
13	410
14	500
15	570
16	300
17	320
18	310
19	400
20	450
21	260
22	420
23	350
24	400
25	360
26	390
27	280
28	350
29	320
30	300

SITE: UNITED CITY

DHK_10	
UNITED CITY PROJECT	
Depth (m)	**Shear Wave Velocity (m/sec)**
0	100
1	120
2	150
3	110
4	100
5	180
6	90
7	80
8	110
9	130
10	170
11	160
12	150
13	140
14	180
15	190
16	160
17	210
18	160
19	190
20	160
21	370
22	300
23	190
24	290
25	340
26	320
30	300

Appendix C

Estimation of Soil Behavior Type Index:

Site: KAWRAN BAZAR

Depth	q	N(60)
1.5	0.495	0
3.0	0.515	2
4.5	0.635	1.840046
6.0	0.73	1.593527
7.5	0.515	2.850587
9.0	0.53	2.602218
10.5	0.655	16.8643
12.0	5.42	16.9019
13.5	12.77	29.74583
15.0	17.65	32.25071
16.5	1.18	29.06141
18.0	1.135	26.41588
19.5	7.015	28.6066
21.0	3.12	32.1286
22.5	1.134	26.42588
24.0	1.76	25.28655
25.5	1.155	18.49509
27.0	7.016	30.7066
28.5	2.26	32.2386
30.0	8.625	35.74348

Site: GULSHAN

Depth	q	N(60)
1.5	1.33	22.49002
3.0	0.76	18.17468
4.5	0.955	9.274727
6.0	1.82	1.60643
7.5	2.6	4.310503
9.0	2.105	6.558222
10.5	0.795	9.714774
12.0	1.005	12.49509
13.5	1.08	12.85144
15.0	1.135	26.41588
16.5	1.18	29.06141
18.0	1.36	26.49002
19.5	3.02	31.1286
21.0	1.79	26.18655

Site: MUGDA

Depth	q	N(60)
1.5	4.665	10
3.0	2.84	12
4.5	2.235	7.419781
6.0	0.78	8.032149
7.5	1.05	1.436834
9.0	0.4	1.311644
10.5	0.46	3.64304
12.0	0.585	2.271835
13.5	0.635	4.283813
15.0	1.72	9.143959
16.5	1.77	25.18655
18.0	7.015	30.6066
19.5	8.525	35.64348

Site: Ashian City

Depth(m)	q	N(60)
1.5	4.535	8
3.0	1.915	10
4.5	0.315	7.419781
6.0	0.35	4.819289
7.5	0.345	4.310503
9.0	0.37	5.246578
10.5	0.425	4.857387
12.0	0.49	7.951422
13.5	3.12	32.1286
15.0	1.885	36.57583
16.5	3.78	40.68597
18.0	2.02	7.419781
19.5	2.92	30.1396

Site: UTTARA

Depth	q	N(60)
1.5	2.195	4
3.0	3.83	6
4.5	3.93	16.69451
6.0	0.5	17.67073
7.5	0.405	18.67885
9.0	2.465	17.05138
10.5	1.34	10.92912
12.0	2.425	13.63101
13.5	1.21	13.92239
15.0	0.98	15.23993
16.5	0.82	13.56199
18.0	0.855	14.83956
19.5	0.94	16.03956

Site: ASULIA

Depth	q	N(60)
1.5	2.61	6
3.0	2.775	4
4.5	0.475	3.709891
6.0	1.055	1.60643
7.5	1.075	2.873669
9.0	0.73	2.623289
10.5	0.64	1.214347
12.0	0.825	1.135917
13.5	1.775	2.141906
15.0	0.865	2.031991
16.5	0.815	0.968714
18.0	0.92	0.927473
19.5	0.89	7.128695

Site: MIRPUR

Depth	q	N(60)
1.5	4.705	12
3.0	6.165	10
4.5	3.015	5.564836
6.0	1.33	8.032149
7.5	0.885	5.747338
9.0	0.97	7.869866
10.5	1.11	9.928695
12.0	1.35	10.62910
13.5	0.78	12.86199
15.0	0.755	15.63256
16.5	4.615	9.419781
18.0	5.48	12.43201
19.5	4.05	18.76073

Site: MOHAMMADPUR

Depth	q	N(60)
1.5	5.03	2
3.0	4.5	6
4.5	4.515	7.419781
6.0	3.05	17.67073
7.5	4.085	5.747338
9.0	5.04	9.181511
10.5	1.915	9.714774
12.0	5.58	13.63101
13.5	1.57	20.28654
15.0	3.55	21.5312
16.5	4.05	15.41336

Site: UNITED CITY

Depth	q	N(60)
1.5	2.61	6
3.0	2.775	4
4.5	0.475	3.709891
6.0	1.055	1.60643
7.5	1.075	2.873669
9.0	0.73	2.623289
10.5	0.64	1.214347
12.0	0.825	1.135917
13.5	1.775	2.141906
15.0	0.865	2.031991
16.5	0.815	0.968714
18.0	0.92	0.927473
19.5	0.89	7.128695

Appendix D

Interface of DEEPSOIL Software

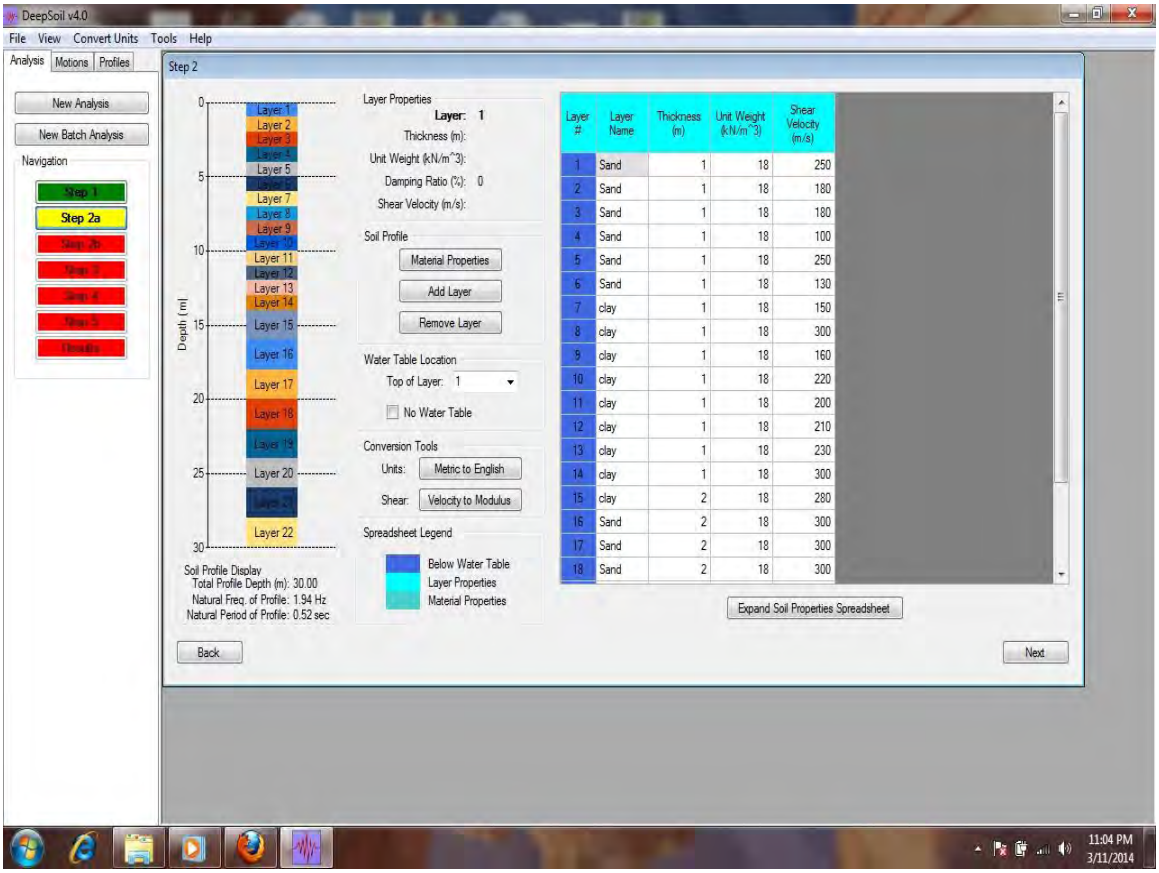

Figure: Soil layers and properties

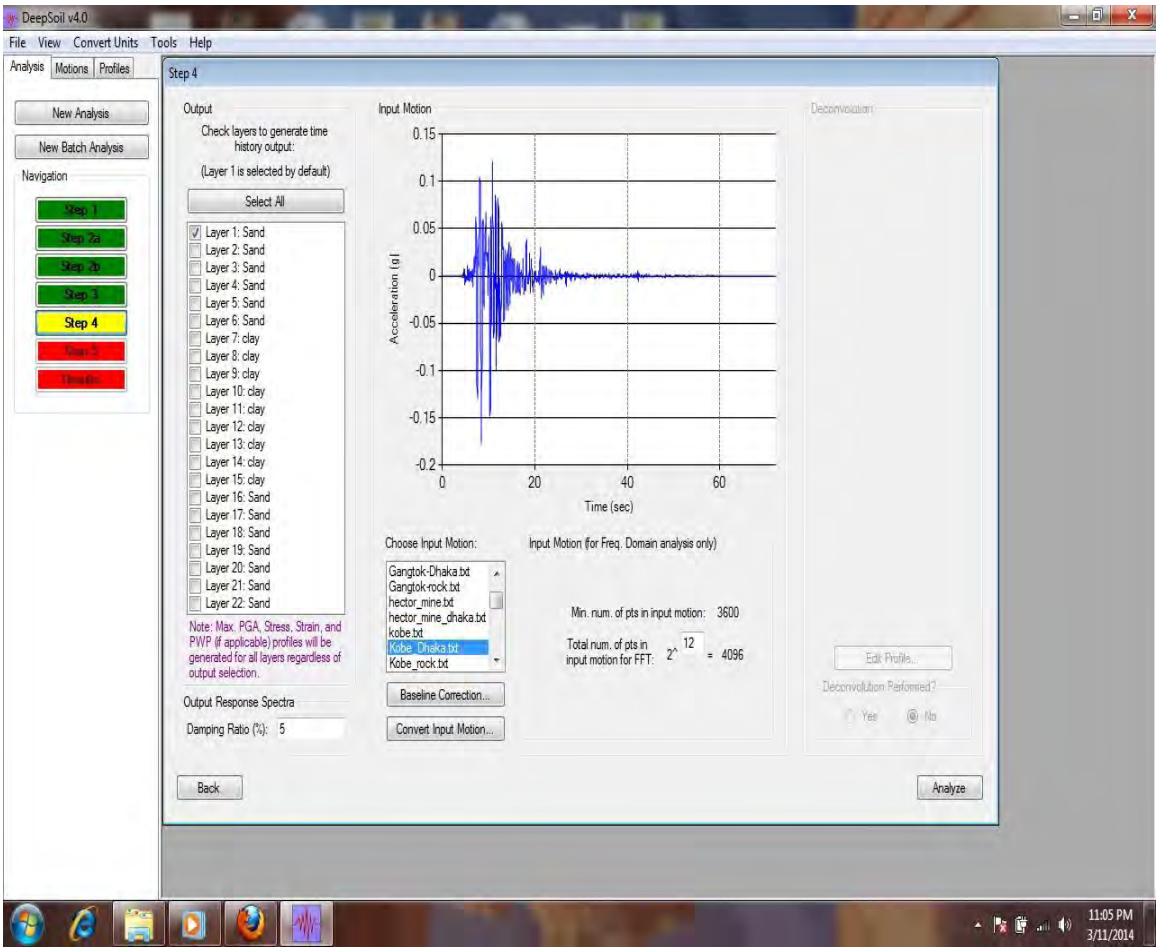

Figure: Input Motion selection

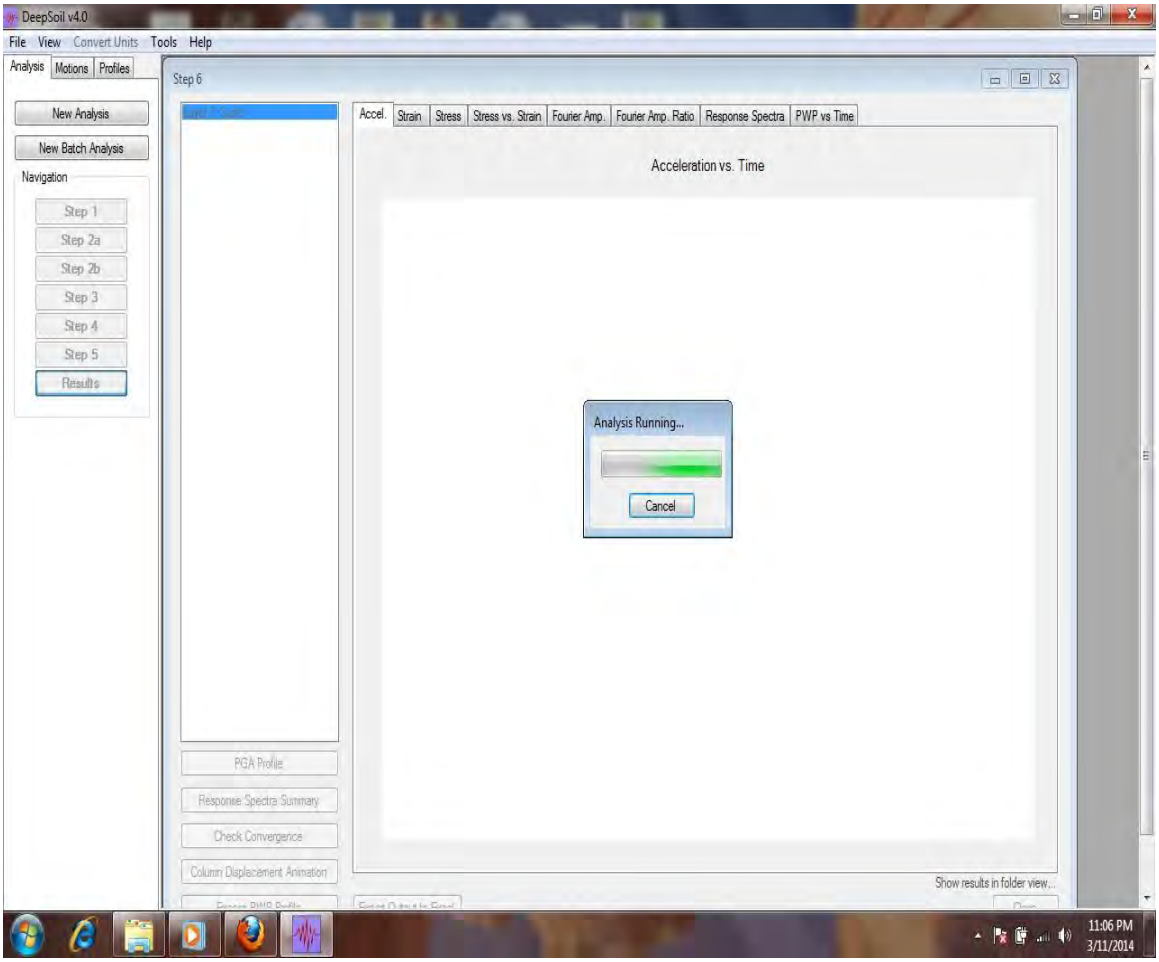

Figure: Analysis is going on

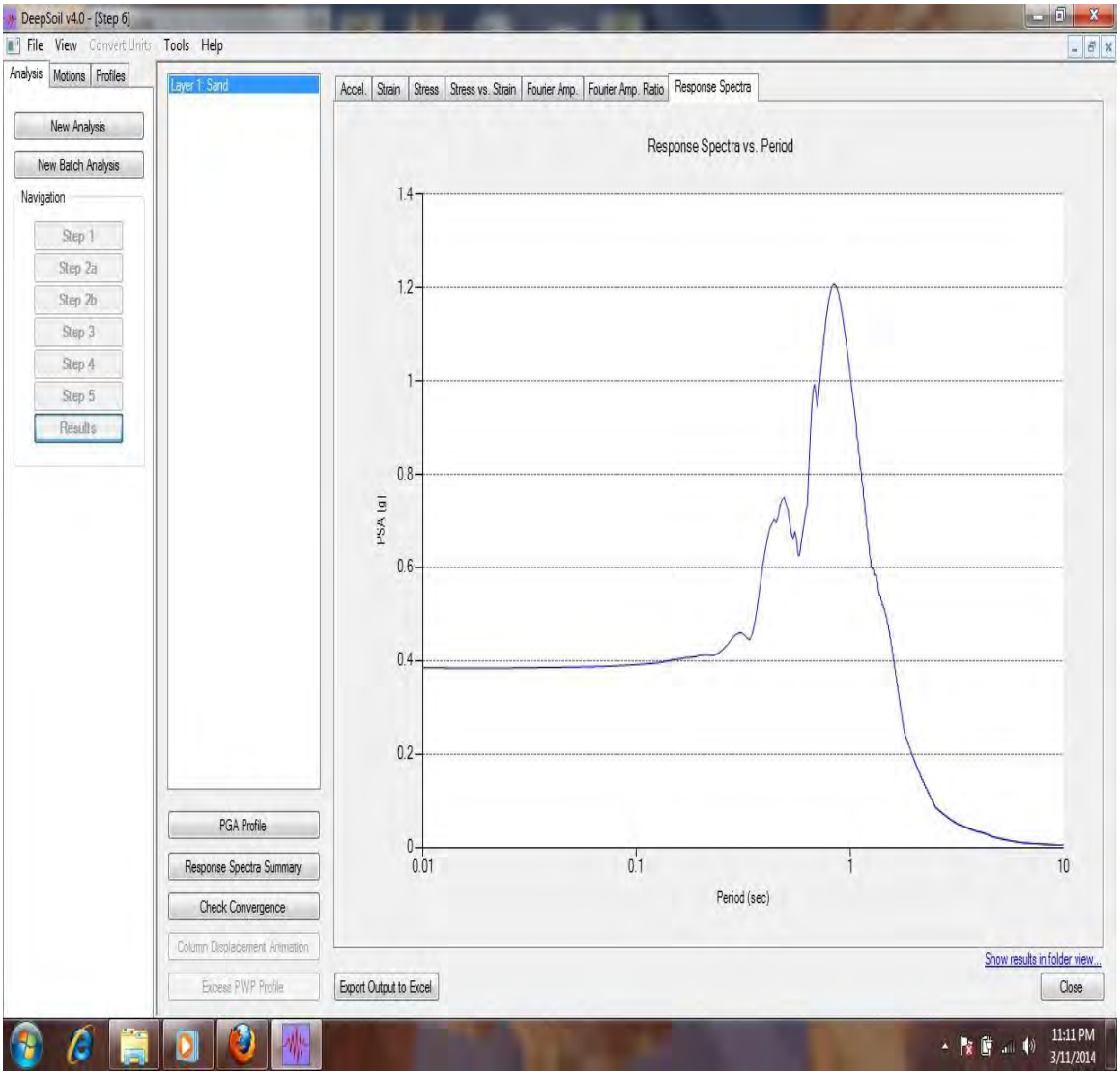

Figure: Analysis Results

CHAPTER ONE
INTRODUCTION

I.1 General

Bangladesh is one of the most natural disaster prone areas in the World. The different types of disasters like flood, cyclonic storms, tidal surges, droughts, tornadoes, river bank erosion, earthquake etc. occur in Bangladesh regularly and frequently. The 1897 Great Indian Earthquake with a magnitude of 8.7, which is one of the strongest earthquakes in the world killed 1542 and affected almost the whole of Bangladesh (Oldham, 1899). Crop and livestock loss was extremely high.

The historical seismicity data and recent seismic activities in Bangladesh and adjoining areas indicate that Bangladesh is at high seismic risk. As Bangladesh is the world's one of the most densely populated area, any future earthquake shall affect more people per unit area than other seismically active regions of the world. Bangladesh including capital city Dhaka is largely an alluvial plain consisting of fine sand and silt deposits with shallow ground water table in most places. Although the older alluvium is less susceptible to site amplification, the deposits along the river flood plains may amplify during a severe earthquake. Human made soil deposits also deserve attention. Loose fills, such as those placed without compaction, are very likely to be susceptible to site amplification.

Over the past 30~40 years Dhaka city has experienced a growth of urban population and it will continue in the future due to several unavoidable reasons. This high population increase demands rapid expansion of the city. Unfortunately, most parts of Dhaka city have already been occupied. As a result, new areas have been reclaimed by both government and private agencies in and around Dhaka city. In many cases, the practice for developing such new areas is just to fill lowlands of the depth 3~12m with dredged material, which is almost silty sand. This causes seismic hazards susceptibility for such areas.

Dhaka is vulnerable to earthquake due to high population density, unplanned structures, lack of preparedness at community level, etc. In the wider metropolitan area the estimated population is 12.8 million while the city population of Dhaka accommodates a large stands approximately 7.0 million as of 2012. Old Dhaka is more vulnerable to earthquake due to its relatively high density of population. Besides, the densely built fabric consisting of vulnerable aged and unreinforced masonry buildings along with narrow local streets makes the locality more susceptible to earthquake. If a large earthquake occurs near Dhaka or within metropolitan area of Dhaka city, the economic impact will be huge and a great number of causalities will take place. This will have severe long term repercussion for the entire country.

One of the most important and most commonly encountered problems in geotechnical earthquake engineering is the evaluation of ground response. Ground response analyses are used to predict ground surface motions for development of design response spectra, to evaluate dynamic stresses and strains for evaluation of seismic hazards, and to determine the earthquake induced forces that can lead to instability of earth and earth retaining structures. Under ideal conditions, a complete ground response analysis would model the rupture mechanism at the source of an earthquake, the propagation of stress waves through the earth to the top of bedrock beneath a particular site and would then determine how the ground surface motion is influenced by the soil that lie above the bedrock. In reality, the mechanism of fault rupture is so complicated and the nature of energy transmission between the source and the site so uncertain that this approach is not so practical for common engineering applications. The problem of ground response analysis then becomes one of determining the response of the soil deposit to the motion of the bedrock immediately beneath it. Despite the fact that seismic waves may travel through tens of kilometers of rock and often less then 100m of soil, the soil plays a very important role in determining the characteristics of the ground surface motion.

The influence of local soil conditions on the nature of earthquake damage has been recognized for many years. Since 1920s, seismologists and more recently geotechnical earthquake engineers have worked toward the development of quantitative methods for predicting the influence of local soil conditions on strong ground motion. Over the

years, a number of techniques have been developed for ground response analysis. The techniques are often grouped according to the dimensionality of the problems they can address, although many of the two and three dimensional techniques are relatively straightforward extensions of corresponding one dimensional technique.

Site amplification of Dhaka City (Rashid, 2000), Sylhet City (Islam, 2005), Chittagong City (Masud, 2007) have been carried out. They have used SHAKE Program to determine site amplification. But they have used SPT-Shear Wave Velocity correlation to estimate Shear Wave Velocity (Vs). Shear wave velocities of each layer have been calculated from the corrected SPT 'N' value using the relation. Shear Wave Velocity (Vs) may not be calculated accurately from SPT-Shear Wave Velocity correlation. In this study Shear Wave Velocity (Vs) has been directly estimated in selected locations of Dhaka City by CPT equipment in the field and detail ground response analysis has been performed. Standard Penetration Test (SPT) has also been conducted in selected locations of Dhaka City.

1.2 Geology of Dhaka City

Dhaka city which is a metropolis as well as the capital city of Bangladesh lies between latitude 23°40' N to 23°54' N and longitude from 90°20' E to 90°30' E and covers an area of about 470 km^2 having the altitude of 6.5 to 9 m above mean sea level. Geologically, it is an integral part in the southern tip of the Madhupur tract an uplifted block in the Bengal basin, with many depressions of recent origin in it. It is bounded by the Tongi khal (Small River) in the North, the Bariganga River in the south and southeast, the Balu River in the East and Turag River in the West.

The subsurface geology of Dhaka city shows that upper formation is Madhupur clay layer and termed as aquitard and it is 6 to 12 m thick in most parts of the city. The Madhupur clay mainly consists of Kaolinite (27~53%) and Illite (14~33%) with very small amount of Illite smectite (2~13%) down to 5m depth (Zahid et al., 2004). However, below the clay layer, medium to coarse grained formation exist. Kamal & Midorikawa (2004) delineated the geomorphology of Dhaka city area, differentiating

the ground of the city into seventeen geomorphic units using aerial photographs. These geomorphic units represent the soil conditions, surface geology of Dhaka with minor anthropogenic modifications. It has been observed that the city has been expanding rapidly even in the low-lying geomorphic units by fill practices for urban growth since 1960. They also classified the fill-sites into four classes based on the thickness of fills. In order to collect the fill-thickness, the boreholes and old topographic map prepared in 1961 are used. Later on, the classified fills are integrated with the pre-urban geomorphic-soil units. This geomorphologic map also illustrates the urban sprawl on the lowlying geomorphic units until 2002. Figure 1.1 shows the Geological map of Bangladesh.

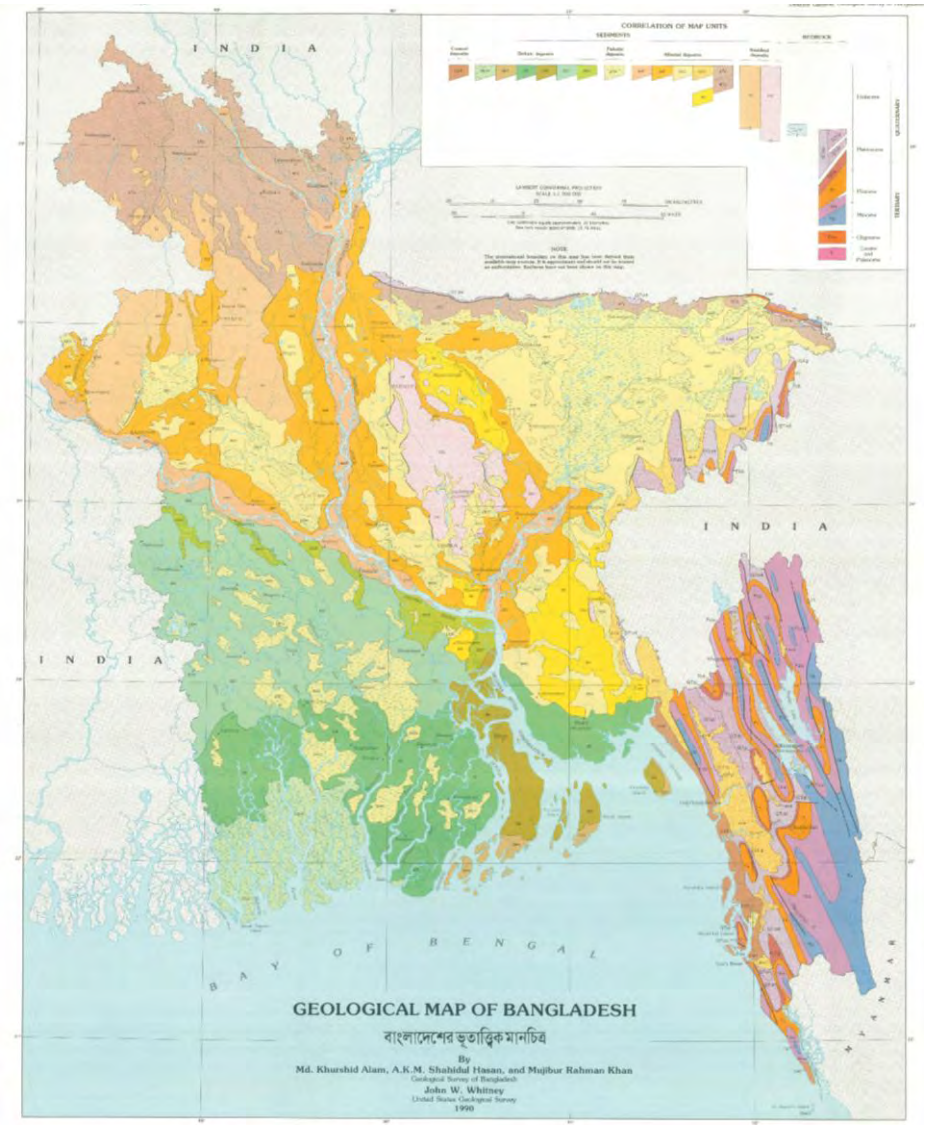

Fig 1.1: Geological map of Bangladesh (Geological survey of Bangladesh, 1990)

Alluvial Silt and Clay: Medium to dark grey Silt to Clay; Colour is darker as amount of organic anmaterial increases. Map unit is a combination of alluvial and paludal deposits; includes flood–basin Silt, backs wamp silty clay, and organic rich Clay in sag ponds and large depressions. Some depressions contain peat. Large areas underlain by this unit are dry only a few months of the years the deeper part of depressions and bhils contains water throughout the year.

Alluvial Silt: Light to medium grey, Fine sandy to clayey silt. Commonly poorly stratified; average grain size decreases away from main channels. Chiefly deposited in flood basins and interstream areas. Units includes small backswamp deposits and varying episodic or unusually large floods. Illite is the most abundant clay mineral. Most areas are flooded annually. Included in this unit are thin veneers of sand spread by episodic large floods over flood plain silts. Historic potery, artifact, and charcoal found in upper 4 m.

Madhupur Clay residuum: light yellowish grey, orange, light to brick red and grayish white, amicaceous silty clay to sandy clay; plastic and abundentey mattled in upper 8 m, contains small clusters of organic matter. Sand fraction dominantly quartz; minor feldspar and mica; sand content increases with depth. Dominant clay minerals are kaolinite and Illite. Iron manganese oxide modules rare.

1.3 Scope and Objectives of Present Research

The purpose of this research is to estimate the Site Amplification through site response analysis of selected locations of Dhaka city based on Shear wave Velocity. In this study, response spectra, amplification factor and peak ground acceleration are estimated by equivalent linear analysis.

The following are the specific objectives of the research:

1. To estimate Shear Wave Velocity directly by CPT equipment at selected locations of Dhaka city.

2. To estimate Site Amplification of those locations of Dhaka city using the program DEEPSOIL.
3. To perform Detailed Ground Response Analysis of Dhaka city.

It is expected that the results obtained from the research can be used for foundation design considerations, placement of lifelines facilities etc. of Dhaka city to minimize future possible hazards caused by earthquake. These will be useful also for the development of microzonation map of Dhaka city.

1.4 Outline of the Study

The Thesis has been comprised of five chapters.

Chapter One is the presentation of a brief introduction to the subject, states the major objects of the study and need for ground response analysis.

Chapter Two presents a brief review of the existing literature on site response with emphasis on methodologies used to solve the site response problem. The procedure of determining Shear Wave Velocity has been discussed in this chapter. Detail Site Amplification analysis procedures by using DEEPSOIL that have been used in this research are also described in details.

Chapter Three presents the CPT equipment test results. The equipments which are used to find out shear wave velocity have been also described here.

Chapter Four consists of detailed site specific ground response analysis using DEEPSOIL software. Using DEEPSOIL tool, response spectra, amplification factor and peak ground acceleration at different locations is estimated.

Chapter Five presents a summary of the results and the findings resulting from this work. It includes recommendations for future research. List of references and appendices follows.

CHAPTER TWO
LITERATURE REVIEW

2.1 General

The objective of this chapter is to analyze the past researches related to Site Amplification in home and abroad. In addition to that detail theoretical aspects of Site Amplification including its estimation procedures and possible mitigation methods are also discussed.

2.2 Seismicity in Bangladesh and problem hazards

Significant damaging historical earthquakes have occurred in and around Bangladesh and damaging moderate magnitude earthquake occur every few years. The country's position adjacent to the very active Himalayan front and ongoing deformation in nearby parts of south-east Asia expose it to strong shaking from a variety of earthquake sources that can produce tremors of magnitude 8 or greater. The potential for magnitude 8 or greater earthquake on the nearby Himalayan front is very high, and the effects of strong shaking from such an earthquake directly affect much of the country. In addition, historical seismicity within Bangladesh indicates that potential for damaging moderate to strong earthquake exists throughout much of the country.

Large earthquakes occur less frequently than serious floods, but they can affect much larger areas and can have long lasting economic, social and political effects. Bangladesh covers one of the largest deltas and one of the thickest sedimentary basins in the world. According to the report on time predictable fault modeling (2009), earthquake and tsunami preparedness component of CDMP have identified five tectonic fault zones which may produce damaging earthquakes in Bangladesh. These are:

a) Madhupur fault zone
b) Dauki fault zone.
c) Plate boundary fault zone-1
d) Plate boundary fault zone-2
e) Plate boundary fault zone-3

Considering fault length, fault characteristics, earthquake records etc, the maximum magnitude of earthquakes that can be produced in different tectonic blocks have been given in Table 2.1.

In the generalized tectonic map of Bangladesh as shown in Figure 2.1 the distribution of epicenters has been found to be linear along the Dauki fault system and random in other regions of Bangladesh. The investigation of the map demonstrates that the epicentres are lying in the weak zones comprising surface or subsurface faults. Figure 2.2 shows the major fault lines which affect the seismicity in Bangladesh. Most of the events are of moderate rank (magnitude 4~6) and lie at a shallow depth, which suggests that the recent movements occurred in the sediments overlying the basement rocks. In the northeastern region (surma basin), major events have been controlled by the Dauki fault system. The events located in and around the Madhupur tract also indicate shallow displacement in the faults separating the block from the alluvium.

Information of earthquake in and around Bangladesh is available for the last 250 years. Among these, during the last 150 years, seven major earthquakes have affected Bangladesh. The surface wave magnitude, maximum intensity according to European Macroseismic scale (EMS) and epicentral distance from Dhaka has been presented in Table 2.3. Characteristics of some recent earthquakes have been also shown in Table 2.2.

Table 2.1 Maximum estimated earthquake magnitude in different tectonic faults (Report of CDMP, 2009)

Fault zone	Earthquake events	Estimated magnitude, m_w
Madhupur fault zone	AD 1885	7.5
Dauki fault zone	AD 1897. AD 1500 to 1630 (AD 1548)	8.0
Plate Boundary-1	AD 1762, AD 680 to 980, BC 150 to AD 60, BC 395 to 740	8.5
Plate Boundary-2	Before 16^{th} century	8.0
Plate Boundary-3	Before 16^{th} century	8.3

Table 2.2 Recent earthquakes in Bangladesh

Date	Place of earthquake	Magnitude	Destructions
13 November, 1997	Chittagong	6.0	It caused minor damage around Chittagong town.
12 july,1999	Maheshkhali Island	5.2	Severely felt around Maheshali island and the adjoining sea.
7 july,2003	Kolabunia union of barkal upazila, Rangamati district	5.1	Houses cracks and landslides.

Table 2.3 List of major earthquake affecting Bangladesh during last 150 years (Ms>7) (sabri, 2002)

Date	Name of earthquake	Surface wave magnitude (m_s)	Maximum intensity (EMS)	Epicentral distance from Dhaka(km)	Basis
10 January, 1869	Cachar earthquake	7.5	IX	250	Back calculation from intensity
14 july,1885	Bengal earthquake	7.0	VII to IX	170	Directly from seismograph
12 June, 1897	Great Indian earthquake	8.7	X	230	
8 July,1918	Srimongal earthquake	7.0	VII to IX	150	
2 July, 1930	Dhubri earthquake	7.1	IX	250	
15 January, 1934	Bihar-nepal earthquake	8.3	X	510	
15 August, 1950	Assum earthquake	8.5	X	780	

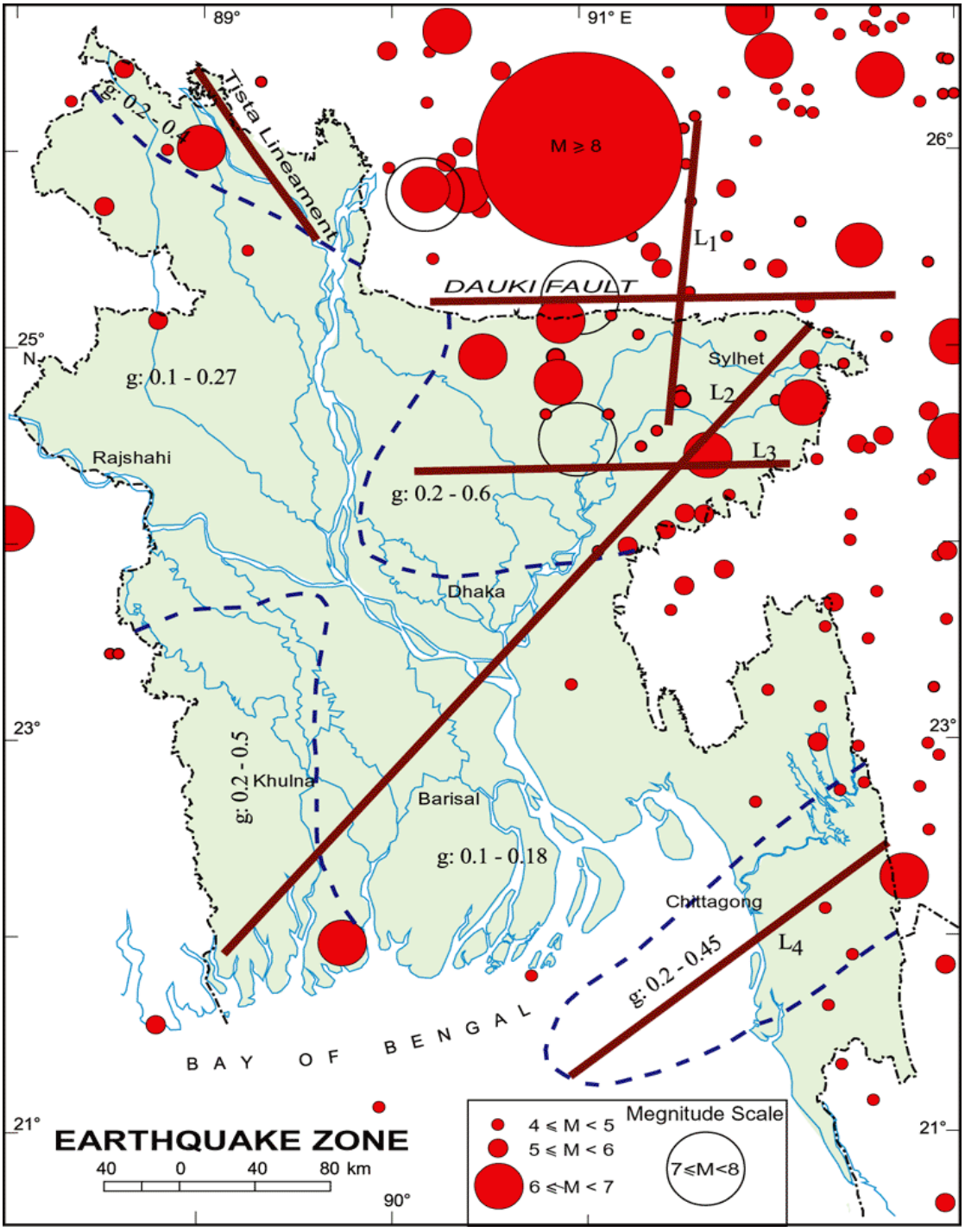

Figure 2.1: Seismo-tectonic lineaments capable of producing damaging earthquakes (Source: www.banglapedia.com)

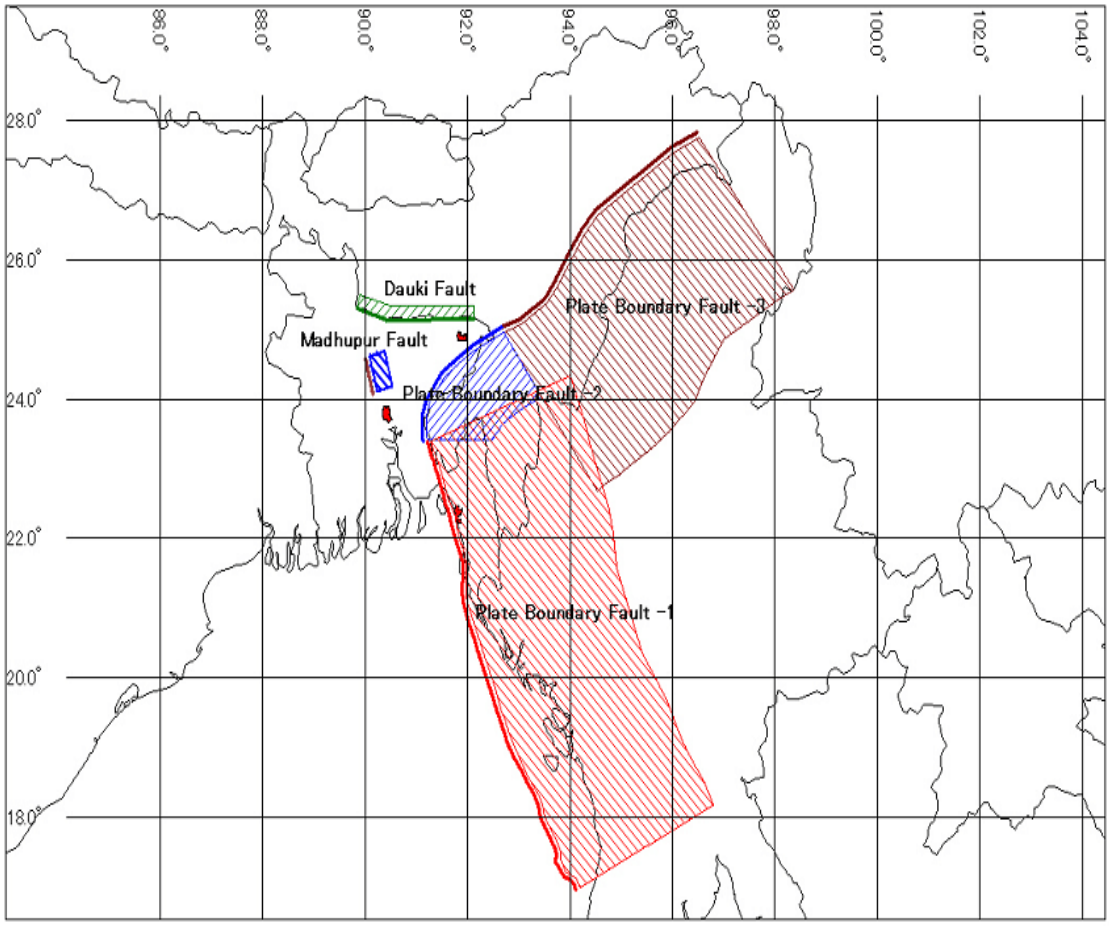

Figure 2.2: The major fault lines which affect seismicity in Bangladesh

(Source: Report on time predictable fault modeling, 2009, earthquake and tsunami preparedness component, CDMP)

Based on the above discussions, the probable hazard scenario for an earthquake to a scale of M_w = 6.5 or above in Dhaka city could cause:

a) Panic among the city dwellers and no knowledge of what is to be done during and immediately after earthquake occurrence.
b) Possible sinking of many of the buildings on filled earth with shallow foundations due to the liquefaction effect.
c) If the earthquake occurs during monsoon time possible damage of the Dhaka flood protection embankment due to liquefaction effect causing sudden submergence of a large area.

d) Large scale damage and some collapse of poorly constructed and /or old building.
e) Possible outbreak of fire in most of the building from the gas lines.
f) Possible damage of power installation and power cut off for identified period.
g) Water supply failure as almost all the deep tube wells are run by power, and possible water line damage.
h) Damage of roads and blockage of traffic due to falling of debris from collapsed buildings and other installations on or near roads.
i) Some of the hospital buildings may collapse killing a large number of inmates and stopping medical for the disaster victims.
j) Some of the school building may collapse killing and injuring a large number of students.
k) An aftershock may cause further collapse of many of the already damaged buildings.
l) A few rescue equipments, whatever is available, cannot be operated due to the lack of guidance, availability of operators, some cannot find access to rescue sports due to road blockage etc.
m) Limited access from outside as most or the highways/bridges, airport may not be functional.

Although during the last decade much advancement has been achieved in the earthquake engineering, modern science has yet to invent any technology that can predict earthquake. But some earthquake induced damages can be evaluated before hand. Therefore, seismic hazard susceptibility of Dhaka soil demands extensive research on ground response analysis in order to mitigate and reduce earthquake induced hazards to the most populated city in the world.

2.2.1 Seismic zoning map of Bangladesh

The seismicity zones and the zone coefficients may be determined from the earthquake magnitude for various return periods and the acceleration attention relationship. It is required that for design or ordinary structures, seismic ground motion having 10% probability of being exceeded in design life of a structure (50 years) is considered critical. An earthquake having 200 years return period originating in sub-Dauki zone have epicentral acceleration of more than 1.0g but at 50 kilometer the acceleration shall be reduced to as low as 0.3g.

Ali (1998) presented the earthquake base and seismic zoning map of Bangladesh. Tectonic frame work of Bangladesh adjoining areas indicate that Bangladesh is situated adjacent to the plate margins of India and Eurasia where devastating earthquakes have occurred in the past. Non-availability of earthquake, geology and tectonic data posed great problem in earthquake hazard mapping of Bangladesh in the past. The first seismic map which was prepared in 1979 was developed considering only the epicentral location of past earthquake and isoseismic map of very few of them. During preparation of National Building Code of Bangladesh in 1993, substantial effort was given in revising the existing seismic zoning map using geophysical and tectonic data, earthquake data, ground motion attenuation data and strong motion data available from within as well as outside of the country. Geophysical and tectonic data were available from Geological survey of Bangladesh. Earthquake data were collected from NOAA data files and geodetic survey, US Dept. of commerce.

Seismic zoning map for Bangladesh has been presented in Bangladesh National Building code (BNBC) published in 1993. The pattern of ground surface acceleration contours having 200 year return period from the basis of this seismic zoning map. There are three zones in the map- zone 1, zone 2 and zone 3. The seismic coefficients of the zones are 0.075g, 0.15g and 0.250g for zone 1, zone 2 and zone 3 respectively. Bangladesh National Building Code (1993) placed Dhaka city area in seismic zone 2 as shown in Figure 2.3. However, the seismic zones in the code are not based on the analytical assessment of seismic hazard and are mainly based on the location of historical data.

The first seismic zoning map of the subcontinent was compiled by the Geological Survey of India in 1935. The Bangladesh Meteorological Department adopted a seismic zoning map in 1972. In 1977, the Government of Bangladesh constituted a Committee of Experts to examine the seismic problem and make appropriate recommendations. The Committee proposed a zoning map of Bangladesh in the same year. Figure 2.4 shows the proposed seismic zoning map of Bangladesh.

According to Bangladesh National Building Code (BNBC, 1993), Bangladesh is divided into 3 earthquake zones (Figure 2.3):

Zone-3 comprising the northern and eastern regions of Bangladesh with the presence of the Dauki Fault system of eastern Sylhet and the deep seated Sylhet Fault, and proximity to the highly disturbed southeastern Assam region with the Jaflong thrust, Naga thrust and Disang thrust, is a zone of high seismic risk with a basic seismic zoning co-efficient of 0.25. Northern Bangladesh comprising greater Rangpur and Dinajpur districts is also a region of high seismicity because of the presence of the Jamuna Fault and the proximity to the active east-west running fault and the Main Boundary Fault to the north in India. The Chittagong-Tripura Folded Belt experiences frequent earthquakes, as just to its east is the Burmese Arc where a large number of shallow depth earthquakes originate.

Zone-2 comprising the central part of Bangladesh represents the regions of recent uplifted Pleistocene blocks of the Barind and Madhupur Tracts, and the western extension of the folded belt. The zone extends to the south covering Chittagong and Cox's Bazar. Seismic zoning coefficient for Zone II is 0.15.

Zone-1 comprising the southwestern part of Bangladesh is seismically quiet, with an estimated basic seismic zoning co-efficient of 0.075.

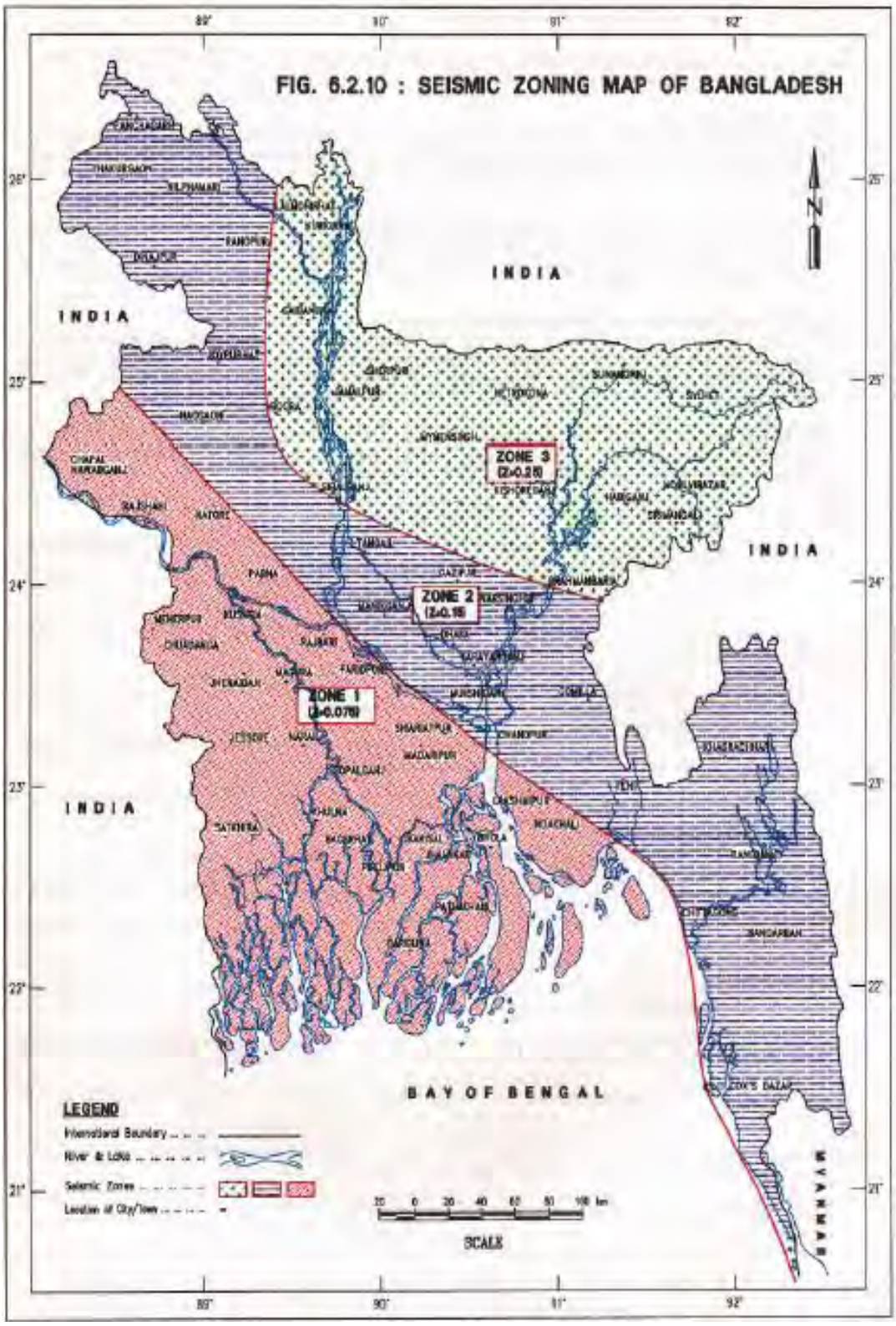

Figure 2.3: Seismic Zoning Map of Bangladesh (After BNBC, 1993)

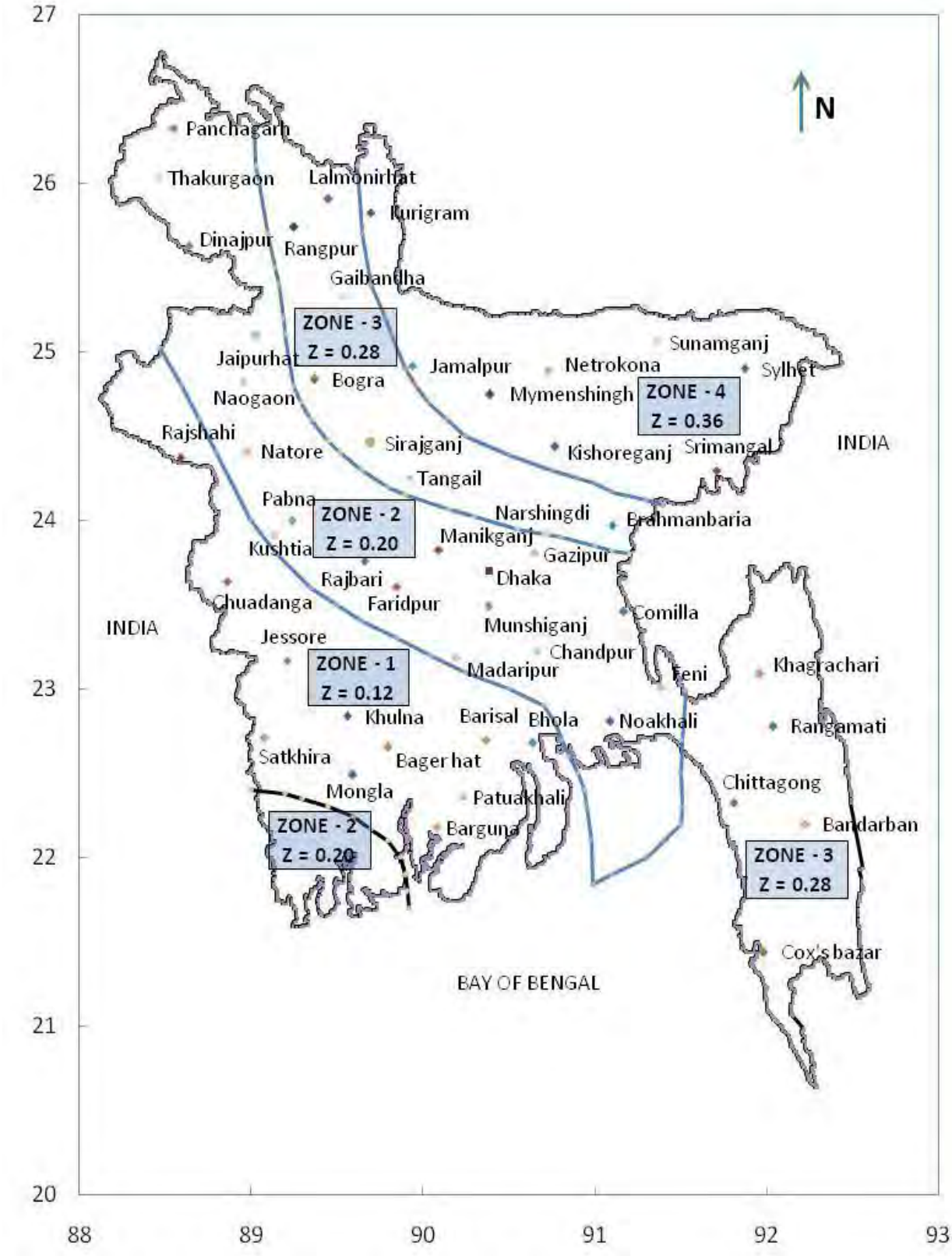

Figure 2.4: Proposed Seismic Zoning Map of Bangladesh

2.2.2 Major Source of Earthquake in Bangladesh

Bangladesh is one of the most earthquake prone countries in the world. Specialists are expecting a severe earthquake in this area in near future, which will cause a serious human casualty, damages of infrastructure and other losses.

Although Bangladesh is extremely vulnerable to seismic activity, the nature and the level of this activity is yet to be defined. In Bangladesh complete earthquake monitoring facilities are not available. The Meteorological Department of Bangladesh established a seismic observatory at Chittagong in 1954. This remains the only observatory in the country.

Since the whole Indian subcontinent is situated on the junction of Indo- Australian plate and Eurasian plate, the tectonic evaluation of Bangladesh can be explained as a result of collision of the north moving Indo- Australian plate with the Eurasian plate. Figure 2.5 shows the tectonic plates.

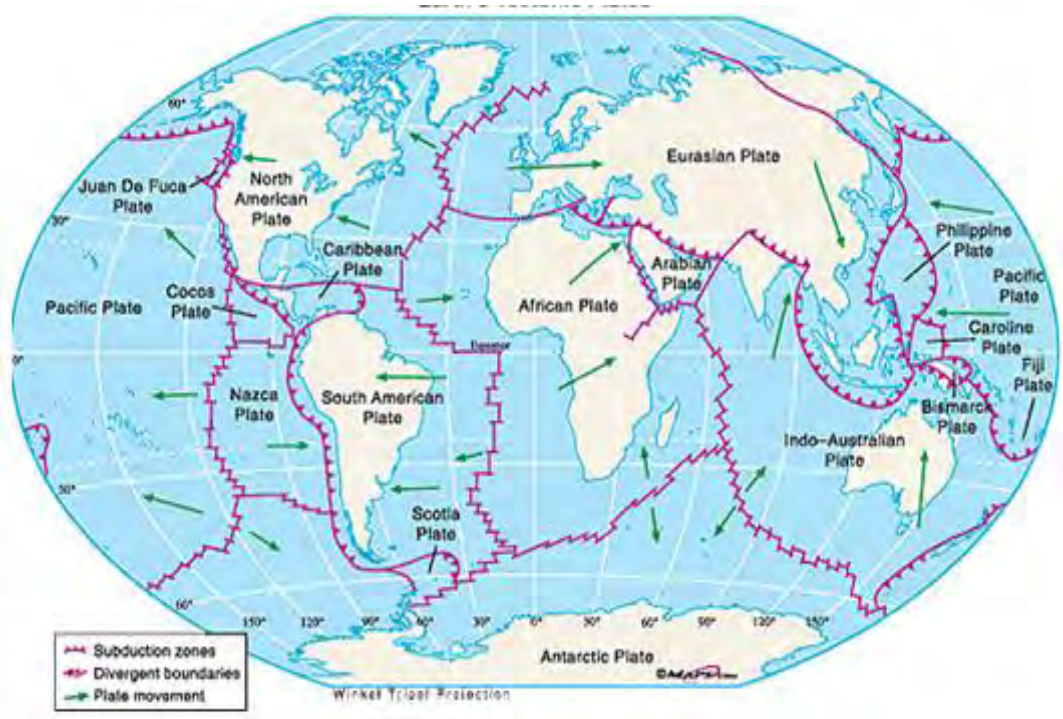

Figure 2.5: Tectonic plates

2.3 Past Research on Site Amplification

Earthquakes in the last 50 years have demonstrated the role of site effects in the distribution and magnitude of the damages associated with a seismic event to be paramount. In 1985, an 8.1 magnitude earthquake caused significant casualties and extensive damage in Mexico City. The occurrence of damage in a city located 350 km from the earthquake epicenter has been attributed to the amplification of seismic waves throughout the city's unconsolidated lacustrine deposit. Seismic events such as the Loma Prieta (1989), Northridge (1994) Kobe (1995), and Chi-Chi earthquakes (1999) have corroborated the significance of local geologic and geomorphologic conditions on the seismic ground response. The changes in the intensity and the frequency content of the motion due to the propagation of the seismic waves in soil deposits and the presence of topographic features, commonly referred to as site effects, have a direct impact on the response of structures during each of these earthquake events. The behavior of soil under cyclic loading is often non-linear and depends on several factors including amplitude of loading, number of cycles, soil type and in situ confining pressure. Even at relatively small strains, soils exhibit non-linear behavior. Thus it is necessary to incorporate soil non-linearity in any site response analysis. One dimensional site response analysis methods are widely used to quantify the effect of soil deposits on propagated ground motions in research and practice. These methods can be divided into two main categories: (1) frequency domain analyses (including the equivalent linear method, e.g. SHAKE 91 (1972)) and (2) time domain analyses (including non-linear analyses).

2.4 Seismic Site Characterization

Strong ground motion are influenced by geological and geotechnical site conditions. Observations from as early as the 1800s exist in the literature indicating the effects of local geology on ground motions (EPRI, 1993). Damaging effects associated with such soft deposits, may lead to local intensity increments as large as 2 to 3 degrees in MM scale (Aki , K. and Irikura, I., 1991; Finn,W.D.L., 1991). Local soil conditions have

significant role in the amplification of seismic waves and have been experienced in the past earthquakes (Ansal, A. et al., 2004; Slob, S. et al., 2002; Street, R. et al., 2001).

To evaluate site effects associated with the local geological and geotechnical conditions, knowledge about the sequence of the geological layers including their depth, lithological and geotechnical characterization is required. The thickness of sediments implies rebounding of the seismic waves leading to site amplification or attenuation. Likewise topographic changes can yield scattering, focusing, or defocusing of incident seismic waves. Soil liquefaction is affected by soil gradation and water table depth. In hilly terrains earthquake triggered landslides are a threat. Such is the effect of local geology that attenuation relationships used for prediction of ground motion levels include a site factor to incorporate the amplification effects. Therefore, site characterization has become one of the most relevant tasks in seismic hazard analysis.

Empirical correlations between surface geology and the increment of the seismic intensity, based on post event observations, are shown in Table 2.4. In the handbook for earthquake ground motion scenarios prepared by Faccioli, E. and Pessina, V., (2003), local ground motion amplification identification based on intensity and elastic response spectra has been given.

Table 2.4 Intensity Increment for each geological unit

Medvedev(1962)	**ΔIMSK**
Granites	0
Limestone, Sandstone, Shale	0.2-1.3
Gypsum, Marl	0.6-1.4
Coarse-material ground	1.0-1.6
Sandy Ground	1.2-1.8
Clayey Ground	1.2-2.1
Fill	2.3-3.0
Moist ground (gravel, sand, clay)	1.7-2.8
Moist fill and soil ground	3.3-3.9
Astroza and Monge (1991)	**ΔIMSK**
Granitic rock	0.0
Volcanic pumicite ashes	1.5-2.5
Gravel	0.5-1.0
Colluvium	1.0-2.0
Lacustrine deposits	2.0-2.5
Faccioli and Pessina (2003)	
Rock or other rock-like geological formation, including at most 5 m of weaker material at the surface	0.0
Deposits of very dense sand, gravel, or very stiff clay, at least several tens of m in thickness, characterised by a gradual increase of mechanical properties with depth	0.0
Deep deposits of dense or medium dense sand, gravel or stiff clay with thickness from several tens to many hundreds of m	0.5
Deposits of loose-to-medium cohesionless soil (with or without some soft cohesive layers), or of predominantly soft to firm cohesive soil	1.0

Relative amplification factors, fag related to surface geology are suggested by Midorikawa, S., (1987). The values suggested can be adopted when the hazard is represented in terms of peak ground acceleration or spectral ordinates. Table 2.5 gives the correlation between surface geology and relative amplification as suggested by different researchers.

Table 2.5 Correlations between surface geology and relative amplification

Borcherdt and Gibbs (1976)	**Relative Amplification**
Bay mud	11.2
Alluvium	3.9
Santaclara formation	2.7
Great valley sequence	2.3
Franciscam formation	1.6
Granite	1.0
Shima (1978)	
Peat	1.6
Humus soil	1.4
Clay	1.3
Loam	1.0
Sand	0.9
Midorikawa (1987)	
Holocene	3.0
Pleistocene	2.1
Quaternary volcanic rocks	1.6
Miocene	1.5
Pre-Tertiary	1.0

Seismic site characterization could be categorized into three different levels depending on level of available data. The manual for zonation on seismic geotechnical hazards, TC4-ISSMGE, (1999) suggests three different levels of methodologies to map out geological units associated to local ground motion amplification. A basic, 'grade I', zonation level consists of compilation and interpretation of existing information available from historic documents (i.e., compiled data on the distribution of damage induced during past destructive earthquake), published reports and other available databases or by direct reference to the site surface geology. The 'grade II' level comprises of collection of additional sources of data obtainable at moderate cost. A very high and detailed zonation level, referred to as 'grade III', typical of site and structural specific studies.

This level is less feasible and unaffordable for investigation on large areas. Once the geotechnical zonation is done, local ground motion amplification could be estimated by different methods. These methods are discusses in the later sections.

2.5 Local Site Effects

Local site effects are considered significant at a radius greater than 50km rather than at locations near to epicentre. The local site effects can be categorised into effects due to basin/soil and due to topography. Rupture directivity, fling step, hanging wall effects are source effects while site effects are due to basin geometry, topography etc. Impedance contrast, resonance, trapping, focusing, basin edge and damping are a part of basin/soil effects whereas ridge, valley, slope variation, discontinuities fall under topography category. Mueller, C.S., (1986) gave a review of state of the art analysis of site effects on ground motion and found that empirical methods yielded better predictions of amplification than theoretical methods that used vertical seismic profiling data.

2.5.1 Site Amplification

The effect of earthquake is often quantified by the damage incurred to manmade structures in addition to the measured ground motions at a site. To estimate the effect of a given earthquake, it is necessary to assess the expected ground motion characteristics, and the subsequent response of both soil and structures to those ground motions. A site amplification phenomenon is dependent on frequency of input motion. The characteristics of earthquake motions are influenced by a number of mechanisms related to the local soil and rock properties. Site amplification is quantified using Eq.2.1, known as the amplification factor (Kramer, S.L., 1996).

$$Amplification\ factor = \frac{u_{ground}}{u_{rock}} \tag{2.1}$$

Where, u= vertical particle displacement

2.5.2 Resonance

Amplification of earthquake motions is highly dependent on the frequency of excitation. Softer soil at larger interface gradient amplifies the low frequency motions whereas stiffer material of smaller interface gradient amplifies motions at a higher frequency. Presence of large amount of frequency content in the strong ground motions makes them vulnerable to amplification effects.

When the natural frequency of the subsoil matches the ground excitation, amplification is caused. Simplified relationships to establish natural frequency of site/structure are given in Eq. 2.2 and 2.3.

$$f_{structure} = \frac{N}{10} \tag{2.2}$$

$$f_{site} = \frac{V_s}{4H} \tag{2.3}$$

f= natural frequency, N = the number of stories in the structure, V_s = the shear wave velocity of the site, H = the thickness of the soil deposit.

2.5.3 Impedance contrast

Shear waves are used to explain the underlying phenomena of site response. Velocity of shear wave is low for dense deposits and is high in case of loose strata. It is common to only consider the effects of vertically propagating, horizontally polarized shear waves in site response analyses.

This is because of vertical orientation of earthquake motions near the surface and the resistance of most structures to lateral loading from the seismic weight of the structure. Material damping and shear wave velocities are useful to quantify the amplification effects in addition to energy flux. Shear wave velocity is evaluated based on density and shear modulus as in Eq. 2.4.

$$Shear\ modulus\ (G) = \rho\ V_s^2 \tag{2.4}$$

ρ = density of soil, V_s = the shear wave velocity of the site

As the stiffness of soil decreases, wave propagation velocity also decreases. But in accordance to the principal of conservation of energy, the amplitude of wave increases and results in a rise in the amplitude of vibration of the surficial soil deposits. The relationship between wave amplitude and total energy of the shear wave are given in Eq. 2.5 (Towhata, I., 2008). Primarily, Aki, K. and Richards, P.G., (1980) have given a relationship (Eq. 2.6) without considering the added effects of scattering and material damping, for the energy flow.

$$Energy\ per\ wavelength = \omega \Pi G E^2 \tag{2.5}$$

$$Energy\ flux = \rho V_s \dot{u}^2 \tag{2.6}$$

ω =frequency of wave, G=shear modulus, E=amplitude of motion, V_s =shear wave velocity, ρ=density of soil

2.5.4 Basin Effects

The effects of alluvial basin geometry on the magnitude and duration of ground motions can be significant. Silva, W. J., (1988) discussed the influence of topology and subsurface irregularities on the amplitude and duration of earthquake motions. The velocity contrast between the soft alluvial soils within the basin and the hard bedrock forming the edge of the basin serves to trap body waves and causes some incident waves to travel through the basin soil as surface waves.

Such trapping of body waves and the creation of slowly attenuating surface waves results in stronger shaking and longer durations than would be experienced under typical one-dimensional conditions (Kramer, S.L., 1996). The generated surface wave amplitude decreases with increase of edge slope. While the effects of geometry are limited towards the center of a large basin, they can be quite significant near the edges. Two and three dimensional site response analyses are required to understand the amplification mechanism in such cases. Induced surface waves are main cause of damage during earthquakes in addition to amplification and prolongation of signal.

2.5.5. Topography

Site effects are associated mainly with the type and spatial distribution of soils, topography of ground which play a significant role in determining the potential damage to engineering facilities during earthquakes. Topography can be distinguished into surface and subsurface topography. Bingol earthquake (2003), North Algerian earthquake (2003) exemplifies the heavy damage concentration along slopes due to topography effects. Table 2.6 discusses the amplification factors given in Eurocode (EC8, 2003) for different site morphology and their corresponding intensity increments.

Table 2.6 Topographic Amplification factors by EC 8(2003) and Paolucci, R. and Rimordi, A. (2002) for different site morphology and corresponding intensity increments ΔI (Faccioli, E. and Pessina,V., 2003)

Site Morphology	Amplification Factors				
	EC8	3D	2D SH	2D SV	ΔI
Isolated Cliff	1.2	1.3	1.22	1.22	1
Ridge crest width << base width Average slope angles >30°	1.4	1.58	1.18	1.32	1.5
Ridge crest width << base width Average slope angles <30°	1.2	1.25	1.09	1.28	1

2.6 Attenuation Relationships

The probability of occurrence of seismic hazard can be predicted by using attenuation relationships. They are widely used to predict the risk of ground motion for the seismic design.

The importance of site effects has been identified and a factor termed as 'site factor' has been and is being incorporated in the old/recently developed attenuation relationships. The use of attenuation relationships permits a more flexible assessment of seismic hazard in design as opposed to the fixed levels of 2% and 10% probability of occurrence in fifty years traditionally used in the codes (Rodriguez-Marek, A., 2000). Abrahamson, N.A., and Shedlock, K.M., (1997) have presented a complete review of attenuation relationships. Some of the attenuation relationships which primarily include site effects are being explained in detail.

2.6.1. Kanno et al. (2006)

To obtain a continuous site correction term Kanno,T. et.al., (2006) used the following relationship to develop a new attenuation relation for strong ground motion in Japan based on recorded data. In the equation, predominant period dependence has been eliminated.

$$G = \log\left(\frac{obs}{pre}\right) = p log\, V_{s30} + q \qquad (2.7)$$

Where, *G* is an additional correction term corresponding to site effects and log (obs/pre) is the residual between the observed amplitude of PGA, PGV, and spectral acceleration (obs) and the values predicted (pre) by the base model. Coefficients *p* and *q* were derived by regression analysis on the residuals averaged at intervals of every 100 m/sec in Vs30.

2.6.2. Campbell and Bozorgnia (2006)

Campbell, K. W. And Bozorgnia, Y., (2006) developed next generation attenuation empirical ground motion model (EGMM) in which the following equation (Eq.2.8) has been used to observe trends in the recorded ground motion data. They found that the model for hanging wall effects given by Abrahamson, N. A. and Silva, W. J. ,(1997) could also be used with this ground motion relation. The general functional form of the EGMM is given by the Eq.2.8. The equation was selected to represent the ground-motion relations for both the average horizontal and vertical components of PGA and PSA.

$$lnY = f_1(M) + f_2(R) + f_3(F) + f_4(HW) + f_5(S) + f_6(D) + \varepsilon_T \qquad (2.8)$$

Where, *fi* =functions of magnitude (M), R= source-to-site distance, F= style of faulting, HW= hanging wall effects, S=shallow site conditions, D= sediment depth.

2.6.3. Abrahamson and Silva (1997)

Attenuation relationship given by Abrahamson, N. A. and Silva, W. J., (1997) is similar to that given by Youngs, R. R., (1993). The relationship is developed for shallow rustal earthquakes in active tectonic regions. The site factor is included as an additive term to the natural logarithm of the corresponding spectral value. Abrahamson, N. A. and Silva, W. J., (1997) indicate that the site factor could also have magnitude dependence.

$$f_5(PGA_{rock}) = a_{10} + a_{11}\, ln\,(PGA_{rock} + c_5) \qquad (2.9)$$

Where, a_{10}, a_{11}, and c_5 are parameters of regression analysis**.**

2.6.4. Boore, Joyner and Fumal (1997)

Joyner W. B. and Boore, D. M., (1981, 1982) proposed an attenuation relationship for shallow crustal earthquakes in active tectonic regions. Further reviews were published by Boore, D. M., Joyner, W. B., and Fumal, T. E., (1993, 1994a and b) and are summarized in Boore, D. M., et al., (1997). The site factor is determined as an additive term to the natural log of the ground motion parameter, and is given by Eq. 2.10. The amplification factors from soil to rock are given in Figure 2.8. Soil is defined by = 310 m/s and 'Rock' is defined by = 620 m/s.

$$Site\ factor = b_v \frac{\overline{V_s}}{V_a} \qquad (2.10)$$

Where, b_v and V_a are regression parameters.

2.6.5. Toro, Abrahamson and Schneider (1997)

Toro, G.R. et al., (1997) developed attenuation relationship for shallow crustal earthquakes in stable continental regions. Soil factors developed by Silva, W. J. et al., (1988) are shown in Figure 2.6. It was proposed that either soil is a homogenizing factor or uncertainty in bedrock motions is lower than that in outcrop motions.

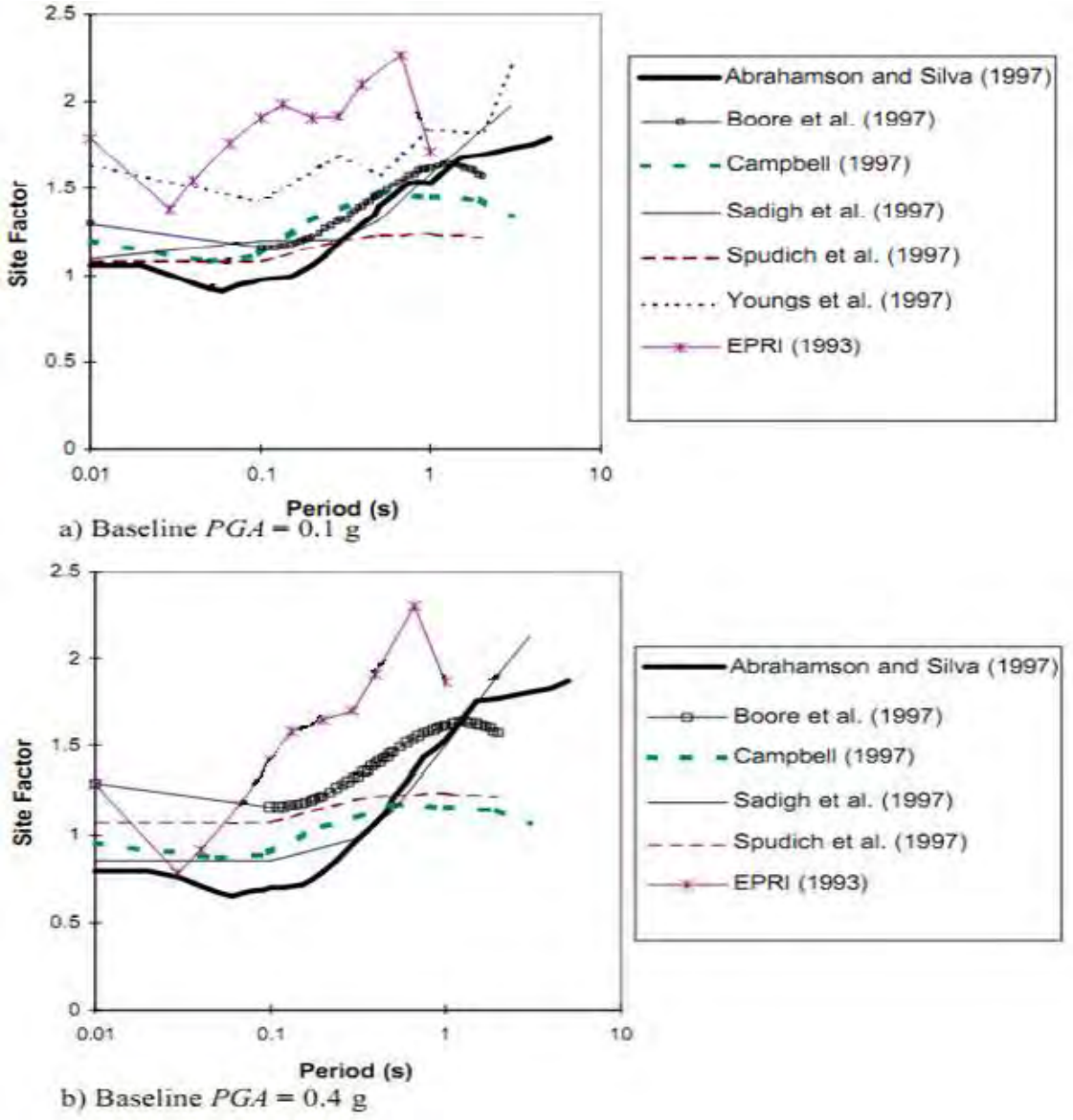

Figure 2.6 (a, b) Site factors used in different ground motion attenuation relationships (Rodriguez-Marek,A., 2000)

2.6.6. Youngs et al. (1997)

A relationship for subduction zone earthquakes has been developed by Youngs, R. R. et al., (1997). The database was divided into deep stiff soil, shallow stiff soil, and rock. In an initial analysis an increase in ratio of soil to rock PGA was observed with an increase in PGA, which contradicts intuitive soil behavior. For the correction of this

error, the relationship was constrained so that soil and rock PGA are equal for small distances to compensate for sparse soil data at small distances.

2.6.7. Campbell (1997)

Campbell, K. W., (1997) ground motion attenuation relationship was developed for shallow earthquakes in active tectonic regions. The database is divided into hard rock, soft rock and firm soil categories. The baseline attenuation relationship is developed for firm soil, with factors for hard rock and soft rock. The relationship includes a depth to basement term that defines a depth to crystalline basement. The attenuation relationship is developed for PGA and normalized spectral periods. The depth to basement term affects only the normalized spectra.

2.6.8. Sadigh et al. (1997)

The attenuation model by Sadigh, K., et al., (1997) is developed for shallow crustal earthquakes in active tectonic regions. The database is divided into rock (bedrock is at least 1 m from surface) and deep soil (a minimum of 20 m of firm soil). Soft soils are excluded from the database. Two different sets of coefficients are given, resulting in both PGA and magnitude dependence in the site amplification factors. There is a large degree of nonlinearity for PGA; in fact, PGA in soil is lower than PGA in rock for PGA values in rock greater than about 0.2 g. The same degree of nonlinearity was inferred by Abrahamson, N. A. and Silva, W. J. (1997). These amplification factors are close to those obtained by Abrahamson, N. A. and Silva, W. J. (1997).

2.6.9. Spudich et al. (1997): Extensional regimes

The relationship of Spudich, P. et al., (1997) for extensional regimes is a modification of the attenuation relationship proposed by Boore, D.M. et al., (1997). Site factors are constant for each period. Relatively low amplification levels at long periods are predicted compared to the other relationships (Fig. 2.6).

2.7 Site Classification

Site effects that represent seismic ground response characteristics are usually incorporated in seismic codal provisions (UBC97, IBC 2000 and EC8 2003). So that site effects can be accounted for while designing. Apart from SPT 'N' and shear strength, V_{30} is also considered in the dynamic site classification. It is the mean value of shear wave velocity for a depth of 30m (Eq.2.11). V_{s30} has been internationally accepted after its inclusion in NEHRP (National Earthquake hazard Reduction Programme, BSSC 2001) provisions for site classification. Shear wave velocity is dependent on the density of the underlying soil therefore; amplification also depends on the shear wave velocity. Brocherdt, R.D., (1992) introduced V_{s30} and the work of Anderson, J.G. et al., (1996) supported it. Though the concept has been accepted by many of the international seismic codes, it is debated if V_{s30} could be capable of representing the complex site amplification relative to the first 30m alone (Wald, L.A. and Mori, J., 2000; Stewart, J.P. et al., 2003; Park, D. and Hashash, Y.M.A., 2004; Di Giacomo, D., et al., 2005; Castellaro, S. et al., 2008).

$$V_{S30} = \frac{30}{\sum_{i=1}^{N} \left(\frac{d_i}{v_i}\right)} \qquad (2.11)$$

Where, di =thickness of the ith soil layer in metres; vi = shear wave velocity for the ith layer in m/s and N= no. of layers in the top 30 m soil strata which will be considered in evaluating V_{s30} values.

Site categories are usually based either on geological criteria or on shear wave velocity of the surficial materials. The use of shear wave velocity has the advantage of being based on an objective measure which affects ground motions in a way that can be modeled. However, it cannot be directly applied to sites that lack shear wave velocity measurements. Also, deeper geological structure such as sedimentary basins and laterally varying structure may have an equally strong or even stronger effect on site response.

Eurocode 8 2003 and IBC 2006

The classification in EC8 is a site classification scheme based on V_{s30}, standard penetration test (SPT) and cone penetration test (CPT) values. EC8 and IBC have a similar classification. Even though both the schemes use similar methods to identify the site classes, the range of V_{s30} values specified for each site class is different in both the methods.

EAK 2000

In the Greek seismic code uncertainty of choosing the soil type is high. Classification is divided into A, B, Γ, Δ and X. Distinct parameters that characterise the soil type are not listed which makes it a weak base for classification. The classification is basically based on thickness, plasticity index and density of the subsoil material. The classification of a site using such simple qualitative criteria does not cater to the current needs and to the present state of knowledge. Table 2.7 gives the site classification methods in different codes.

Table 2.7 Site classification in different seismic codes worldwide

Author	Site Class	Soil Profile	Average properties in top 30m		
			Soil shear wave velocity, V_s (m/s)	Standard penetration resistance, N	Soil undrained shear strength, S_u (kN/m^2)
IBC (2006)	A	Hard Rock	V_s>1500	N/A	N/A
	B	Rock	7600<V_s≤1500	N/A	N/A
	C	Very dense soil and soft rock	360<V_s≤760	N>50	S_u ≥100
	D	Stiff soil profile	180<V_s≤360	15≤N≤50	50≤S_u ≤100
	E	Soft soil profile	V_s<180	N<15	S_u <50
	E	---	Any profile with more than 3m of soil having the following characteristics: PI>20, w>40% , S_u<25 kN/m^2		

	F	---	Any profile with having one or more of the following characteristics: 1. Soils vulnerable to potential failure or collapse under seismic loading such as liquefiable soils, quick and highly sensitive clays, collapsible, weak cemented soils. 2. Peats and highly organic clays (H>3m of peat and/or highly organic clay where H=thickness of soil). 3. Very highly plastic clays(H>7.5m with PI>75) 4. Very thick soft/medium stiff clays (H>36m)			
Eurocode8 (2003)	A	Rock or other rock like geological formation, including utmost 5 m of weaker material at the surface	V_s > 800 m/s	N > 50	S_u > 250 kN/m^2
	B	Deposits of very dense sand, gravel or very stiff clay, at least several tens of metres in thickness, characterized by a gradual increase of mechanical properties with depth	V_s :360 – 800 m/s	N:15 - 50	S_u :70 - 250 kN/m^2
	C	Deep deposits of dense or medium dense sand gravel or stiff clay with thickness from several tens to many hundreds of metres	V_s :180 – 360 m/s	N < 15	S_u < 70 kN/m^2
	D	Deposits of loose to medium cohesionless soil (with or without some soft cohesive layers), or of predominantly soft to firm cohesive soil	V_s < 180 m/s		
	E	A soil profile consisting of a surface alluvium layer with V_{s30} values of type C or D and thickness varying between about 5 m and 20 m, underlain by stiffer material with V_{s30} > 800 m/s			
	Special case-1	Deposits consisting or containing a layer at least 10 m thick of soft clays/silts with a high plasticity index (PI > 40) and high water content	V_s < 100 m/s (indicative)		S_u:10 - 20 kN/m^2
	Special case-2	Deposits of liquefiable soils, of sensitive clays, or any other soil profile not included in types A – E or S1			

EAK 2000	A	Rock or semi rock formations extending in wide area and large depth provided that they are not strongly weathered. Layers of dense granular material with little percentage of silt-clay mixtures having thickness less than 70 m. Layers of stiff over consolidated clay with thickness less than 70 m.
	B	Strongly weathered rocks or soils which can be considered as granular materials in terms of their mechanical properties. Layers of granular material of medium density with thickness larger than 5 m or of high density with thickness over 70 m. Layers of stiff over consolidated clay with thickness over 70 m.
	Γ	Layers of granular material of low relative density with thickness over 5 m or of medium density with thickness over 70 m. Silt-clay soils of low strength with thickness over 5 m.
	Δ	Soft clays of high plasticity index (PI > 60) with total thickness over 12 m
	X	Loose fine grained silt-sand soils under the water table which may liquefy (unless a specific study proves that such a hazard can be excluded or their mechanical characteristics will be improved). Soils which are close to apparent tectonic faults. Steep slopes covered with loose debris. Loose granular soils or soft silty clayey soils which have been proved hazardous in terms of dynamic compaction or loss of strength. Recent loose backfills, organic soils, soils of class Γ with excessively steep inclination.

Rodriguez-Marek (2000) and Pitilakis (2004)

Rodriquez-Marek, A., (2000) classified soil into categories from class A to class F based on V_{s30} and soil depth. The stiffness of soil and the shear wave velocity are considered to correlate with the geological units. Pitilakis, K. et al., (2004) similar to Rodriguez-Marek, A., (2000) classified soils based on their stiffness from class A to

class F with a qualitative description of the site. This classification follows EC8 (2003) except with some subclasses involved. Time period of the ground has been considered for the classification too. Classification by both the researchers is shown in Table 2.8.

Table 2.8 Site classification by Pitilakis, K. et al., (2004) and Rodriguez-Marek, A., (2000)

Pitilakis (2004)	A1	Intact rock formations	
	A2	Slightly weathered / segmented rock formations provided that the weak, highly weathered surficial layer has a thickness of less than 5.0 m	Weak layer: $V_s \geq 300$ m/s Rock form: $V_s \geq 800$ m/s
		Geologic formations which resemble rock formations in their mechanical properties and their composition (e.g. conglomerates)	$V_s \geq 800$ m/sec
	B1	Highly weathered rock formations whose weathered layer has a considerable thickness of 5.0-30.0m	Weathered layer: $V_{s(1)} \geq 300$ m/s
		Soft rock formations of great thickness or formations which resemble these in their mechanical properties (e.g. stiff marls)	$V_s = 400 - 800$ m/s $N_{(2)} > 50$ $S_{u(3)} > 200$KPa
		Homogeneous soil formations of very dense sand-sand gravel and/or very stiff clay and small thickness (less than 30.0m)	$V_s = 400 - 800$ m/s $N > 50$ $S_u > 200$Kpa
	B2	Soil formations of very dense sand-sand gravel and/or very stiff clay, of homogeneous nature and medium thickness (30.0-60.0m), whose mechanical properties increases with depth	$V_s = 400 - 800$ m/s $N > 50$ $S_u > 200$Kpa
	C1	Soil formations of dense to very dense sand–sand gravel and/or stiff to very stiff clay of great thickness (>60.0m), whose mechanical properties and strength are constant and/or increasing with depth	$V_s = 400 - 800$ m/s $N > 50$ $S_u > 200$KPa
	C2	Soil formations of medium dense sand – sand gravel and/or medium stiffness clay (PI > 15, fines percentage > 30%) of medium thickness (20.0m – 60.0m)	$V_s = 200 - 400$ m/s $N > 20$ $S_u > 70$KPa

	C3	Category C2 soil formations of great thickness (>60.0 m), homogenous or stratified that are not interrupted by any other soil formation with a thickness of more than 5.0m and of lower strength and V_s velocity	V_s = 200 - 400 m/s N > 20 S_u >70KPa
	D1	Recent soil deposits of substantial thickness (up to 60m), with the prevailing formations being soft clays of a high plasticity index (PI>40), with a high water content and low values of strength parameters	$V_s \leq$200 m/s N < 20 S_u <70KPa
	D2	Recent soil deposits of substantial thickness (up to 60m), with prevailing fairly loose sandy to sandy silt formations with a substantial fines percentage (so as not to be considered susceptible to liquefaction)	$V_s \leq$200 m/s N < 20
	D3	Soil formations of category C with V_s>300m/s and great overall thickness (>60.0m), interrupted at the first 40 meters by soil layers of category D1 or D2 of a small thickness (5 – 15m)	
	E	Surface soil formations of small thickness (5-20m),small strength and stiffness likely to be classified as category C and D according to geotechnical properties ,which overlie category A formations($V_s \geq$ 800m/s)	Surface soil layers: V_s = 150 - 300 m/s
	X	Loose fine sandy-silty soils beneath the water table, susceptible to liquefaction (unless a special study proves no such dangers, or if the soil's mechanical properties are improved); Soils near obvious tectonic faults steep slopes covered with loose lateral deposits, loose granular or soft silty clayey soils; provided they have been proven to be hazardous in terms of dynamic compaction or loss of strength. Recent loose landfills; Soils with a very high percentage in organic material	

Rodriguez-Marek,A., (2000)	A	Hard rock	Crystalline bedrock; $V_{s30} \geq$ 1500 m/s
	B	Competent bed rock	V_{s30} > 600 m/s or < 6 m of soil. Most un -weathered California rock cases
	C1	Weathered rock	V_{s30}~ 300 m/s increasing to > 600 m/s, weathering zone > 6 m and < 30 m
	C2	Shallow stiff soil	Soil depth > 6 m and < 30 m
	C3	Intermediate depth stiff soil	Soil depth > 30 m and < 60 m
	D1	Deep stiff Holocene soil	Soil depth > 60 m and < 200 m
	D2	Deep stiff Pleistocene soil	Soil depth > 60 m and < 200 m
	D3	Very deep stiff soil	Soil depth > 200 m
	E1	Medium thickness soft clay	Thickness of soft clay layer 3 – 12 m
	E2	Deep soft clay	Thickness of soft clay layer > 12 m
	F	Potentially liquefiable sand	Holocene loose sand with high water table, $Z_w \leq$ 6m

2.8 Standard Penetration Test (SPT)

The standard penetration test, developed in 1927, is currently the most popular and economical means to obtain subsurface information. It has been estimated that 85 to 90 percent of conventional foundation design in North and South America is made using the SPT. This test is also widely used in other geographic regions. The method has been standardized as ASTM D 1586 since 1958 with periodic revisions to date.
The test consists of:

1. Driving the standard split-barrel sampler of dimensions. a distance of 460 mm (18 in) into the soil at the bottom of the boring.
2. Counting the number of blows to drive the sampler the last 305 mm (12 in) to obtain the N number.
3. Using a 63.5 kg (140 lb) driving mass (or hammer) falling "free" from a height of 760 mm (30 in). Several hammer configurations have been shown in Fig. 2.7.

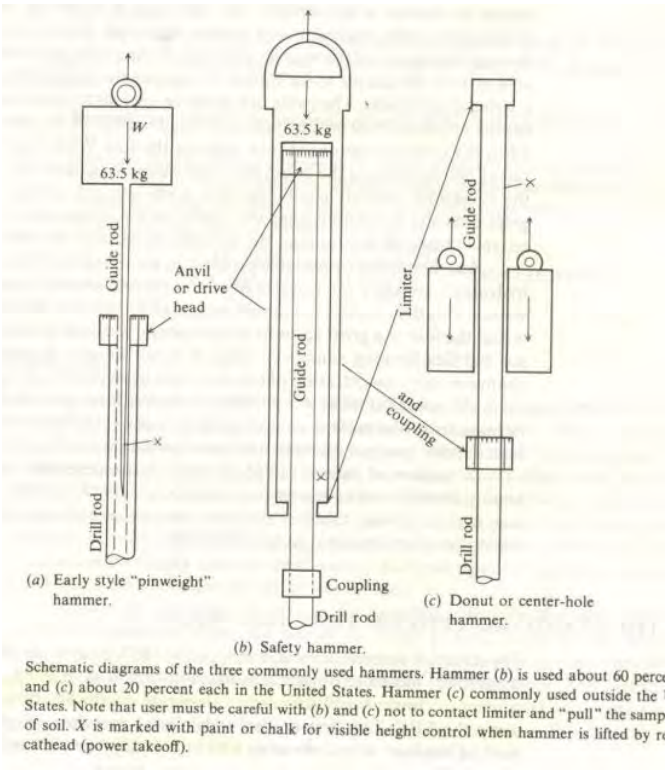

Schematic diagrams of the three commonly used hammers. Hammer (*b*) is used about 60 perc and (*c*) about 20 percent each in the United States. Hammer (*c*) commonly used outside the States. Note that user must be careful with (*b*) and (*c*) not to contact limiter and "pull" the samp of soil. *X* is marked with paint or chalk for visible height control when hammer is lifted by r cathead (power takeoff).

Figure 2.7: Several hammer configurations.

Table 2.9: Penetration Resistance and Soil Properties on Basis of the Standard Penetration Test.

Sands		Clays	
Number of blows per ft, N	**Relative Density**	**Number of blows per ft, N**	**Consistency**
		Below 2	Very soft
0-4	Very loose	2-4	Soft
4-10	Loose	4-8	Medium
10-30	Medium	8-15	Stiff
30-50	Dense	15-30	Very stiff
Over 50	Very dense	Over 30	Hard

2.9 Methods of Site Response Analysis

Site response is primarily influenced by properties that influence wave propagation, particularly stiffness and damping. Ground failure is influenced by the shear strength of soil. Site response has been studied in large number of earthquakes since 1960. Soil is the most nonlinear material dealt by engineers and its behaviour during strong shaking is very complex. Seismologists have traditionally treated soil as a linear material and rarely considered soil nonlinearity in the assessment of site conditions (Finn, W.D.L., 1991). Soil nonlinearity is prevalent even at low strain values (strains less than 10-2). The pioneering work of Seed, H.B. and Idriss, I.M., (1969) brought attention to the nonlinear behaviour of soils during seismic shaking. Observations during 1964 Alaska, Niigata earthquakes and the 1967 Caracas earthquake formed the basis for the work. Since then, site response has become an integral part of geotechnical earthquake engineering.

Not until the 1985 Michoacan earthquake, soft soils were thought to deamplify motions at peak ground accelerations larger than 0.1 to 0.2 g (Seed, H.B. et al., 1983), while

motions at stiff soils were thought to be largely unaffected by the ground motion intensity. The Mexico City earthquake (1985) also brought attention to the need for a better understanding of the dynamic properties of soft clays (Finn, W.D.L., 1991). The development of design codes has followed the advancements in understanding of site response. The use of spectral shapes without amplification factors for peak acceleration reflected the observations by Seed, H.B. et al., (1976) that accelerations in soils and rocks were approximately equal. Factors that underlain the ground response are peak ground acceleration, predominant frequency and amplitude. Techniques used widely to quantify site response include the following:

i. Experimental Methods
    a. Standard Spectral Ratio (SSR)
    b. Microtremor Measurements
        - H/V noise ratio (Nogoshi-Nakamura technique)
        - H/V spectral ratio of weak motion

ii. Numerical Methods
    a. One dimensional site response analysis
        - Transfer functions
        - Equivalent linear approximation of nonlinear response
        - Deconvolution
    b. Advanced Methods

iii. Empirical and Semi-Empirical Methods
    a. Empirical attenuation laws

2.9.1. Experimental Methods

2.9.1.1. Standard Spectral Ratio (SSR) Method

In this method the recordings at nearby site are compared which are subjected to source and path effects. Introduced by Borcherdt, R.D., (1970), this method provides a reliable estimate of site response possible only if the reference site is free from site effects. The recording site has to be unaffected by any site effects and the reference site must be justifiable for the assumption of behavioral difference unaffected by source radiation or

travel path. For this reason, reference site has to be located near to the location of testing to ensure that the difference in the records is due to only site effects but not due to source or path effects (caused when hypocentral distance is more than 10 times of array aperture). SSR technique gives an upper bound of actual site effects at high frequencies and under estimation at frequencies below fundamental frequency for site effects.

2.9.1.2. Microtremor Measurements

Microtremors are caused by artificial disturbances in the ground such as traffic, industrial machines and so on. Their amplitude of motions is 0.1-1microns. Kanai, K. and Tanaka, T., (1960) from systematic measurements of microtremors carried out at several thousands of places in Japan have inferred that the properties of ground can be identified from the characteristics of microtremors and can be utilized for determining the seismic factor for estimating seismic hazard.

The spectral analysis of microtremors is an alternate way to characterize site response. The relationship between local site response and microtremor characteristics, such as predominant period or resonant frequency, site amplification and liquefaction vulnerability, was first studied many years ago (Gutenberg,B., 1957; Kanai,K., and Tanaka,T., 1961). Kanai,K. et al., (1954) proposed a method to classify the ground into four categories, which is used by the Japan Building Code (Table 2.10).

Table 2.10 Microzones of Japan Building code (Kanai,K. and Tanaka,T.,1961)

Zones	Soil description
I	Ground consisting of rock, hard and sandy soils or gravely deposits
II	Ground consisting of sandy gravel, hard sandy clay, loam or alluvial gravel with thickness of 5m or more
III	Standard ground other than zone I,II or IV
IV	Ground consisting of soft soil alluvial delta deposits, top soils or mud thickness of 3m or more where less than 30yrs has elapsed since the time of reclamation

This classification is based on the detailed comparison of microtremor results and ground conditions. Since then, many researchers have used microtremor motions to understand the influence of basin geology on ground motions (Katz, L.J., 1976; Kagami,H. et al., 1982; Field, E. H. et al., 1990). An approach by Nakamura,Y., (1989) uses HVSR from ambient noise at a single sediment site. This technique has been implemented by many researchers (Ohmachi, T., et al., 1991; Field, E. H. and Jacob, K., 1993, 1995; Lermo, J. and Chavez-Garcia, F.J. , 1993, 1994; Yamanaka, H., et al., 1993; Suzuki, T. et al., 1995; Bonilla, L. F., et al., 1997; Hartzell, S., et al., 1998; Bodin, P. and Horton, S., 1999; Huang, H. C. and Teng, T. L., 1999, 2002; Horike, M., et al., 2001; Huang, H. C., 2002; Hardesty, K., et al., 2010).

H/V Noise Ratio method

It has been shown by many researchers (Ohmachi, T., et. al., 1991; Lermo, J. et al., 1992; Field, E.H. and Jacob, K., 1993, 1995) on how H/V ratio of noise can be used to identify the fundamental resonant frequency and amplification factor of sediments. This method doesn't depend on reference site. It is also called as Nogoshi-Nakamura technique which was introduced in early seventies. 'H' represents the horizontal component of the Fourier Spectra of micro tremors and 'V' is the corresponding vertical component. H/V is more stable than the raw noise spectra. It exhibits a clear peak in soft soils which could be correlated with the fundamental resonant frequency. Field observations combined with several theoretical investigations corroborate the randomly distributed near surface source lead to H/V ratios. Though the frequency of the peak correlated to the peak frequency of the ground, amplitude of this peak is not well correlated with the S wave amplification at the site's resonant frequency. Amplitude is highly sensitive to poisons ratio near the surface. This technique is rather inexpensive and noninvasive in character. Figure 2.8 represents the H/V method and SSR method of recording. Even though this technique is one of the popular methods for site response evaluation there has been debate amount the science peers regarding the reliability of results. Mucciarelli, M., (1998) has demonstrated that many of the difficulties attributed to the Nakamura technique (1989) maybe due to the differences in measurement setup, data collection and varying environment and urban conditions.

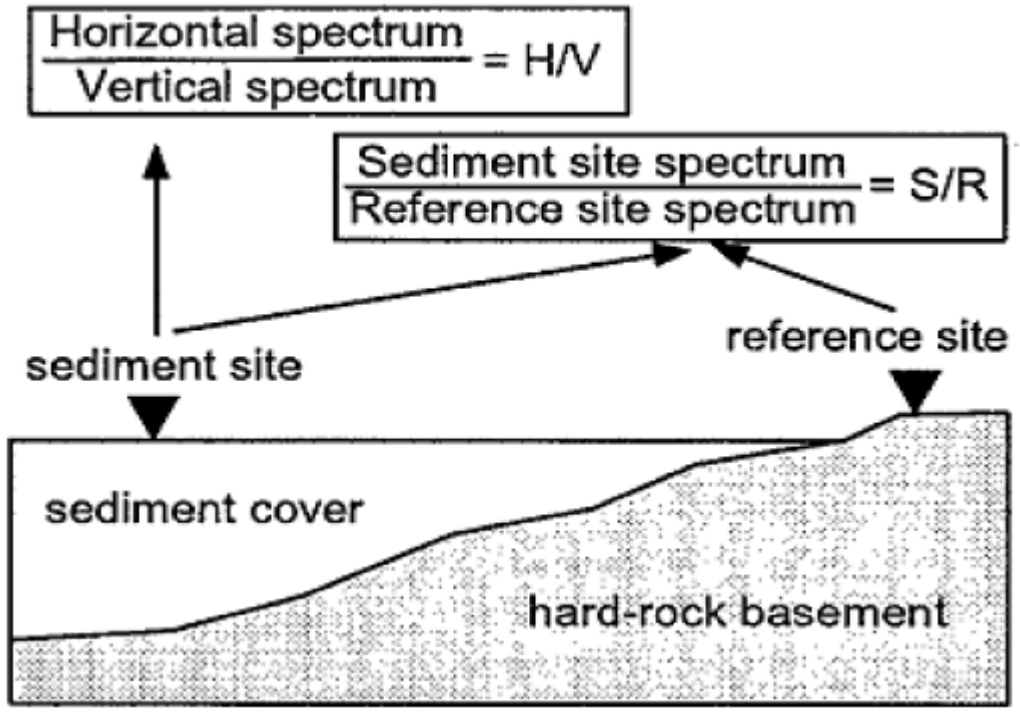

Figure 2.8 Different methods for estimating site frequency using ambient noise vibrations (Ibsvon Seht, M. and Wohlenberg, J., 1999)

H/V spectral ratio of weak motion

The H/V spectral ratio (HVSR) method is an experimental technique to evaluate some characteristics of soft sedimentary (soil) deposits. HVSR technique is a combination of Langston's receiver function method and Nakamura's proposal to use HVSR ratio with recordings of ambient vibrations. Receiver function method was used for determining the velocity structure of the crust from the horizontal to vertical spectral ratio (HVSR) of the teleseismic P-waves. H/V method is based on the records of the ambient noise (microtremors) in environment. Microtremor consists of both body and surface waves. Suzuki, T. (1933) pointed out that H/V spectrum ratio of Rayleigh waves reflects the surface structure. Nogoshi, M., and Igarashi, T. (1971) in their paper distinguished the components of the microtremor whether body waves or surface waves. Nakamura,Y., (1989) estimated that some site characteristics are related with the site transfer function, using microtremor measurements. It consists in deriving the ratio between the Fourier spectra of the horizontal and the vertical components of the microtremor recording obtained at the surface; this ratio is called thereafter the H/V ratio. It was first applied

to the S wave portion of the earthquake recordings obtained at three different sites in Mexico by Lermo, J. and Chavez Garcia, F.J. (1994a). The technique has also been checked on various sets of weak and strong motion data (Chavez Garcia, F.J. et al., 1996; Lachet, C. et al., 1996; Theodulidis et al., 1996; Bonilla, L. F., et al., 1997; Yamazaki, T. Y. and Ansary, M. A., 1997; Riepl J., et al., 1998; Zaré, M. et al., 1999). The HVSR shape exhibits a very good experimental stability. It can be well correlated with surface geology and it is less sensitive to source and path effects. When classical spectral ratios are compared with surface or downhole recordings and with theoretical 1D computations (Lachet, C. and Bard, P. Y., 1994) it was identified that absolute level of HVSR depends on the type of incident waves.

The horizontal to vertical spectral ratio is also termed as Quasi transfer spectra (QTS). The purpose of Nakamura,Y., (1989) was to estimate the amplification factor caused by multiple reflected vertical incident SH waves and peak frequency. Microtremor can be divided into two parts, Rayleigh wave and the other wave. A typical geological structure has been shown in Fig.2.9.

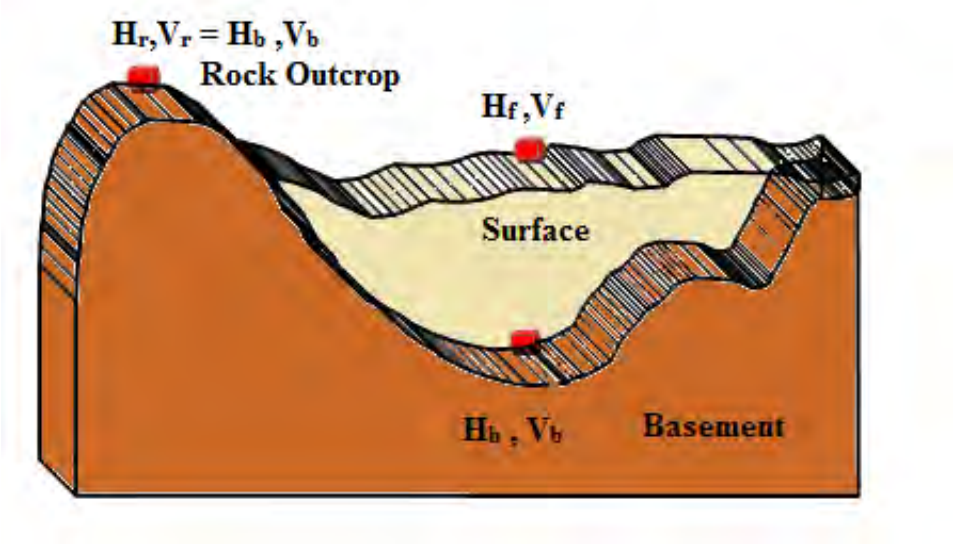

Figure 2.9 Typical geological structure of sedimentary basin (modified from Nakamura,Y., 2000)

Due to its low cost both for the survey and analysis, H/V technique is useful in calibrating site response studies at specific locations. It is very effective in estimating the natural frequency of soft soil sites when there is a large impedance contrast with the underlying bedrock. The method is especially recommended in areas of low and moderate seismicity, due to the lack of significant earthquake recordings, as compared to high seismicity areas (SESAME, 2004). Many scientists only trust the peak frequency of this ratio, interpreted as linked to the Rayleigh wave's ellipticity and representative of the fundamental S wave resonance frequency for sites with large impedance contrast, some other claim the H/V ratio provides a satisfactory estimate of the site S wave transfer function. However, it should be pointed out that the H/V technique alone is not sufficient to characterise the complexity of site effects and in particular the absolute values of seismic amplification (SESAME, 2004).

Some practical guidelines for field experiment design have been provided in SESAME (2004) manual. It details on data processing and interpretation of the results for the implementation of the H/V spectral ratio technique using ambient vibrations. Manual recommends that in-situ soil/sensor coupling should be handled with care; Concrete and asphalt provide good results, whereas measuring on soft / irregular soils such as mud, grass, ploughed soil, ice, gravel, uncompacted snow, etc., should be looked at with more attention.

Koller, M. et al., (2004) evaluated the influence of experimental parameters on stability and reproducibility of H/V estimations from ambient vibrations. The influence of various types of parameters has been tested on the results of H/V curves both in frequency and amplitude. For each tested parameter, H/V data was compared with a 'reference situation'. The results of the study are based on 593 recordings that were used to test 60 parameters. The parameters are categorised into 8 main heads.

The results of the study are summarized as follows. The standard recording / instrument / sensor setting parameters have no strong influence on the H/V curves. In situ soil / sensor coupling should be handled with care. Concrete and asphalt provide good results, whereas measuring on soft / irregular soils such as mud, grass, ploughed soil, ice, gravel, not compacted snow, etc. should be avoided. Artificial soil/ sensor coupling

should be avoided unless it is absolutely necessary, for example, to compensate a strong inclination of the soil. In such a case, either a pile of sand, or a trihedron should be used. Recording above underground structures must be avoided.

Nearby surface structures should be considered with care, particularly under windy conditions. Measurements under wind or strong rain should be avoided. Some noise sources should be considered with care (or avoided using an anti-trigger window selection to remove the transients, see next chapter), these are: close steps, close high speed car or truck traffic, close machinery, etc. Results are stable with time (if other parameters, such as weather conditions, etc. are kept constant)

2.9.2. Numerical Methods

Site effects can be estimated using numerical analysis if the site characteristics are well known.
These methods are favored when high quality geotechnical data is available. Numerically based zoning can be done when sufficient density of boreholes and geotechnical information is available. But, such approach requires an in depth understanding of both analytical models and of the numerical schemes that are used. Lack of such expertise in numerical analyses may lead to less reliable results.

2.9.2.1 One Dimensional Analysis

The most general method of site response analysis is one dimensional analysis. Two dimensional and three dimensional analyses can be employed using finite element method, finite difference method and thin layer methods that even assess the effect of topography and basin structure on wave propagation (Bielak, J. et al., 1999; Law, H. K. and Lam, I. P., 1999). This method is widely used for response analysis as it provides conservative results, evaluated from case histories of different earthquakes. In this analysis 1D propagation of the seismic waves are considered. One of the basic

assumption in one dimensional analysis is that all boundaries are horizontal and response of soil is reliant on vertical propagation of SH wave from the bedrock below. The soil and bedrock are assumed to be infinite in horizontal direction. The assumptions are justified as velocity of wave generally decreases from the earth's interior towards the surface, and hence stress waves from the focus are bent by successive refractions into a nearly vertical path. By Snell's law of refraction, the waves trapped in the soil by refraction at the interface of firm ground and soil will propagate nearly vertical even though the waves are propagating in a shallow inclined direction from the firm ground. Vertical ground motions are generally not as important from the standpoint of structural design as horizontal ground motions. Soil properties generally vary more rapidly in the vertical direction than in the horizontal direction.

In reality, a complete ground response analysis must take into account the various factors mentioned before including the additional factors such as rupture mechanism at the origin of earthquake, propagation of seismic waves through the crust to the top of bedrock. These factors are difficult to quantify and hence a complete ground response analysis becomes highly complicated. Therefore, one-dimensional ground response analyses are used extensively due to its simplicity.

Methods of analyses

The genesis of the methods of analysis is from numerous field observations and laboratory testing. Difference in each of the methods is in the assumptions, representation of stress–strain relations and the method of integration of equation of motion (Govindarajulu, L., et al., 2004).
The methods of analysis can be broadly categorized as follows:

1. Linear analysis
2. Equivalent linear analysis
3. Nonlinear analysis

- ***Linear analysis***

In one dimensional analysis, linear approach is the simplest approach to evaluate ground response. Its basis is the principle of superposition. Nonlinear behaviour of soil is approximated by iterative procedure with equivalent linear soil properties. Linear approach has been implemented in the following procedures, which are commonly used for ground response analysis (Kramer, S.L., 1996).

- Transfer functions
- Equivalent linear approximation of non linear response
- Deconvolution

Many packages are available for one dimensional analysis such as SHAKE, DEEPSOIL, EDUSHAKE, PROSHAKE, Cyber Quake, EERA etc. The main advantage in these methods is flexibility and versatility, which have lead to significant breakthroughs in the understanding of site effects during the last two decades. Using these methods phenomenological and parametric studies can be done and can also be used to assess the uncertainty in a seismic site response.

Linear and equivalent linear analysis is performed in frequency domain whereas nonlinear analysis is performed in time domain. In frequency domain, soil modeled as linear viscoelastic.

The strain variation throughout the loading time is approximated by a reference strain that is constant throughout the analysis. In linear analysis, soil deposit is assumed to consist of one uniform layer with soil stiffness either constant or varying with depth. However, as the behavior of soil is not elastic and material properties change spatially, numerical techniques such as finite element or finite difference method can be used. In one dimensional time domain analysis soil is idealized as discrete lumped mass system. The dynamic equation is solved using methods like central difference, Newmark 'β' and Wilson 'θ' methods.

- ***Nonlinear Approach***

The linear approach is very simple and is easy to compute but non linear response of soil cannot be evaluated precisely. This limitation can be overcome by using the nonlinear response of soil using direct numerical integration in small time intervals in time domain. Nonlinear analysis is usually performed by using a discrete model such as finite element and lumped mass models, and performing time domain step-by-step integration of equations of motion. For nonlinear analysis to give meaningful results, the stress-strain characteristics of the particular soil must be realistically modeled. The integration of motion in small time intervals will permit the use of any linear or non linear stress-strain models. The data from borings or measurements of shear wave velocity are used to construct the soil model. When such data are not available, generic ground conditions can be used (Shima, E. and Imai, T., 1982). Since all soils have highly nonlinear properties, nonlinearity in site characterization and analysis has to be taken under serious consideration.

Moreover nonlinear behaviour can also be observed in the earthquake ground motion records (Tokimatsu, K. and Midorikawa, S., 1982; Chang, C.Y. et al., 1991). There are many types of software, which can incorporate the nonlinear response of soils such as PLAXIS, SASSI2000, FLAC, QUAKE/W, DEEPSOIL etc.

2.9.2.2. Two Dimensional Analysis

The one dimensional site response analysis will be useful for level or gently sloping ground with parallel soil layers. Since these conditions are not so common, one dimensional analysis may not give very accurate results in most of the cases. In the case of sites where embedded structures like pipe lines or tunnels are present, one dimensional analysis will not yield desired results. Two dimensional analysis can be done either based on frequency domain or time domain methods.

This analysis can be done using dynamic finite element methods adopting either equivalent linear approach or nonlinear approach (Kramer, S.L., 1996). Numerical modeling software like PLAXIS, FLAC, QUAKE/W etc can be used for modeling two

dimensional cases. Due to the high computational cost involved in the dynamic finite nonlinear element methods, various researchers proposed number of alternatives to this approach such as shear beam approach and layered inelastic shear beam approach. Shear beam approach is widely used for the analysis of earthen dams.

2.9.2.3. Three Dimensional Analysis

There may be cases in which there is variation in soil profile in three dimensions and the two dimensional approach may not be adequate. This is ideal for studying the response of three dimensional structures. The method and the approaches adopted is similar to the two dimensional approach. Equivalent linear finite element approach, nonlinear finite element approach etc are the adopted approaches.

2.9.3. Empirical and Semi-empirical methods

Available strong motion recordings have provided fundamental basis for many empirical attenuation laws. The empirical attenuation relationships are developed from one particular set of data where both earthquake observations and information on surface geology are available, which can be applied at other sites where only geological information is known. All these laws relate a given ground motion parameter (PGA, PGV, Sa, duration, Arias intensity etc) to the magnitude and distance of the seismic event, and they also very often take into account a site parameter. The site parameter is usually a binary descriptor, such as "rock" and "non-rock". Only rarely is the site geology characterized in a more refined manner, for instance with distinction between thin and thick deposits, or with S wave velocity values.

2.10 Ground Response Analysis

Propagation of seismic waves through soil column during earthquake alters the amplitude, frequency and duration of ground motion by the time it reaches the surface. The effects of ground motion are propagated in the form of waves from one medium to another. So, physically it is problem of prediction of ground motion characteristics whereas mathematically it is a problem of the wave propagation in continuous medium. The evaluation of such response of the site to dynamic loading is termed as ground response analysis. Site effects can be quantified by empirical correlations between rock outcrop motion and motion at soil sites. Different correlations are used for stiff soils and deep cohesionless soils. Depending on the geometry and loading conditions different analysis i.e, one, two and three dimensional are suggested.

Idriss, I.M., (1990) developed a correlation between peak acceleration at rock outcrop and soft soil which is independent of earthquake magnitude. It is an empirical relationship developed from the recordings during Loma Prieta earthquake, 1989 in San Francisco bay and Mexico City in 1985. Figure 2.10 shows the Relationship between peak acceleration of rock sites and soil sites. It can be inferred that sites subjected to low values of PGA had more amplification than those compared to higher values. Also for very strong ground motion the amplitude of vibration at soft soil sites is lower compared to rock sites. Various empirical relationships have also been discussed in detail for the estimation of site effects.

Ground response analysis also termed as soil amplification study comprises the calculation of site natural periods, ground motion amplification, evaluation of liquefaction potential, stability analysis etc. The important features that are considered for analysis are characteristics of soil overlying bedrock, bedrock location and inclination, topography of bedrock and soil deposits, faults in the soil deposits. A complete ground response analysis considers source, path and site amplification effects. Damping factors of the soil are difficult to be assessed. Important steps in site specific ground response analysis are dynamic characterization of the site and selection of rock motions.

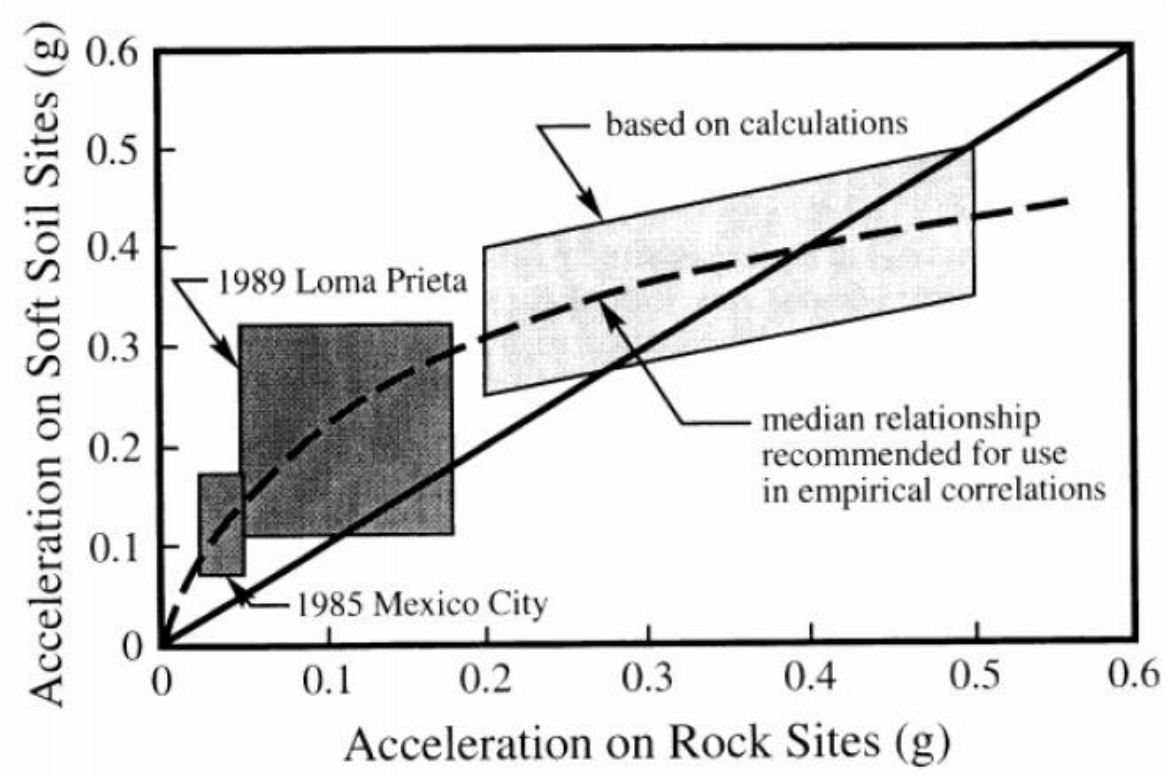

Figure 2.10 Relationship between peak acceleration of rock sites and soil sites (Idriss, I.M., 1990)

Empirical relationships are useful when large area is considered for response analysis and time is constrained. But due to scanty data and the range of applicable site conditions, empirical relationships cannot be applied to all situations. Numerical simulations are practical in such situations as they cover a range of ground motions and site effects for the locations where previous information is not available.

2.10.1. Cyclic soil behavior

Soils behave linearly in low strains and nonlinearity prevails at high strains. When the strain induced in the soil increased a limiting value of about 10-5, soil is said to behave nonlinearly.

This behavior plays a major role in ground motion propagation. For site response analysis, shear modulus and cyclic soil behavior are required. Estimation of shear

modulus can be done by different geophysical methods and cyclic behavior can be studied by high and low strain laboratory tests. The response of a soil under cyclic loading is as shown in Figure 2.11 (a).

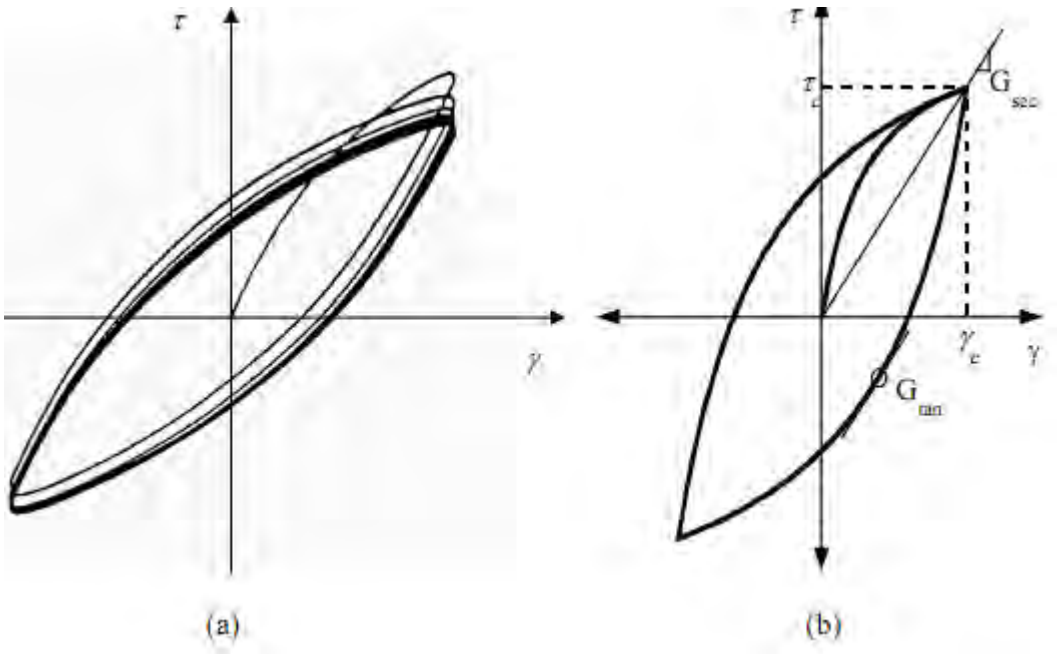

Figure 2.11 (a, b) Stress-strain behavior of typical clay (EPRI, 1993) and idealized hysteresis loop

An idealized hysteresis loop of soil can be represented by two parameters shear modulus and damping. Shear modulus describes the stiffness of soil. Shear modulus can be either tangent modulus or secant modulus. Tangent shear modulus, G_{tan} is given by the inclination of loop at every point of time whereas secant shear modulus, G_{sec} which is average modulus for a given load cycle and is given as shown in Fig. 2.11 (b). Maximum shear modulus G_{max} corresponds to the initial shear modulus. The actual hysteresis loop is defined in terms of shear modulus degradation and damping ratio curves as shown in Fig. 2.11 (b). Inclination of the hysteresis loop is dependent on the stiffness of soil and energy dissipation is given by the breadth/area of the loop. Clearly, inclination of the loop is represented by shear modulus and breadth by damping ratio. The energy dissipated is given by the Equation 2.12 and is called as damping ratio.

$$\xi = \frac{E_D}{4\pi E_S} \; ; \; E_s = \frac{1}{2} G_{sec} \gamma_c^2 \qquad 2.12$$

E_D is the energy dissipated in one cycle of loading, ES is the strain energy stored in the system, γc is the cyclic shear strain.

As the soil becomes more non linear damping ratio increases whereas secant modulus decreases with increase in cyclic shear strain. Several researchers have developed curves for modulus degradation and damping curves for different soils. Figure 2.12 (a and b) gives the relations between G/G_{max} versus shear strain and damping ratio versus shear strain curves for different soil plasticity for normally and over consolidated clays (Vucetic, M. and Dobry, R., 1991). Several researchers (Idriss, I.M., 1990; Seed, H.B., and Sun, J. I., 1989; Seed, H.B. et al., 1986; Seed, H.B., and Idriss, I.M., 1970) developed the curves for different types of soils (Figure 2.13 and 2.14).

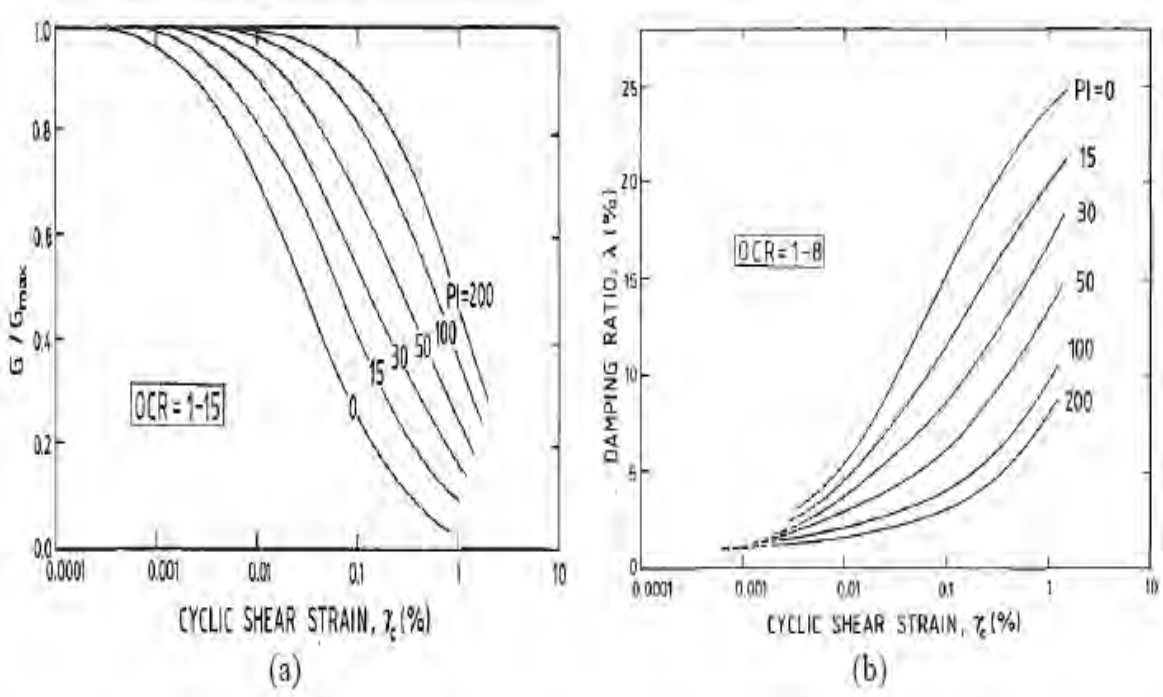

Figure 2.12 (a,b) Relations between G/G_{max} versus shear strain, and Damping ratio versus shear strain curves for different soil plasticity for normally and over consolidated clays (Vucetic, M. and Dobry, R., 1991)

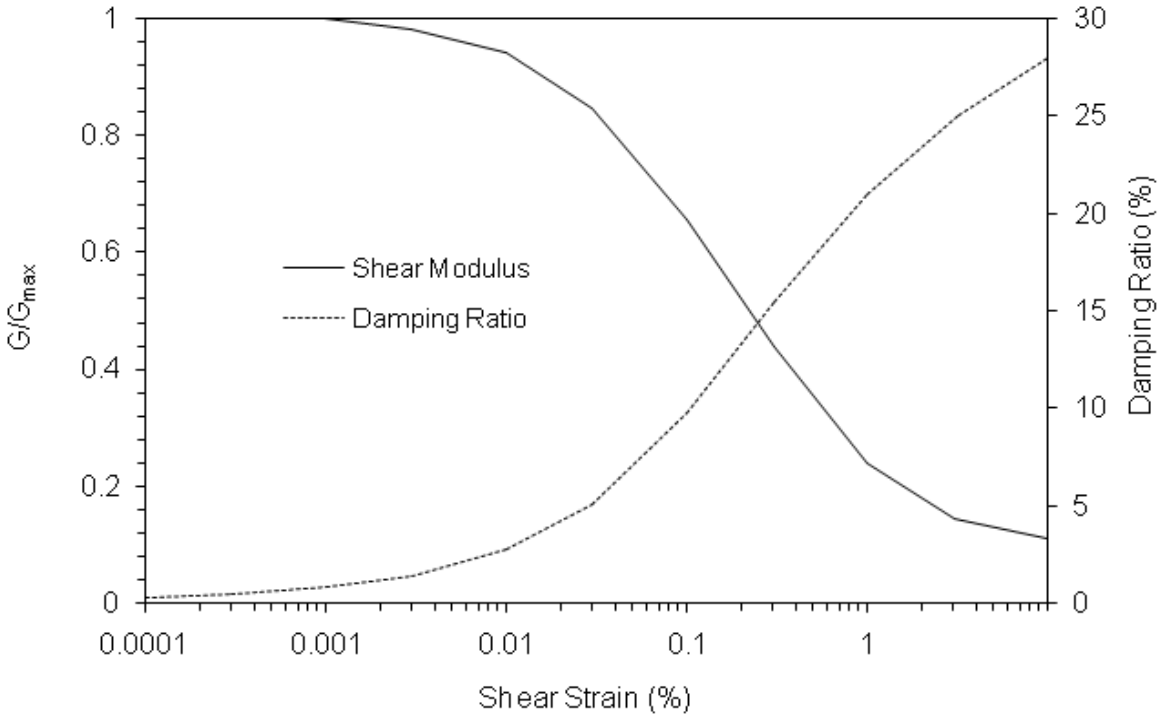

Figure 2.13 Modulus for clay (Seed, H.B., and Sun, J. I., 1989) upper range and damping for clay (Idriss, I.M., 1990)

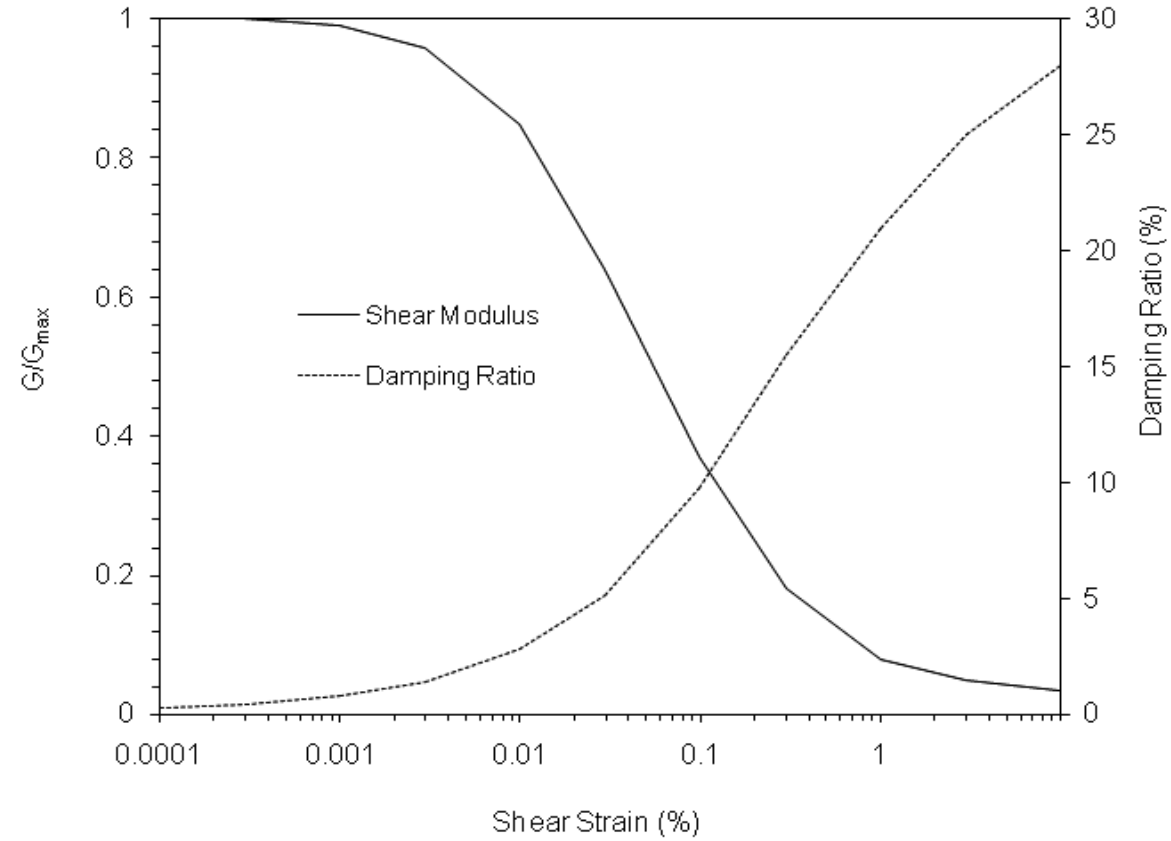

Figure 2.14 Modulus for sand (Seed, H.B., & Idriss, I.M., 1970) upper range and damping for sand (Idriss, I.M., 1990)

Different factors influence the cyclic behavior of soil. The factors can be classified as environmental and loading factors. Some of the primary factors are strain amplitude, void ratio, degree of saturation for cohesive soils, effective mea principal stress, and number of cycles of loading. The secondary factors include octahedral shear stress, thixotropy (time effects), effective strength parameters ('c' and 'φ'), over consolidation ratio (OCR). In case of deep soil deposits, confining pressure plays a major role in influencing the cyclic behavior. The effects of different factors are given by Hardin, B.O. and Drnevich, V.P. (1972), Vucetic, M. and Dobry, R., (1987) and are summarized in Table 2.11 below.

Table 2.11 Conditions influencing cyclic soil behavior of normally consolidated and moderately consolidated soils (Vucetic, M. and Dobry, R., 1987)

Factors	G/G_{max}	Damping Ratio
Effective confining pressure, σ_v	Increases with σ_v; effect decreases with increasing PI	Decreases with σ_v; effect decreases with increasing PI
Void ratio, e	Decreases with e	Increases with e
Geologic age, t_g	May increase with t_g	May decrease with t_g
Cementation, c	May increase with c	May decrease with c
Overconsolidation ratio, OCR	Not affected	Not affected
Plasticity Index, PI	Increase with PI	Decrease with PI
Cyclic strain, γ_c	Decrease with γ_c	Increases with γ_c
Strain rate, $\dot{\gamma}$	G increases with $\dot{\gamma}$,but G/G_{max} are measured at same $\dot{\gamma}$	Stays constant or may increase with $\dot{\gamma}$
Number of loading cycles, N	Decreases after N cycles of large γ_c (G_{max} measured before N cycles) for clays; for sands, can increase (under drained conditions) or decrease under undrained conditions	Not significant for moderate γ_c and N

2.10.2. Material constitutive models

For the analysis of the cyclic soil behavior the material has to be simulated realistically. A constitutive model relating the stress to strain has to be carefully selected or designed. It is difficult to develop a constitutive model as it requires simulation of complex phenomena such as nonlinearity, hardening and softening, anisotropy, residual or initial stress, volume change during shear, stress history and stress paths, three dimensional state of stress and strain, fluid in pores (Park and Hashash,Y.M.A., 2004). Performing quality laboratory tests on undisturbed soil samples is difficult and also soil properties vary spatially in a large site. Such difficulties lead to simplification of soil behavior and usage of simplified models for the representation of soil model. Different simple models used are listed below:

- Linear visco-elastic model
- Kelvin-Voigt model
- Hysteretic model
- Udaka model (1975)
- Nonlinear simple shear model
- Nonlinear simple shear hyperbolic model
- Nonlinear simple shear modified hyperbolic model
- Romberg-Osgood model
- Plasticity based model

The simplest constitutive law is associated with linear visco-elastic model. Energy dissipating characteristics of the soil are to be inputted whereas the stress-strain characteristics are considered linear which mean Hooke's law holds good. It is valid for weak ground motion, propagation of motions through stiff or rocky material where strain is very minimal.

Kelvin-Voigt model

In this model a spring and a dashpot are connected in parallel (Figure 2.15). When the force is applied, both the spring and the dashpot move simultaneously. The deformation (i.e. the displacement) is the same for both. However, the dashpot and spring stresses are in parallel and thus the total stress is the sum of the stress in the spring and the stress in the dashpot. Kelvin-voigt model has the constitutive equation given in Eq. 2.13

$$\tau = G\gamma + \eta\dot{\gamma} \qquad 2.13$$

Where, η is the viscosity of the dashpot.

For a harmonic shear strain of $\gamma = \gamma_0 \sin\omega t$ the energy dissipated in a single cycle is given by Eq.2.14.

$$E_D = \int_{t_0}^{t_0+2\pi/w} \tau \, d\gamma = \int_{t_0}^{t_0+\frac{2\pi}{w}} \tau \, (\partial \gamma/\partial t) \, dt = \pi\omega\eta\gamma_o^2 \qquad 2.14$$

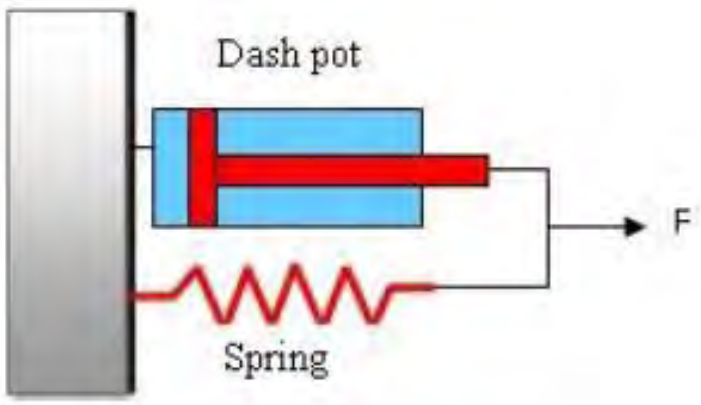

Figure 2.15 Kelvin-Voigt model

Viscous damping of Kelvin-Voigt model is frequency dependent and hence cannot actually simulate the damping of soils.

Hysteritic model

In this model to eliminate the frequency dependence of damping, rate independent dashpot is used. Viscosity η is represented in terms of damping ratio ξ defined in Eq.2.15. Rearranging the equation and using equation 2.17 or 2.18, damping becomes independent of frequency.

$$\xi = \frac{E_D}{4\pi E_S} = \frac{\eta\omega}{2G} \qquad 2.15$$

Rearranging, we get

$$\eta = \frac{2G}{\omega}\,\xi$$

$$\tau = G^*\gamma \qquad 2.16$$

G* is complex shear modulus defined as:

$$G^* = G(1 + i2\xi) \qquad 2.17$$

The imaginary term represents the phase lag and hence the damping property of soil. If damping is assumed to be small, an approximation of complex shear modulus is defined as shown below.

$$G^* = G(1 - \xi^2 + i2\xi) \qquad 2.18$$

The approximation of complex shear modulus is done as follows

$$v_s^* = \sqrt{\frac{G^*}{\rho}} = \sqrt{\frac{G(1 + i2\xi)}{\rho}} \approx \sqrt{\frac{G}{\rho}}(1 + i\xi) = v_s(1 + i\xi) \qquad 2.19$$

2.10

Udaka model (1975)

Udaka model consists of a complex shear modulus derived from back calculation. This model gives identical response amplitude to that of Kelvin–Voigt model. This is an approximate solution used to provide a better simulation understanding of Kelvin–Voigt model and has the same limitations. The complex shear modulus is given by

$$G^* = G\left(1 - 2\xi^2 + i2\xi\sqrt{1-\xi^2}\right) \qquad 2.20$$

2.10.3. Equivalent linear analysis

Simulation of complex cyclic behavior of soil is required for performing ground response analysis. To capture the nonlinear cyclic response of soil within frequency domain solution equivalent linear analysis has been developed by Schnabel, P.B. et al., 1972. This method is widely used for engineering applications as the results well converged with the field recordings. Schnabel, P.B. et al., (1972) addressed nonlinear hysteretic stress–strain properties of sand by using an equivalent linear method of analysis. The method was originally based on the lumped mass model of sand deposits resting on rigid base to which the seismic motions were applied. Later, this method was generalized to wave propagation model with an energy transmitting boundary. The seismic excitation could be applied at any level in the new model. Up to a strain of 10^{-3} soil model can be simplified to a equivalent linear model. Equivalent linear method implies that strain always returns to a value of zero after cyclic loading and failure cannot occur. In a frequency domain analysis it is assumed that modulus and damping properties are constant. For a given ground motion time history, propagated ground motion is calculated using an initial estimate of modulus and damping. The strain histories for each layer for which maximum strain values is obtained are calculated. Effective shear strain equal to 65% of maximum strain is computed for a given soil layer and corresponding shear modulus and damping are obtained from the curves

shown in Fig.2.12, 2.13 and 2.14. The process is repeated to achieve a converging solution.

The limitation of this method is nothing but the assumption. Usage of constant shear modulus and damping throughout the analysis might eliminate important high frequency components and can overestimate stiffness at large strains. Sugito, M., et al., (1994) and Assimaki, D. et al. (2000) proposed the usage of frequency dependent modulus degradation and damping in equivalent linear analysis to overcome this limitation. To estimate frequency dependent modulus and damping, Assimaki, D. et al., (2000) proposes the use of strain Fourier spectrum. Even this does not simulate the actual behavior as the relationship between frequency, damping and shear modulus is not linear.

Toro, G. R. et al., (1997) observed the decline of uncertainity for motion of high intensity when analyzed by equivalent linear method. This decrease apparently offsets the increased uncertainty associated with high strain dynamic properties of soils. For the current study, equivalent linear approach is adopted to perform the site-specific ground response analysis at selected locations in the Dhaka city.

2.10.4. Analysis using DEEPSOIL

A computer program DEEPSOIL (Hashash, Y.M.A. et al., 2011), for equivalent linear approximation of layered soils is used to compute the seismic response of horizontally layered soil deposits of the study area. It is a one-dimensional site response analysis program that can perform linear, equivalent linear and non-linear approach of analysis. The linear analysis can be done either in frequency domain or time domain. Frequency domain methods are the most widely used to estimate site effects due to their simplicity, flexibility and low computational requirements. However, in cases of high seismic intensities at rock base and/or high strain levels in the soil layers, an equivalent soil stiffness and damping for each layer cannot represent the behavior of the soil column over the entire duration of a seismic event. In such cases also ground motion propagation through deep soil deposits can be simulated using this tool. The equivalent

linear approach implemented in DEEPSOIL is similar to that in SHAKE (Schnabel, P.B. et al., 1972). Any number of material properties and layers can be used and the user can choose frequency dependent or independent complex shear modulus formulations (Park, D. and Hashash, Y.M.A., 2004).

For performing 1D equivalent linear analysis following inputs about soil are required i.e, number of layers of the profile, thickness of layer, shear wave velocity/shear modulus, % of damping, unit weight and water table depth. The steps involved in the analysis are:

- Selection of analysis method
    - Frequency Domain
        - Linear
        - Equivalent Linear
    - Time Domain
        - Linear
        - Nonlinear
- The method to define the soil curve:
    - Discrete Points
    - Pressure-Dependent Hyperbolic Model
- Defining of soil properties and soil model properties
    - Layer thickness, damping, shear property, unit weight
    - Soil model – Sand/Clay
- Defining of rock properties
    - Elastic/rigid half space
    - Rock properties such as shear property, unit weight, damping
- Analysis control
    - Fourier transform type
    - Type of complex shear modulus
- Input ground motion
- Output

For the input ground motion, array recordings or rock outcrop records are used to simulate field response. In the absence of such records, synthetic motions can be used. For evaluation of 1D response, the generated input ground motions are propagated through the soil profiles. Damping and shear modulus properties can be selected from the database or user defined curves can be inputted. Different steps to be followed in the analysis are shown through flow chart in the Figure 2.16.

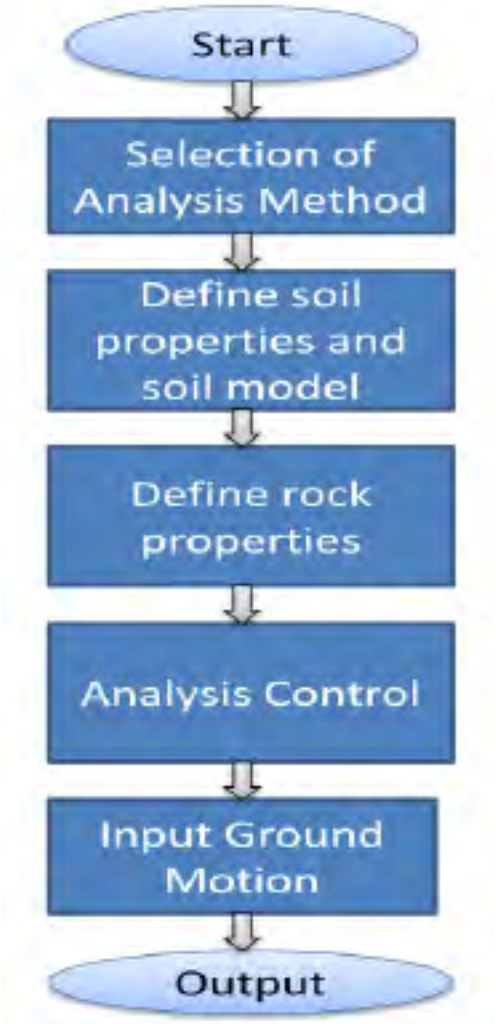

Figure 2.16 Flowchart for equivalent linear analysis

2.11 Seismic Waves

The acceleration of the ground surface is due to various seismic waves generated by the fault rupture during earthquake. There are two basic types of seismic waves: body waves and surface waves. P and S waves are both called body waves because they can travel through the interior of the earth. Surface waves are only observed close to the surface of the earth, and they are subdivided into Love waves and Rayleigh waves. Surface waves result from the interaction between body waves and the surficial earth materials. The four types of seismic waves are further discussed below.

1. P wave (body wave)

   The P wave is also known as the primary wave, compressional wave or longitudinal wave. It is a seismic wave that causes a series of compressions and dilations of the materials through it travels. The P wave is the fastest wave and is the first to arrive at a site. Being a compression-dilation type of wave, P waves can travel through both solids and liquids. Because soil and rock are relatively resistant to compression-dilation effects, the P wave usually has the least impact on ground surface movements.

2. S wave (body wave)

   The S wave is also known as the secondary wave, shear wave, or transverse wave. The S wave causes shearing deformations of the materials through which it travels. Because liquids have no shear resistance, S waves can only travel through solids. The shear resistance of soil and rock is usually less than the compression-dilation resistance, and thus an S wave travels more slowly through the ground than a P wave. Soil is weak in terms of its shear resistance, and S waves typically have the greatest impact on ground surface movements.

3. Love wave (surface wave)

   Love waves are analogous to S waves in that are transverse shear waves that travel close to the ground surface.

4. Rayleigh wave (surface wave)

   Rayleigh waves have been described as being similar to the surface ripples produced by a rock thrown into a pond. These seismic waves produce both vertical and horizontal displacement of the ground as the surface waves propagate outward.

It is important to recognize that the peak acceleration a_{max} will be most influenced by the S waves and in some cases, by surface waves. For example, Kramer (1996) states that at distances greater than about twice the thickness of the earth's crust, surface waves, rather than body waves, will produce peak ground motions.

2.12 Concluding Remarks

In this chapter past researches related to site amplification have been discussed. A detailed review on dynamic site characterisation, local site effects and factors affecting them has been discussed. The information about the local site effects is useful in the simulation of strong ground motions and hence, the results of the site response studies are one of the most important inputs for seismic hazard assessment of a region. From the review it is clear that results of site characterization and ground response analysis can be used for mitigation, land use planning and safe construction practices to avoid the losses from the future earthquakes. Several inputs regarding the site specific geological, geophysical, geotechnical, seismo-tectonic, ground motion parameters are required to study their effects on the structures and soil that pronounce earthquake effects like soil amplification, liquefaction of soils etc. Ground response analysis and methods of shear wave velocity determination based on CPT equipment had been also discussed.

CHAPTER THREE
COLLECTION OF DATA

3.1 General

The objective of this chapter is to describe the different parts of the CPT equipment. It also describes the procedure for determination of Shear Wave Velocity. The Shear Wave Velocity measured at selected locations of Dhaka City has been presented in this chapter. Standard Penetration Test (SPT) results at selected locations of Dhaka City have also been presented. Here the locations of the tests for the research have also been described.

3.2 Standard Penetration Test (SPT)

Standard Penetration Test (SPT) has been conducted at all ten selected areas of the Dhaka City. SPT is being used for the determination of soil characteristics. To utilize SPT results in determining soil characteristics, SPT have been conducted according to ASTM D1586 (ASTM, 2000).

3.3 General Specification of CPT Equipment

Intended for 1 meter 36mm dia CPT rods. Pushes down the CPT cone at a nominal rate of 2 cm per second. Pull up rate is 5 cm per second. Handled by 2 men, the complete equipment can be transported on a pick-up van. After that the soil anchors have been installed, the machine is positioned on the test site, the wheels are removed and the reaction beams are installed and secured. The anchors can give between 8 and 16 tons reaction force. The Machine can also be used as a separate standalone unit with the wheels arrangement removed. Figure 3.1 shows the CPT equipment used for this research.

Figure 3.1: CPT Equipment

3.3.1 Soil Anchors: Arranging the Soil Anchors

Start to install the 4 Soil Anchors in a square configuration with the size 1.3 x 1.6 m. Install the Manual Cross Head or the Motor Drive on top of the Soil Anchor using two 12 mm bolts. Use 2 or 3 CPT rods to turn the Soil Anchor into the ground. Screw down the auger until the top of the rod is 0.6 m above the ground. If the soil is hard, it can be enough with the soil anchor rod, but if the upper soil is soft, use the extension rods. Use wood pieces to support the pusher and erect it horizontally. The supports shall be high enough so that the wheels are free from the ground. Remove the Wheels, Remove the bolts that are locking the wheel and pull out the wheels. Anchoring beams, Insert the two short beams inside the machine like the picture shows.

3.3.2 Hydraulic Pump

Before connecting the hydraulic hoses, clean the quick coupling with a rag. Before starting the engine, the pump valve shall be in **OPEN** position. Check the oil level in the engine.

3.3.3 Start Engine

Turn the fuel valve to OPEN. To apply choke on a cold engine, turn the choke lever to the left. Put the ignition switch to ON. Start the engine by pulling the starter line.

3.3.4 Operation

Firstly close the pump valve. Then run the cylinders up. With no load or light load on the machine, Both VALVES can be used to increase the speed going upwards. This does not function going down. Pull the right lever for push down. The speed is regulated by changing the engine rpm. For CPT, the standard Rate of Penetration shall be 1.2 meter/minute + / - 25 %.

3.3.5 Preparation for CPT

Before the penetration can be started, the Memocone must have been prepared. This includes filling the filter point and connecting to the Datalogger for start up and zero readings. When the Memocone has been prepared and started up together with the Datalogger, put it inside the machine. Adjust the Depth Sensor Wheel, Turn the LEVER to the right. Adjust if necessary on the screw so that the wheel is turning when the Memocone is moving up and down. Do not press the wheel too hard against the Memocone, only so much that it turns the wheel safely.

Depth Sensor

Connect the depth sensor cable with the Datalogger. Insert the PUSHING HEAD or MICROPHONE into the ANVIL. It will stay in position by the means of magnets. Move the head down and guide the Memocone into the center. When the head makes contact with the Memocone, press the + button on the Datalogger and start the penetration. When the resistance is getting higher, check that the automatic locks are gripping OK. PUSH about 0.5 meter.

3.3.6 Pressure Reading

It is possible to know the pushing force by checking the hydraulic pressure.

50 Bar = 6 ton
100 Bar = 12 ton
150 Bar = 18 ton
200 Bar = 24 ton

3.3.7 Maintenance

Every 1 year should be executed the following scheme:

1. Change engine oil.
2. Lubricate the depth sensor wheel with oil.

Every 2 year:

1. Change the hydraulic oil.

3.3.8 PC-Mon

PC-Mon stands for PC Interface monitor. This unit is the link between the CPTu probes Memocone and a portable PC. The software PC-Mon v 1.0 or later has to be installed in the portable PC. The handling of the PC-Mon is totally menu operated. All possibilities at upstart, operation, registration of data and collection of data is clearly described on the screen. All input is done by the keyboard and arrow-up and arrow-down buttons.

Figure 3.2: PC Mon

Technical specification:

Size: 420 x 300 x 55 mm
Weight: 5 Kg
Cabinet: Machined Aluminium
Power requirement: 12 V DC (Car battery)
Consumption: 1 A, FUSE: 6 A
Inputs: 12 Volts power, CPT Probe, Depth transducer encoder, Microphone, Pressure sensor (Bosch type)
Outputs: 12 Volts for PC, USB port

3.4 Procedure for Determination of Shear Wave Velocity

3.4.1 Methodology

In this research, CPT equipment has been used to measure shear-wave velocity. This is special CPT equipment fitted with a seismic cone. During a pause in cone penetration, a shear wave can be created at the ground surface that will propagate into the ground on a hemi-spherical front and a measurement made of the time taken for the seismic wave to propagate to the seismometer in the cone. By repeating this measurement at another depth, one can determine, from the signal traces, the interval time and so calculate the average shear wave velocity over the depth interval between the seismometers. A repetition of this procedure with cone advancement yields a vertical profile of vertically propagating shear wave velocity. Figure 3.3 shows schematic arrangement of the SCPT and a typical arrangement of the surface shear wave source.

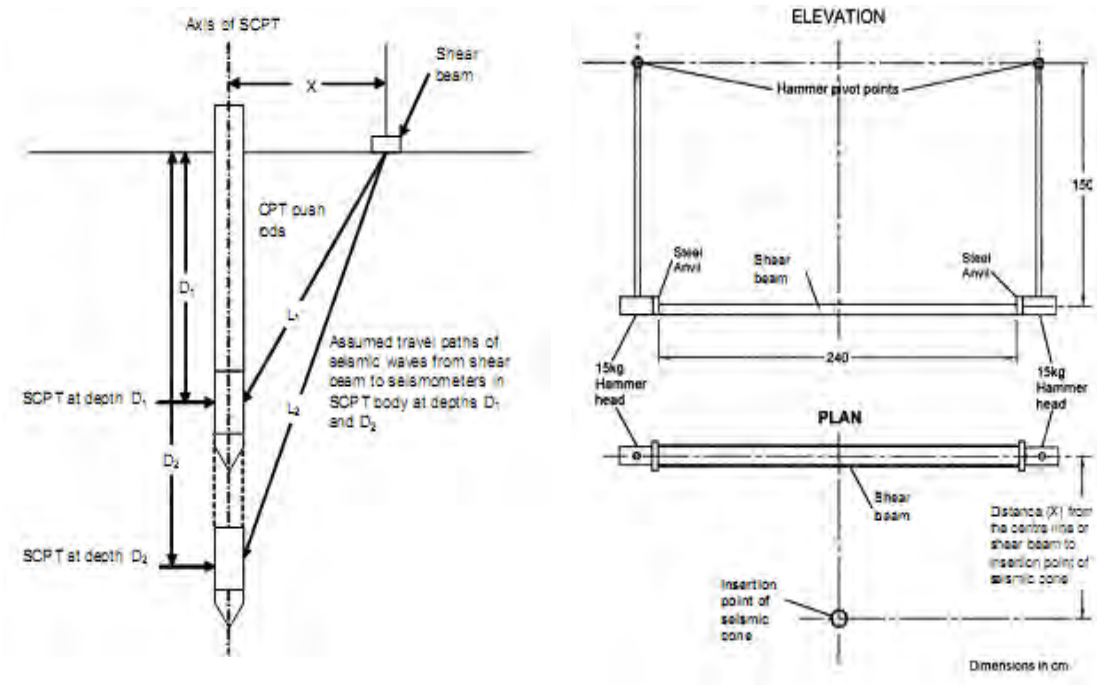

Figure 3.3 Schematic arrangement of the SCPT and a typical arrangement of the surface shear wave source

3.4.2 Equipment

The seismometer is fitted inside the cone barrel. The seismometer is mounted firmly in the cone barrel with the active axis in the horizontal direction and the axis alignment indicated on the outside of cone body. The cone barrel at the location of the seismometer should be of a greater diameter than the sections immediately below the location of the seismometer to ensure good acoustic coupling between the cone barrel and the surrounding soil. In variable and layered ground conditions, with ambient noise or ground structures that would corrupt the received signals, wave characteristics of the source can be used to identify the shear wave amongst the other waves. The inclusion of a vertically orientated seismometer will allow the P wave element of the seismic wave to be assessed or P wave arrival measured if a P wave source is used.

The shear beam can be metal or wood encased at the ends and bottom with minimum 25 mm thick steel. The strike plates or anvils at the ends are welded to the bottom plate and the bottom plate should have cleats welded to it, to penetrate the ground and prevent sliding when struck. The shear beam is placed on the ground and loaded by the leveling jacks of the cone pushing equipment or the axle load from vehicle wheels. The ground should be prepared to give good continuous contact along the whole length of the beam to ensure good acoustic coupling between the beam and the ground. The Shear Beam should not move when struck by the hammers otherwise energy is dissipated and does not travel into ground and does not pro-duce repeatable seismic shear waves. The anvils, on the ends of the Shear Beam, when struck in the direction of the long axis of the Shear Beam, will produce shear waves of opposite polarity. The beam can be continuous (approximately 2.4 m long) i.e. greater than the width of a vehicle or equipment used to load the beam and 150 mm wide or alternatively can be two shorter beams placed and loaded so that the anvils oppose and can be struck by the hammers to produce shear waves of opposite polarity. Care must be taken to position the beams and strike direction to maximise S waves and minimise the production of P waves.

Heavy hammer(s) with head mass of between 5 to 15 kg to strike the plate or anvil on the end of the shear beam in a direction parallel to the long axis of the shear beam and the active axis of seismometer. A typical setup is shown in Figure 3.3. The data

recording equipment can be a digital oscilloscope, a PC with installed A/D board and oscilloscope software or a commercial data acquisition system such as a seismograph. The data recording equipment must be able to record at 50 μs (microsecond) per point interval, or faster, to ensure clear uncorrupted signals and to start the logging of the seismometer outputs using an automatic trigger. An analogue anti aliasing filter should be used to avoid corruption of signal frequencies above the device limits. Commercial data recording equipment usually include amplifiers and signal filters to help enhance recorded signals. The effect of these processes on the recorded signals must be considered before their use. For example filtering can cause phase shift of signals and amplification is usually limited to a frequency range. In either case the signals may not be directly comparable. Experience has shown that there is a significant advantage to record the unprocessed data and then the effect of filtering and processing can be assessed during post processing. Most modern acquisition equipment allows the viewing of filtered signals during acquisition (to assess quality and repeat-ability) but saves the data un-filtered. Most modern acquisition equipment allows signal stacking to improve signal to noise ratio. The trigger can be fixed to the hammer head or the beam. The trigger is required to be very fast (less than 10 microsecond reaction time) and repeatable. When the hammer hits the shear beam, the electrical reaction of the trigger activates the trigger circuit that outputs to the signal recording equipment. A seismic trigger mounted on the beam may be used if it is fast enough, repeatable and delay time is checked and known or a contact trigger that works the instant contact is made between the hammer and the anvil.

3.4.3 Test Procedures

The test procedure for estimating shear-wave velocity using seismic cone is described in ASTM D7400. At the start of the SCPT, the body of the cone should be rotated until the axis of a seismometer is parallel to the long axis of the shear beam.

a) The cone is pushed into the ground, monitoring the inclination of the cone barrel during the push. It is important to know the exact location of the receivers in all three axes and the inclinometer in the cone barrel will give the horizontal component and the depth measuring system of the CPT the vertical component.

b) The penetration of the cone is stopped and the depth to the seismometer/s is recorded. The horizontal offset distance, X, from cone to centre of the shear beam should also be recorded. Typically this procedure is carried out at depths greater than about 2-3m in order to minimize the interference of surface wave effects. If the seismic cone includes a fully operative electric cone then it will be advanced at 2 cm/s and stopped typically at a rod break at 1m intervals or for pore water pres-sure dissipation tests. If acceptable such stoppages can also be used for downhole seismic wave measurements. Alternatively the seismic cone can be pushed to a predetermined depth at which the shear wave velocities are required and the measurements made. To avoid the possible effects of time between stop-ping, pushing and making measurements it is advisable to keep this time interval consistent. The horizontal distance, X, between the entry point of the seismic cone and the source should be kept at around 1m. Greater distances will require the effects of curved travel paths, that particularly affect single array SCPT's, to be addressed. It is advisable at the first depth of measurement to monitor the output of the receivers without activating the source to determine the ambient seismic noise in the ground and thereby enable the filtering, as far as possible, the ambient noise. Experience has shown that ambient noise can be reduced by retracting the cone pushing system, so that the drive rods are unloaded and there is no contact between the shear beam system and the cone drive rods through the cone drive vehicle and the cone driving equipment motors are not running.

c) The shear beam is struck by the hammer and the trigger activates the recording equipment that then displays the time based signal trace received by the seismometer. For quality assurance, it is recommended to reset the trigger and repeat the procedure until a consistent and reproducible trace is obtained. The voltage-time traces should lie one over the other. If they do not, continue repeating until measured responses are identical. If the seismic wave velocity appears too high then there may be a connection between the cone drive system and the seismic cone so allowing the seismic waves to travel through the cone drive rods instead of the ground.

d) The trigger is reset and the shear beam is then struck by the hammer on the opposite end on the other side of vehicle (causing initial particle motion in the opposite direction and a shear wave of opposite polarity) and procedure in step c) is again completed.

e) Show the traces from step c) and d) together and identify the shear wave (usually clearly seen with traces from the opposite polarity shear waves as a mirror image in time) and pick an arrival time. An example of signals is shown in Figure 3.4.

The average shear wave velocity for the given depth interval in units of m/s and assuming straight ray paths is given by Equation (3.1):

$$V_s = \frac{L_1 - L_2}{T_1 - T_2} \quad \ldots\ldots\ldots\ldots\ldots\ldots\ldots\ldots\ldots\ldots \quad (3.1)$$

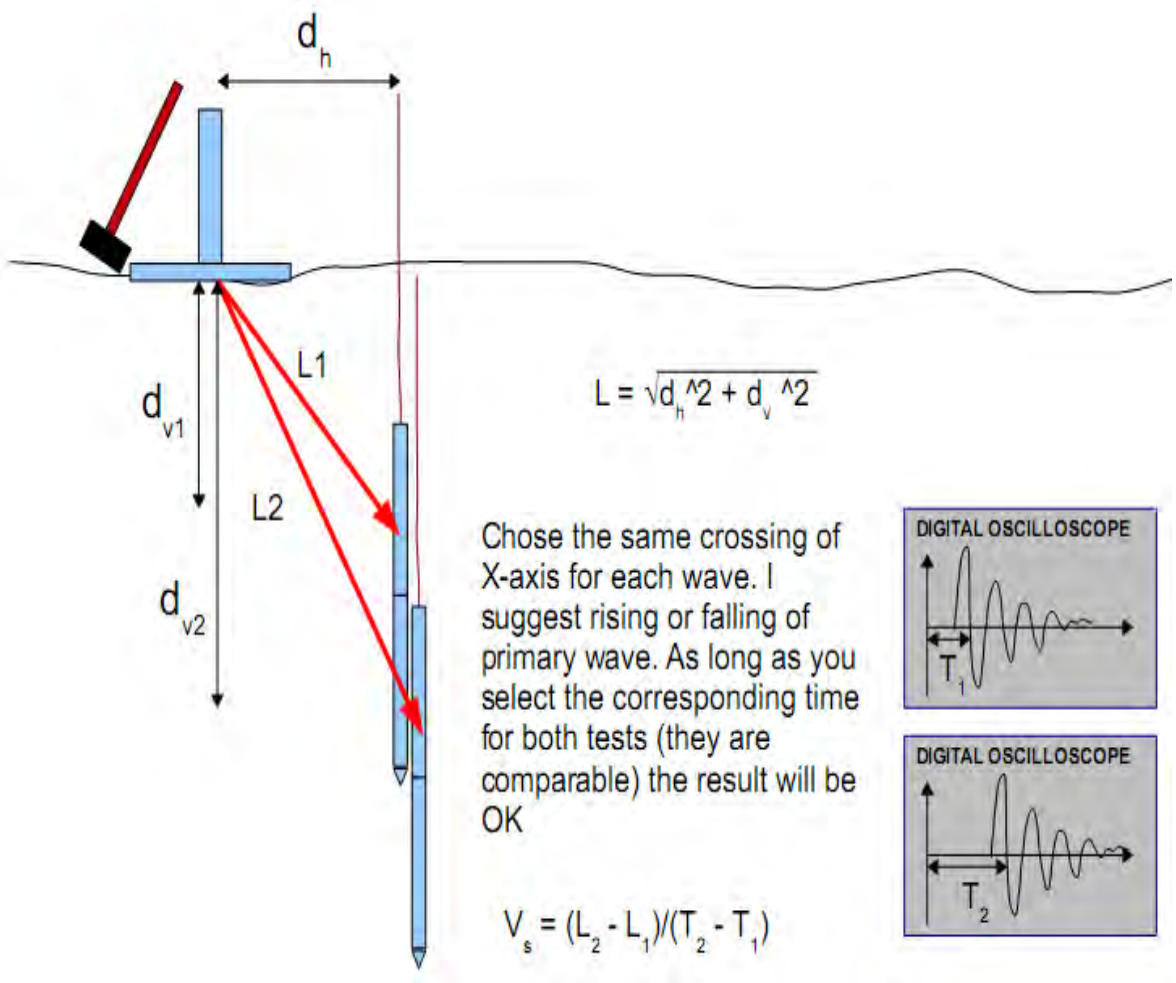

Figure 3.4: An example of shear wave traces showing the interval time T2 – T1

3.5 Selected Areas for the Research

Total ten locations of the Dhaka city have been selected for this research. The main targeted areas have been reclaimed recent fill and loose lands since some of these lands found susceptible to Site Amplification. Total ten areas have been selected which almost surround the Dhaka city. The selected areas are **Kawran Bazar**, **Gulshan**, **Mugda**, **Ashian City**, **Uttara, Asulia, Mirpur, Mohammadpur, Mothertek and United City**. Figure 3.5 shows the selected areas of Dhaka City for this research.

Figure 3.5: Map showing the selected areas of Dhaka City for this Research

3.6 Determination of Shear Wave Velocity

Shear wave velocity has been estimated by using CPT equipment at all ten selected locations of Dhaka city. Shear wave velocity is being used for the estimation of Site Amplification. Shear Wave velocity is estimated according to the procedure described in ASTM D7400. :

3.6.1 SITE: KAWRAN BAZAR

This site has been situated in middle-eastern part of Dhaka city. The depth of clay layer is 7.5 m from existing ground level. After that 3.0 m is silt layer. Then 19.5 m is fine sand layer. The maximum value of SPT N is 36 and the minimum value of SPT N is 1. The average shear wave velocity of this site is 164 m/s. The maximum value of shear wave velocity is 300 m/s and the minimum value of shear wave velocity is 60 m/s. Figure 3.6 shows the shear wave velocity profile at Kawran Bazar location.

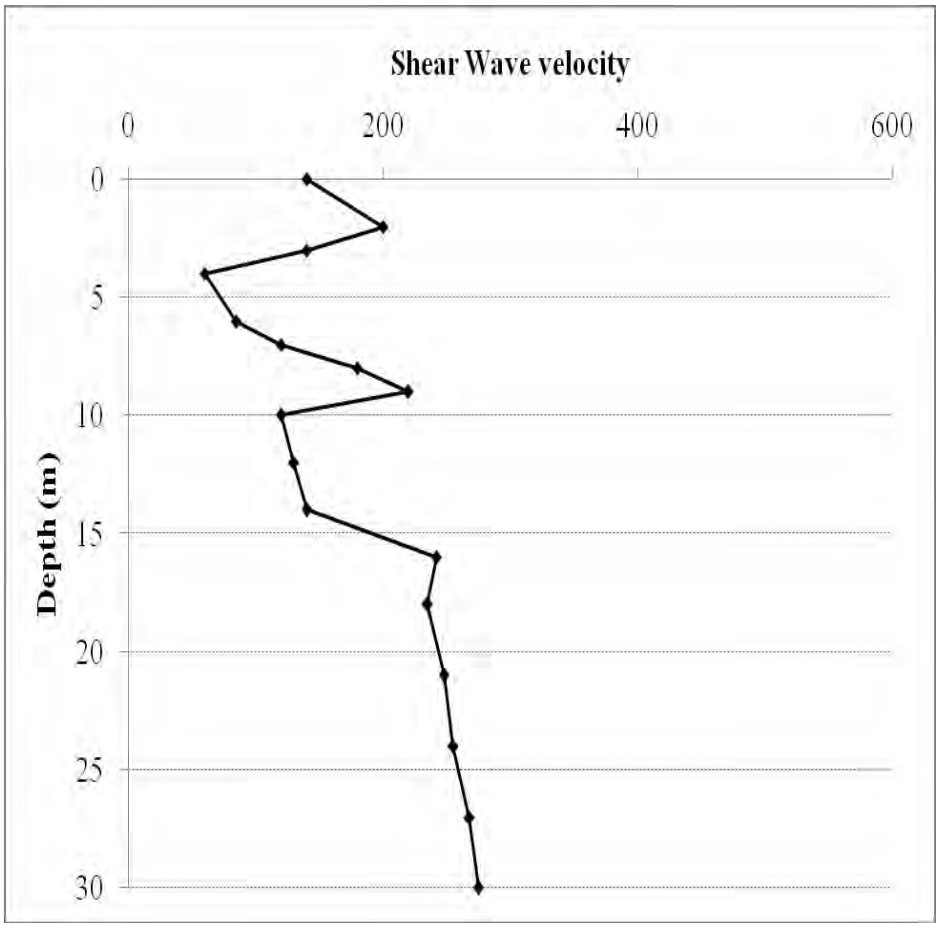

Figure 3.6: Shear wave velocity profile at Kawran Bazar

SPT Results:

SPT has been conducted in the area following procedure described in ASTM D1586. The SPT N values of the boreholes are shown in the Table 3.1. The SPT N value of clay layers varies from 2 to 15. The maximum value of SPT N is 36. The minimun value of SPT N is 1.

Table 3.1: SPT Result of Kawran Bazar site

Depth(m)	Description of Soil	SPT N Value
1.5	Clay	1
3.0	Clay	1
4.5	Clay	1
6.0	Clay	2
7.5	Clay	2
9.0	Silt	14
10.5	Silt	15
12.0	Fine Sand	28
13.5	Fine Sand	32
15.0	Fine Sand	33
16.5	Fine Sand	35
18.0	Fine Sand	26
19.5	Fine Sand	28
21.0	Fine Sand	30
22.5	Fine Sand	28
24.0	Fine Sand	30
25.5	Fine Sand	32
27.0	Fine Sand	35
28.5	Fine Sand	33
30.0	Fine Sand	36

3.6.2 SITE: GULSHAN

This site has been situated in central part of Dhaka city. The depth of fine sand filling is 4.5 m from existing ground level. The organic clay layer exists from 4.5 m to 7.5 m from EGL. After that 6.0 m is silty clay layer. Then 4.5 m is sandy silt. Then 12.0 m is fine sand. The maximum value of SPT N is 38 and the minimum value of SPT N is 1. The average shear wave velocity of this site is 234 m/s. The maximum value of shear wave velocity is 300 m/s and the minimum value of shear wave velocity is 100 m/s. Figure 3.7 shows the shear wave velocity profile at Gulshan location.

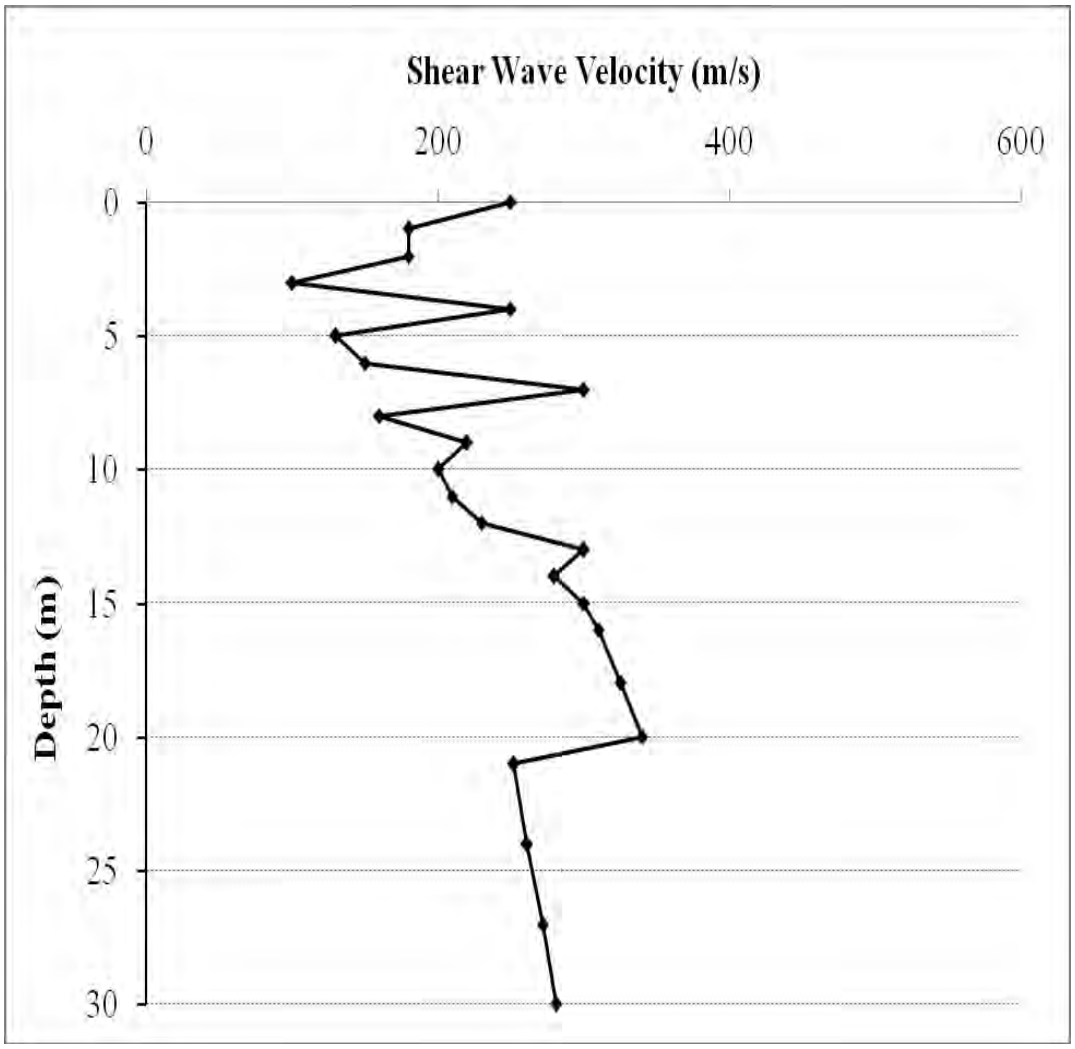

Figure 3.7: Shear wave velocity profile at Gulshan

SPT Results:

SPT has been conducted in the area following procedure described in ASTM D1586. The SPT N values of the boreholes have been shown in the Table 3.2 The uncorrected SPT N value of filling fine sand varies from 5 to 7. The SPT N value of silty clay layers varies from 5 to 12. The maximum value of SPT N is 40. The minimum value of SPT N is 1.

Table 3.2: SPT Result of Gulshan site

Depth(m)	Description of Soil	SPT N Value
1.5	Filling Sand	7
3.0	Filling Sand	8
4.5	Filling Sand	5
6.0	Organic Clay	1
7.5	Organic Clay	3
9.0	Silty Clay	5
10.5	Silty Clay	8
12.0	Silty Clay	11
13.5	Silty Clay	12
15.0	Sandy Silt	26
16.5	Sandy Silt	30
18.0	Sandy Silt	33
19.5	Fine Sand	38
21.0	Fine Sand	32
22.5	Fine Sand	30
24.0	Fine Sand	34
25.5	Fine Sand	36
27.0	Fine Sand	38
28.5	Fine Sand	37
30.0	Fine Sand	40

3.6.3 SITE: MUGDA

This site has been situated in eastern part of Dhaka city. The depth of filling sand is 3.0 m from existing ground level. The silty clay layer exists from 3.0 m to 15.0m from EGL. After that 4.5 m is silt layer. Then 10.5 m is fine sand. The maximum value of SPT N is 40 and the minimum value of SPT N is 1. The average shear wave velocity of this site is 220 m/s. The maximum value of shear wave velocity is 360 m/s and the minimum value of shear wave velocity is 90 m/s. Figure 3.8 shows the shear wave velocity profile at Mugda location.

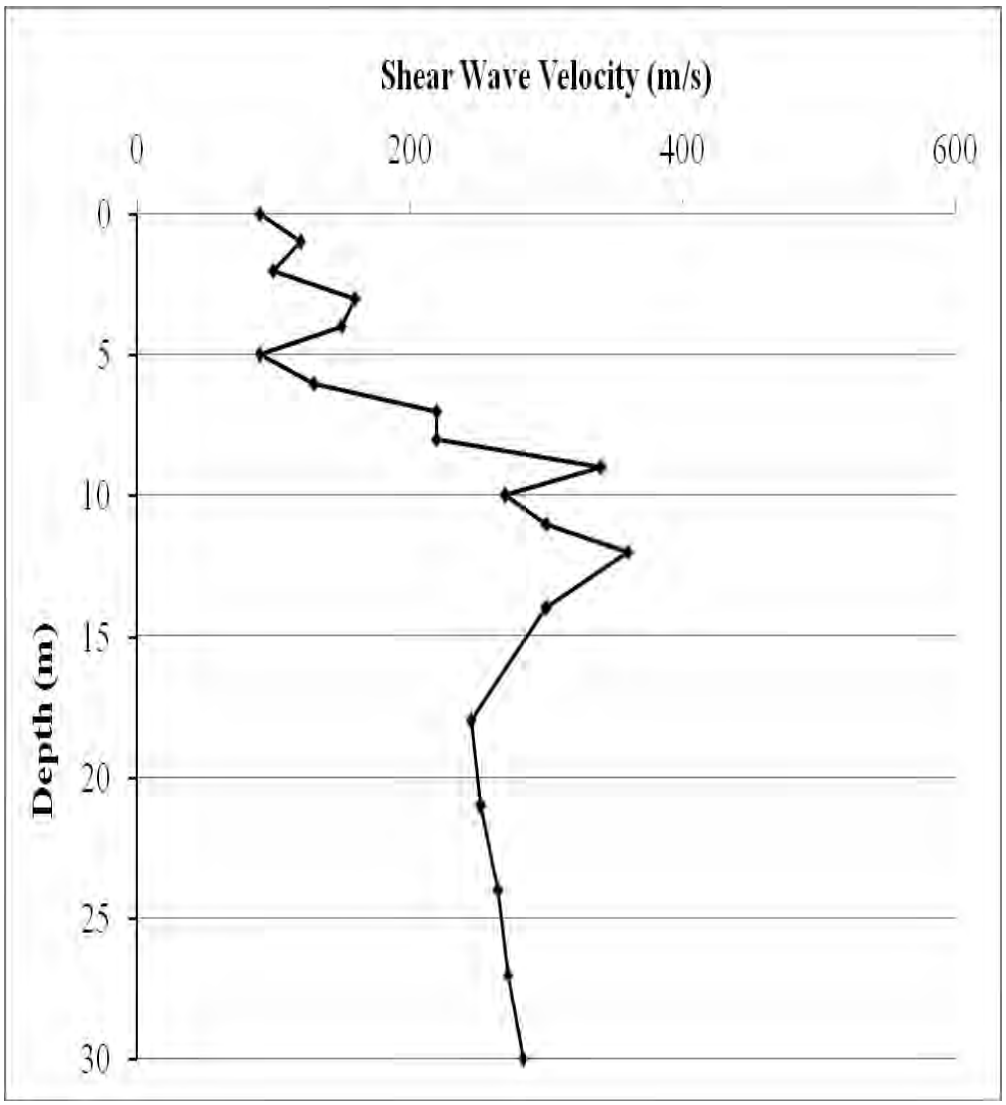

Figure 3.8: Shear wave velocity profile at Mugda

SPT Results:

SPT has been conducted in the area following procedure described in ASTM D1586. The SPT N values of the boreholes have been shown in the Table 3.3 The uncorrected SPT N value of filling fine sand varies from 5 to 6. The SPT N value of silty clay layers varies from 1 to 9. The maximum value of SPT N is 42. The minimum value of SPT N is 1.

Table 3.3: SPT Result of Mugda site

Depth(m)	Description of Soil	SPT N Value
1.5	Filling Sand	5
3.0	Filling Sand	6
4.5	Silty Clay	4
6.0	Silty Clay	5
7.5	Silty Clay	1
9.0	Silty Clay	1
10.5	Silty Clay	3
12.0	Silty Clay	2
13.5	Silty Clay	4
15.0	Silty Clay	9
16.5	Silt	26
18.0	Silt	33
19.5	Silt	36
21.0	Sand	32
22.5	Sand	34
24.0	Sand	37
25.5	Sand	35
27.0	Sand	38
28.5	Sand	40
30	Sand	42

3.6.4 SITE: ASIAN CITY, DAKHIN KHAN

This site has been situated in Northern part of Dhaka city. The depth of fine sand filling is 3.0 m from existing ground level. The silty clay layer exists from 3.0 m to 10.5 m from EGL. After that 3.0 m is fine sand layer. Then 3.0 m is silty clay. After that 13.5 m is dense sand layer. The maximum value of SPT N is 42 and the minimum value of SPT N is 3.The average shear wave velocity of this site is 205 m/s. The maximum value of shear wave velocity is 520 m/s and the minimum value of shear wave velocity is 80 m/s. Figure 3.9 shows the shear wave velocity profile at Asian City location.

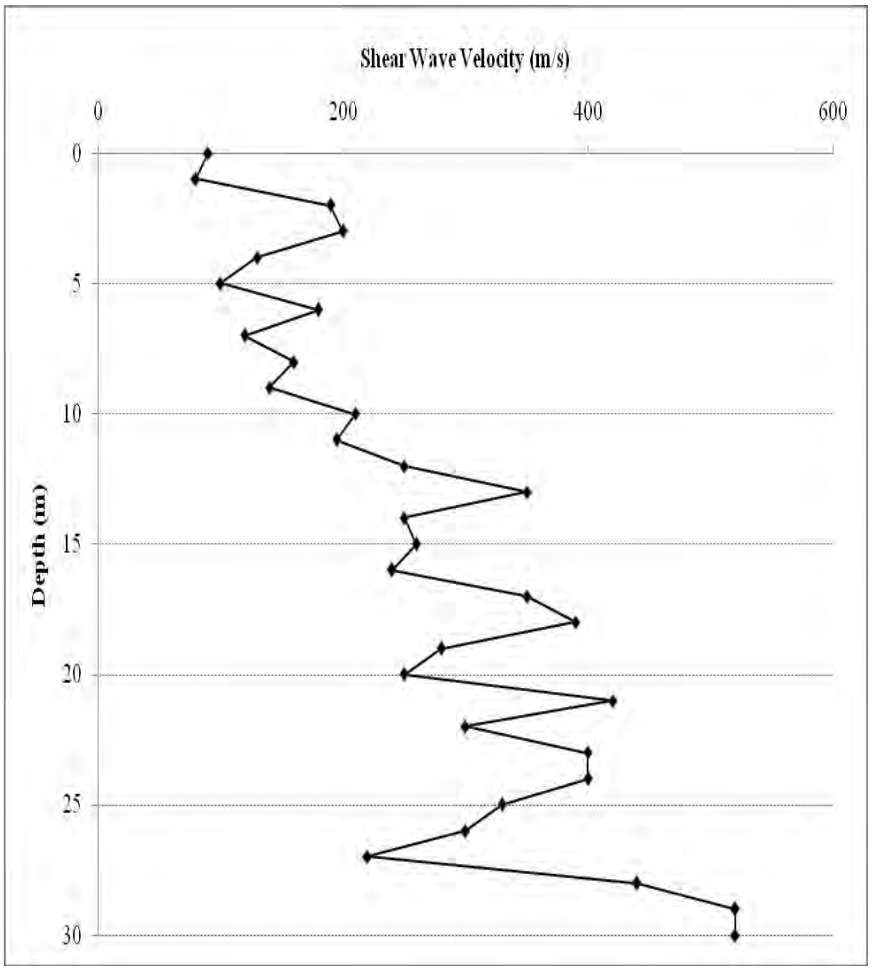

Figure 3.9: Shear wave velocity profile at Asian city

SPT Results:

SPT is conducted in the area following procedure described in ASTM D1586. The SPT N values of the boreholes are shown in the Table 3.4. The uncorrected SPT N value of filling fine sand varies from 4 to 5. The SPT N value of silty clay layers varies from 3 to 33. The maximum value of SPT N is 56. The minimum value of SPT N is 3.

Table 3.4: SPT Result of Asian City site

Depth(m)	Description of Soil	SPT N Value
1.5	Filling Sand	4
3.0	Filling Sand	5
4.5	Silty Clay	4
6.0	Silty Clay	3
7.5	Silty Clay	3
9.0	Silty Clay	4
10.5	Silty Clay	6
12.0	Sand	5
13.5	Sand	13
15.0	Silty Clay	19
16.5	Silty Clay	33
18.0	Dense Sand	35
19.5	Dense Sand	38
21.0	Dense Sand	35
22.5	Dense Sand	39
24.0	Dense Sand	50
25.5	Dense Sand	45
27.0	Dense Sand	56
28.5	Dense Sand	42
30.0	Dense Sand	39

3.6.5 SITE: UTTARA

This site has been situated in north of Dhaka city. The depth of fine sand filling is 4.5 m from existing ground level. The clay layer exists from 4.5 m to 27.0 m from EGL. After that 3.0 m is dense sand layer. The maximum value of SPT N is 18 and the minimum value of SPT N is 2. The average shear wave velocity of this site is 188 m/s. The maximum value of shear wave velocity is 500 m/s and the minimum value of shear wave velocity is 80 m/s. Figure 3.10 shows the shear wave velocity profile at Uttara location.

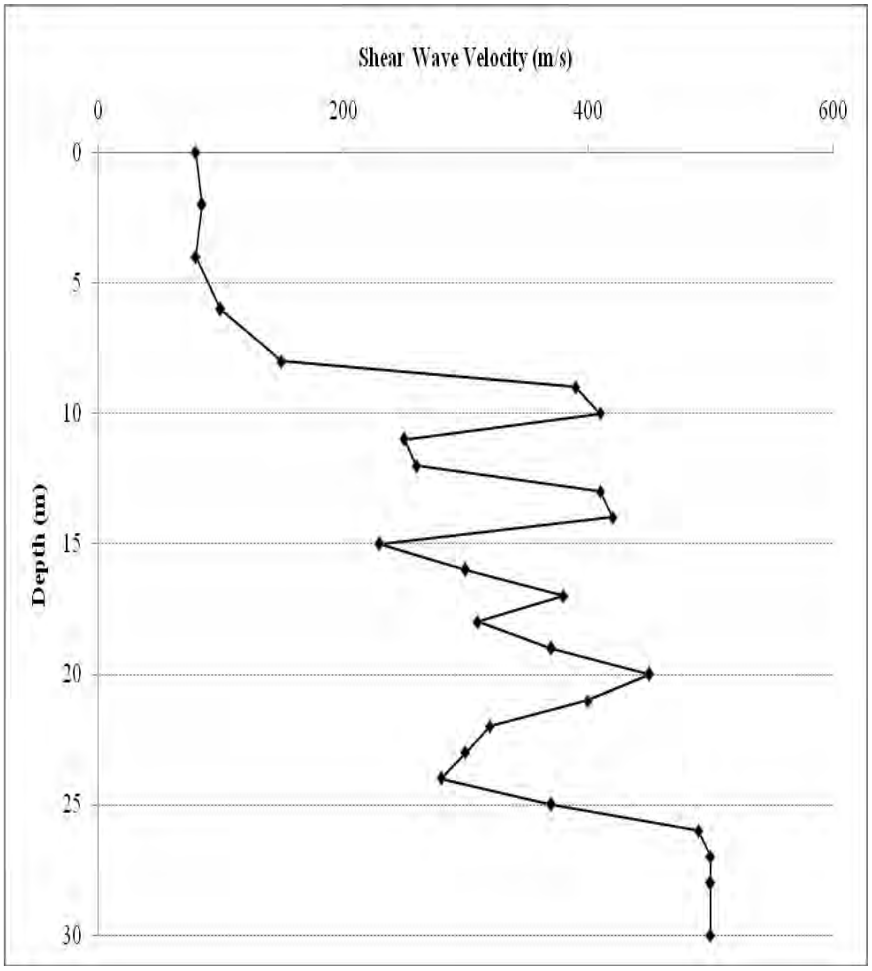

Figure 3.10: Shear wave velocity profile at Uttara

SPT Results:

SPT has been conducted in the area following procedure described in ASTM D1586. The SPT N values of the boreholes are shown in the Table 3.5. The uncorrected SPT N value of filling fine sand varies from 5 to 25. The SPT N value of clay layers varies from 21 to 29. The maximum value of SPT N is 57. The minimum value of SPT N is 5.

Table 3.5: SPT Result of Uttara site

Depth(m)	Description of Soil	SPT N Value
1.5	Filling Sand	5
3.0	Filling Sand	12
4.5	Filling Sand	25
6.0	Clay	22
7.5	Clay	21
9.0	Clay	20
10.5	Clay	23
12.0	Clay	22
13.5	Clay	21
15.0	Clay	28
16.5	Clay	29
18.0	Clay	23
19.5	Clay	24
21.0	Clay	31
22.5	Clay	30
24.0	Clay	36
25.5	Clay	41
27.0	Clay	49
28.5	Dense Sand	57
30.0	Dense Sand	50

3.6.6 SITE: ASULIA

This site has been situated in north-west part of Dhaka city. It is a private land development project where main filing is done by dredged river sand. The depth of fine sand filling is 1.5 m from existing ground level. The silty clay layer exists from 1.5 m to 18.0 m from EGL. After that 3.0 m is fine sand layer. Then 4.5 m is clay layer. After that 4.5 m is dense sand layer. The average shear wave velocity of this site is 139 m/s. The maximum value of shear wave velocity is 700 m/s and the minimum value of shear wave velocity is 50 m/s. Figure 3.11 shows the shear wave velocity profile at Asulia location.

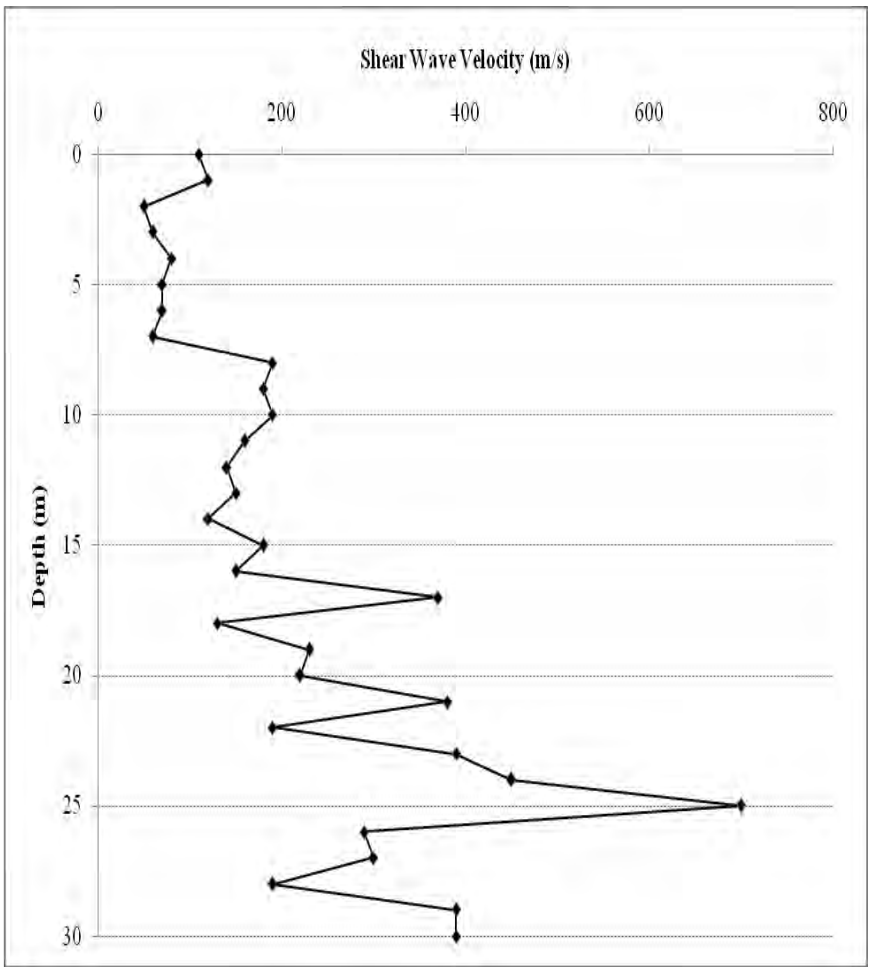

Figure 3.11: Shear wave velocity profile at Asulia

SPT Results:

SPT has been conducted in the area following procedure described in ASTM D1586. The SPT N values of the boreholes are shown in the Table 3.6. The SPT N value of silty clay layers varies from 1 to 14. The maximum value of SPT N is 47. The minimum value of SPT N is 1.

Table 3.6: SPT Result of Asulia site

Depth(m)	Description of Soil	SPT N Value
1.5	Filling Sand	1
3.0	Silty Clay	2
4.5	Silty Clay	2
6.0	Silty Clay	1
7.5	Silty Clay	4
9.0	Silty Clay	6
10.5	Silty Clay	4
12.0	Silty Clay	3
13.5	Silty Clay	2
15.0	Silty Clay	3
16.5	Silty Clay	7
18.0	Silty Clay	14
19.5	Sand	8
21.0	Sand	22
22.5	Clay	12
24.0	Clay	17
25.5	Clay	30
27.0	Dense Sand	37
28.5	Dense Sand	43
30.0	Dense Sand	47

3.6.7 SITE: MIRPUR

This site has been situated in north-west part of Dhaka city. The depth of clay layer is 30.0 m from existing ground level. The maximum value of SPT N is 74 and the minimum value of SPT N is 14. The average shear wave velocity of this site is 320 m/s. The maximum value of shear wave velocity is 810 m/s and the minimum value of shear wave velocity is 190 m/s. Figure 3.12 shows the shear wave velocity profile at Mirpur location.

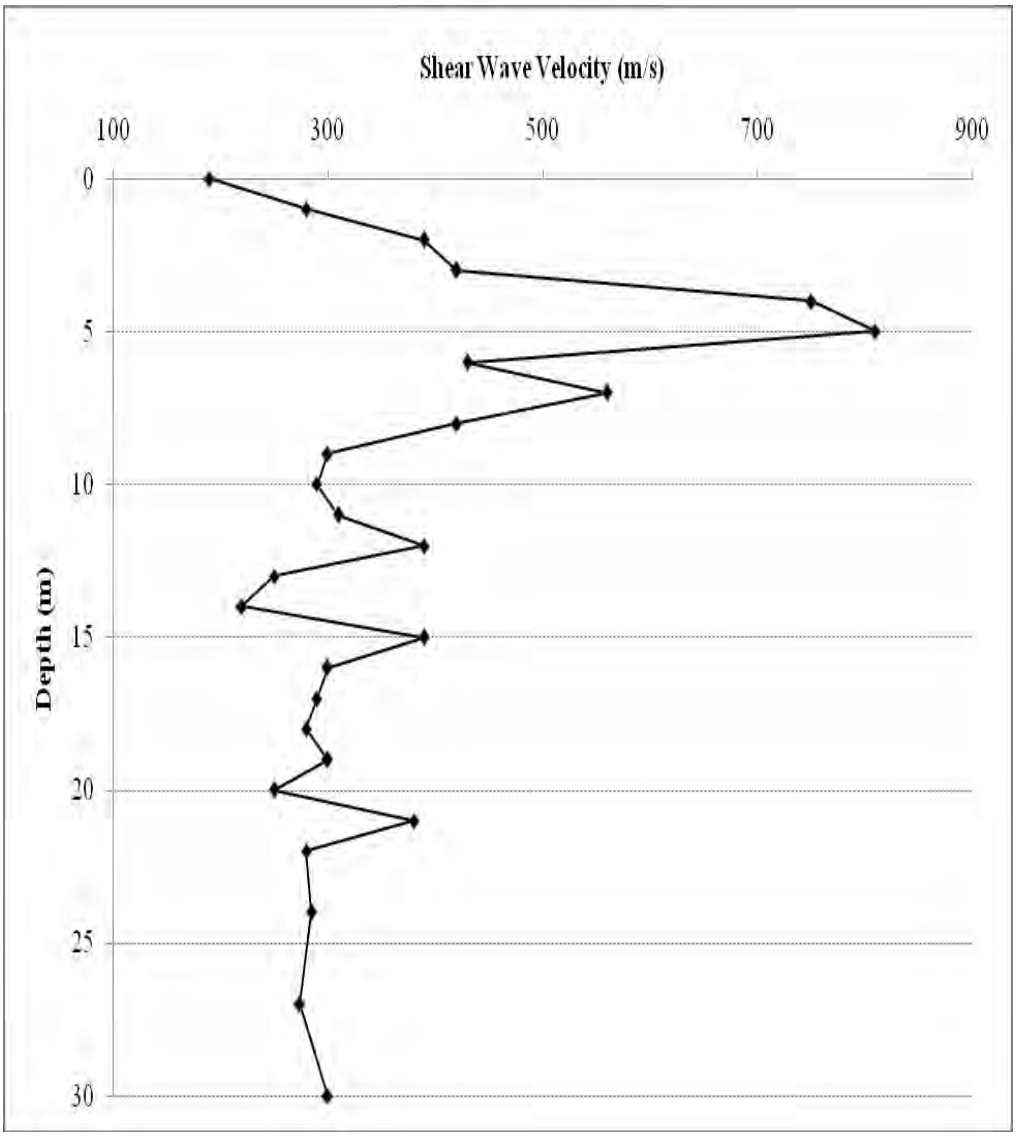

Figure 3.12: Shear wave velocity profile at Mirpur

SPT Results:

SPT has been conducted in the area following procedure described in ASTM D1586. The SPT N values of the boreholes are shown in the Table 3.7. The SPT N value of clay layers varies from 14 to 74.

Table 3.7: SPT Result of Mirpur site

Depth(m)	Description of Soil	SPT N Value
1.5	Clay	22
3.0	Clay	46
4.5	Clay	52
6.0	Clay	48
7.5	Clay	62
9.0	Clay	31
10.5	Clay	14
12.0	Clay	22
13.5	Clay	23
15.0	Clay	25
16.5	Clay	28
18.0	Clay	24
19.5	Clay	23
21.0	Clay	38
22.5	Clay	74
24.0	Clay	55
25.5	Clay	36
27.0	Clay	40
28.5	Clay	25
30.0	Clay	29

3.6.8 SITE: MOHAMMADPUR

This site has been situated in west part of Dhaka city. It is a private land development project. The depth of fine sand filling is 4.5 m from existing ground level. The silty clay layer exists from 4.5 m to 10.5 m from EGL. After that 19.5 m is sand layer. The maximum value of SPT N is 55 and the minimum value of SPT N is 2. The average shear wave velocity of this site is 194 m/s. The maximum value of shear wave velocity is 750 m/s and the minimum value of shear wave velocity is 50 m/s. Figure 3.13 shows the shear wave velocity profile at Mohammadpur location.

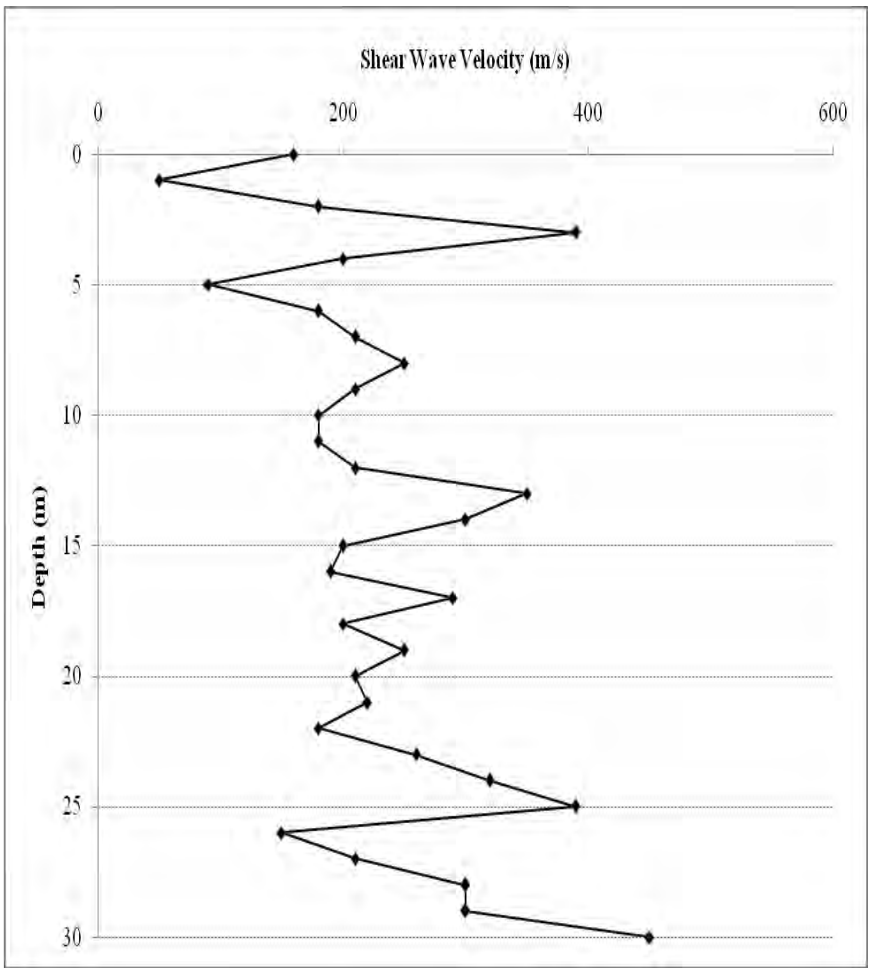

Figure 3.13: Shear wave velocity profile at Mohammadpur

SPT Results:

SPT has been conducted in the area following procedure described in ASTM D1586. The SPT N values of the boreholes are shown in the Table 3.8. The uncorrected SPT N value of filling fine sand varies from 2 to 3. The SPT N value of silty clay layers varies from 9 to 17. The maximum value of SPT N is 55. The minimum value of SPT N is 2.

Table 3.8: SPT Result of Mohammadpur site

Depth(m)	Description of Soil	SPT N Value
1.5	Filling Sand	3
3.0	Filling Sand	2
4.5	Filling Sand	3
6.0	Silty Clay	9
7.5	Silty Clay	11
9.0	Silty Clay	13
10.5	Silty Clay	17
12.0	Sand	19
13.5	Sand	26
15.0	Sand	20
16.5	Sand	16
18.0	Sand	25
19.5	Sand	27
21.0	Sand	29
22.5	Sand	27
24.0	Sand	29
25.5	Sand	33
27.0	Sand	32
28.5	Sand	38
30.0	Sand	55

3.6.9 SITE: EAST NANDIPARA, MOTHERTEK

This site has been situated in eastern part of Dhaka city. The depth of recent fill (fine sand) is 3.0 m from existing ground level. After that 27 m is clay layer. The maximum value of SPT N is 62. The minimum value of SPT N is 2. The average shear wave velocity of this site is 265 m/s. The maximum value of shear wave velocity is 570 m/s and the minimum value of shear wave velocity is 70 m/s. Figure 3.14 shows the shear wave velocity profile at Mothertek location.

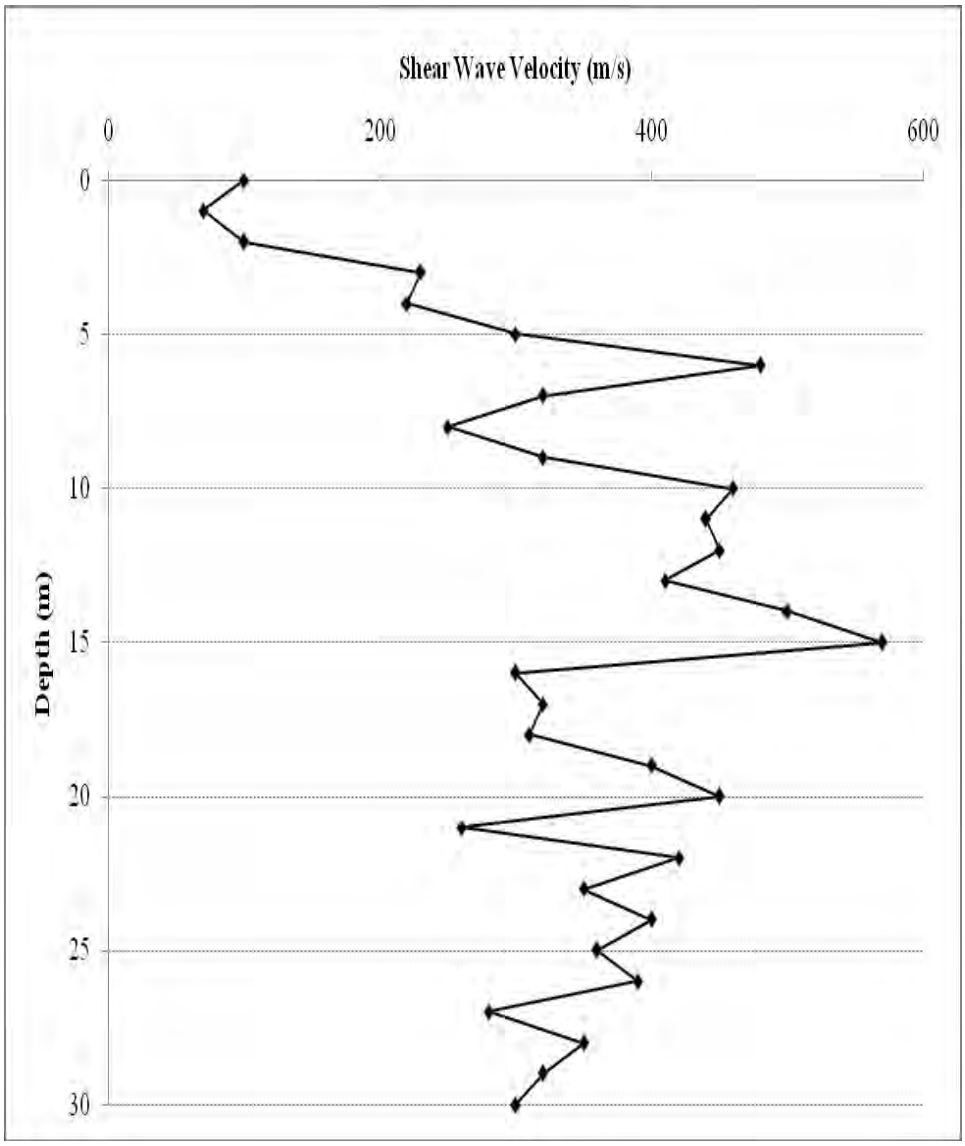

Figure 3.14: Shear wave velocity profile at Mothertek

SPT Results:

SPT has been conducted in the area following procedure described in ASTM D1586. The SPT N values of the boreholes are shown in the Table 3.9. The uncorrected SPT N value of filling filling sand varies from 2 to 5. The SPT N value of clay layers varies from 8 to 62. The maximum value of SPT N is 62. The minimum value of SPT N is 2.

Table 3.9: SPT Result of Mothertek site

Depth(m)	Description of Soil	SPT N Value
1.5	Filling Sand	2
3.0	Filling Sand	5
4.5	Clay	8
6.0	Clay	15
7.5	Clay	10
9.0	Clay	13
10.5	Clay	14
12.0	Clay	27
13.5	Clay	21
15.0	Clay	36
16.5	Clay	38
18.0	Clay	18
19.5	Clay	27
21.0	Clay	22
22.5	Clay	34
24.0	Clay	39
25.5	Clay	55
27.0	Clay	36
28.5	Clay	28
30.0	Clay	62

3.6.10 SITE: UNITED CITY

This site has been situated in Eastern part of Dhaka city. The depth of fine sand filling is 4.5 m from existing ground level. The silty clay layer exists from 4.5 m to 12.0 m from EGL. After that 4.5 m is fine sand layer. Then 4.5 m is silty clay layer. After that 9.0 m is clay layer. The maximum value of SPT N is 15 and the minimum value of SPT N is 3.The average shear wave velocity of this site is 161 m/s. The maximum value of shear wave velocity is 370 m/s and the minimum value of shear wave velocity is 80 m/s. Figure 3.15 shows the shear wave velocity profile at United City location.

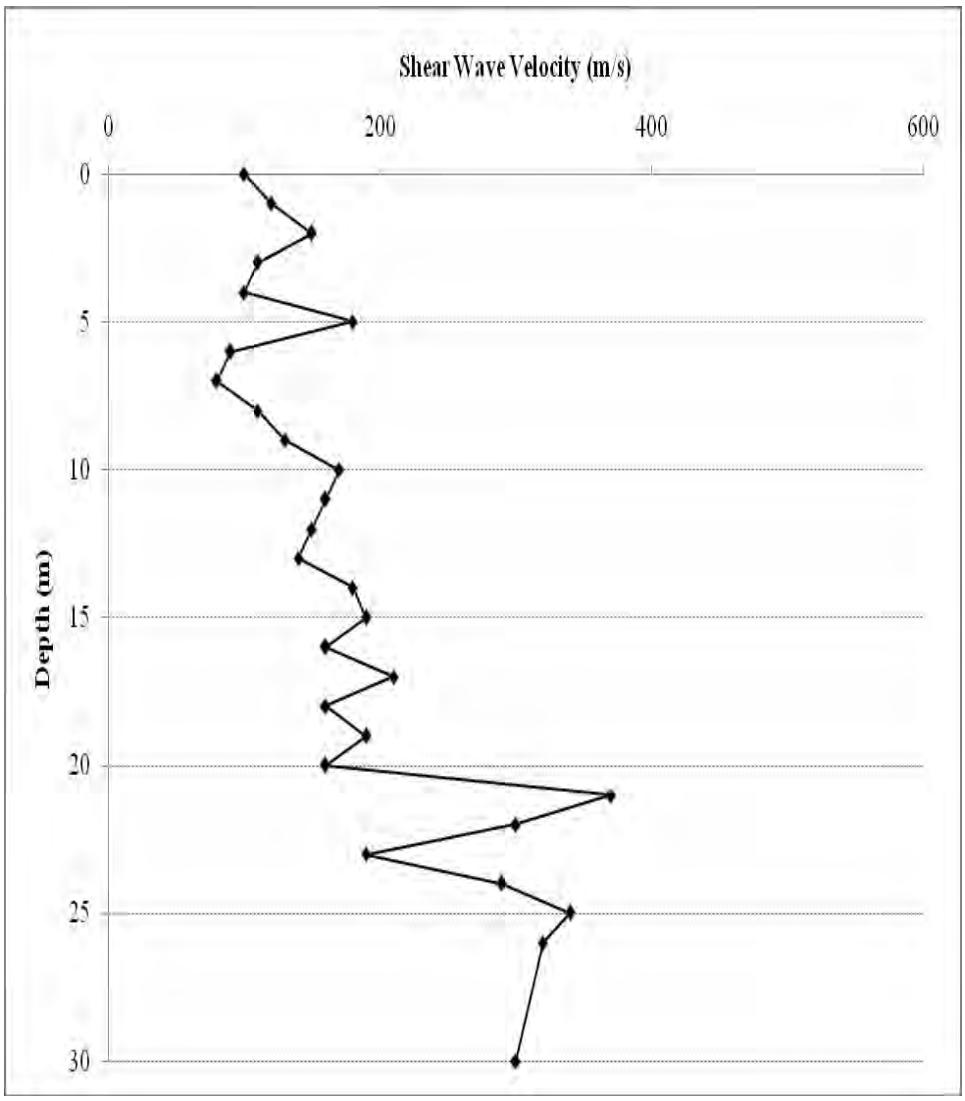

Figure 3.15: Shear wave velocity profile at United City

SPT Results:

SPT has been conducted in the area following procedure described in ASTM D1586. The SPT N values of the boreholes are shown in the Table 3.10. The uncorrected SPT N value of filling fine sand varies from 2 to 3. The SPT N value of clay layers varies from 10 to 38. The maximum value of SPT N is 42. The minimum value of SPT N is 1.

Table 3.10: SPT Result of United City site

Depth(m)	Description of Soil	SPT N Value
1.5	Filling Sand	3
3.0	Filling Sand	3
4.5	Filling Sand	2
6.0	Silty Clay	7
7.5	Silty Clay	4
9.0	Silty Clay	3
10.5	Silty Clay	2
12.0	Silty Clay	1
13.5	Sand	1
15.0	Sand	1
16.5	Sand	1
18.0	Silty Clay	1
19.5	Silty Clay	1
21.0	Silty Clay	42
22.5	Clay	34
24.0	Clay	10
25.5	Clay	26
27.0	Clay	38
28.5	Clay	28
30.0	Clay	20

3.7 Concluding Remarks

The maximum value of shear wave velocity is 810 m/s from the ten selected sites. The minimum value shear wave velocity is 50 m/s from the ten selected sites. The variation of shear wave velocities with depth for ten selected locations of the Dhaka city has been described in this chapter.

CHAPTER FOUR
DETAILED GROUND RESPONSE ANALYSIS

4.1. General

Earthquake effects are usually quantified on the basis of degree of damage in addition to the recorded ground motions at a site. Heterogeneity in the soil media of different layers cause the disparity in the characteristics of seismic waves as they propagate from bed rock to the ground surface form one site to another. Also the attenuation of these waves and trapping of body waves augment damaging scenario. During 1994 Northridge earthquake (M 6.7) high ground motions were recorded (PGA 1.82g) whereas the predicted PGA at 100m was 0.46g (Silva, W. J., 2000). The curvature of a sediment-filled basin structure in particular can confine body waves and can cause some incident body waves to propagate through the alluvium as surface waves resulting in stronger shaking effects and longer duration of strong ground motion (Kramer,S.L., 1996). Such is the effect of seismic wave propagation and amplification. So, estimation of site specific dynamic response is important for the estimation of seismic hazard. The results of ground response analysis form the important parameter in case of performance based design. Cramer, C. H., and Real, C. R. (1992) concluded that variability in the geotechnical model associated with uncertainty in stiffness and damping characteristics more significantly impacted the predicted motions than variability between different methods of analysis utilizing relatively consistent velocity profiles (i.e., from preferred versus standard geotechnical models).

Dhaka City is underlain by loose sandy silts and silty clay which makes it vulnerable to damage caused due to the ground motion amplification of the young, loose soil deposits in the area. Site response analysis consists of estimation of local site effects and surface ground motion. This chapter deals with the estimation of surface ground motion for Dhaka city.

The main objective of this chapter is to present the ground responses analysis of the selected locations in Dhaka city. Shear wave velocities of the selected areas have been determined by CPT equipment (Chapter 3.3).

4.2. Ground Response Analysis

Propagation of seismic waves through soil column during earthquake alters the amplitude, frequency and duration of ground motion by the time it reaches the surface. The effects of ground motion are propagated in the form of waves from one medium to another. So, physically it is problem of prediction of ground motion characteristics whereas mathematically it is a problem of the wave propagation in continuous medium. The evaluation of such response of the site to dynamic loading is termed as ground response analysis.

Shear wave velocity (Vs)

Shear wave velocity (Vs) is one of the most important input parameter to represent the stiffness of the soil layers. Total ten locations have been selected for Site Amplification Analysis in Dhaka city in this research. Shear wave velocity (Vs) is measured in ten selected locations of Dhaka city by using CPT equipment (Chapter 3.4).

In Dhaka City the depth of bedrock was unavailable due to lack of deep boreholes. In DEEPSOIL (Hashash,Y.M.A. et al., 2011), rock depth is assumed to be below the last layer, so to prevent erroneous results the last layer was assumed to be the same upto a depth of 100m.

For site response analysis by equivalent linear method the results are considered to be accurate for estimating PGA upto 3sec for general projects (Finn W.D.L., 1995; Martin, G.R., 1994; Durward, J.A., 1996; Dobry, R., 2000; Dickenson, S. E., 1995). Selection of a ground motion for dynamic analysis is tedious. Input ground motion have to be selected in such way that they represent the regional seismicity and must incorporate the anticipated earthquakes. The selection of ground motion can be done based on expected magnitude and distance, soil profile, strong motion duration, seismo tectonic environment, acceleration to

vertical ratio, spectral matching etc. In this study, Kobe earthquake (Mb = 6.8) of 17th January 1995, Loma Prieta earthquake (Mb = 6.9) of 17th October 1989, Northridge earthquake (Mb = 6.7) of 17th January 1994, Sikkim earthquake (Mb = 6.9) of 18th September 2011, Coalinga earthquake, Hector Mine earthquake, Michocan earthquake, Nahanni earthquake, Ofunata earthquake and Parkfield earthquake, is selected as the input ground motions (Fig.4.1). The input rock motion for Dhaka is scaled to 0.19g value (Hossaini et al, 2012). The magnitude of earthquake is almost similar to that expected in Dhaka City. So, the rock properties have been defined and the shear modulus has been considered which is frequency independent. During the analysis, number of iterations also affects the results, after serious reflection 25 iterations have been considered. Table 4.1 summarizes the surface PGA evaluated at different locations and Table 4.2 shows the Site amplification factor at different locations of Dhaka City. Table 4.3 shows the PSA based Surface Input ratio.

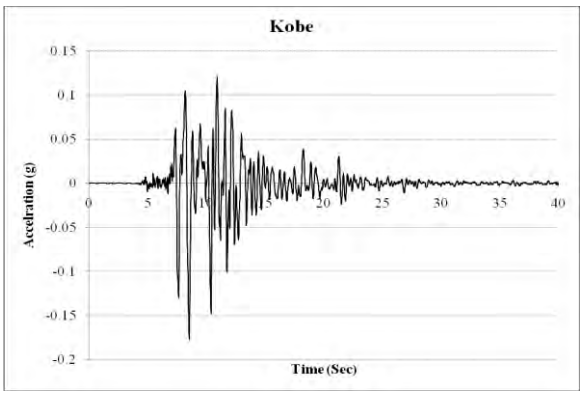

(a) Kobe earthquake, 1995; Mb= 6.8

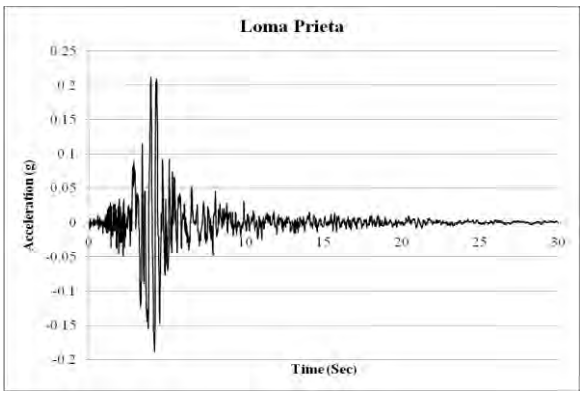

(b) Loma Prieta earthquake, 1989; Mb=6.9

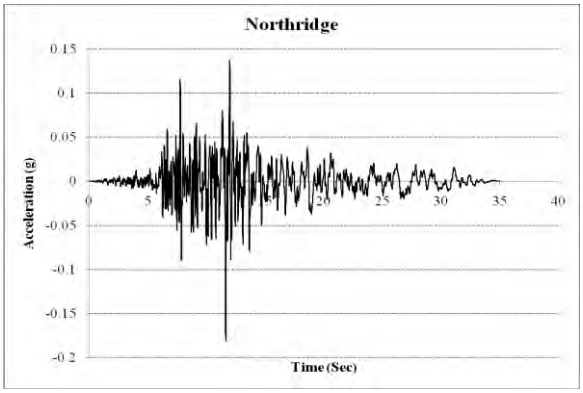

(c) Northridge earthquake, 1994; Mb=6.7

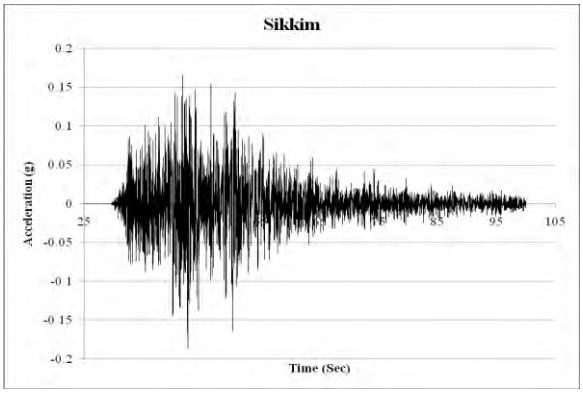

(d) Sikkim earthquake, 2011; Mb=6.9

Figure 4.1(a) Scaled Input Ground motion (a) Kobe earthquake, (b) Loma Prieta earthquake, (c) Northridge earthquake and (d) Sikkim earthquake

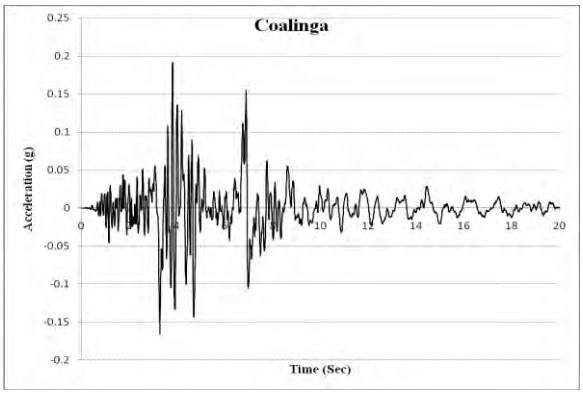

(a) Coalinga earthquake

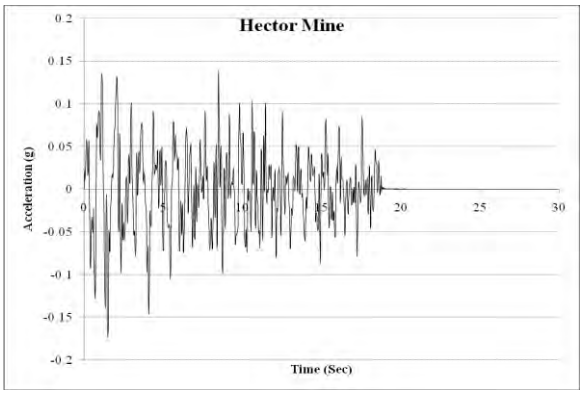

(b) Hector Mine earthquake

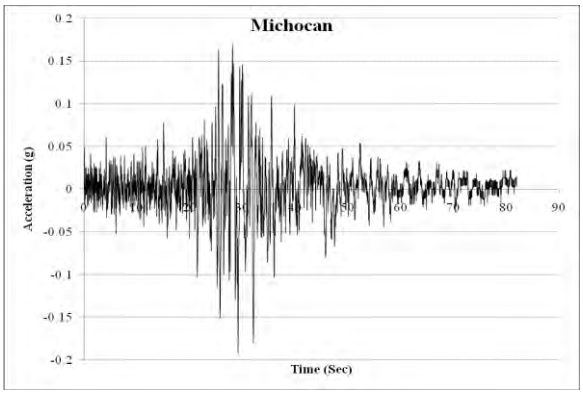

(c) Michocan earthquake

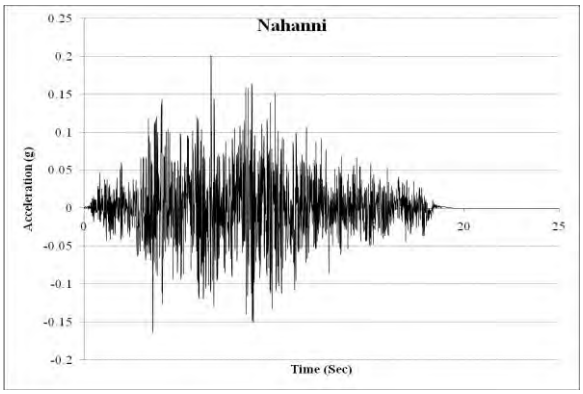

(d) Nahanni earthquake

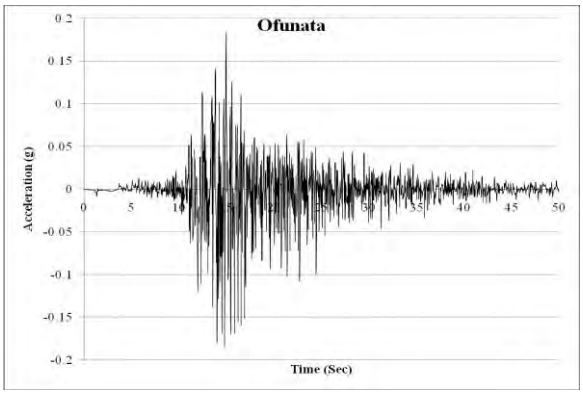

(e) Ofunata earthquake

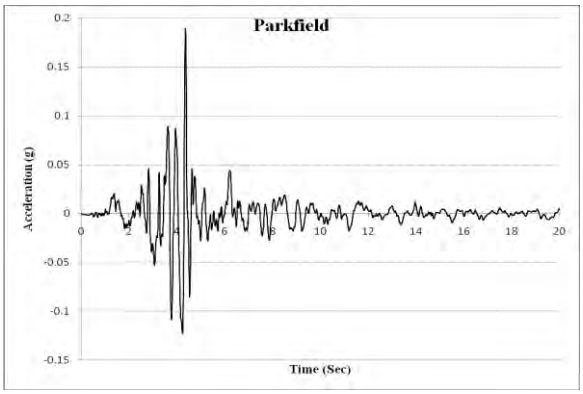

(f) Parkfield earthquake

Figure 4.1(b) Scaled Input Ground motions (a) Coalinga earthquake, (b) Hector Mine earthquake, (c) Michocan earthquake, (d) Nahanni earthquake, (e) Ofunata earthquake and (f) Parkfield earthquake

Figure 4.2 shows the comparison of input PSA for different input ground motions and figure 4.3 shows the comparison of mean and standard deviation for different input ground motions that are used for analysis.

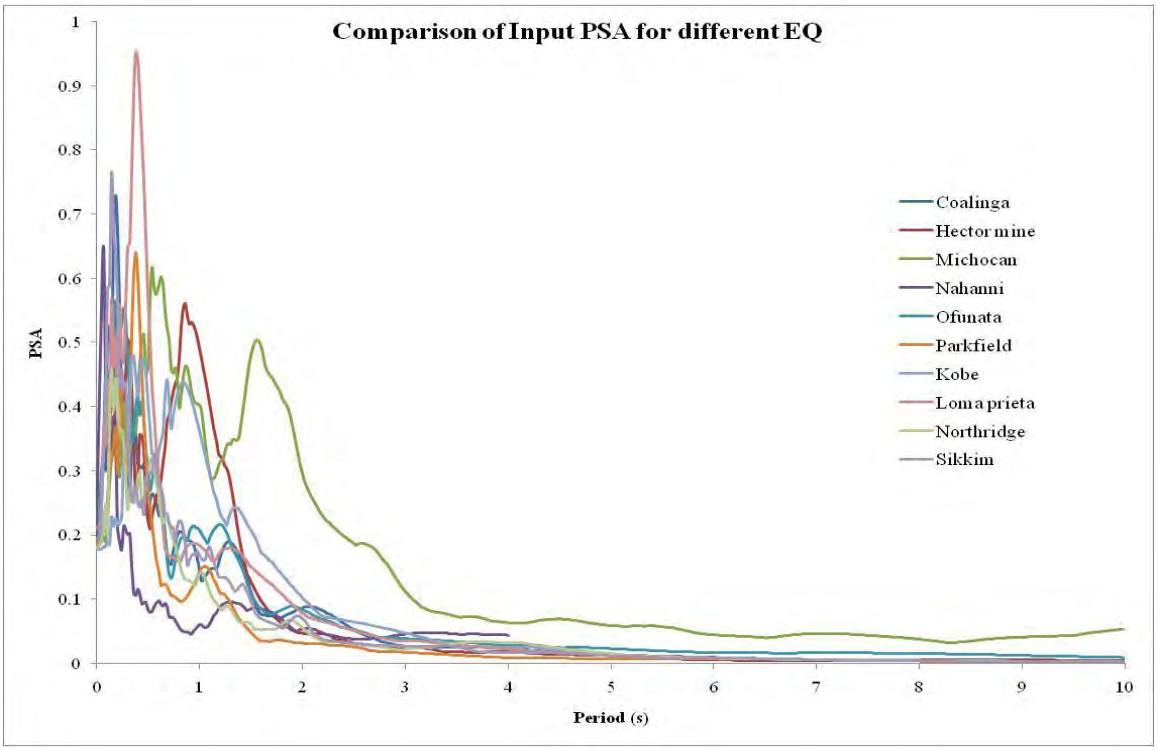

Figure 4.2 Comparison of input PSA for different input ground motion

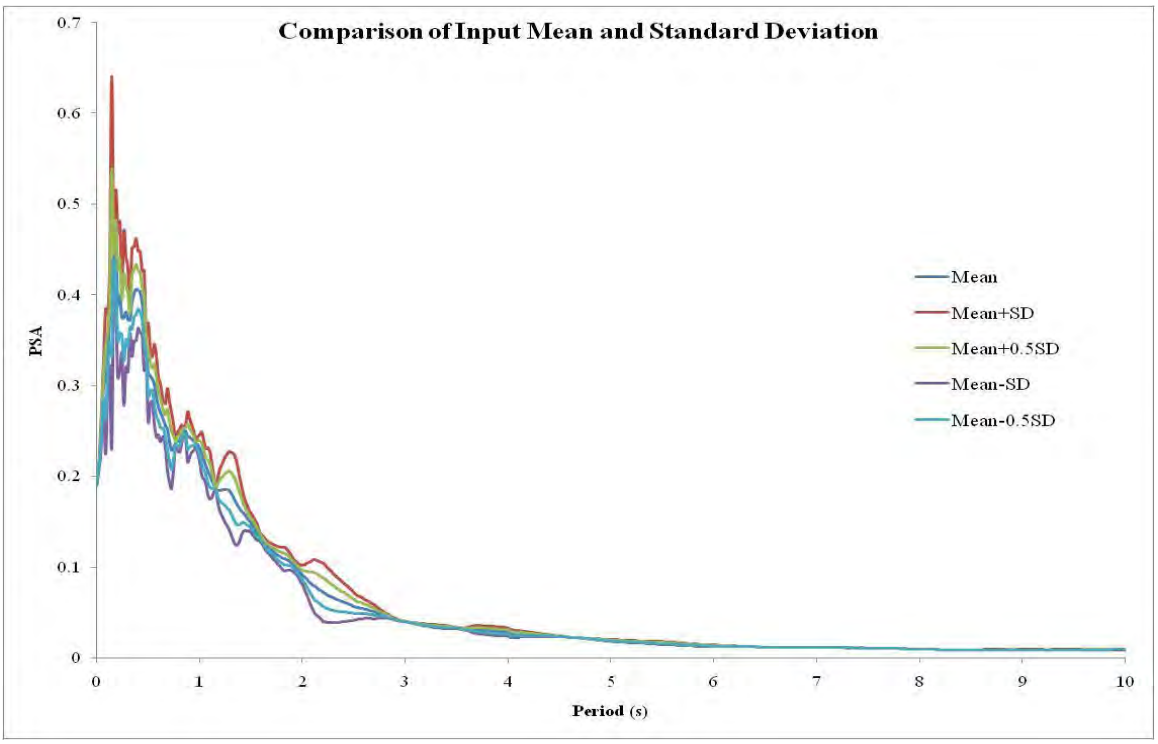

Figure 4.3 Comparison of Mean and Standard Deviation for different input ground motion

4.2.1 SITE: KAWRAN BAZAR

This site has been situated in middle-eastern part of Dhaka city. Different geotechnical and geophysical test are conducted to characterize the site. Design soil profile is given in Figure 4.4 with average shear wave velocity for each layer. Average shear wave velocity for 30m layer (V_{30avg}) is

$$V_{30\,avg} = \frac{\sum_{i=1}^{N} h_i}{\sum_{i=1}^{N} \frac{h_i}{V_i}} = 164 \text{ m/s}$$

Where, h is the thickness of soil layer, and V is the respective shear wave velocity.

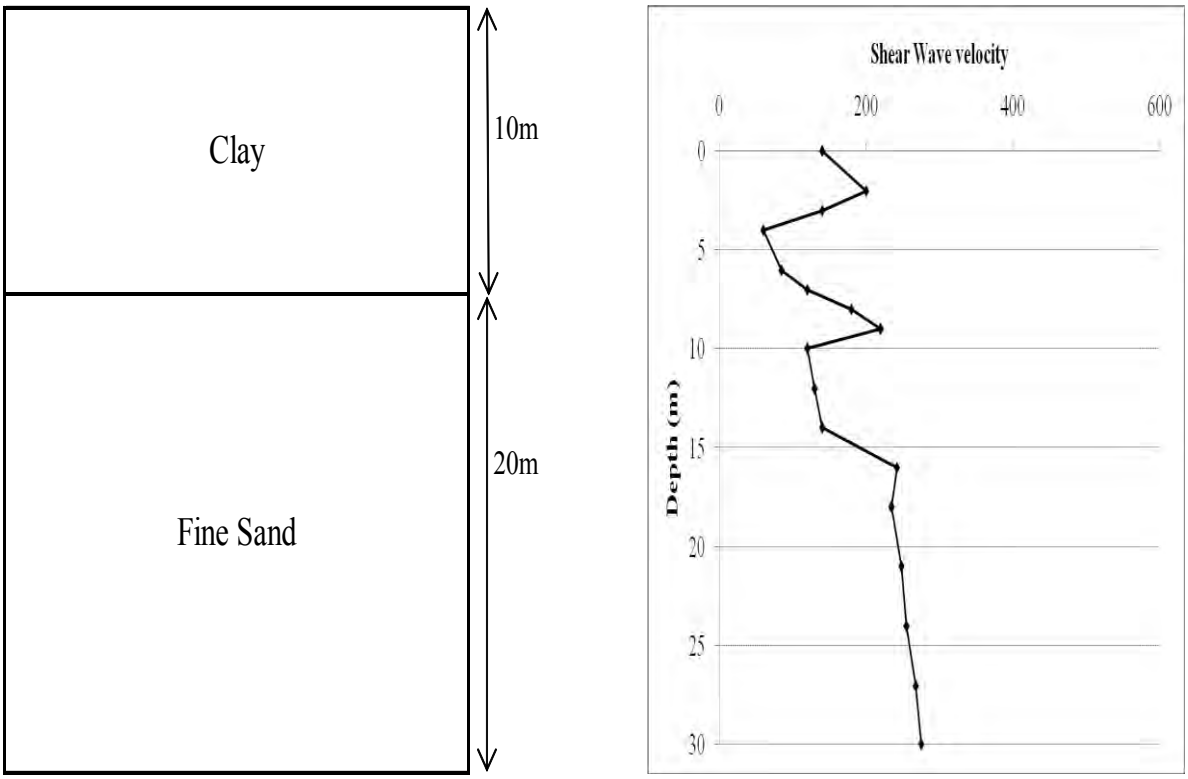

a) Design soil profile

b) Shear wave velocity profile

Figure 4.4: Site Characterization

Response Spectra

Response spectra of four earthquakes are shown in Figure 4.5. Among the four earthquakes, Kobe earthquake produces highest (0.35g) peak spectral acceleration (PSA) for this site and Northridge earthquake produces lowest (0.0029g) peak spectral acceleration (PSA). It is observed that initially soil surface response is less than input response for all four earthquakes for this site. But gradually surface response increases.

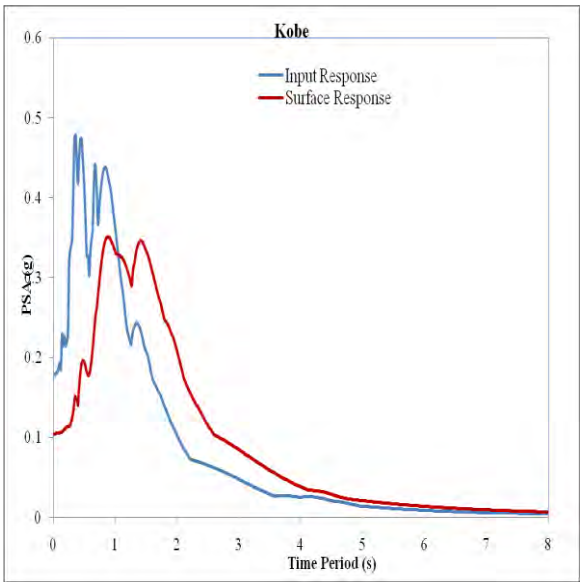

a) Kobe earthquake

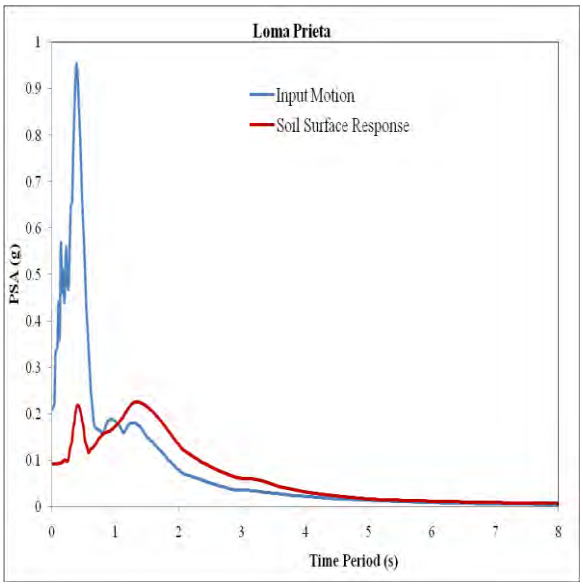

b) Loma prieta earthquake

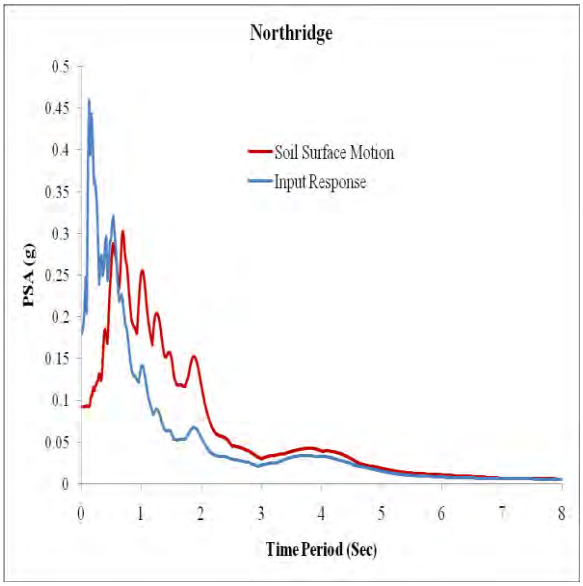

c) Nothridge earthquake

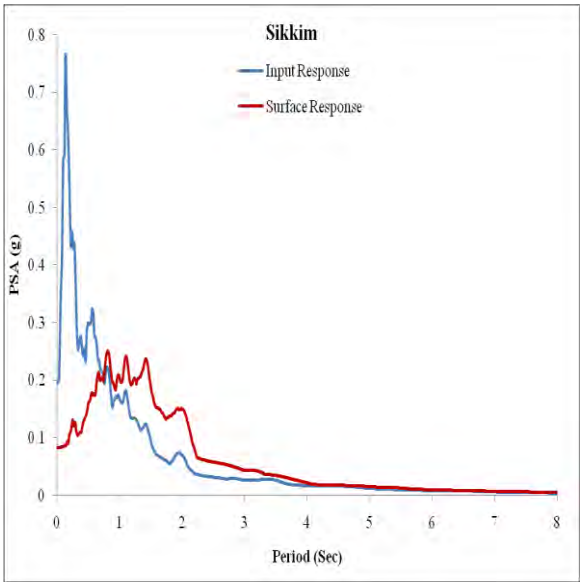

d) Sikkim earthquake

Figure 4.5: Response Spectra

Time Histories

The design soil profile is excited with input motion of four earthquakes to determine the dynamic response of local soil. Equivalent linear approach is used for site response analysis. As the seismic waves travel up and down, the soil vibrates. The acceleration of soil at the ground surface is shown in Figure 4.6. It is noted that the PGA and the ordinates of the response spectra increased.

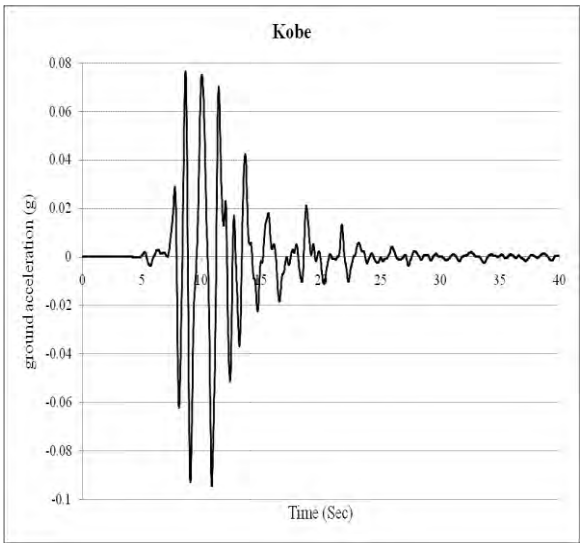

a) Kobe earthquake

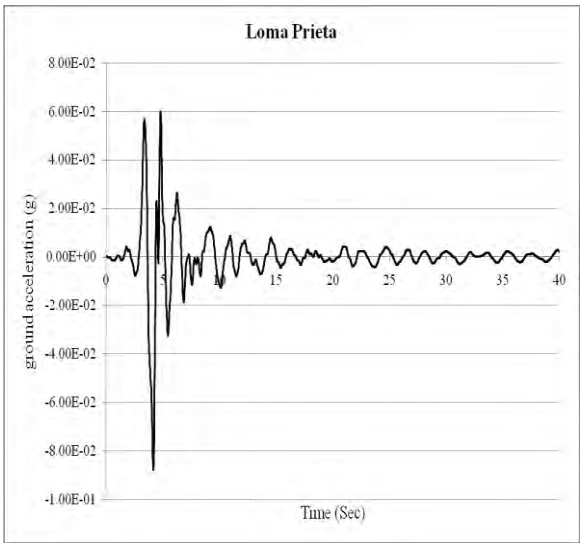

b) Loma prieta earthquake

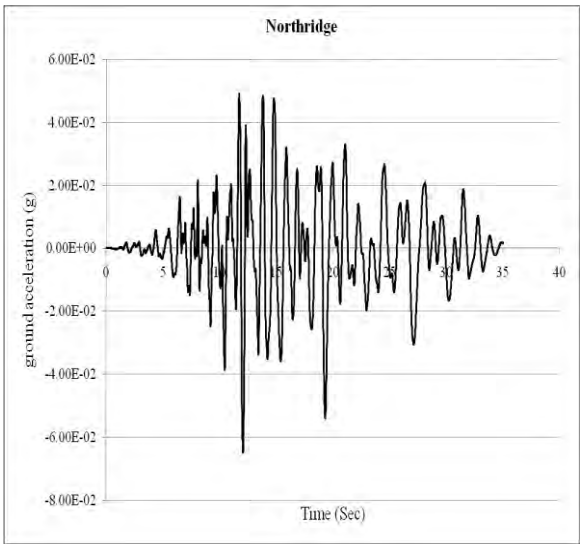

c) Nothridge earthquake

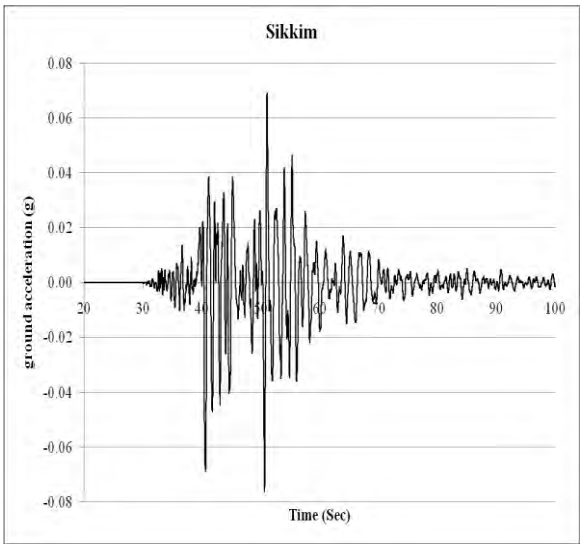

d) Sikkim earthquake

Figure 4.6: Time histories for local site effects

Maximum Peak Ground Acceleration (PGA)

Maximum Peak Ground Acceleration (PGA) at different depths of four earthquakes for this site is shown in figure 4.7. PGA at surface and that at bedrock is obtained from the analysis. The peak ground acceleration values at surface are observed to be in the range of 0.079g (Northridge) to as high as 0.105g (Kobe) and that of the bedrock were observed to vary from 0.177g (Kobe) to 0.212g (Loma prieta). The impedance in the acceleration values can be observed. Such as, a sudden rise within few meters can cause considerable damage to the sub and super structure resulting in huge loss.

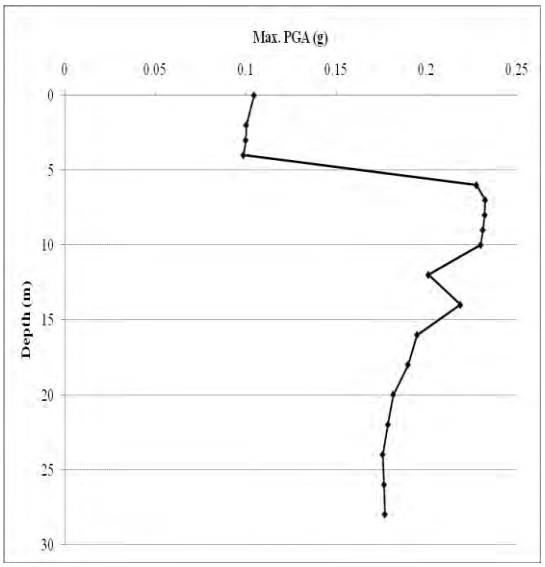

a) Kobe earthquake

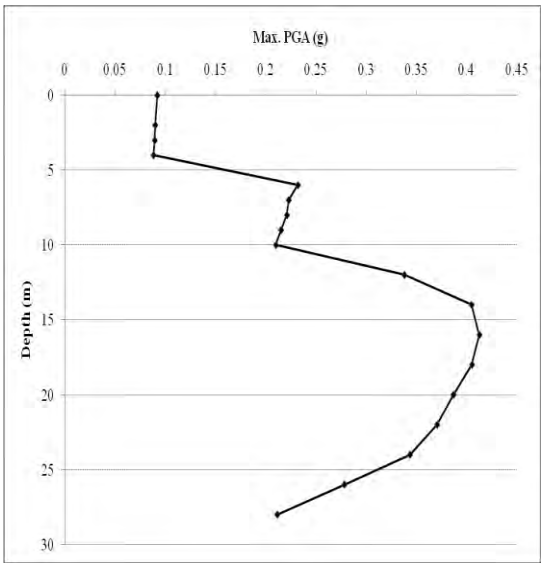

b) Loma prieta earthquake

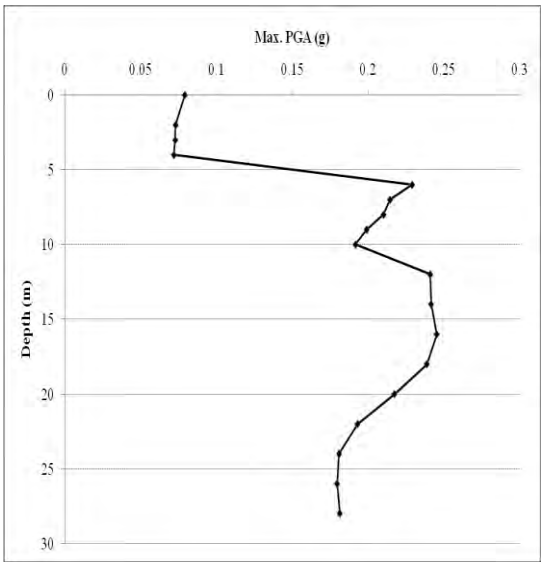

c) Nothridge earthquake

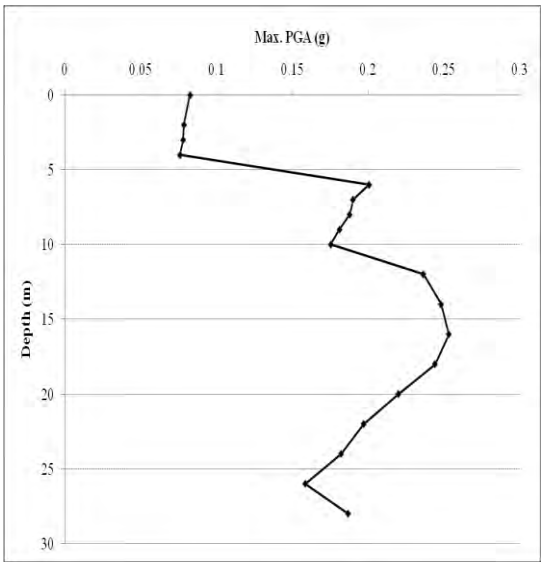

d) Sikkim earthquake

Figure 4.7: Maximum Peak Ground Acceleration for local site effects

Site amplification factors at sub surface layers are often used as one of the parameters for estimation of ground response. The amplification factor is the ratio of peak ground acceleration at surface to that of acceleration at hard rock. The amplification factors are determined as;

Amplification Factor = PGA recorded at ground surface / PGA recorded at hard rock
Amplification Factor (For Kobe earthquake) = 0.105/0.177 = 0.59
Amplification Factor (For Loma prieta earthquake) = 0.092/0.212 = 0.43
Amplification Factor (For Northridge earthquake) = 0.079/0.181 = 0.44
Amplification Factor (For Sikkim earthquake) = 0.082/0.187 = 0.44

Hence, the amplification factors have also been computed and it has been identified that similar to the peak ground acceleration values, the variation is within 0.43 (Loma prieta) to 0.59 (Kobe).

Maximum Stress Ratio

Maximum Stress Ratio at different depths of four earthquakes for this site is shown in figure 4.8. Maximum stress ratio at different depths of four earthquakes for this site is obtained from the analysis. The Maximum stress ratio values for Kobe earthquakes are observed to be in the range of 0.142 to as high as 0.237. The Maximum stress ratio values for Loma prieta earthquakes are observed to be in the range of 0.177 to as high as 0.351. The Maximum stress ratio values for Northridge earthquakes are observed to be in the range of 0.083 to as high as 0.181. The Maximum stress ratio values for Sikkim earthquakes are observed to be in the range of 0.133 to as high as 0.222.

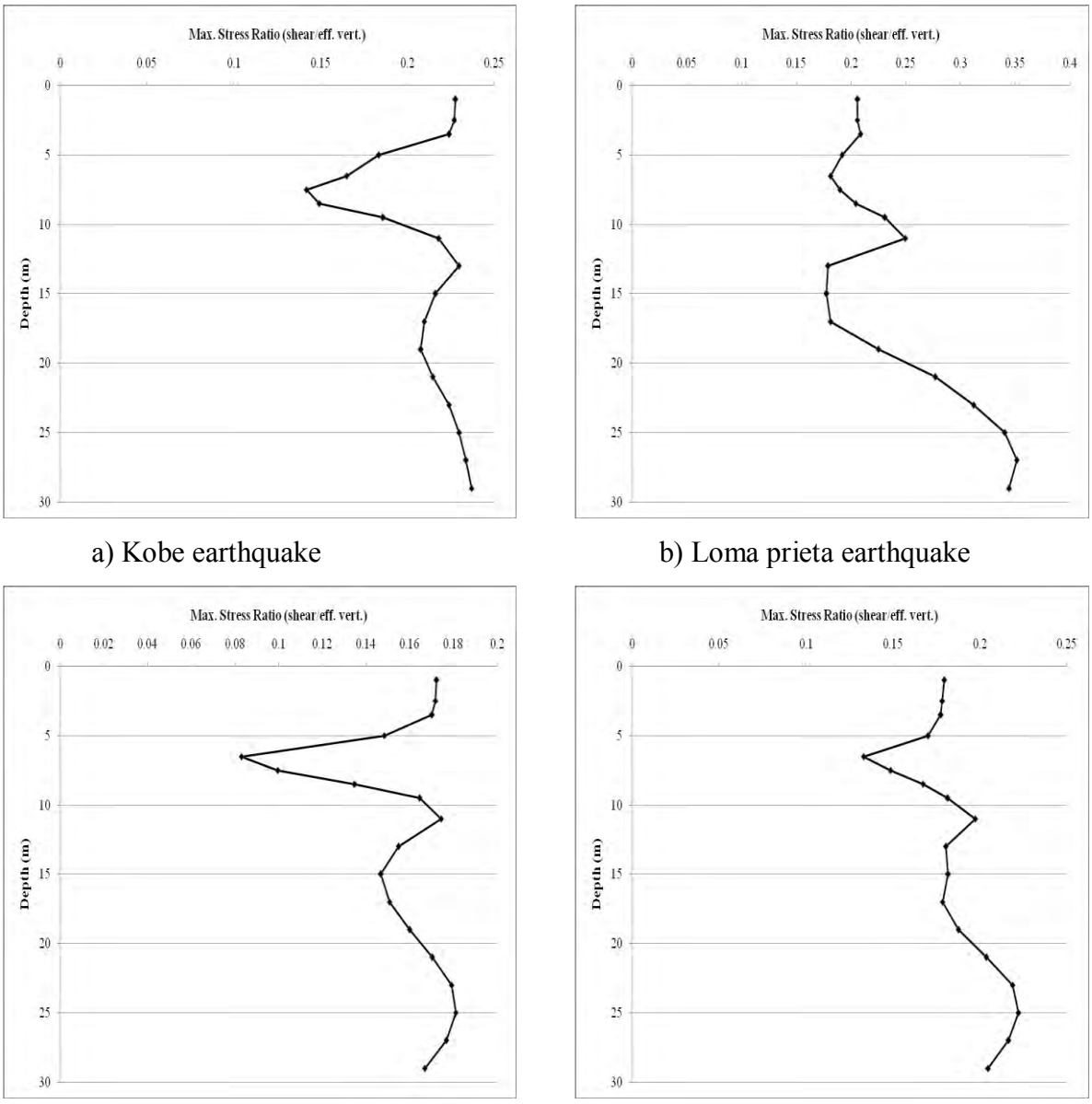

a) Kobe earthquake b) Loma prieta earthquake

c) Nothridge earthquake d) Sikkim earthquake

Figure 4.8: Maximum stress ratio for local site effects

Maximum Strain

Maximum Strain at different depths of four earthquakes for this site is shown in figure 4.9. Maximum strain values at different depths of four earthquakes for this site are obtained from the analysis. The Maximum strain values for Kobe earthquakes are observed to be in the range of 0.0061 to as high as 3.30. The Maximum strain values for Loma prieta earthquakes are observed to be in the range of 0.0054 to as high as 3.77. The Maximum strain values for Northridge earthquakes are observed to be in the range of 0.0044 to as high as 1.49. The Maximum strain values for Sikkim earthquakes are observed to be in the range of 0.0047 to as high as 2.262.

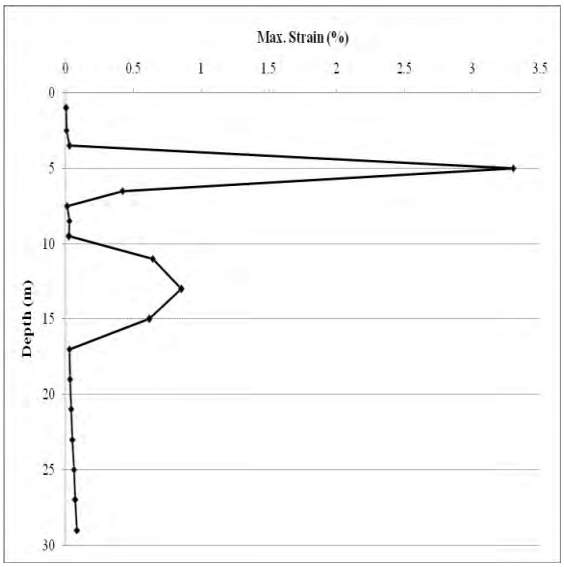

a) Kobe earthquake

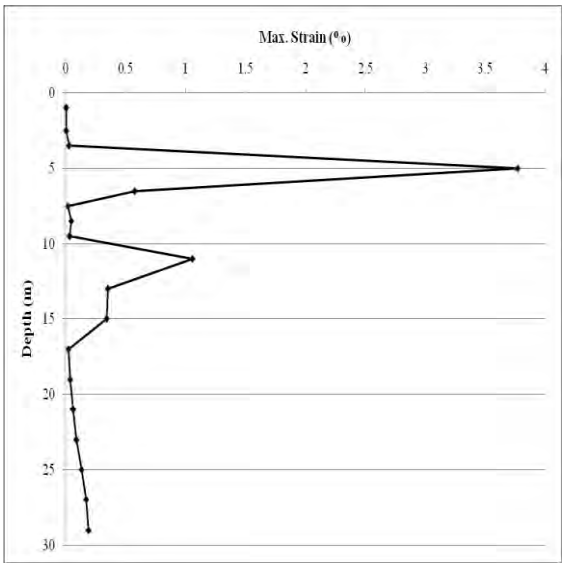

b) Loma prieta earthquake

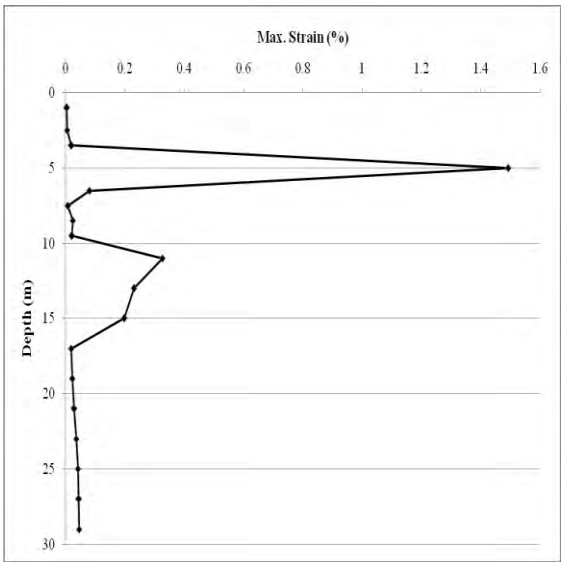

c) Nothridge earthquake

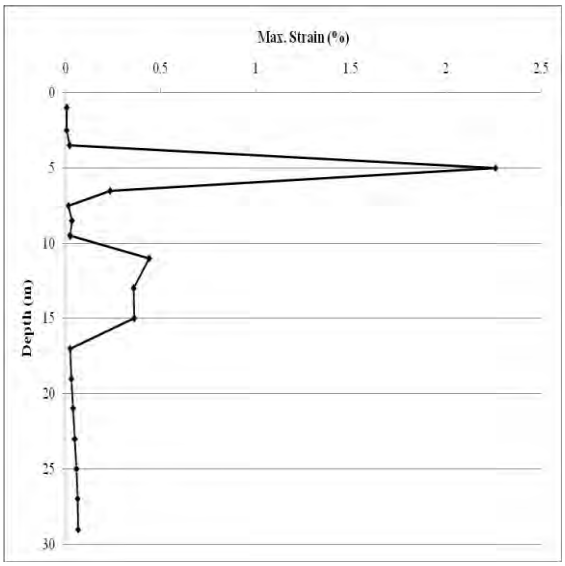

d) Sikkim earthquake

Figure 4.9: Maximum strain for local site effects

Figure 4.10 shows the comparison of Mean and Standard Deviation for surface PSA and Figure 4.11 shows the comparison of Surface PSA which are produced for different input motions.

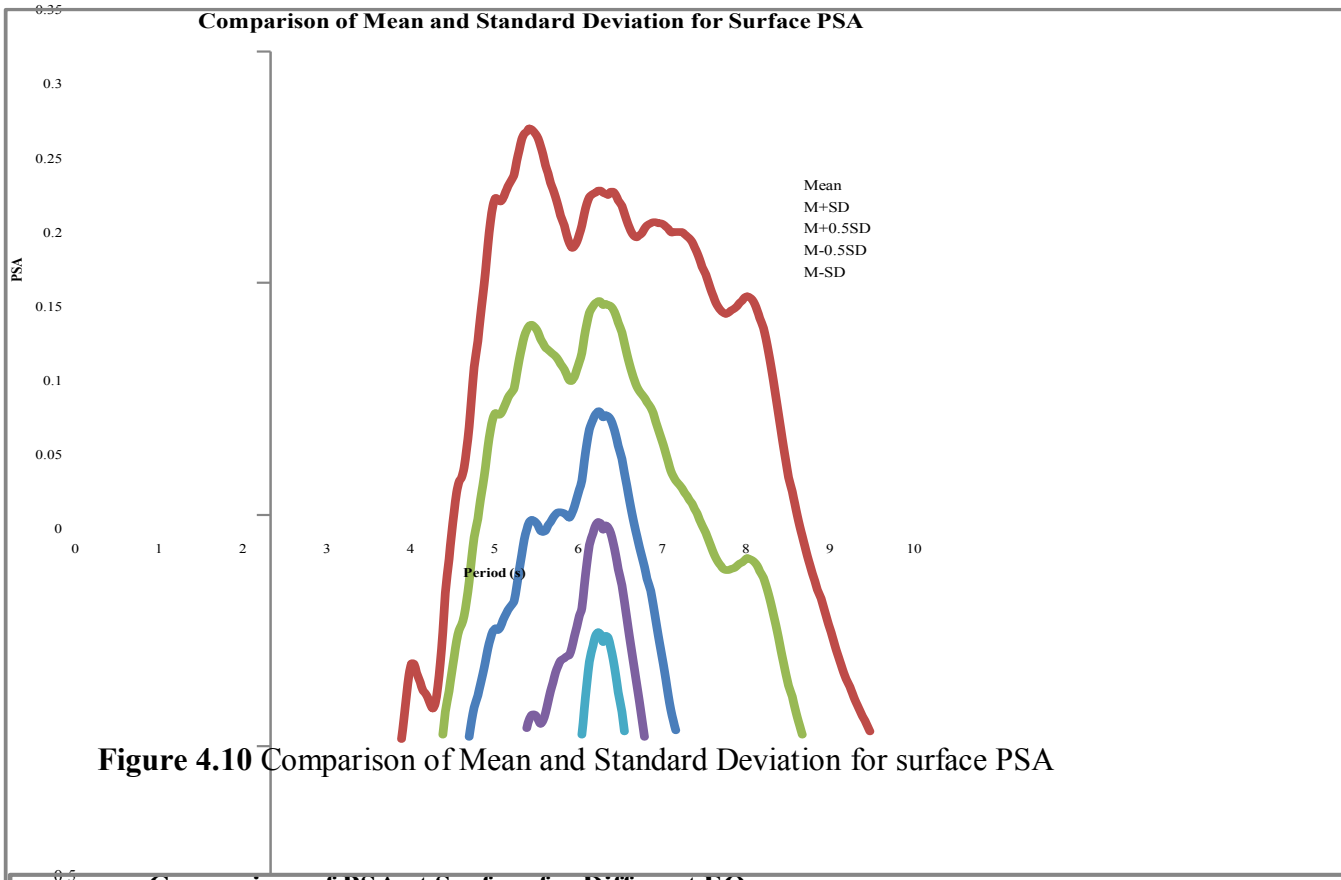

Figure 4.10 Comparison of Mean and Standard Deviation for surface PSA

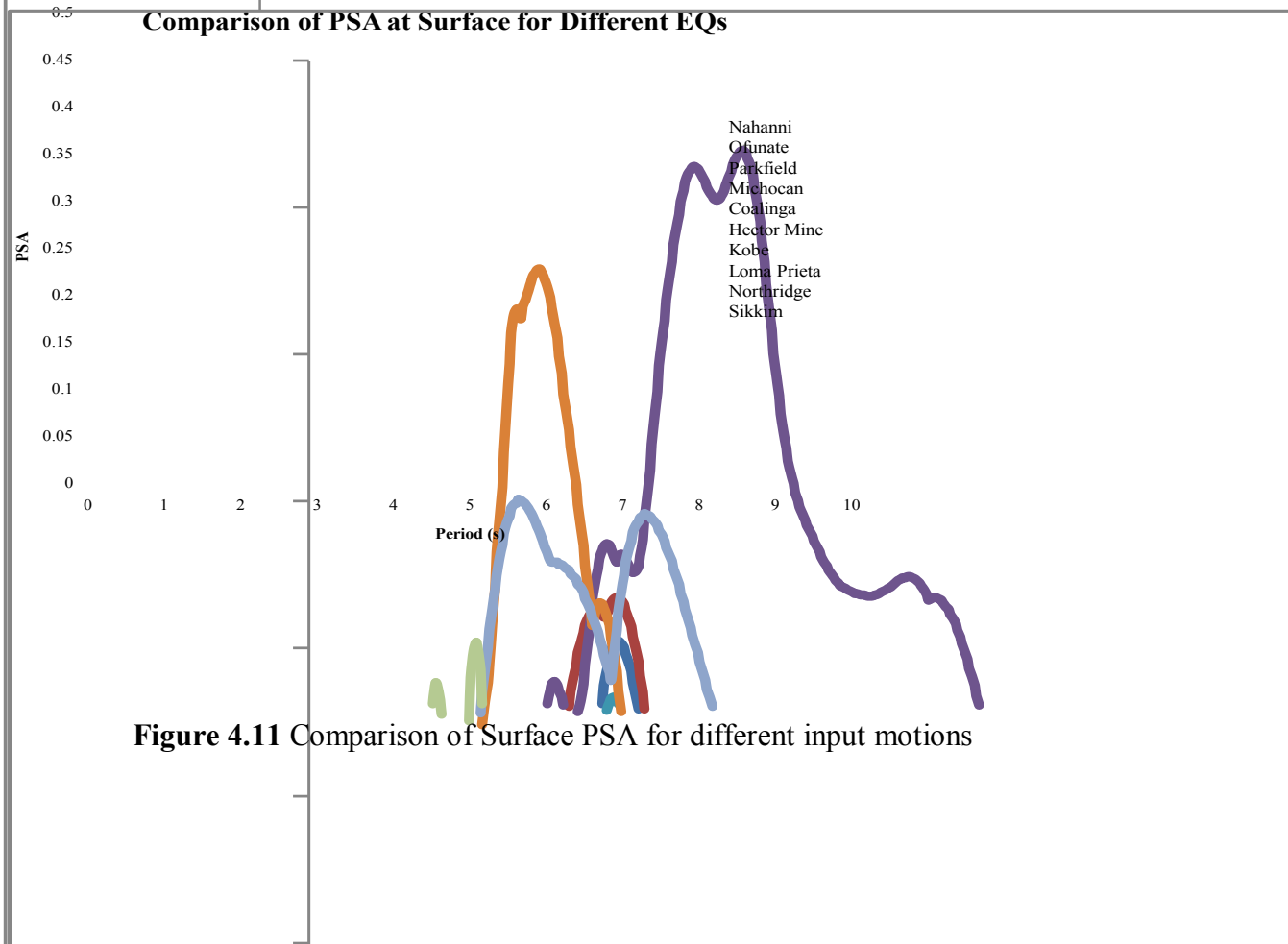

Figure 4.11 Comparison of Surface PSA for different input motions

Figure 4.12 shows the comparison of Mean Input PSA and Mean Surface PSA produced for different input motions.

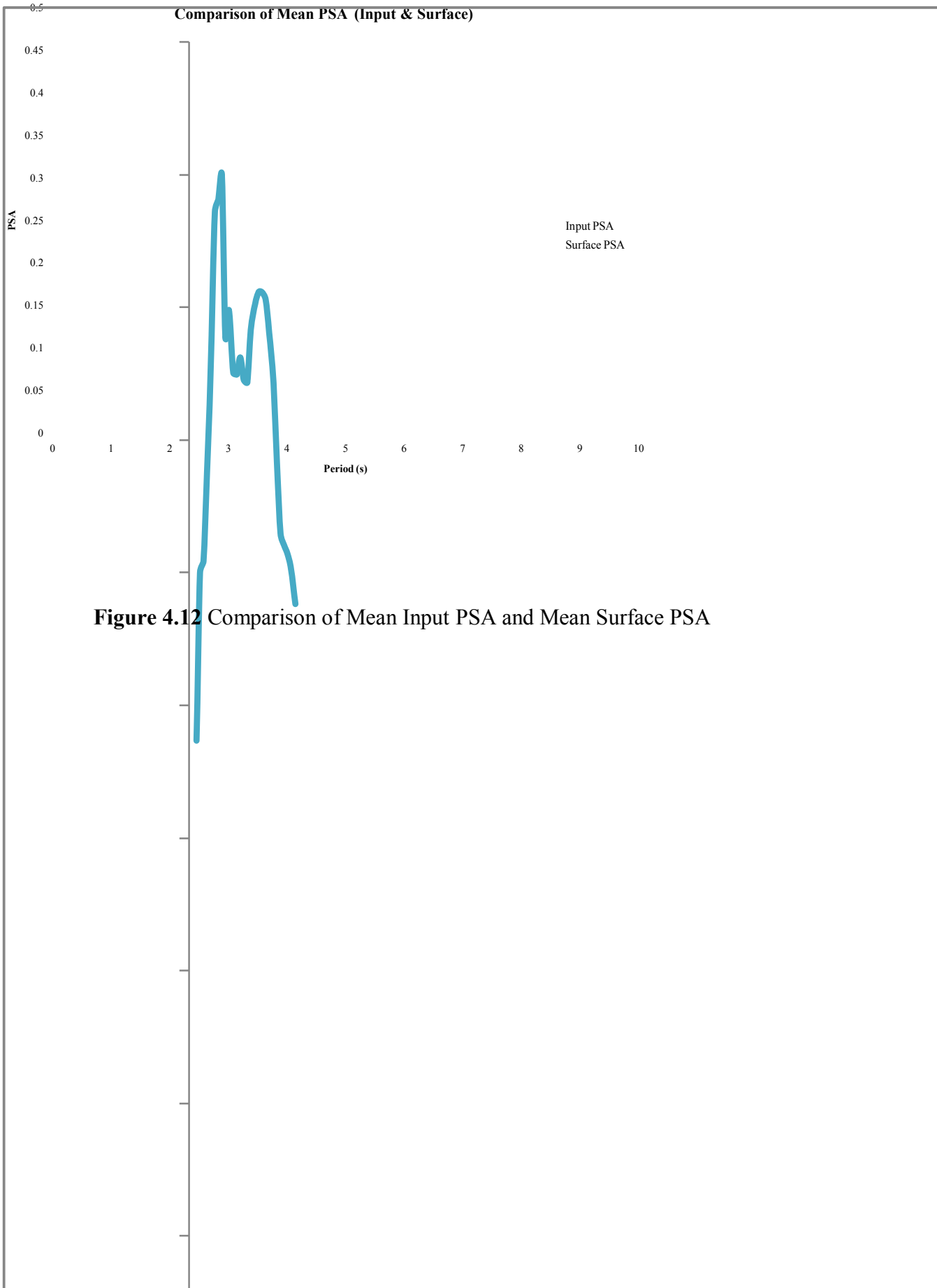

Figure 4.12 Comparison of Mean Input PSA and Mean Surface PSA

4.2.2 SITE: GULSHAN

This site has been situated in central part of Dhaka city. Different geotechnical and geophysical test are conducted to characterize the site. Design soil profile is given in Figure 4.13 with average shear wave velocity for each layer. Average shear wave velocity for 30m layer (V_{30avg}) is

$$V_{30\,avg} = \frac{\sum_{i=1}^{N} h_i}{\sum_{i=1}^{N} \frac{h_i}{V_i}} \quad = 234 \text{ m/s}$$

Where, h is the thickness of soil layer, and V is the respective shear wave velocity.

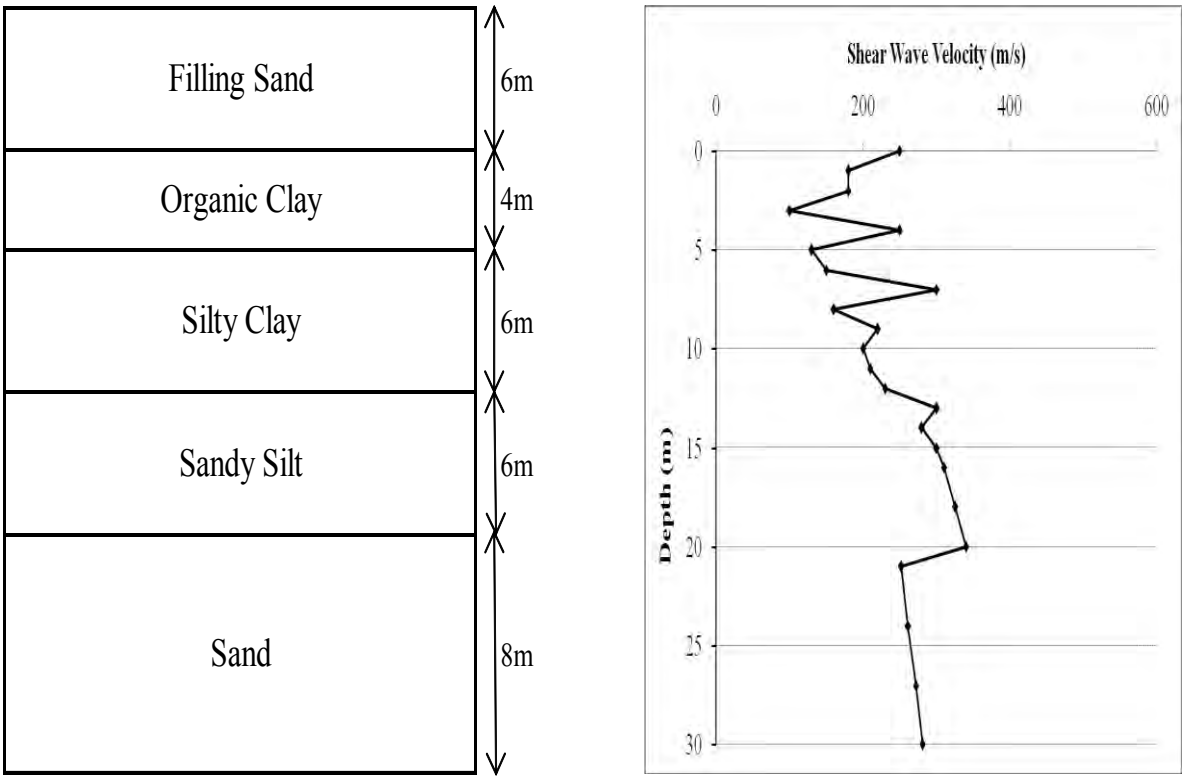

a) Design soil profile b) Shear wave velocity profile

Figure 4.13: Site Characterization

Response Spectra

Response spectra of four earthquakes are shown in Figure 4.14. Among the four earthquakes, Kobe earthquake produces highest (1.21g) peak spectral acceleration (PSA) for this site and Northridge earthquake produces lowest (0.0028g) peak spectral acceleration (PSA). It is observed that initially soil surface response is less than input response for all four earthquakes for this site. But gradually surface response increases.

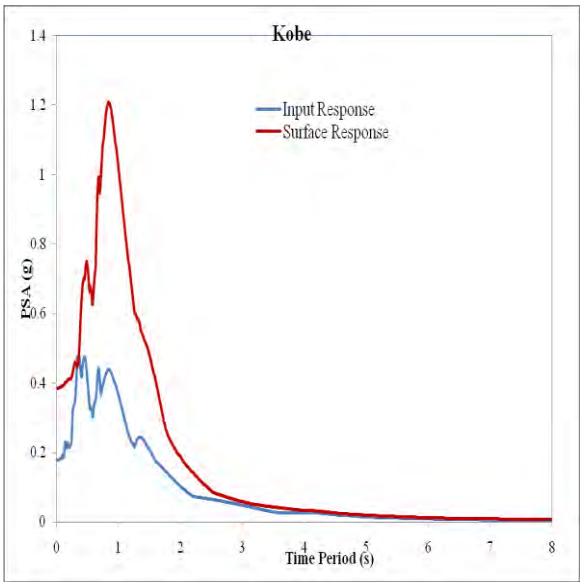

a) Kobe earthquake

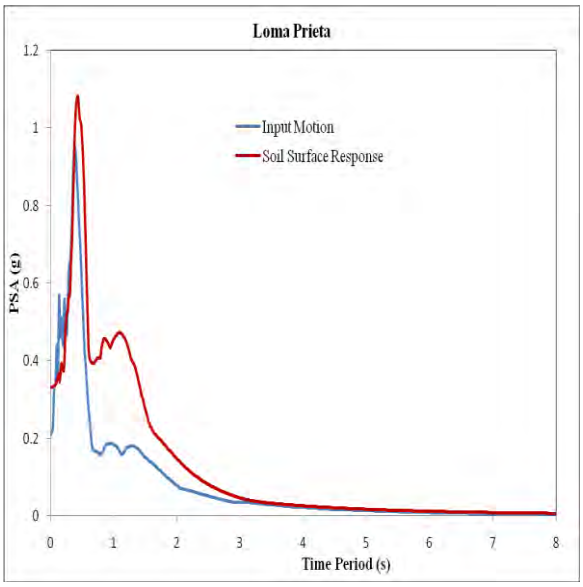

b) Loma prieta earthquake

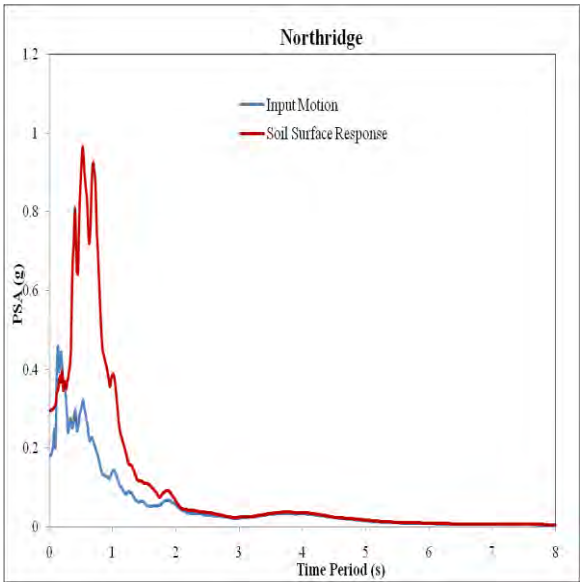

c) Nothridge earthquake

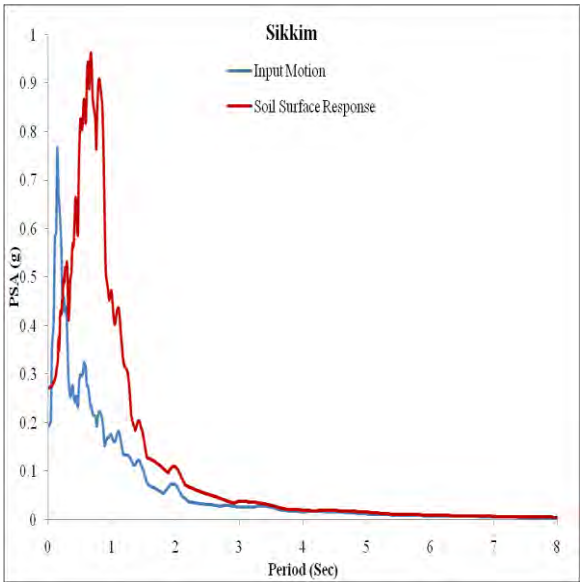

d) Sikkim earthquake

Figure 4.14: Response Spectra

Time Histories

The design soil profile is excited with input motion of four earthquakes to determine the dynamic response of local soil. Equivalent linear approach is used for site response analysis. As the seismic waves travel up and down, the soil vibrates. The acceleration of soil at the ground surface is shown in Figure 4.15. It is noted that the PGA and the ordinates of the response spectra increased.

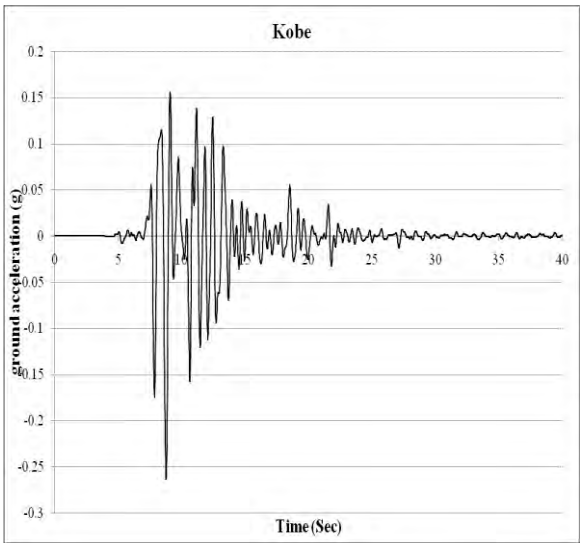

a) Kobe earthquake

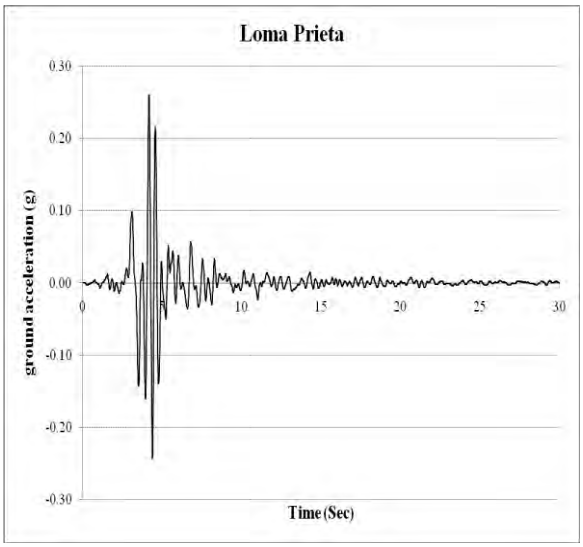

b) Loma prieta earthquake

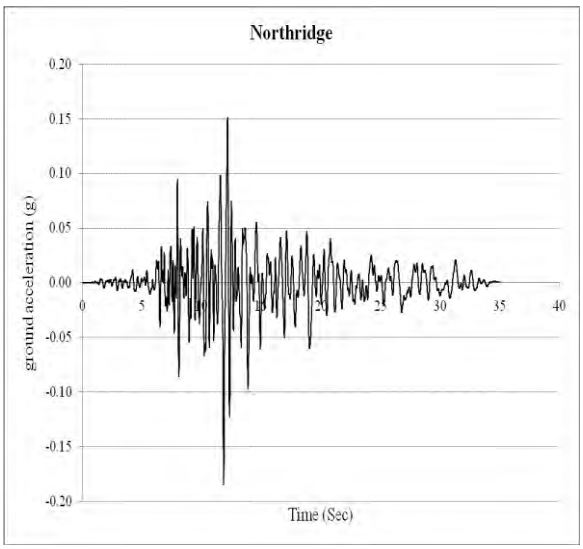

c) Nothridge earthquake

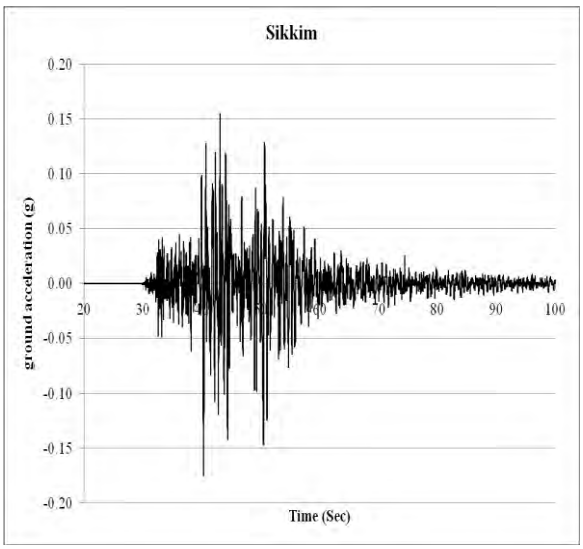

d) Sikkim earthquake

Figure 4.15: Time histories for local site effects

Maximum Peak Ground Acceleration (PGA)

Maximum Peak Ground Acceleration (PGA) at different depths of four earthquakes for this site is shown in figure 4.16. PGA at surface and that at bedrock is obtained from the analysis. The peak ground acceleration values at surface are observed to be in the range of 0.272g (Sikkim) to as high as 0.385g (Kobe) and that of the bedrock were observed to vary from 0.177g (Kobe) to 0.212g (Loma prieta). The impedance in the acceleration values can be observed. Such as, a sudden rise within few meters can cause considerable damage to the sub and super structure resulting in huge loss.

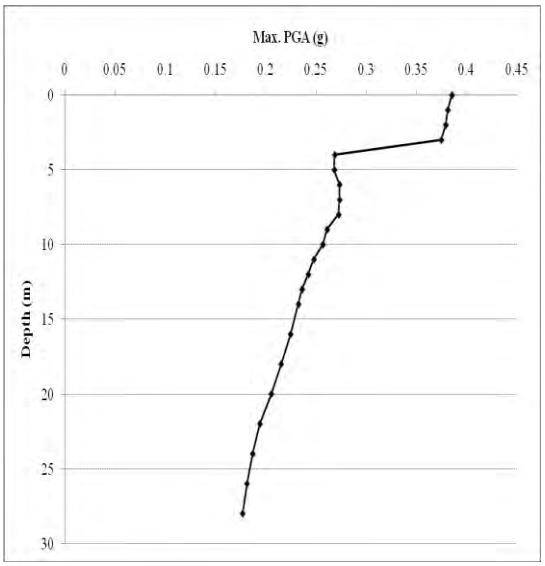

a) Kobe earthquake

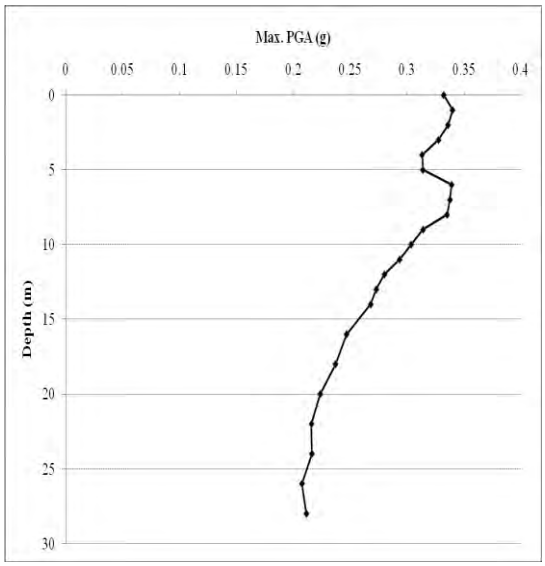

b) Loma prieta earthquake

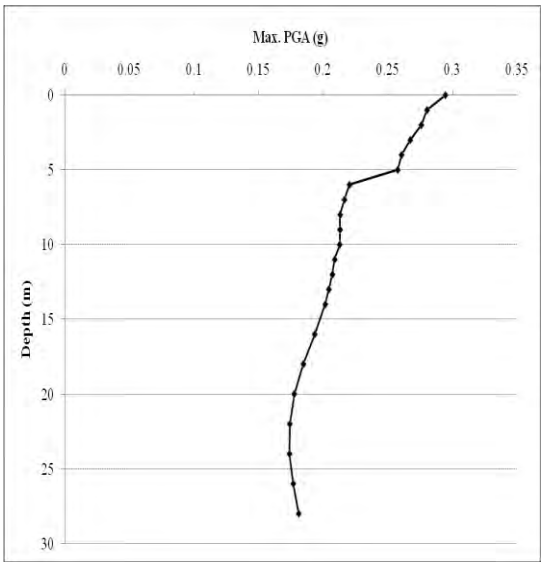

c) Nothridge earthquake

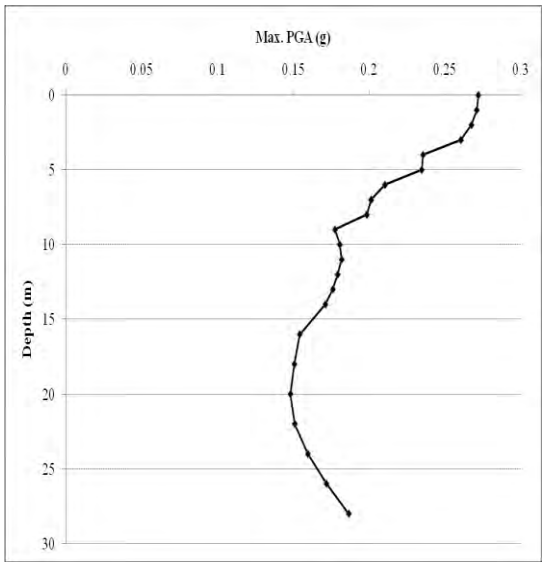

d) Sikkim earthquake

Figure 4.16: Maximum Peak Ground Acceleration for local site effects

Site amplification factors at sub surface layers are often used as one of the parameters for estimation of ground response. The amplification factor is the ratio of peak ground acceleration at surface to that of acceleration at hard rock. The amplification factors are determined as;

Amplification Factor = PGA recorded at ground surface / PGA recorded at hard rock
Amplification Factor (For Kobe earthquake) = 0.385/0.177 = 2.18
Amplification Factor (For Loma prieta earthquake) = 0.332/0.212 = 1.57
Amplification Factor (For Northridge earthquake) = 0.295/0.181 = 1.63
Amplification Factor (For Sikkim earthquake) = 0.272/0.187 = 1.45

Hence, the amplification factors have also been computed and it has been identified that similar to the peak ground acceleration values, the variation is within 1.45 (Sikkim) to 2.18 (Kobe).

Maximum Stress Ratio

Maximum Stress Ratio at different depths of four earthquakes for this site is shown in figure 4.17. Maximum stress ratio at different depths of four earthquakes for this site is obtained from the analysis. The Maximum stress ratio values for Kobe earthquakes are observed to be in the range of 0.351 to as high as 0.853. The Maximum stress ratio values for Loma prieta earthquakes are observed to be in the range of 0.314 to as high as 0.733. The Maximum stress ratio values for Northridge earthquakes are observed to be in the range of 0.212 to as high as 0.648. The Maximum stress ratio values for Sikkim earthquakes are observed to be in the range of 0.235 to as high as 0.601.

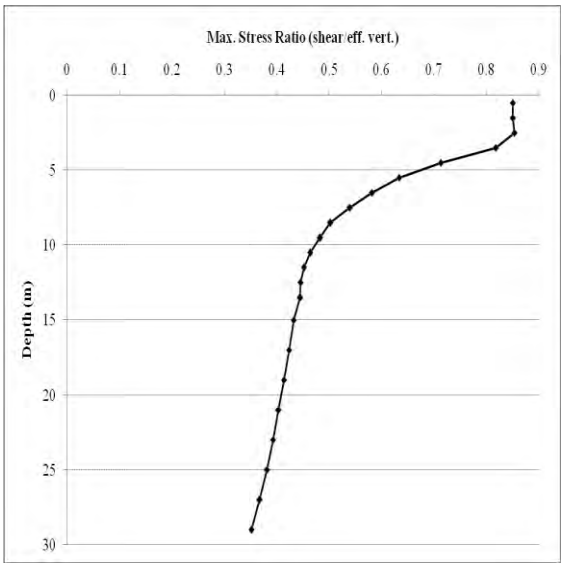

a) Kobe earthquake

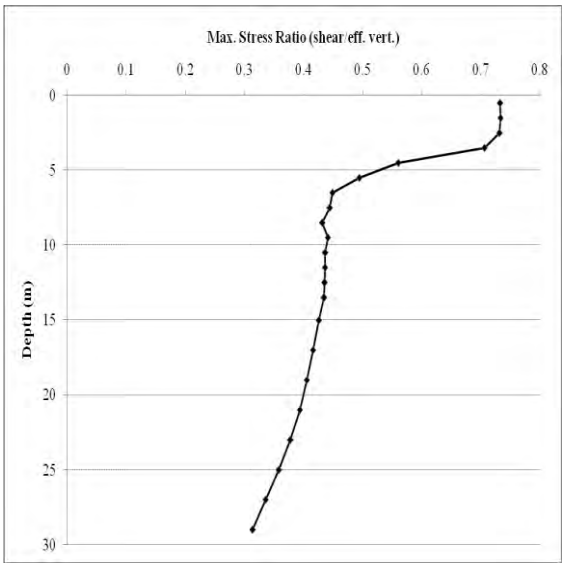

b) Loma prieta earthquake

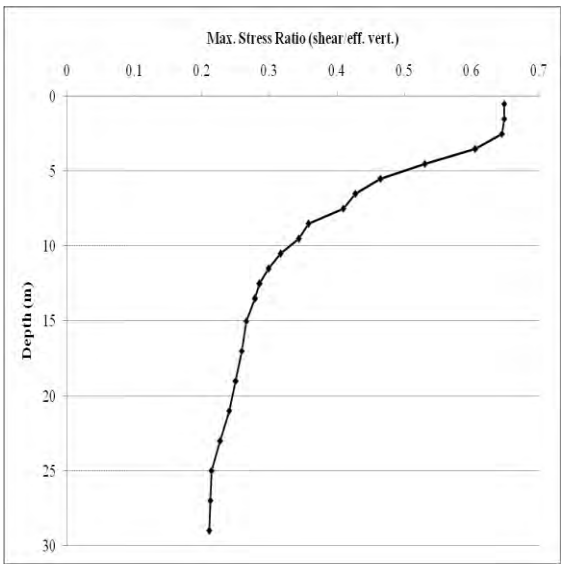

c) Nothridge earthquake

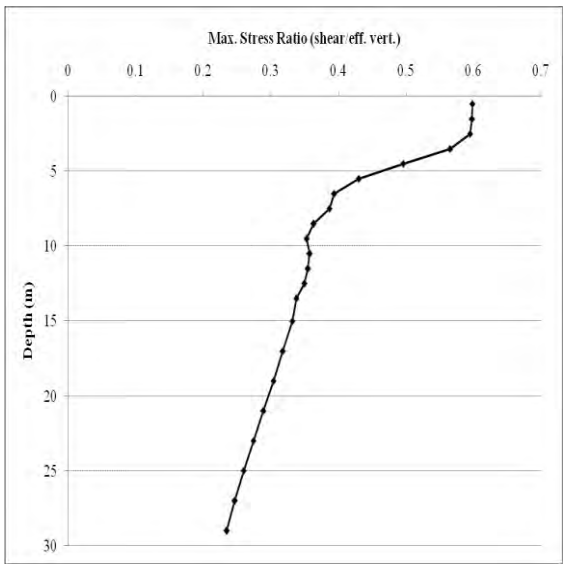

d) Sikkim earthquake

Figure 4.17: Maximum stress ratio for local site effects

Maximum Strain

Maximum Strain at different depths of four earthquakes for this site is shown in figure 4.18. Maximum strain values at different depths of four earthquakes for this site are obtained from the analysis. The Maximum strain values for Kobe earthquakes are observed to be in the range of 0.0033 to as high as 5.25. The Maximum strain values for Loma prieta earthquakes are observed to be in the range of 0.0028 to as high as 2.89. The Maximum strain values for Northridge earthquakes are observed to be in the range of 0.0196 to as high as 1.63. The Maximum strain values for Sikkim earthquakes are observed to be in the range of 0.0023 to as high as 1.20.

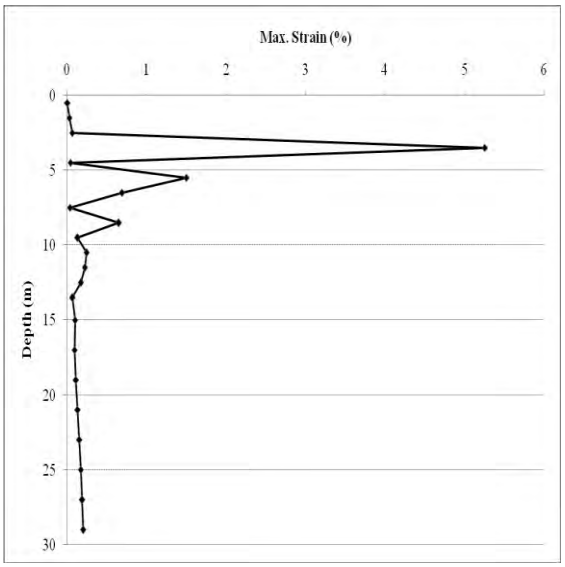

a) Kobe earthquake

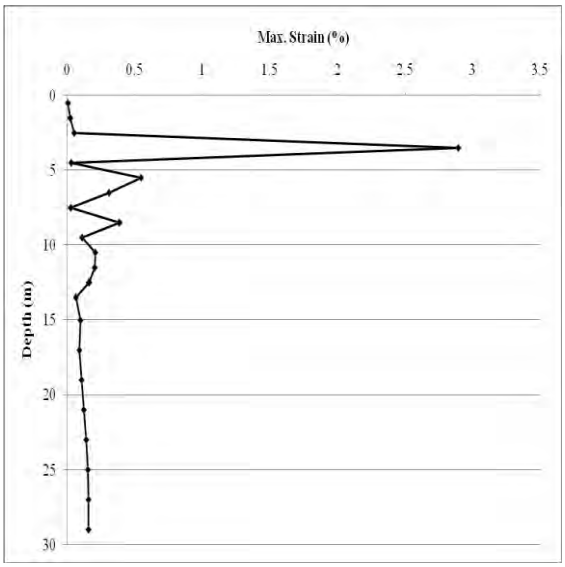

b) Loma prieta earthquake

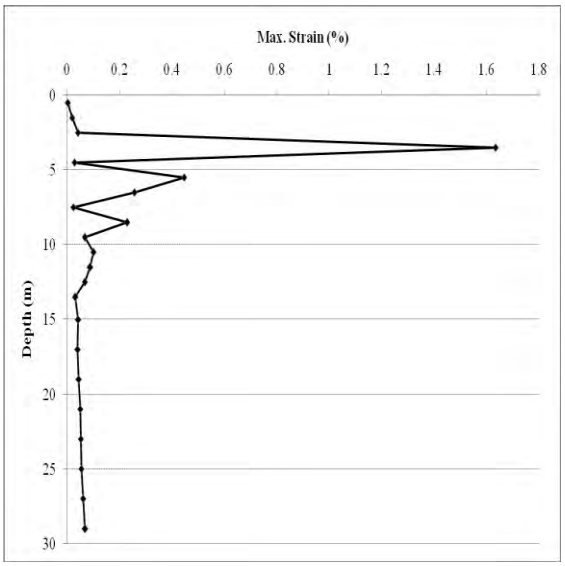

c) Nothridge earthquake

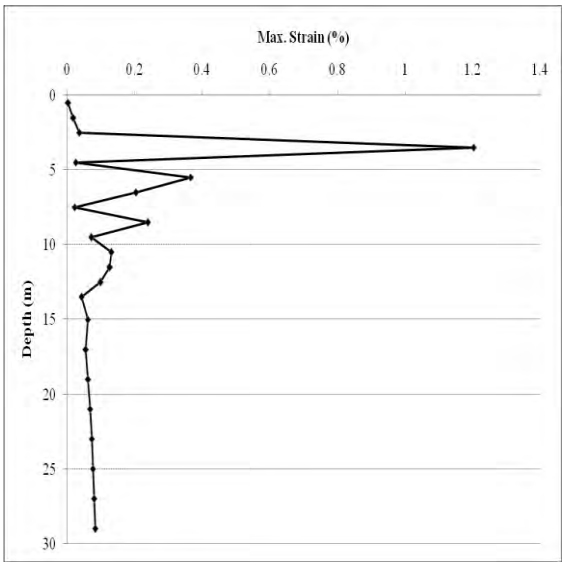

d) Sikkim earthquake

Figure 4.18: Maximum strain for local site effects

Figure 4.19 shows the comparison of Mean and Standard Deviation for surface PSA and Figure 4.20 shows the comparison of Surface PSA which are produced for different input motions.

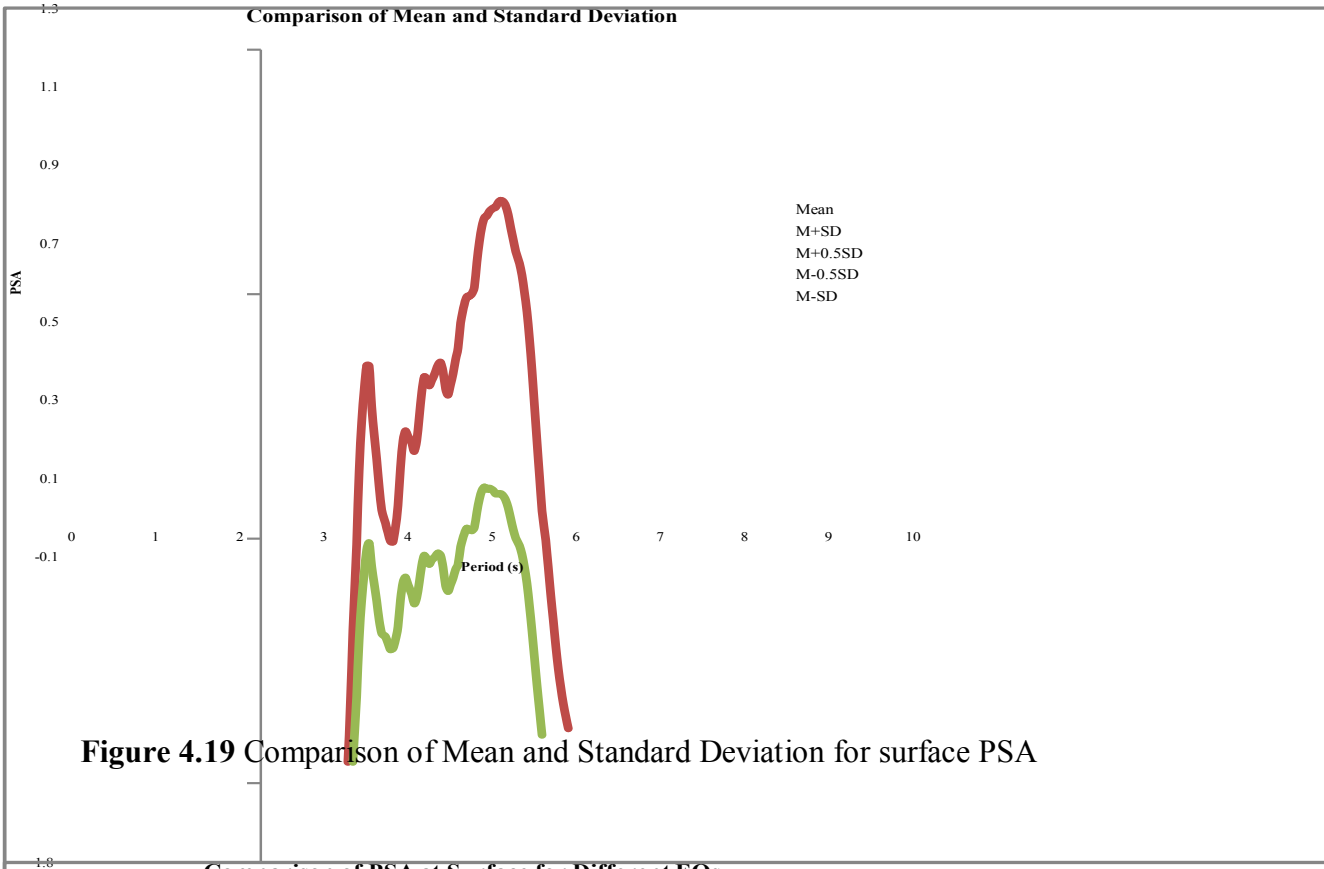

Figure 4.19 Comparison of Mean and Standard Deviation for surface PSA

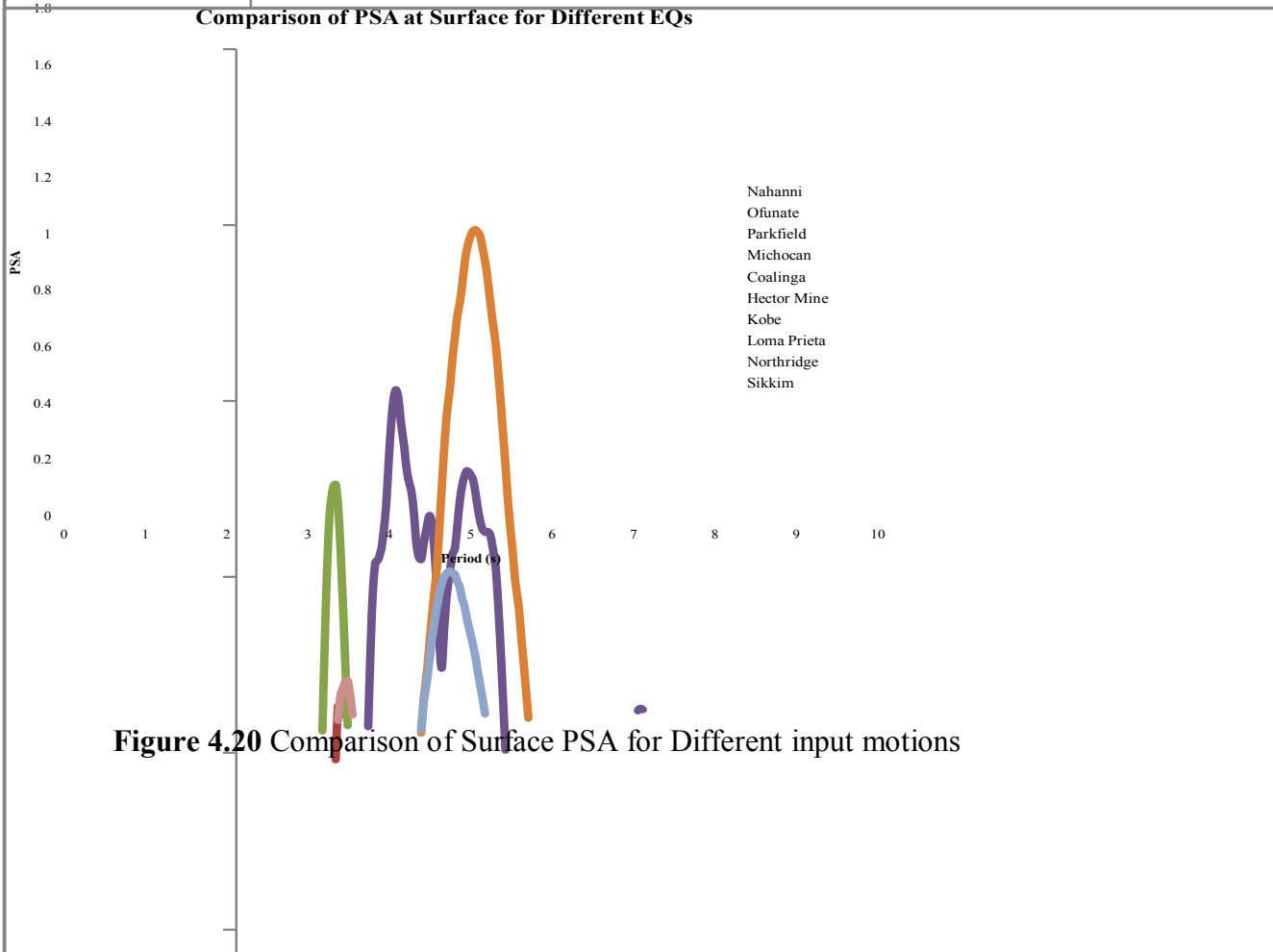

Figure 4.20 Comparison of Surface PSA for Different input motions

Figure 4.21 shows the comparison of Mean Input PSA and Mean Surface PSA produced for different input motions.

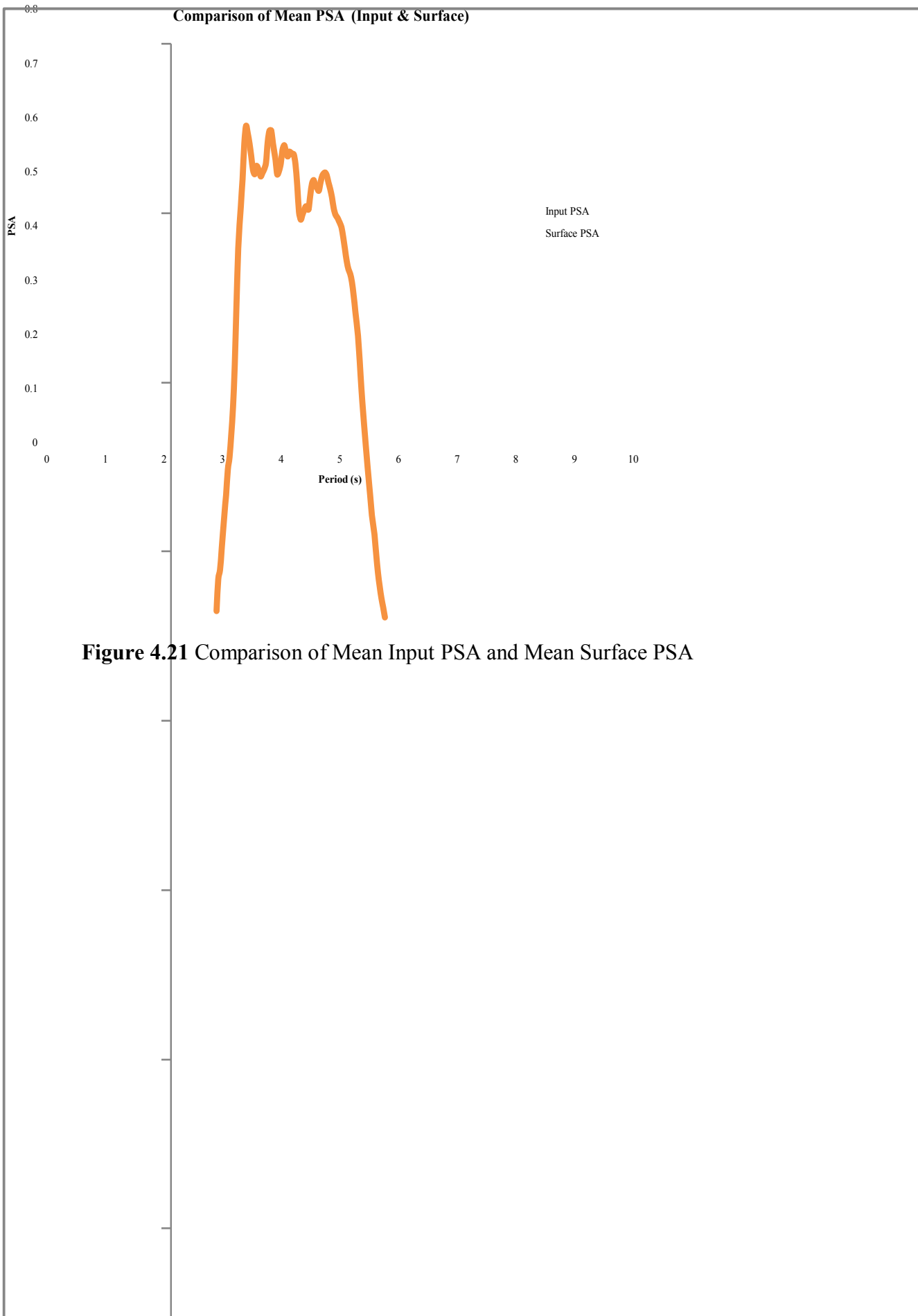

Figure 4.21 Comparison of Mean Input PSA and Mean Surface PSA

4.2.3 SITE: MUGDA

This site has been situated in eastern part of Dhaka city. Different geotechnical and geophysical test are conducted to characterize the site. Design soil profile is given in Figure 4.22 with average shear wave velocity for each layer. Average shear wave velocity for 30m layer (V_{30avg}) is

$$V_{30\,avg} = \frac{\sum_{i=1}^{N} h_i}{\sum_{i=1}^{N} \frac{h_i}{V_i}} \quad = 220 \text{ m/s}$$

Where, h is the thickness of soil layer, and V is the respective shear wave velocity.

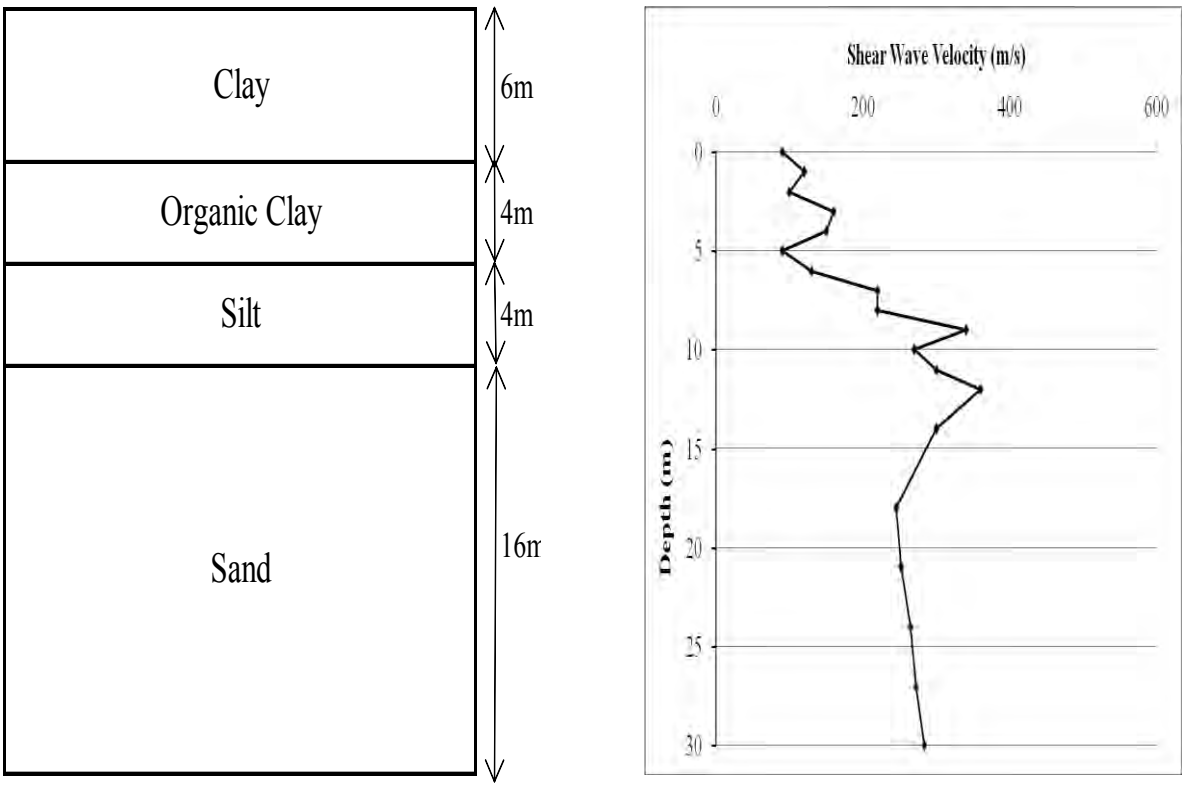

a) Design soil profile b) Shear wave velocity profile

Figure 4.22: Site Characterization

Response Spectra

Response spectra of four earthquakes are shown in Figure 4.23. Among the four earthquakes, Kobe earthquake produces highest (0.66g) peak spectral acceleration (PSA) for this site and Northridge earthquake produces lowest (0.0028g) peak spectral acceleration (PSA). It is observed that initially soil surface response is less than input response for all four earthquakes for this site. But gradually surface response increases.

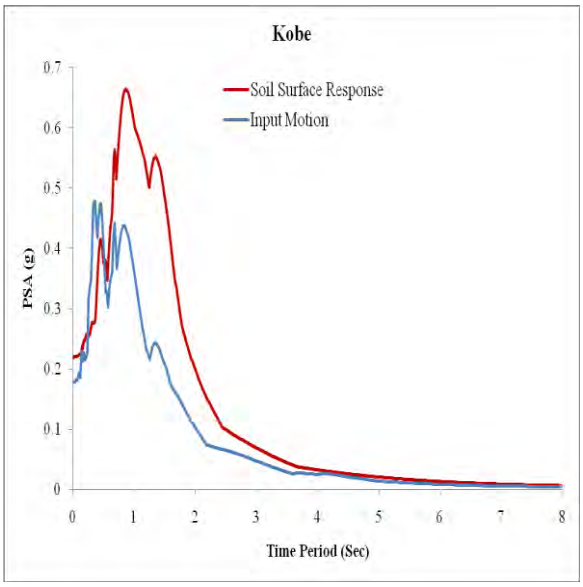

a) Kobe earthquake

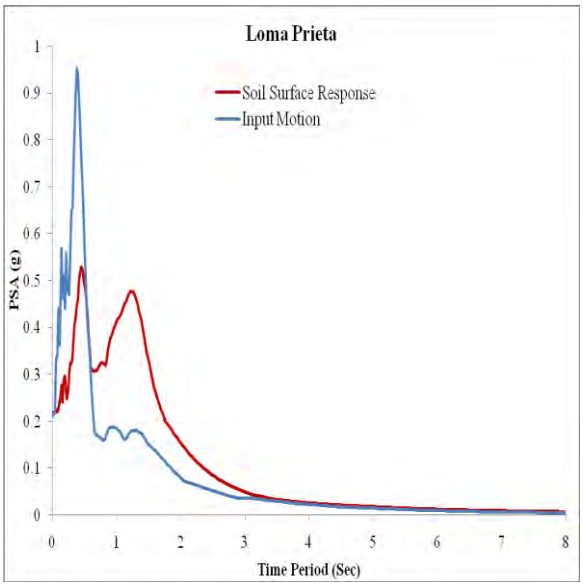

b) Loma prieta earthquake

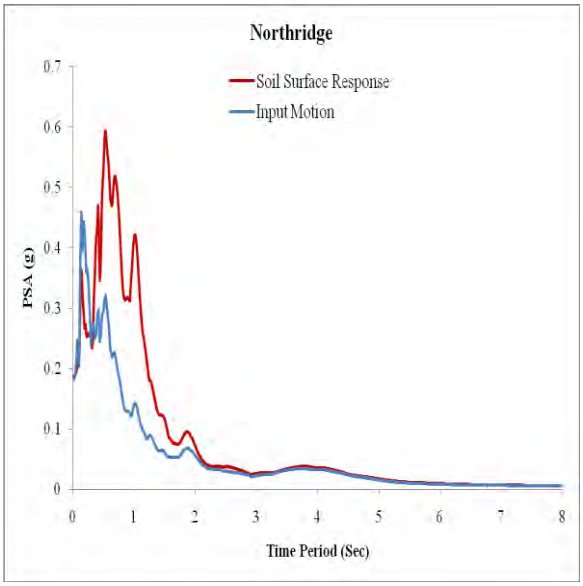

c) Nothridge earthquake

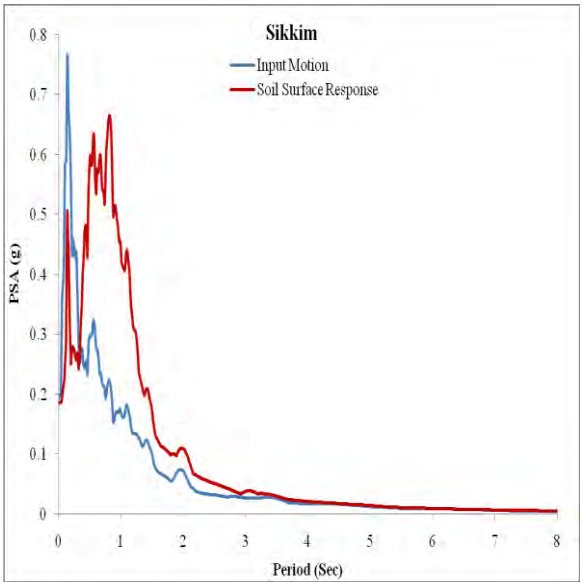

d) Sikkim earthquake

Figure 4.23: Response Spectra

Time Histories

The design soil profile is excited with input motion of four earthquakes to determine the dynamic response of local soil. Equivalent linear approach is used for site response analysis. As the seismic waves travel up and down, the soil vibrates. The acceleration of soil at the ground surface is shown in Figure 4.24. It is noted that the PGA and the ordinates of the response spectra increased.

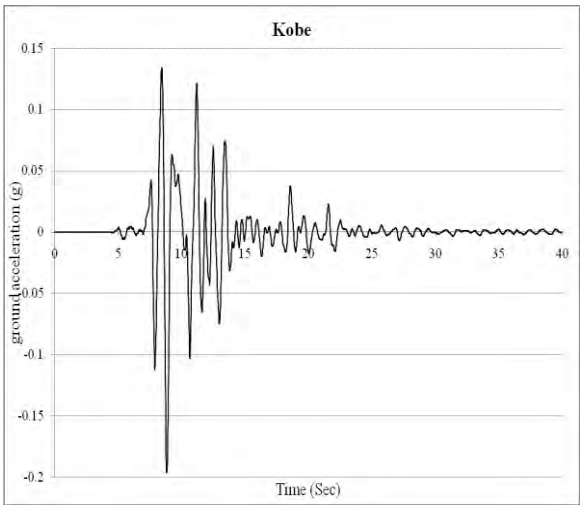

a) Kobe earthquake

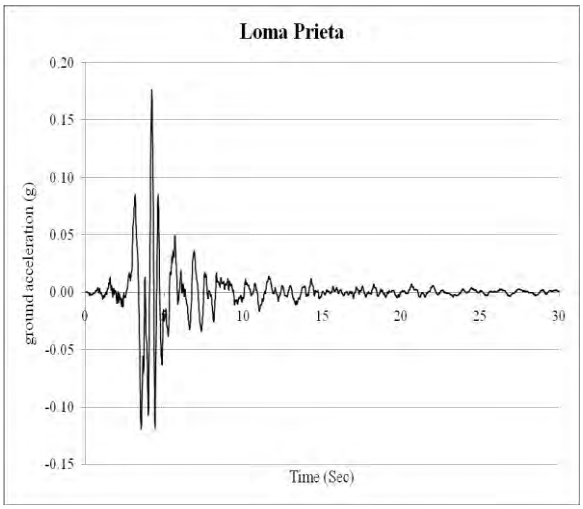

b) Loma prieta earthquake

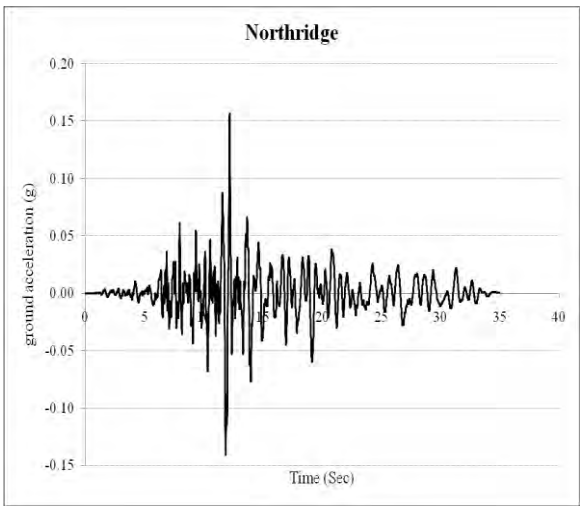

c) Nothridge earthquake

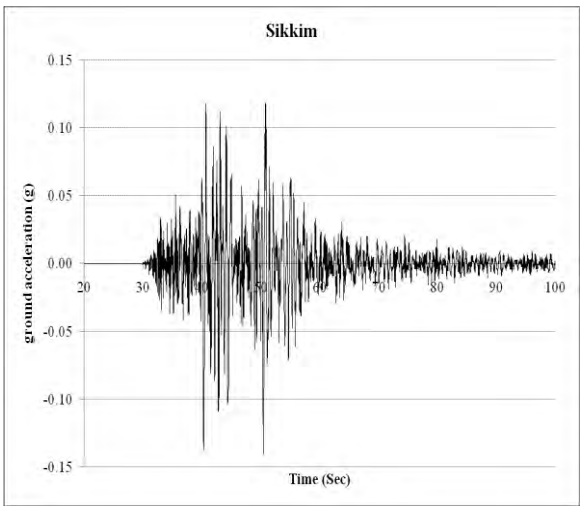

d) Sikkim earthquake

Figure 4.24: Time histories for local site effects

Maximum Peak Ground Acceleration (PGA)

Maximum Peak Ground Acceleration (PGA) at different depths of four earthquakes for this site is shown in figure 4.25. PGA at surface and that at bedrock is obtained from the analysis. The peak ground acceleration values at surface are observed to be in the range of 0.185g (Sikkim) to as high as 0.220g (Kobe) and that of the bedrock were observed to vary from 0.177g (Kobe) to 0.212g (Loma prieta). The impedance in the acceleration values can be observed. Such as, a sudden rise within few meters can cause considerable damage to the sub and super structure resulting in huge loss.

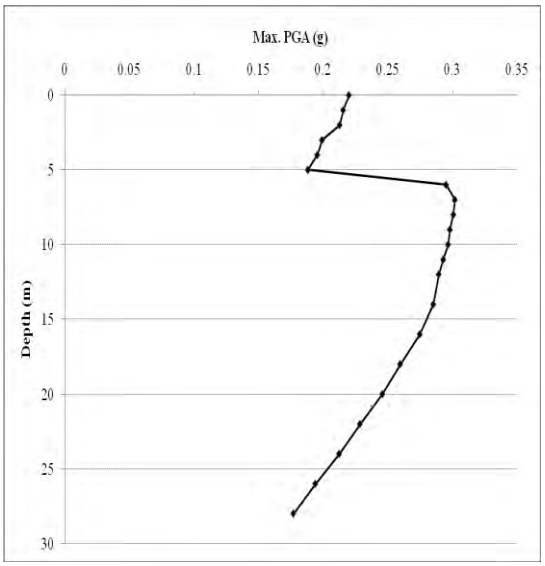

a) Kobe earthquake

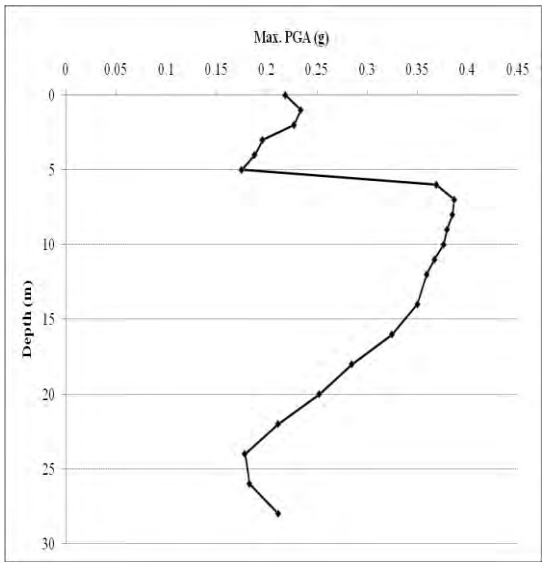

b) Loma prieta earthquake

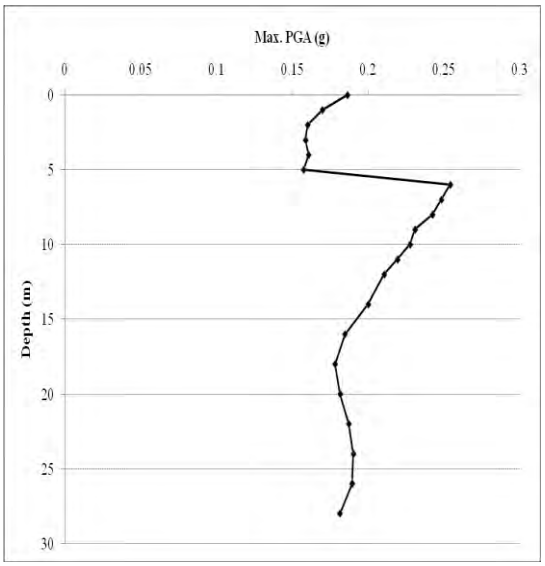

c) Nothridge earthquake

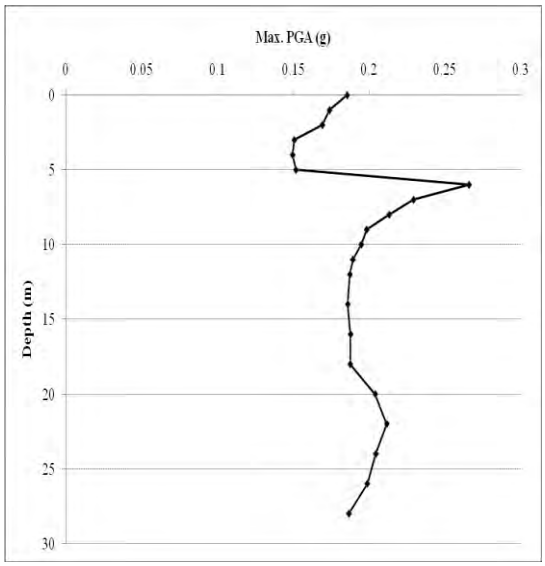

d) Sikkim earthquake

Figure 4.25: Maximum Peak Ground Acceleration for local site effects

Site amplification factors at sub surface layers are often used as one of the parameters for estimation of ground response. The amplification factor is the ratio of peak ground acceleration at surface to that of acceleration at hard rock. The amplification factors are determined as;

Amplification Factor = PGA recorded at ground surface / PGA recorded at hard rock
Amplification Factor (For Kobe earthquake) = 0.220/0.177 = 1.24
Amplification Factor (For Loma prieta earthquake) = 0.219/0.212 = 1.03
Amplification Factor (For Northridge earthquake) = 0.186/0.181 = 1.03
Amplification Factor (For Sikkim earthquake) = 0.185/0.187 = 0.99

Hence, the amplification factors have also been computed and it has been identified that similar to the peak ground acceleration values, the variation is within 0.99 (Sikkim) to 1.24 (Kobe).

Maximum Stress Ratio

Maximum Stress Ratio at different depths of four earthquakes for this site is shown in figure 4.26. Maximum stress ratio at different depths of four earthquakes for this site is obtained from the analysis. The Maximum stress ratio values for Kobe earthquakes are observed to be in the range of 0.255 to as high as 0.477. The Maximum stress ratio values for Loma prieta earthquakes are observed to be in the range of 0.263 to as high as 0.473. The Maximum stress ratio values for Northridge earthquakes are observed to be in the range of 0.222 to as high as 0.401. The Maximum stress ratio values for Sikkim earthquakes are observed to be in the range of 0.236 to as high as 0.402.

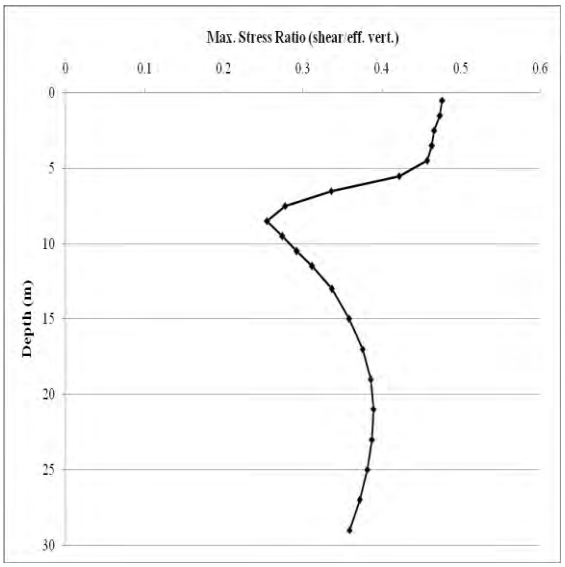

a) Kobe earthquake

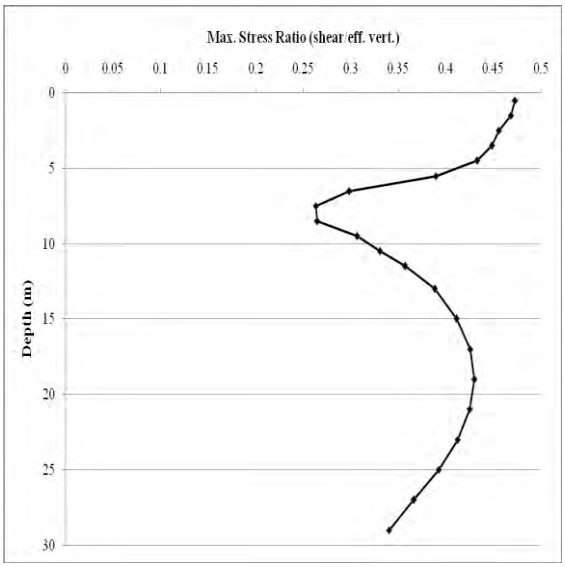

b) Loma prieta earthquake

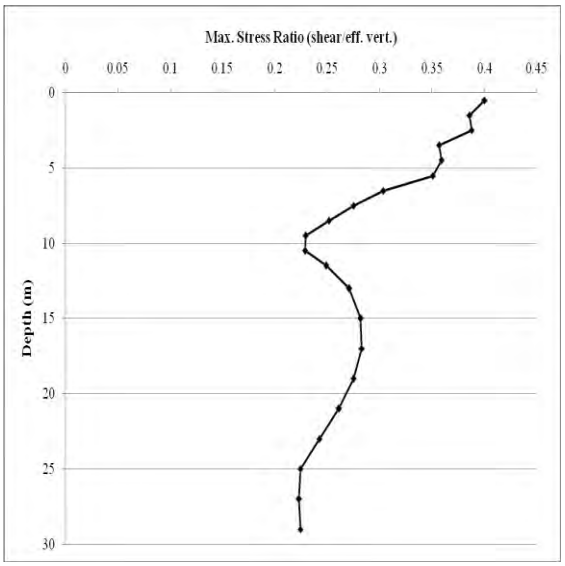

c) Nothridge earthquake

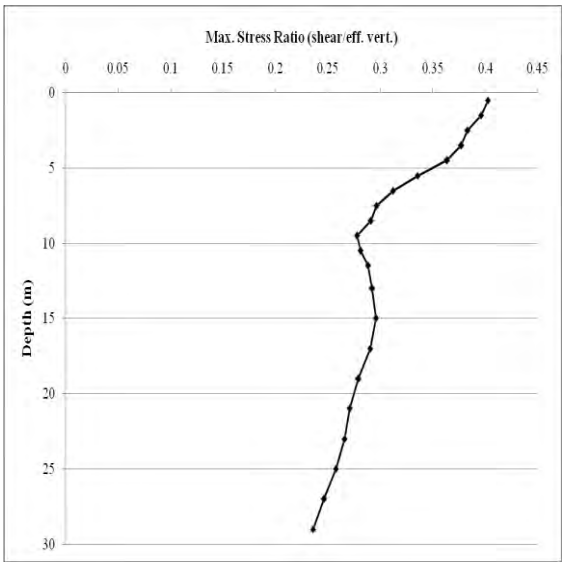

d) Sikkim earthquake

Figure 4.26: Maximum stress ratio for local site effects

Maximum Strain

Maximum Strain at different depths of four earthquakes for this site is shown in figure 4.27. Maximum strain values at different depths of four earthquakes for this site are obtained from the analysis. The Maximum strain values for Kobe earthquakes are observed to be in the range of 0.014 to as high as 6.43. The Maximum strain values for Loma prieta earthquakes are observed to be in the range of 0.0154 to as high as 3.68. The Maximum strain values for Northridge earthquakes are observed to be in the range of 0.0108 to as high as 2.33. The Maximum strain values for Sikkim earthquakes are observed to be in the range of 0.0136 to as high as 1.99.

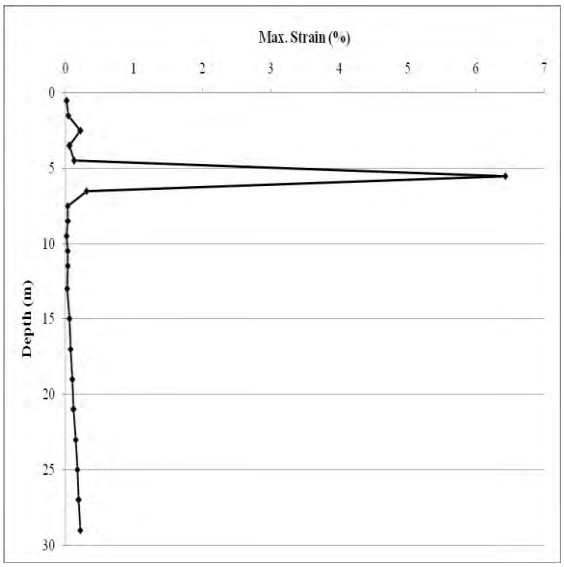

a) Kobe earthquake

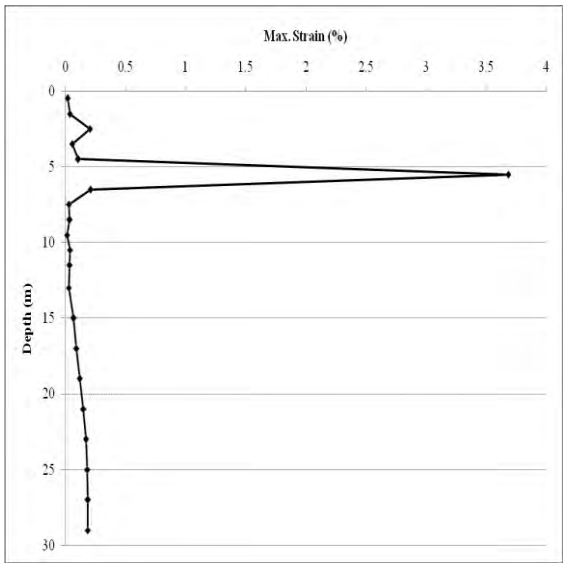

b) Loma prieta earthquake

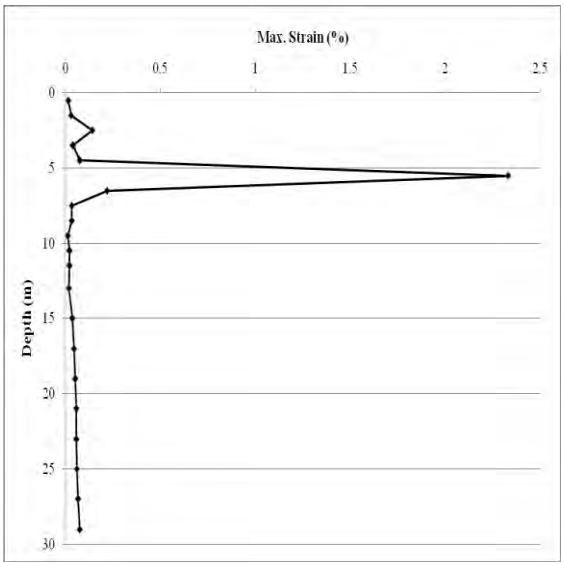

c) Nothridge earthquake

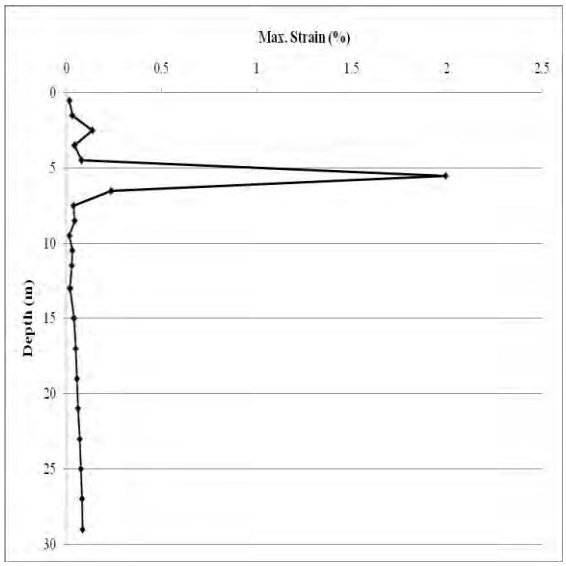

d) Sikkim earthquake

Figure 4.27: Maximum strain for local site effects

Figure 4.28 shows the comparison of Mean and Standard Deviation for surface PSA and Figure 4.29 shows the comparison of Surface PSA which are produced for different input motions.

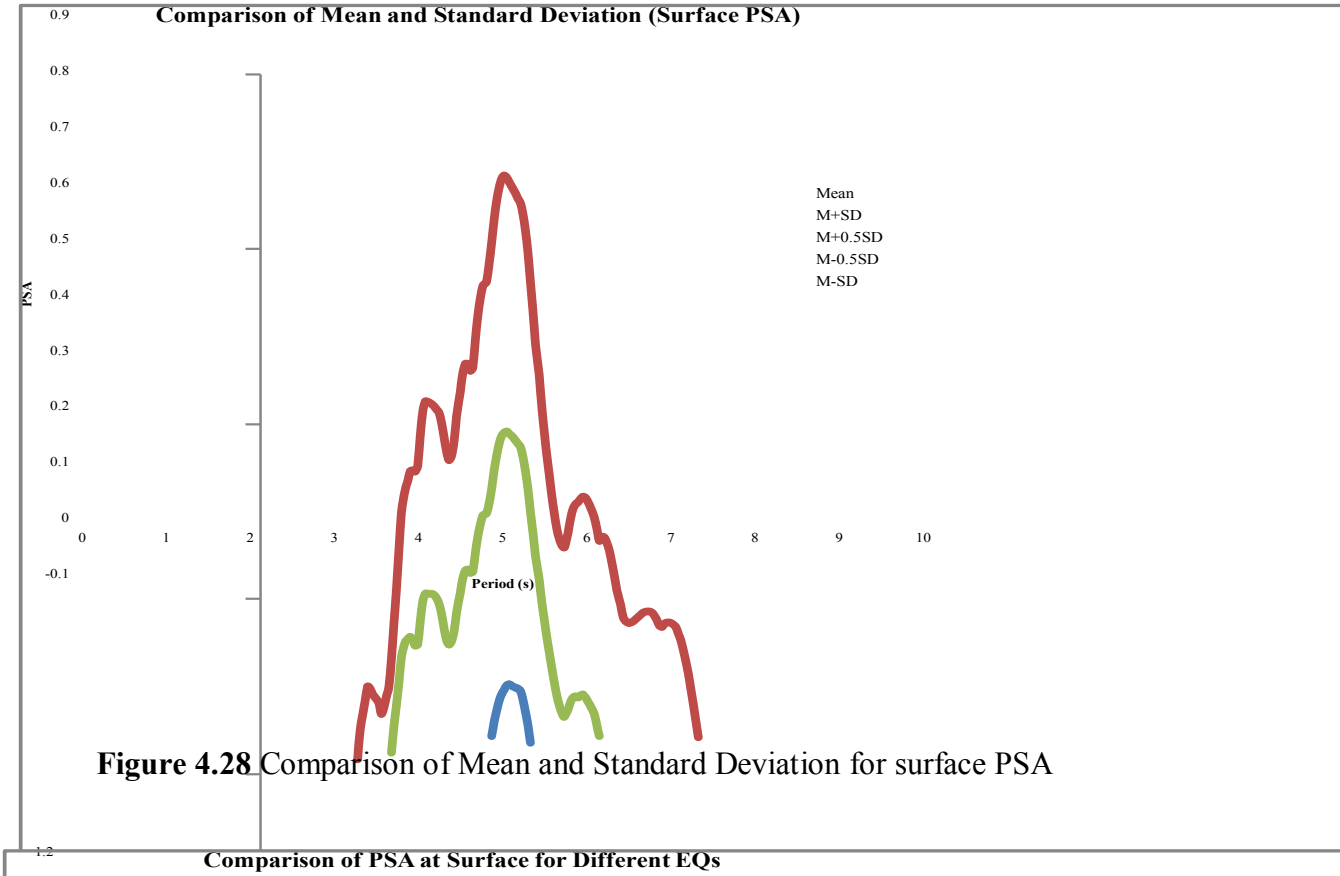

Figure 4.28 Comparison of Mean and Standard Deviation for surface PSA

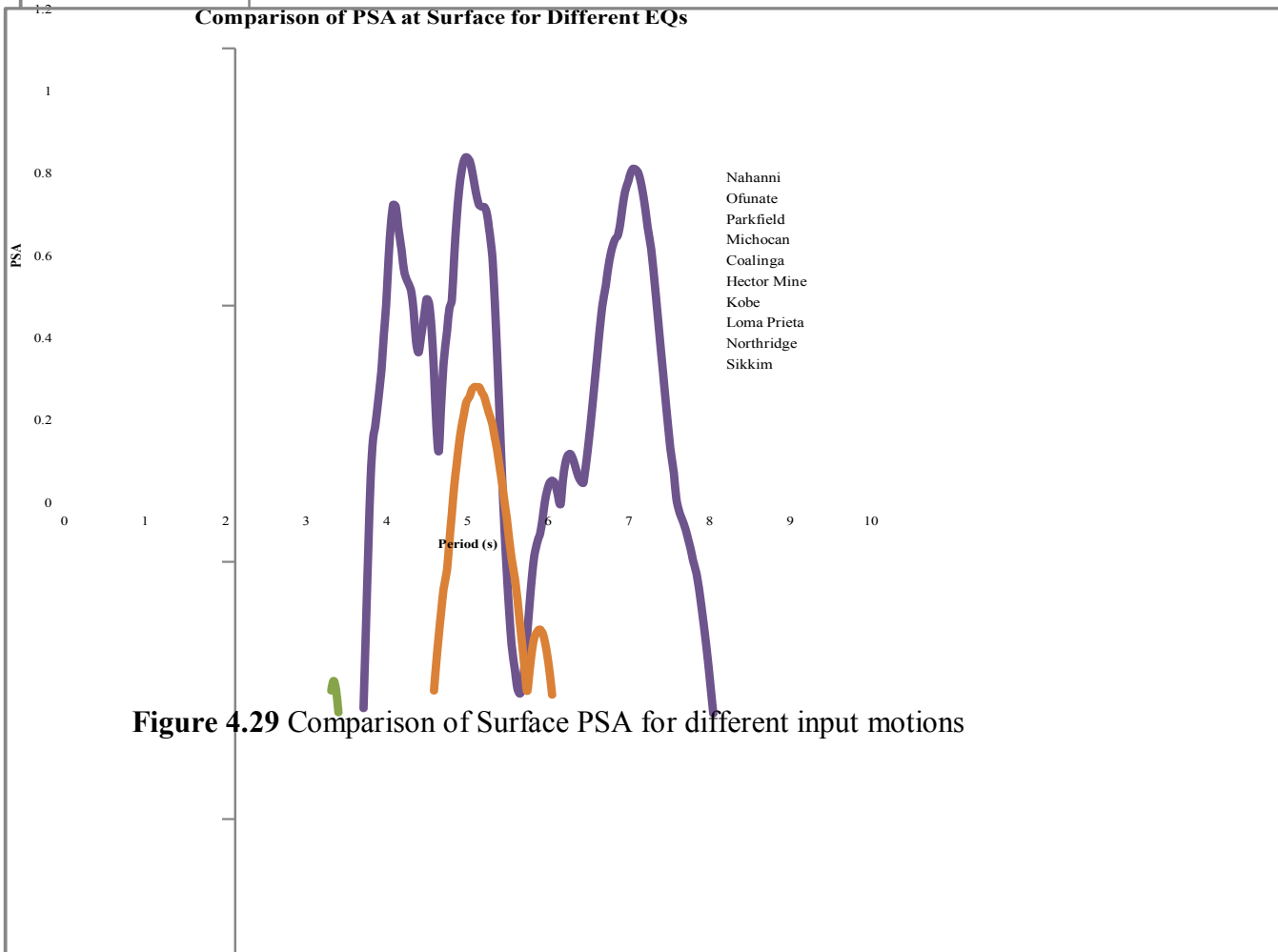

Figure 4.29 Comparison of Surface PSA for different input motions

Figure 4.30 shows the comparison of Mean Input PSA and Mean Surface PSA produced for different input motions.

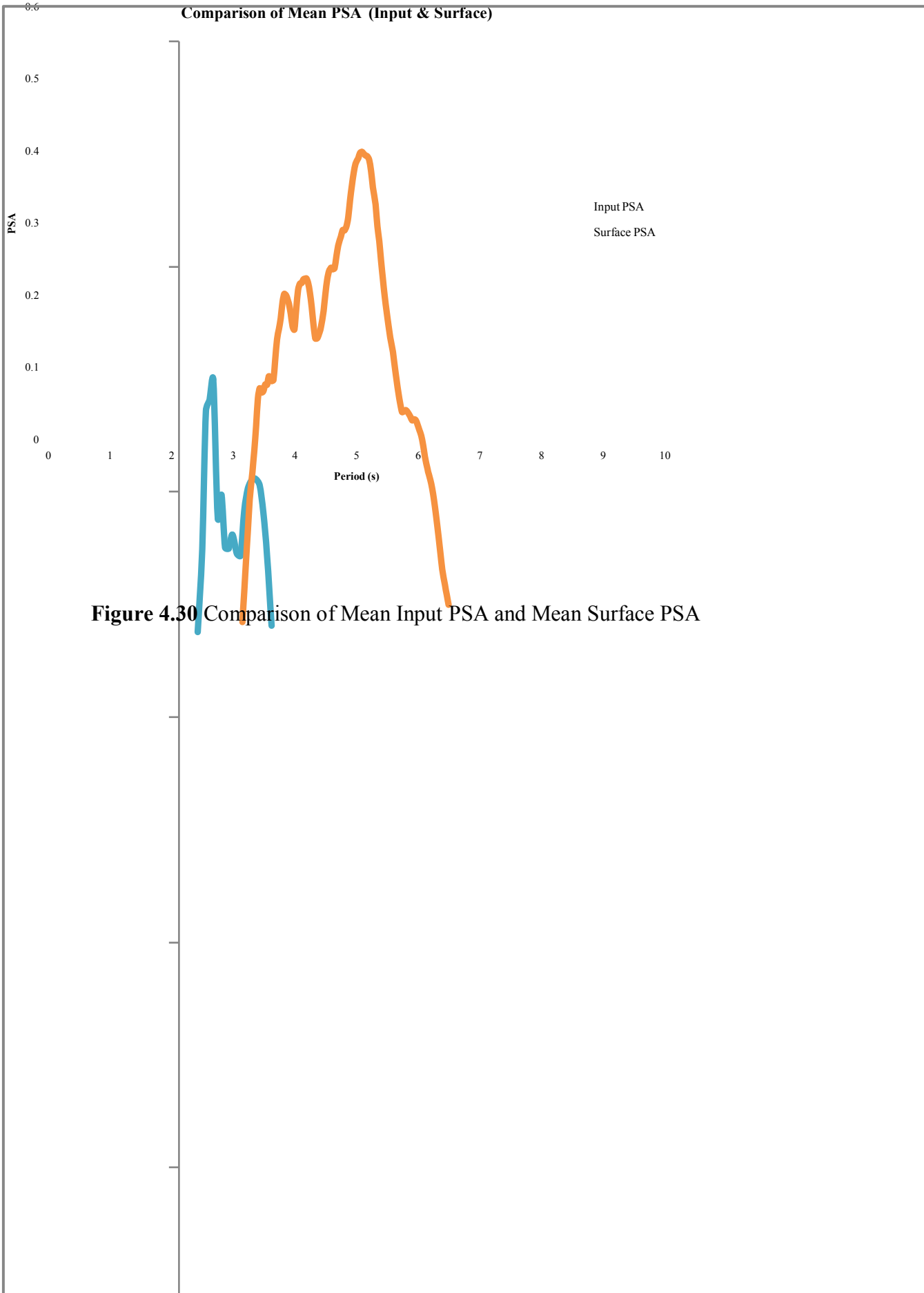

Figure 4.30 Comparison of Mean Input PSA and Mean Surface PSA

4.2.4 SITE: ASIAN CITY, DAKHIN KHAN

This site has been situated in Northern part of Dhaka city. Different geotechnical and geophysical test are conducted to characterize the site. Design soil profile is given in Figure 4.31 with average shear wave velocity for each layer. Average shear wave velocity for 30m layer (V_{30avg}) is

$$V_{30\,avg} = \frac{\sum_{i=1}^{N} h_i}{\sum_{i=1}^{N} \frac{h_i}{V_i}} \quad = 205 \text{ m/s}$$

Where, h is the thickness of soil layer, and V is the respective shear wave velocity.

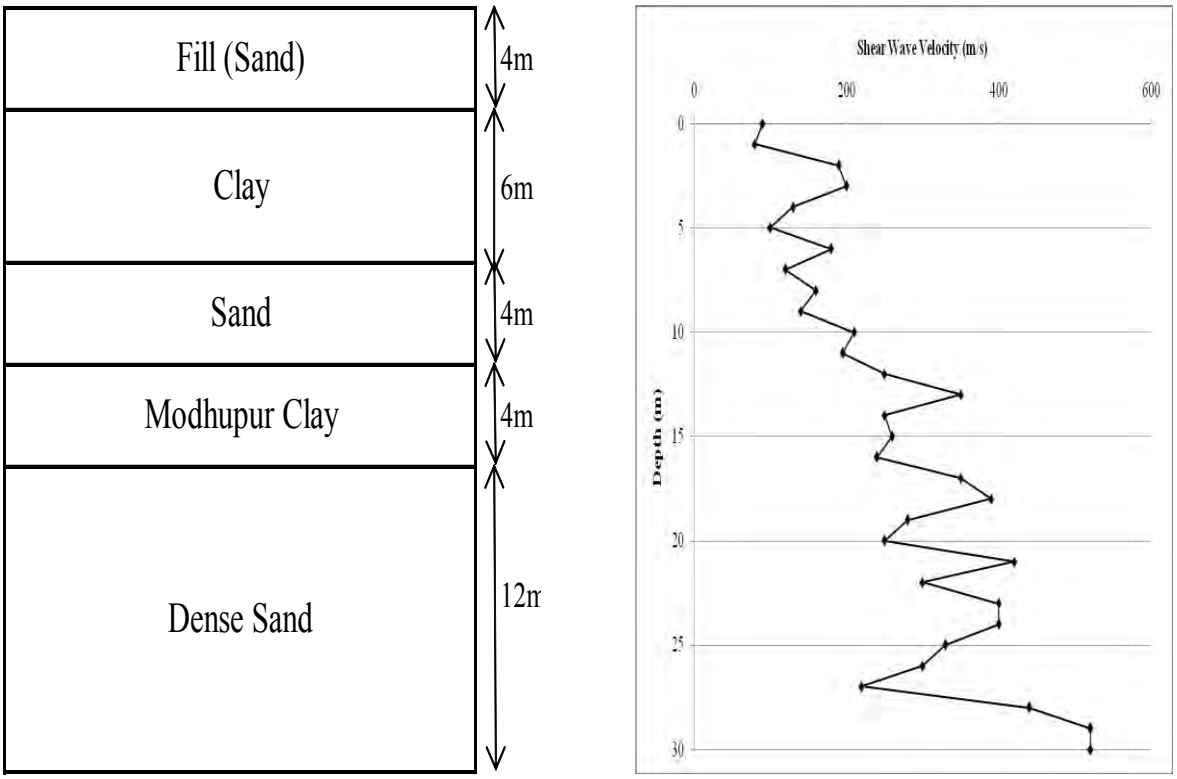

a) Design soil profile b) Shear wave velocity profile

Figure 4.31: Site Characterization

Response Spectra

Response spectra of four earthquakes are shown in Figure 4.32. Among the four earthquakes, Kobe earthquake produces highest (0.76g) peak spectral acceleration (PSA) for this site and Northridge earthquake produces lowest (0.0028g) peak spectral acceleration (PSA). It is observed that initially soil surface response is less than input response for all four earthquakes for this site. But gradually surface response increases.

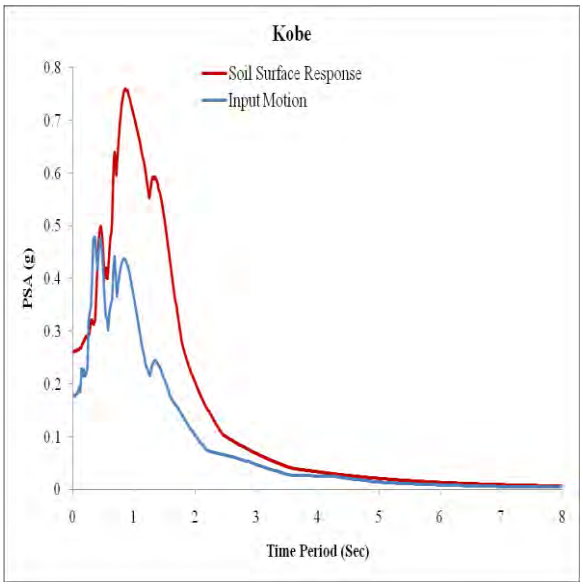

a) Kobe earthquake

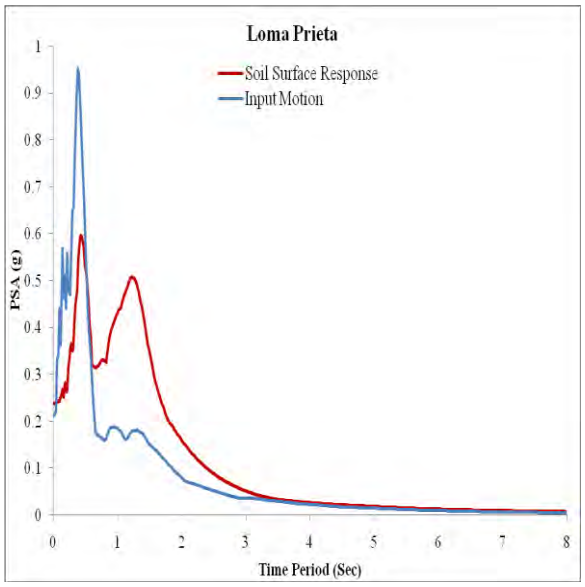

b) Loma prieta earthquake

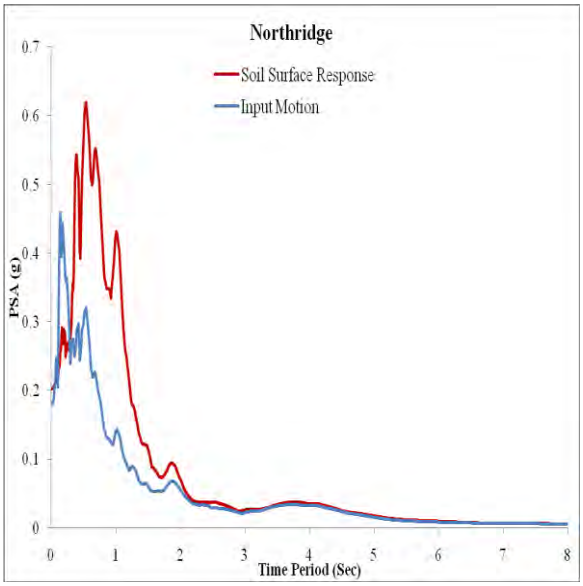

c) Nothridge earthquake

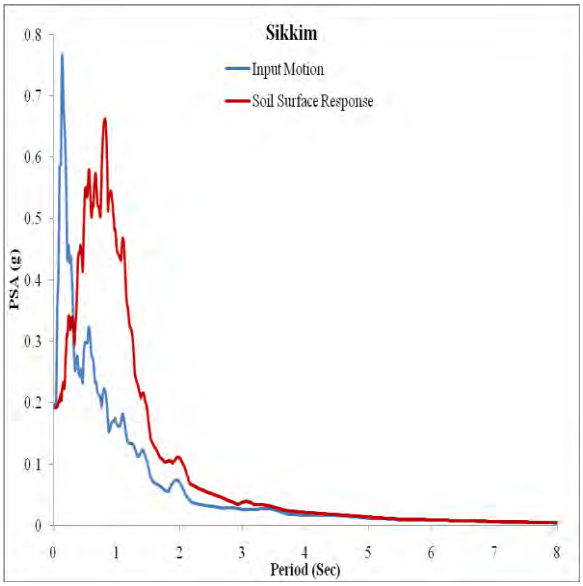

d) Sikkim earthquake

Figure 4.32: Response Spectra

Time Histories

The design soil profile is excited with input motion of four earthquakes to determine the dynamic response of local soil. Equivalent linear approach is used for site response analysis. As the seismic waves travel up and down, the soil vibrates. The acceleration of soil at the ground surface is shown in Figure 4.33. It is noted that the PGA and the ordinates of the response spectra increased.

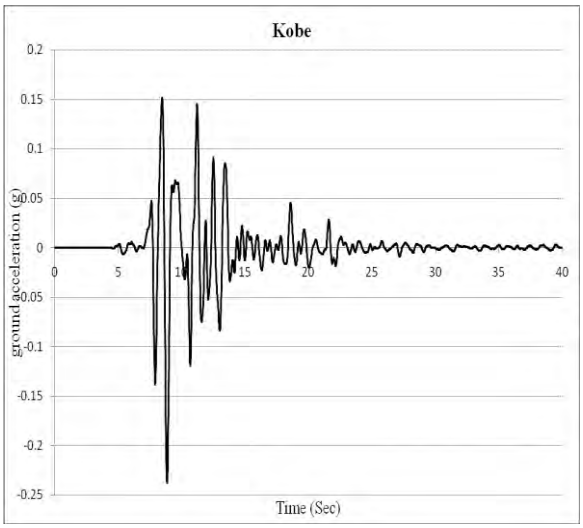

a) Kobe earthquake

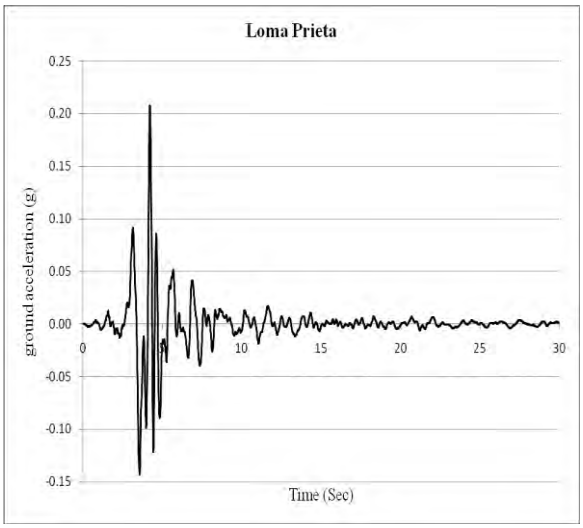

b) Loma prieta earthquake

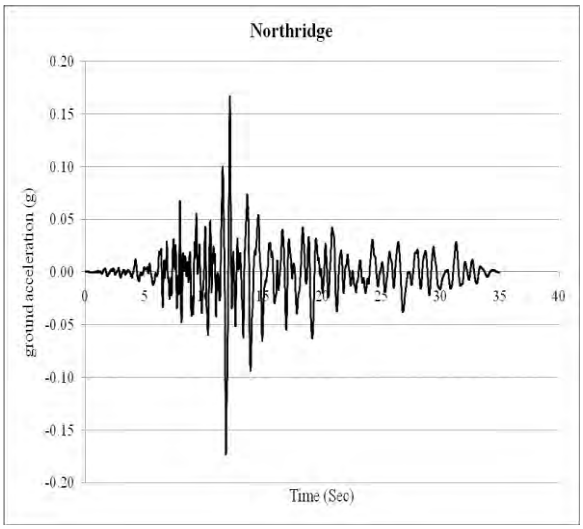

c) Nothridge earthquake

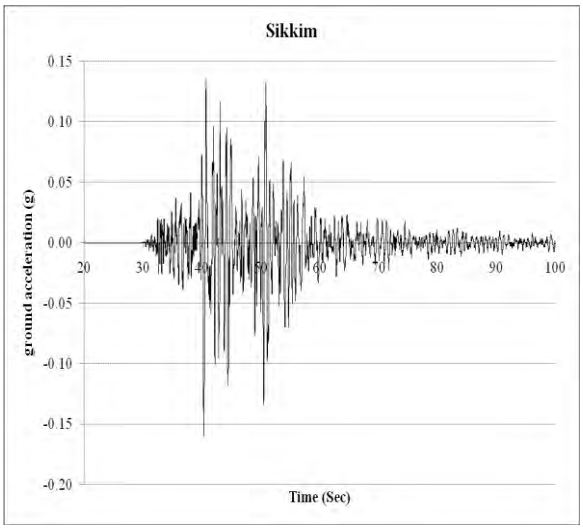

d) Sikkim earthquake

Figure 4.33: Time histories for local site effects

Maximum Peak Ground Acceleration (PGA)

Maximum Peak Ground Acceleration (PGA) at different depths of four earthquakes for this site is shown in figure 4.34. PGA at surface and that at bedrock is obtained from the analysis. The peak ground acceleration values at surface are observed to be in the range of 0.192g (Sikkim) to as high as 0.262g (Kobe) and that of the bedrock were observed to vary from 0.177g (Kobe) to 0.212g (Loma prieta). The impedance in the acceleration values can be observed. Such as, a sudden rise within few meters can cause considerable damage to the sub and super structure resulting in huge loss.

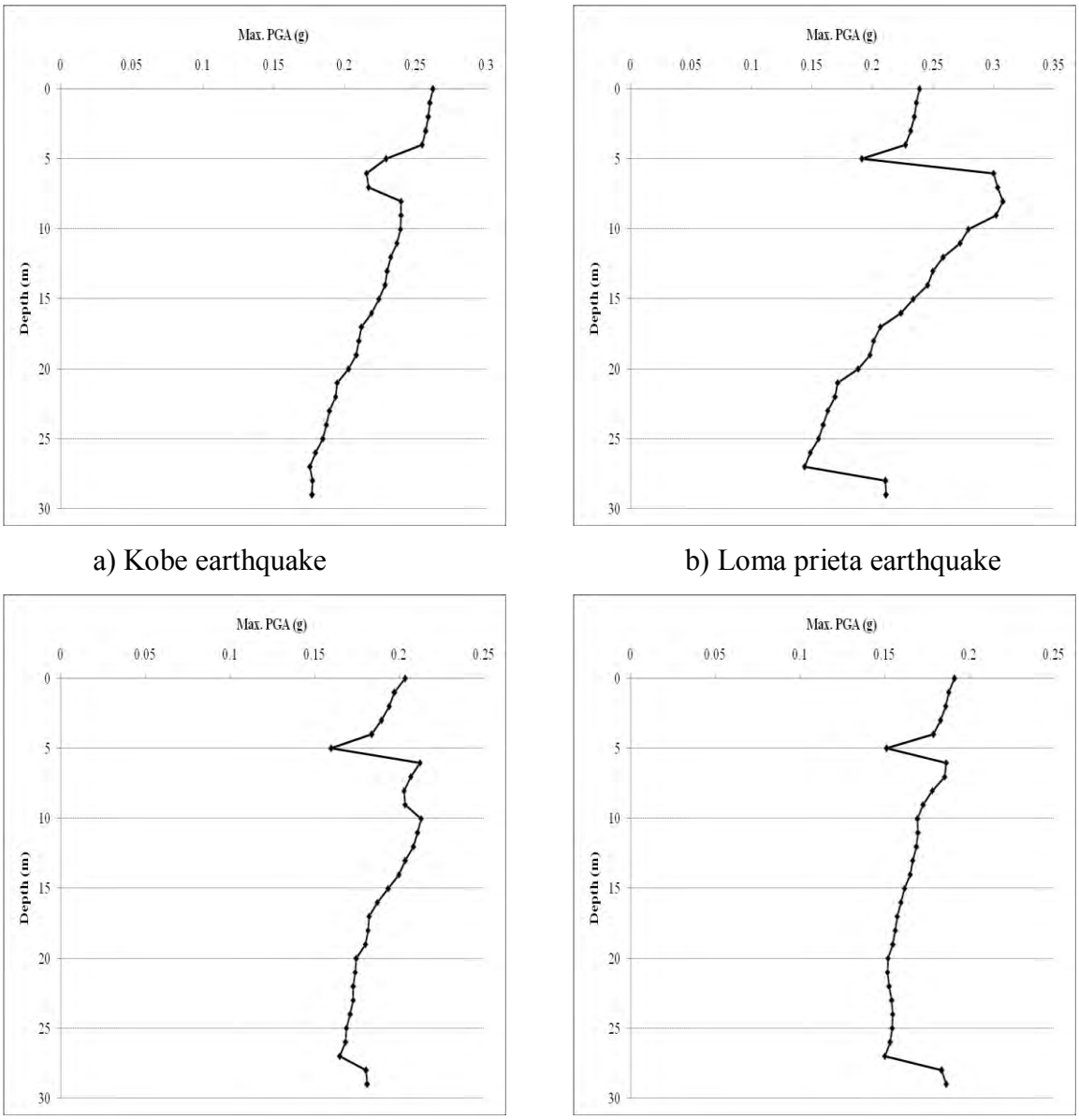

a) Kobe earthquake

b) Loma prieta earthquake

c) Nothridge earthquake

d) Sikkim earthquake

Figure 4.34: Maximum Peak Ground Acceleration for local site effects

Site amplification factors at sub surface layers are often used as one of the parameters for estimation of ground response. The amplification factor is the ratio of peak ground acceleration at surface to that of acceleration at hard rock. The amplification factors are determined as;

Amplification Factor = PGA recorded at ground surface / PGA recorded at hard rock
Amplification Factor (For Kobe earthquake) = 0.262/0.177 = 1.48
Amplification Factor (For Loma prieta earthquake) = 0.239/0.212 = 1.12
Amplification Factor (For Northridge earthquake) = 0.204/0.181 = 1.13
Amplification Factor (For Sikkim earthquake) = 0.192/0.187 = 1.03

Hence, the amplification factors have also been computed and it has been identified that similar to the peak ground acceleration values, the variation is within 1.03 (Sikkim) to 1.48 (Kobe).

Maximum Stress Ratio

Maximum Stress Ratio at different depths of four earthquakes for this site is shown in figure 4.35. Maximum stress ratio at different depths of four earthquakes for this site is obtained from the analysis. The Maximum stress ratio values for Kobe earthquakes are observed to be in the range of 0.283 to as high as 0.572. The Maximum stress ratio values for Loma prieta earthquakes are observed to be in the range of 0.281 to as high as 0.520. The Maximum stress ratio values for Northridge earthquakes are observed to be in the range of 0.184 to as high as 0.438. The Maximum stress ratio values for Sikkim earthquakes are observed to be in the range of 0.205 to as high as 0.418.

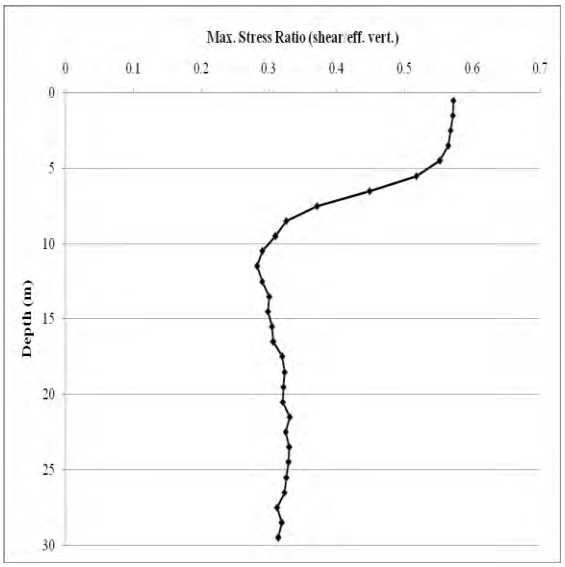

a) Kobe earthquake

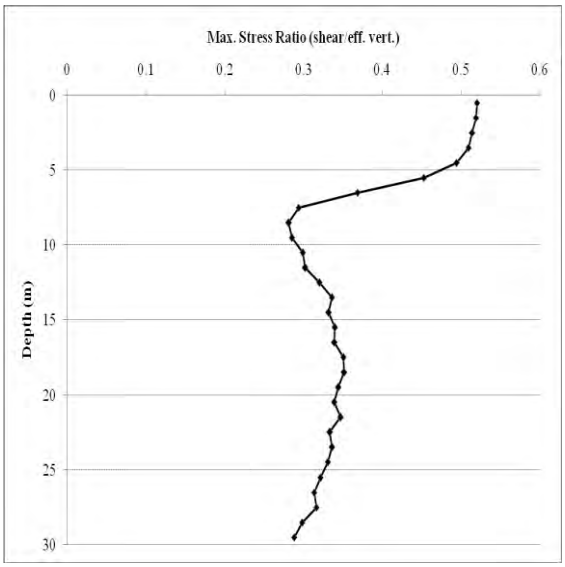

b) Loma prieta earthquake

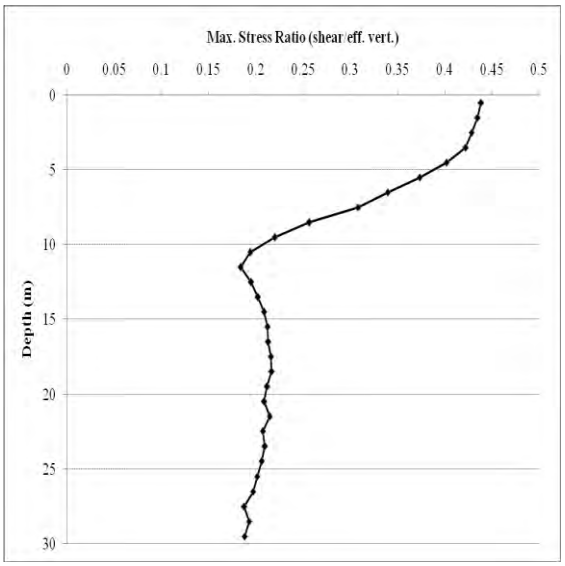

c) Nothridge earthquake

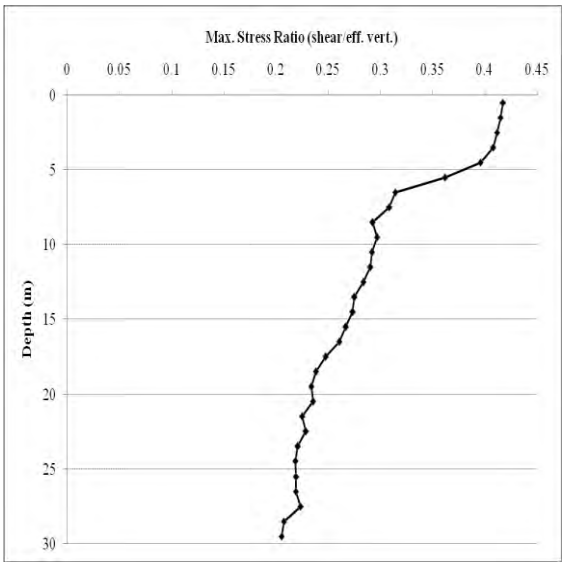

d) Sikkim earthquake

Figure 4.35: Maximum stress ratio for local site effects

Maximum Strain

Maximum Strain at different depths of four earthquakes for this site is shown in figure 4.36. Maximum strain values at different depths of four earthquakes for this site are obtained from the analysis. The Maximum strain values for Kobe earthquakes are observed to be in the range of 0.0165 to as high as 5.03. The Maximum strain values for Loma prieta earthquakes are observed to be in the range of 0.0145 to as high as 3.11. The Maximum strain values for Northridge earthquakes are observed to be in the range of 0.0117 to as high as 1.45. The Maximum strain values for Sikkim earthquakes are observed to be in the range of 0.0112 to as high as 1.24.

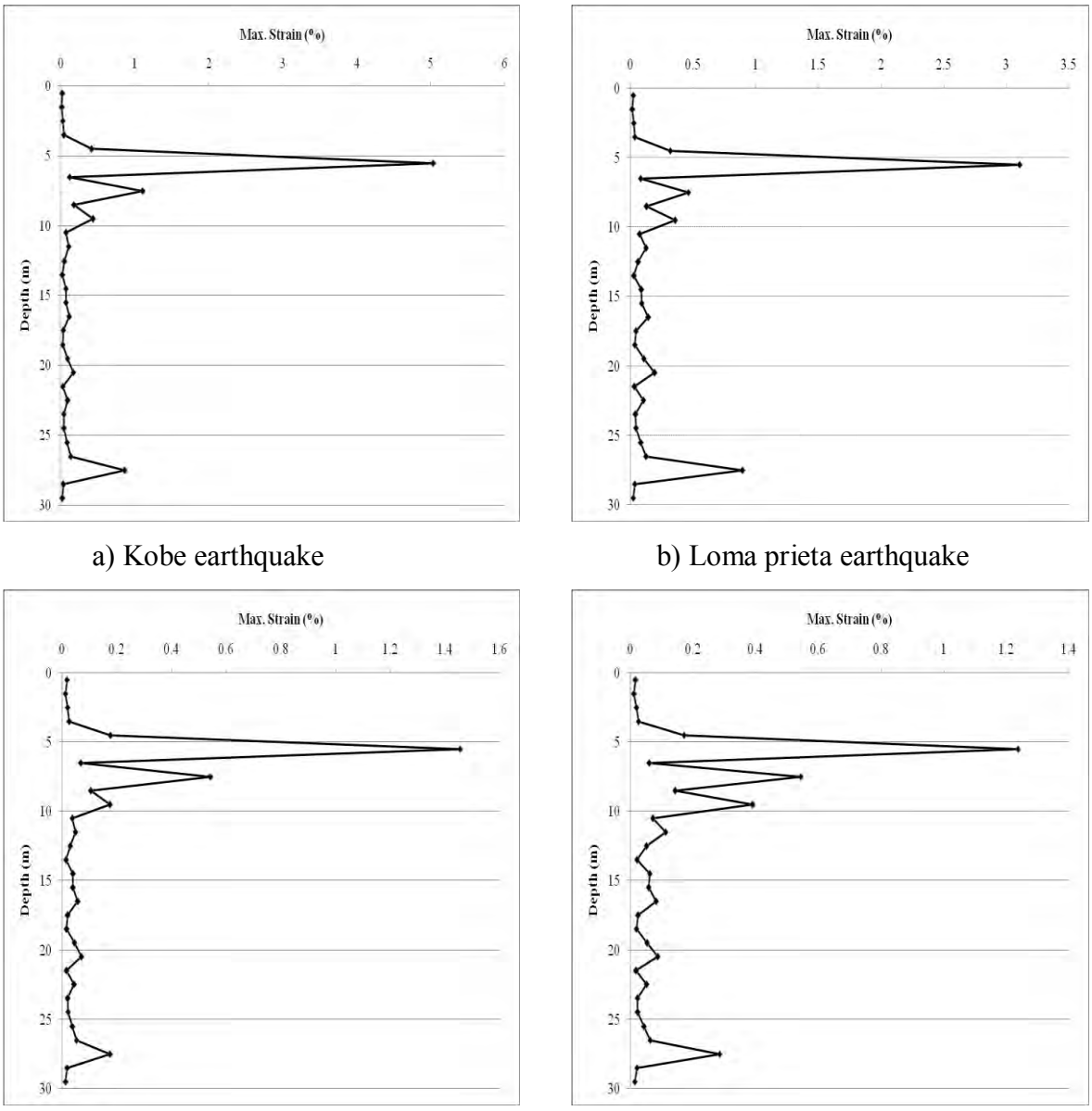

a) Kobe earthquake

b) Loma prieta earthquake

c) Nothridge earthquake

d) Sikkim earthquake

Figure 4.36: Maximum strain for local site effects

Figure 4.37 shows the comparison of Mean and Standard Deviation for surface PSA and Figure 4.38 shows the comparison of Surface PSA which are produced for different input motions.

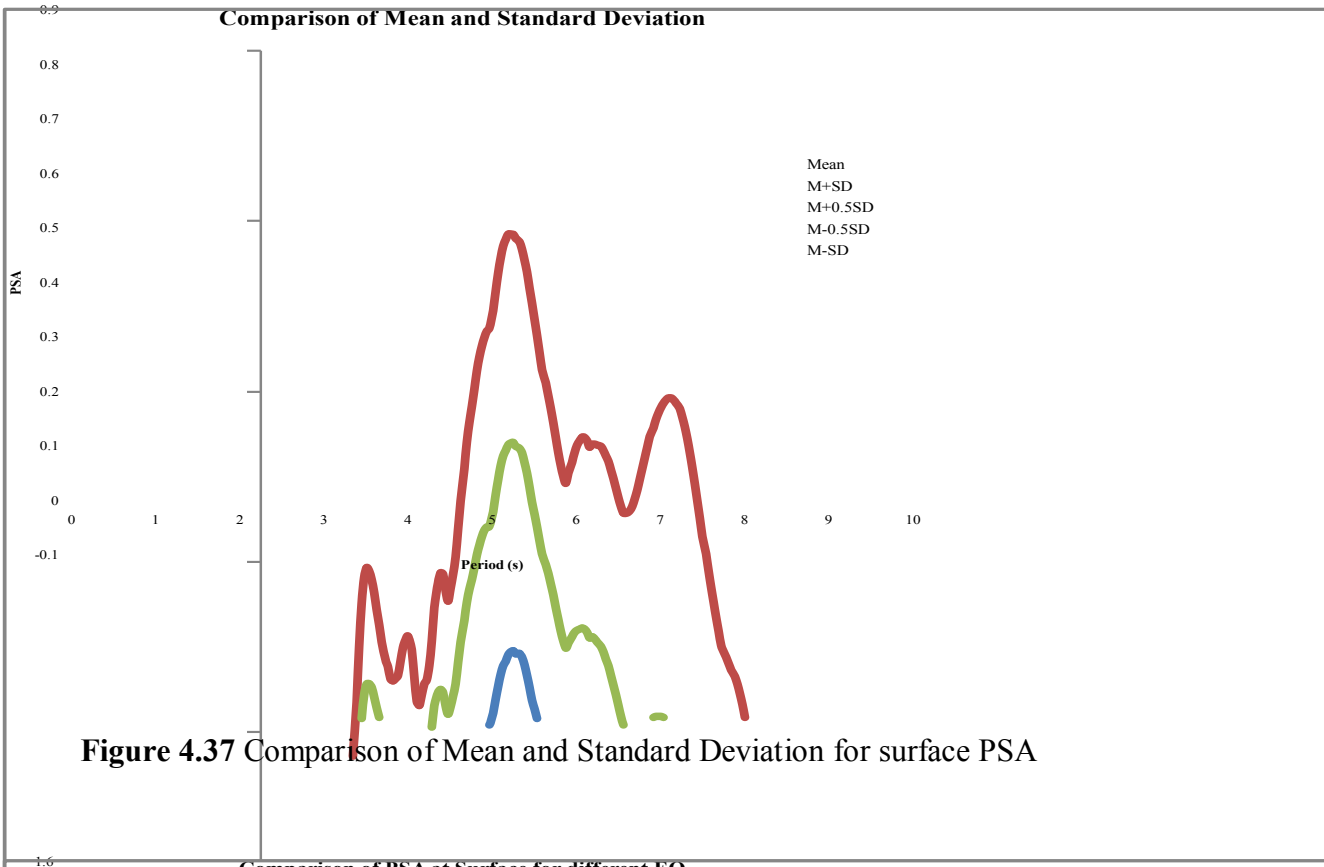

Figure 4.37 Comparison of Mean and Standard Deviation for surface PSA

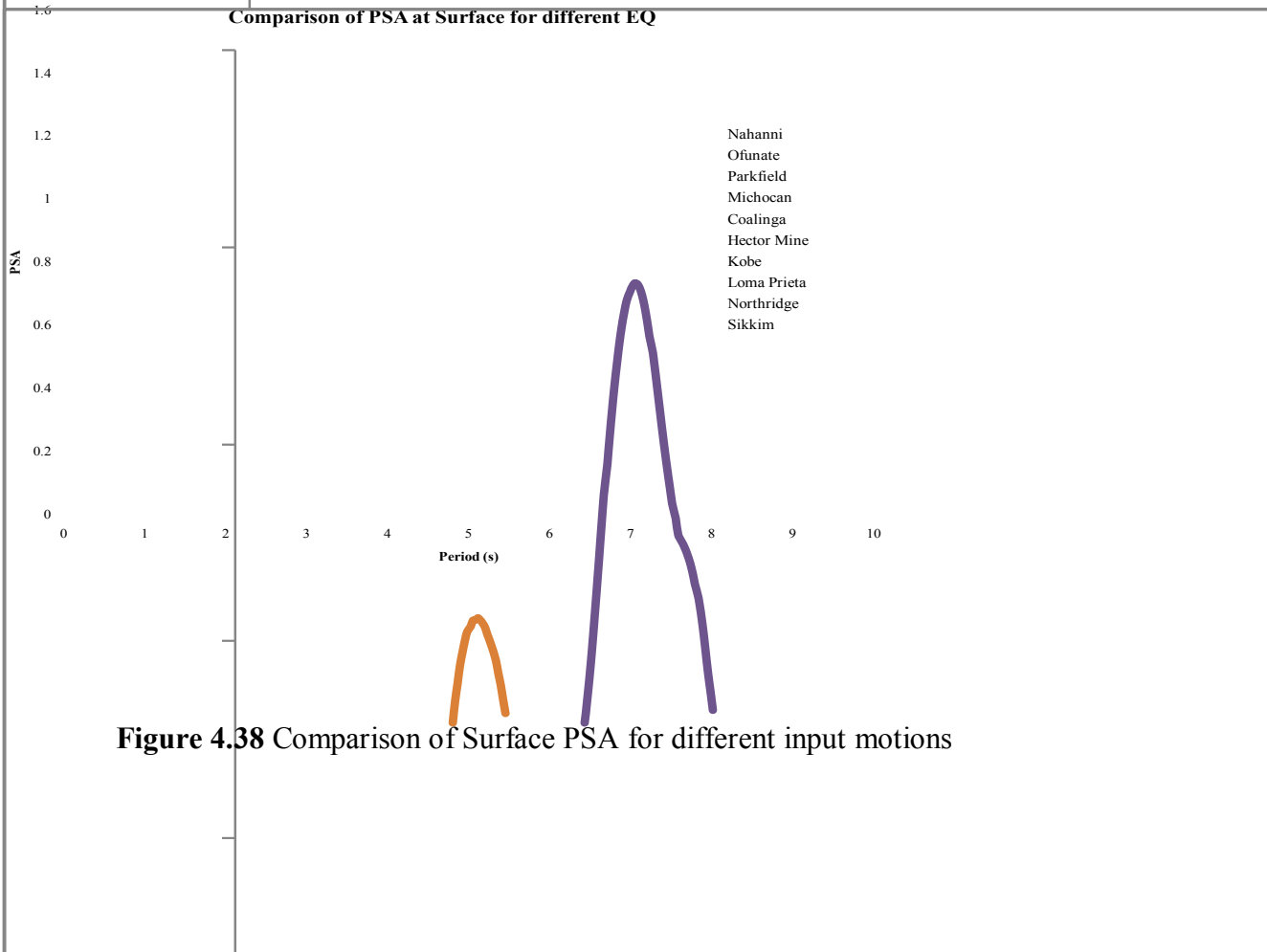

Figure 4.38 Comparison of Surface PSA for different input motions

Figure 4.39 shows the comparison of Mean Input PSA and Mean Surface PSA produced for different input motions.

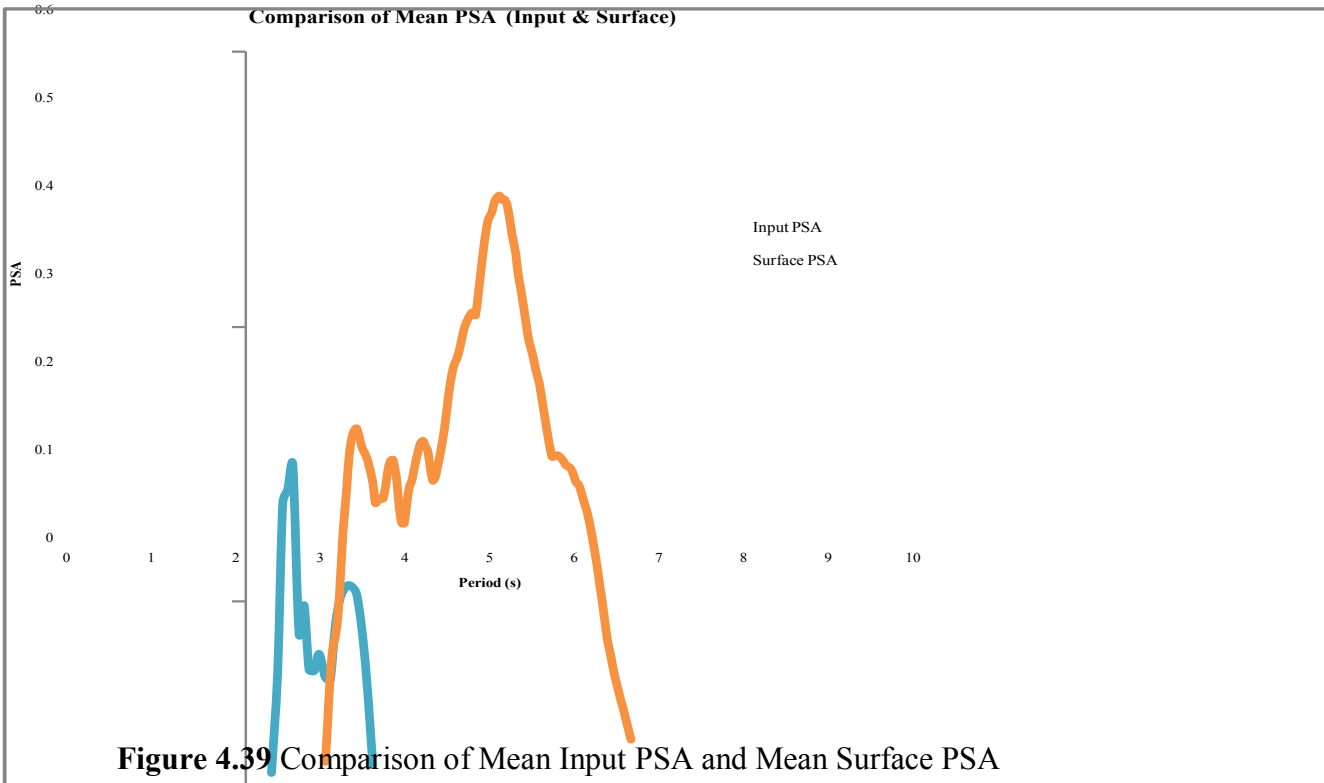

Figure 4.39 Comparison of Mean Input PSA and Mean Surface PSA

4.2.5 SITE: UTTARA

This site has been situated in north of Dhaka city. Different geotechnical and geophysical test are conducted to characterize the site. Design soil profile is given in Figure 4.40 with average shear wave velocity for each layer. Average shear wave velocity for 30m layer (V_{30avg}) is

$$V_{30\,avg} = \frac{\sum_{i=1}^{N} h_i}{\sum_{i=1}^{N} \frac{h_i}{V_i}} = 188 \text{ m/s}$$

Where, h is the thickness of soil layer, and V is the respective shear wave velocity.

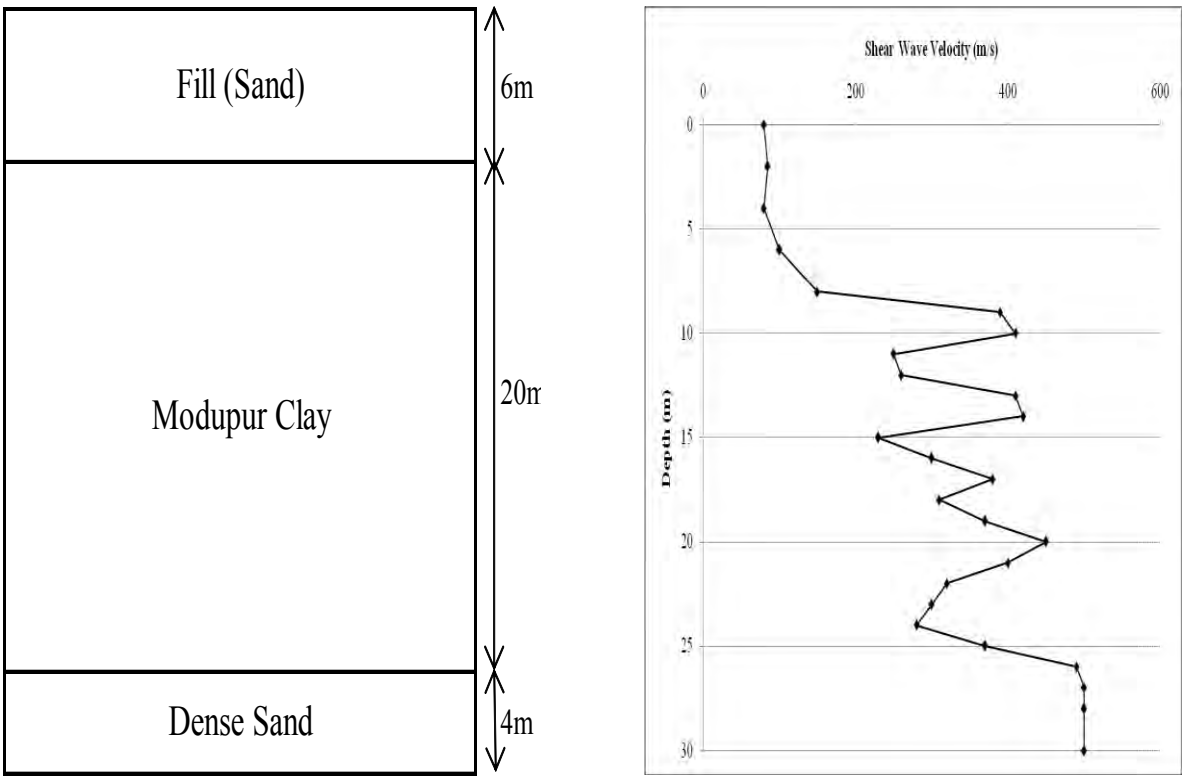

a) Design soil profile b) Shear wave velocity profile

Figure 4.40: Site Characterization

Response Spectra

Response spectra of four earthquakes are shown in Figure 4.41. Among the four earthquakes, Loma prieta earthquake produces highest (0.93g) peak spectral acceleration (PSA) for this site and Northridge earthquake produces lowest (0.0029g) peak spectral acceleration (PSA). It is observed that initially soil surface response is less than input response for all four earthquakes for this site. But gradually surface response increases.

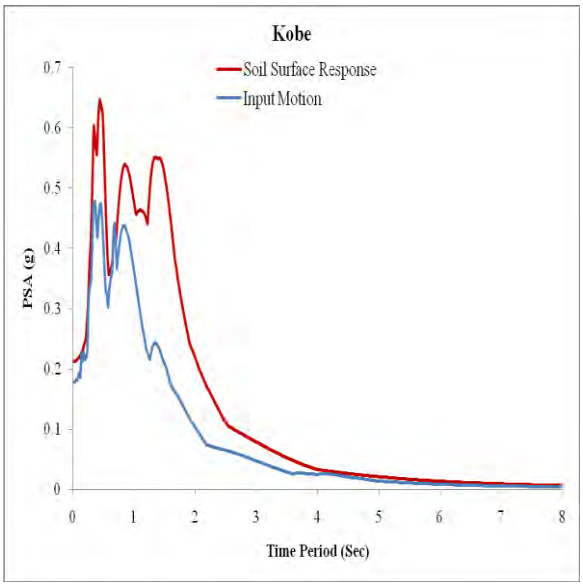

a) Kobe earthquake

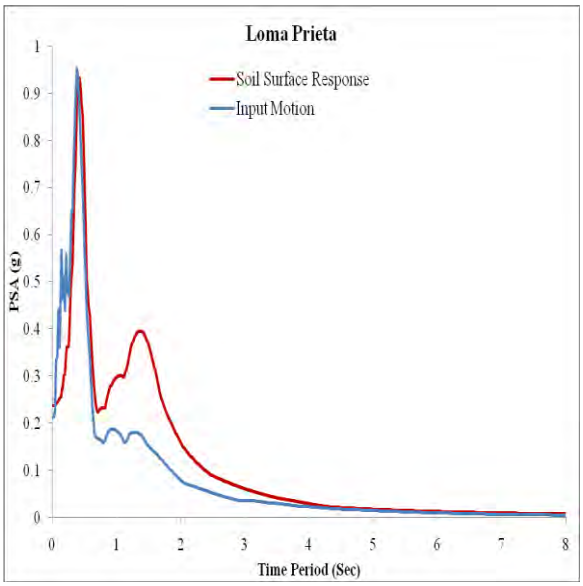

b) Loma prieta earthquake

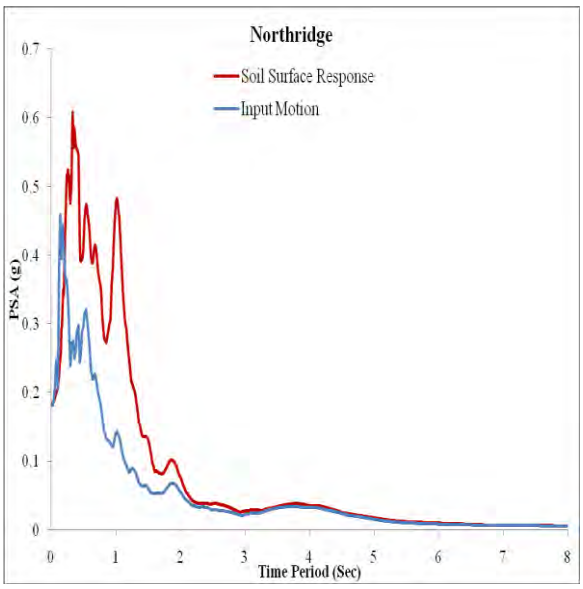

c) Nothridge earthquake

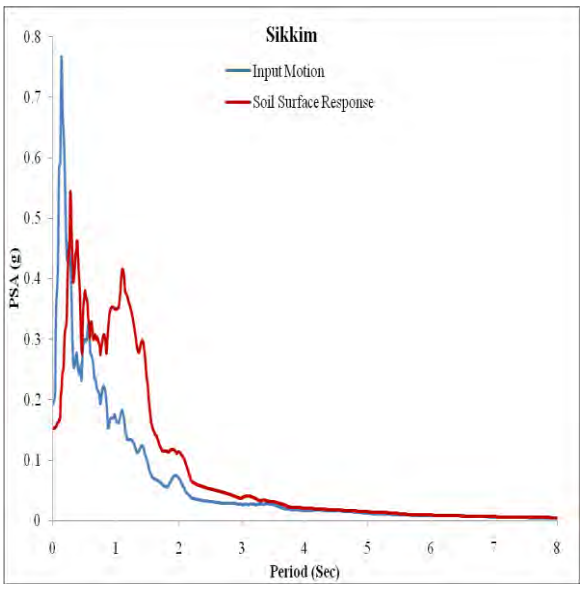

d) Sikkim earthquake

Figure 4.41: Response Spectra

Time Histories

The design soil profile is excited with input motion of four earthquakes to determine the dynamic response of local soil. Equivalent linear approach is used for site response analysis. As the seismic waves travel up and down, the soil vibrates. The acceleration of soil at the ground surface is shown in Figure 4.42. It is noted that the PGA and the ordinates of the response spectra increased.

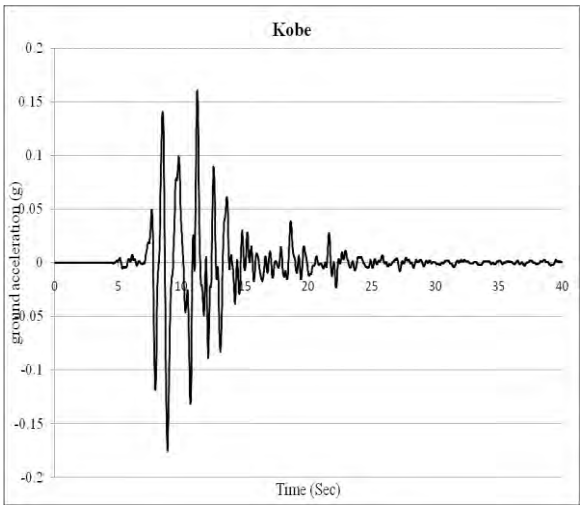

a) Kobe earthquake

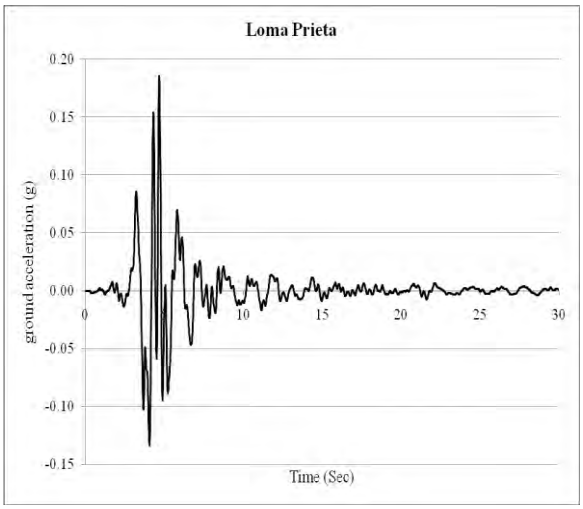

b) Loma prieta earthquake

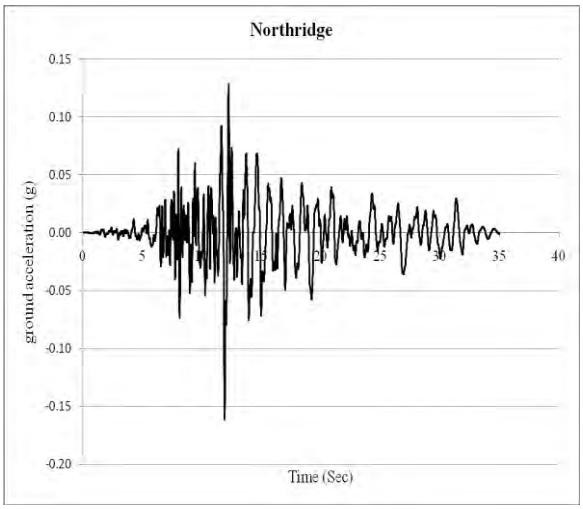

c) Nothridge earthquake

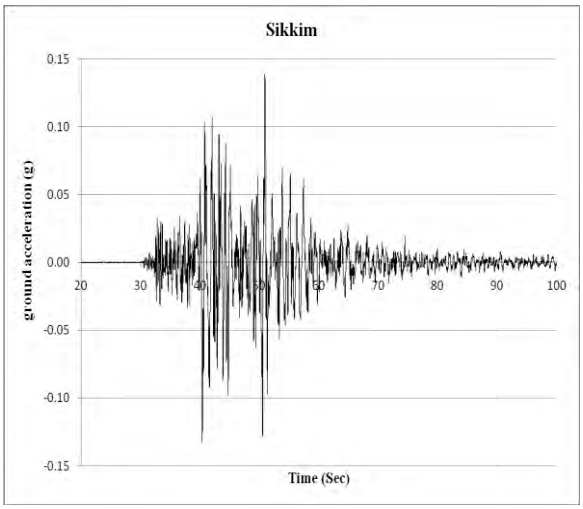

d) Sikkim earthquake

Figure 4.42: Time histories for local site effects

Maximum Peak Ground Acceleration (PGA)

Maximum Peak Ground Acceleration (PGA) at different depths of four earthquakes for this site are shown in figure 4.43. PGA at surface and that at bedrock is obtained from the analysis. The peak ground acceleration values at surface are observed to be in the range of 0.152g (Sikkim) to as high as 0.238g (Loma prieta) and that of the bedrock were observed to vary from 0.177g (Kobe) to 0.212g (Loma prieta). The impedance in the acceleration values can be observed. Such as, a sudden rise within few meters can cause considerable damage to the sub and super structure resulting in huge loss.

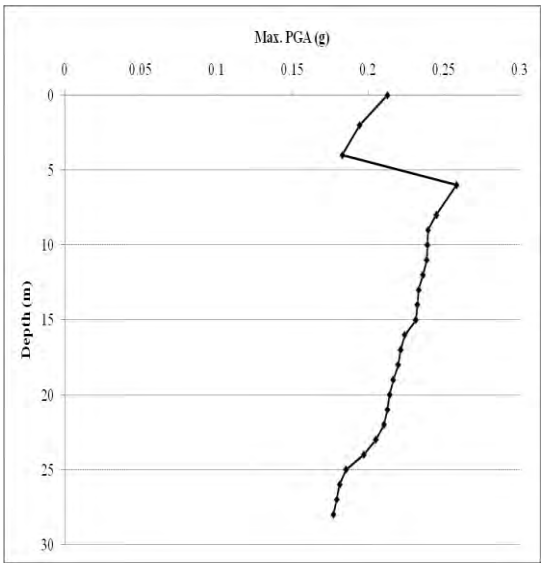

a) Kobe earthquake

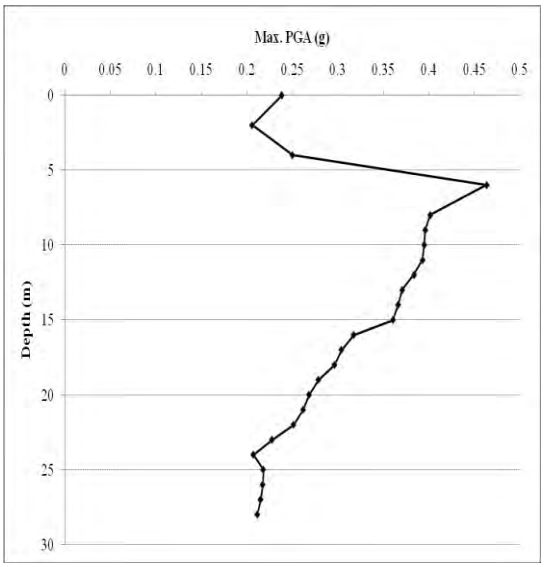

b) Loma prieta earthquake

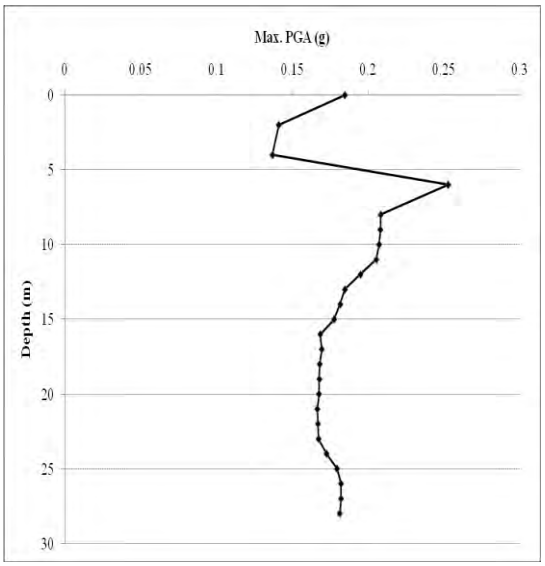

c) Nothridge earthquake

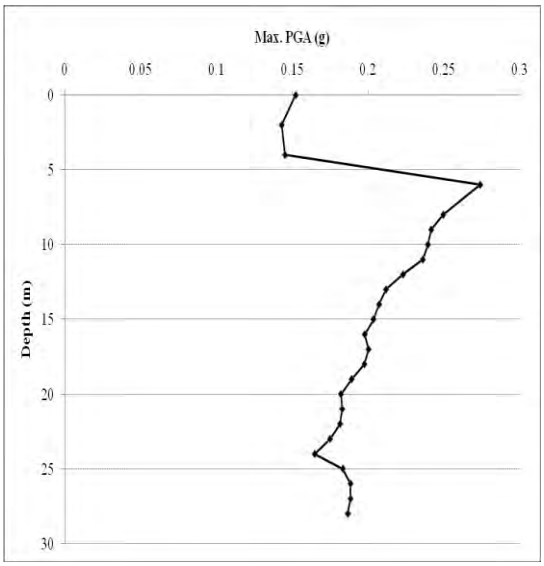

d) Sikkim earthquake

Figure 4.43: Maximum Peak Ground Acceleration for local site effects

Site amplification factors at sub surface layers are often used as one of the parameters for estimation of ground response. The amplification factor is the ratio of peak ground acceleration at surface to that of acceleration at hard rock. The amplification factors are determined as;

Amplification Factor = PGA recorded at ground surface / PGA recorded at hard rock
Amplification Factor (For Kobe earthquake) = 0.213/0.177 = 1.20
Amplification Factor (For Loma prieta earthquake) = 0.238/0.212 = 1.12
Amplification Factor (For Northridge earthquake) = 0.185/0.181 = 1.02
Amplification Factor (For Sikkim earthquake) = 0.152/0.187 = 0.81

Hence, the amplification factors have also been computed and it has been identified that similar to the peak ground acceleration values, the variation is within 0.81 (Sikkim) to 1.12 (Kobe).

Maximum Stress Ratio

Maximum Stress Ratio at different depths of four earthquakes for this site is shown in figure 4.44. Maximum stress ratio at different depths of four earthquakes for this site is obtained from the analysis. The Maximum stress ratio values for Kobe earthquakes are observed to be in the range of 0.271 to as high as 0.464. The Maximum stress ratio values for Loma prieta earthquakes are observed to be in the range of 0.297 to as high as 0.525. The Maximum stress ratio values for Northridge earthquakes are observed to be in the range of 0.180 to as high as 0.393. The Maximum stress ratio values for Sikkim earthquakes are observed to be in the range of 0.215 to as high as 0.341.

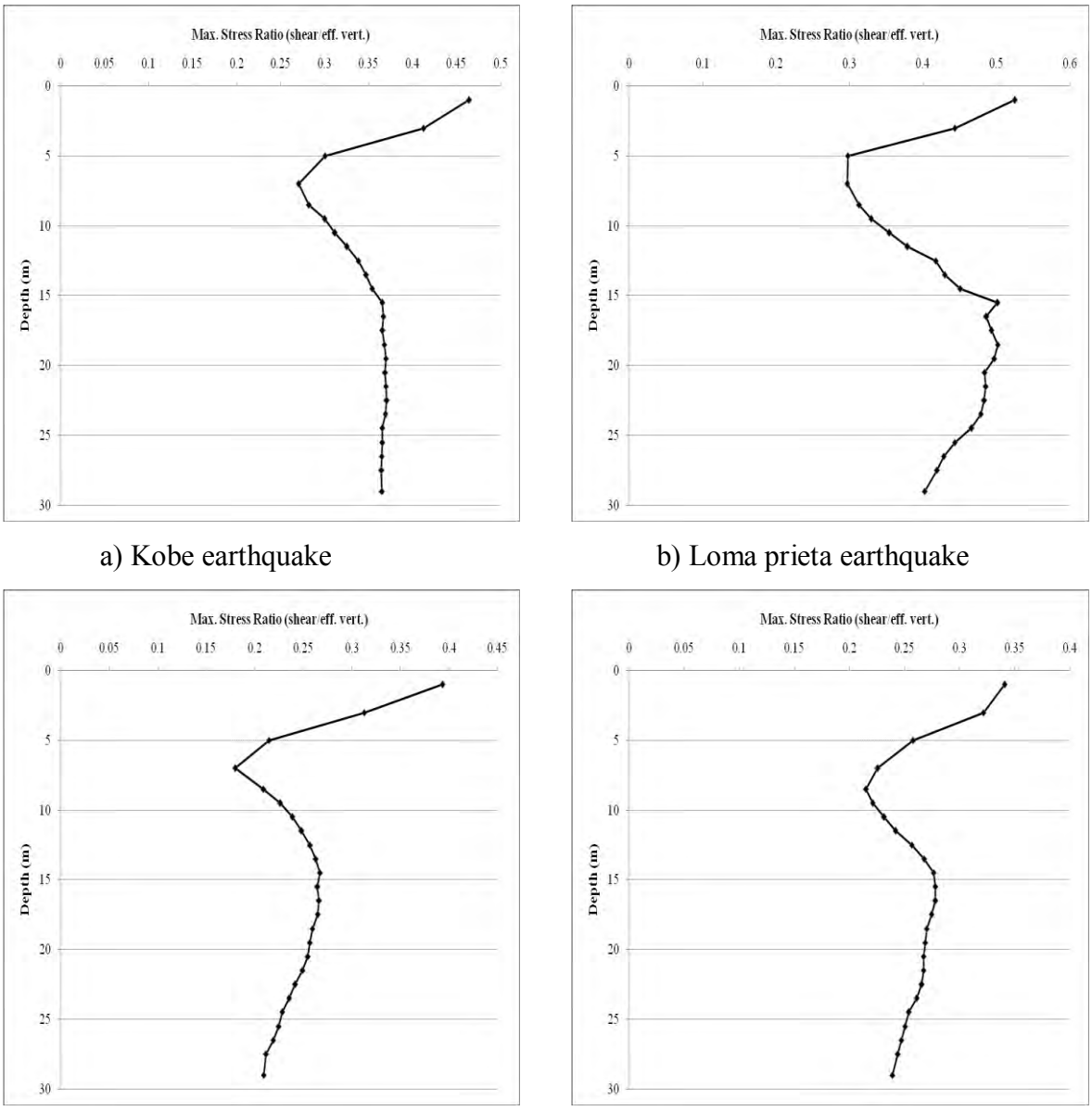

a) Kobe earthquake b) Loma prieta earthquake

c) Nothridge earthquake d) Sikkim earthquake

Figure 4.44: Maximum stress ratio for local site effects

Maximum Strain

Maximum Strain at different depths of four earthquakes for this site is shown in figure 4.45. Maximum strain values at different depths of four earthquakes for this site are obtained from the analysis. The Maximum strain values for Kobe earthquakes are observed to be in the range of 0.0107 to as high as 2.21. The Maximum strain values for Loma prieta earthquakes are observed to be in the range of 0.0120 to as high as 2.14. The Maximum strain values for Northridge earthquakes are observed to be in the range of 0.0076 to as high as 0.67. The Maximum strain values for Sikkim earthquakes are observed to be in the range of 0.0074 to as high as 1.30.

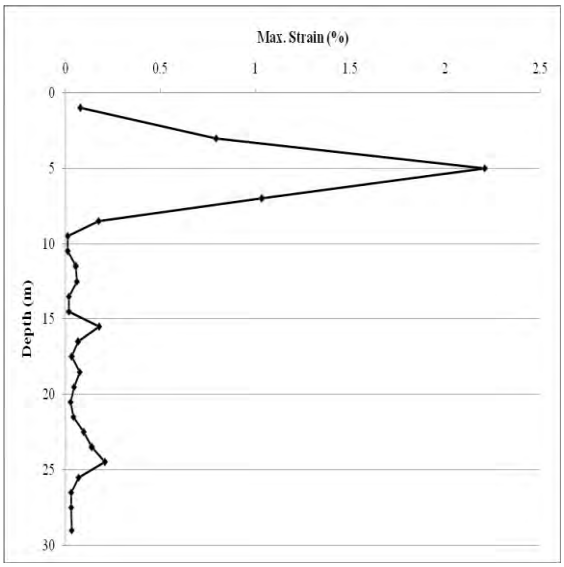

a) Kobe earthquake

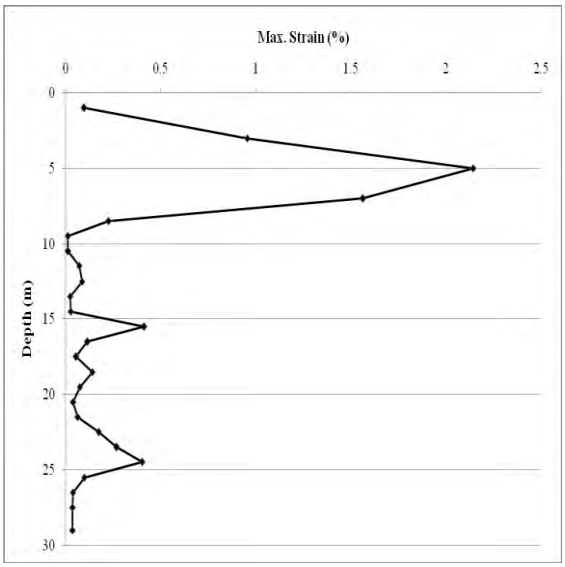

b) Loma prieta earthquake

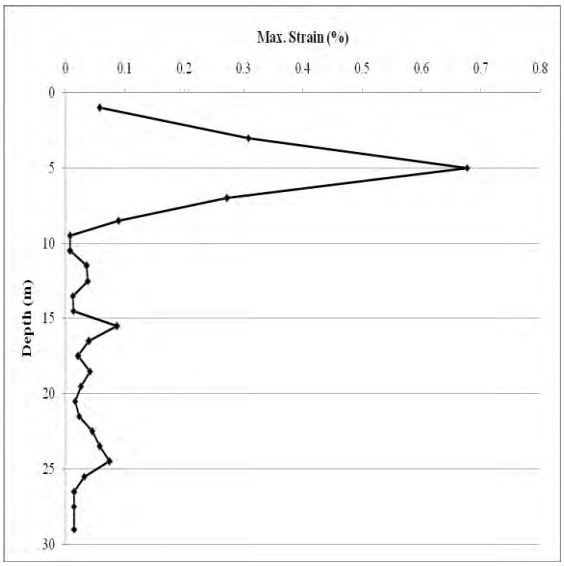

c) Nothridge earthquake

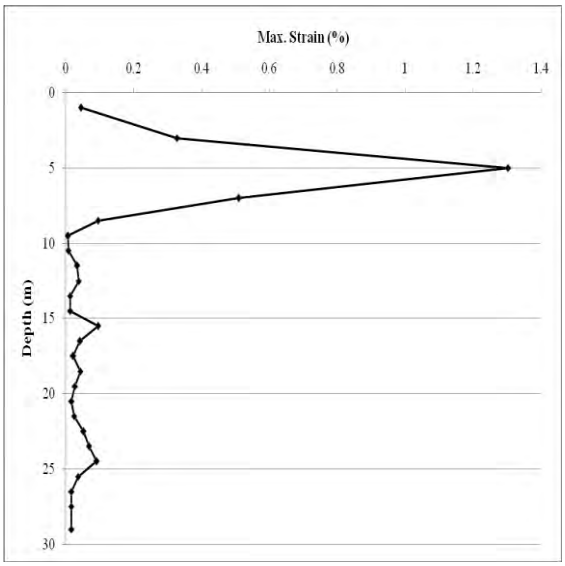

d) Sikkim earthquake

Figure 4.45: Maximum strain for local site effects

Figure 4.46 shows the comparison of Mean and Standard Deviation for surface PSA and Figure 4.47 shows the comparison of Surface PSA which are produced for different input motions.

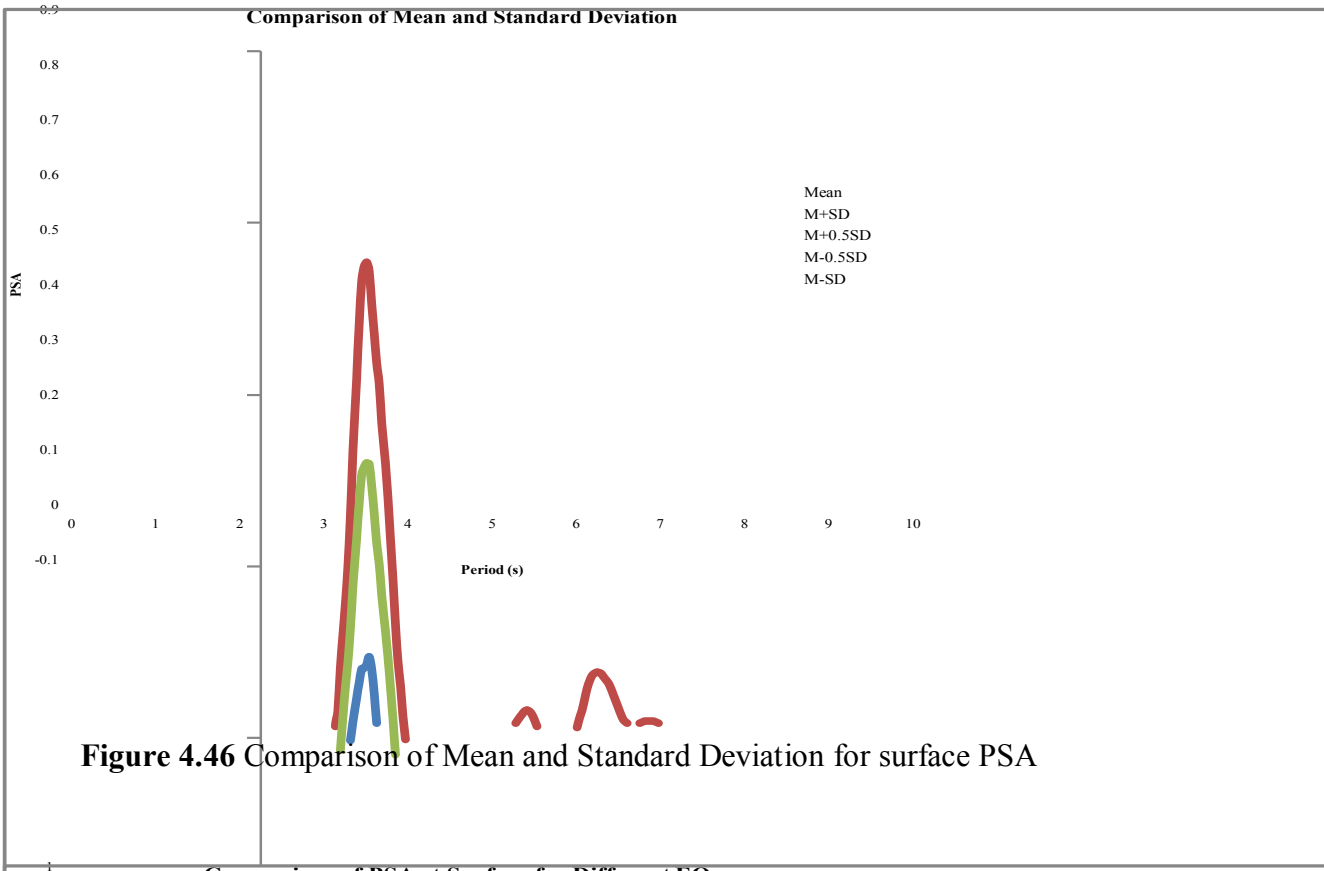

Figure 4.46 Comparison of Mean and Standard Deviation for surface PSA

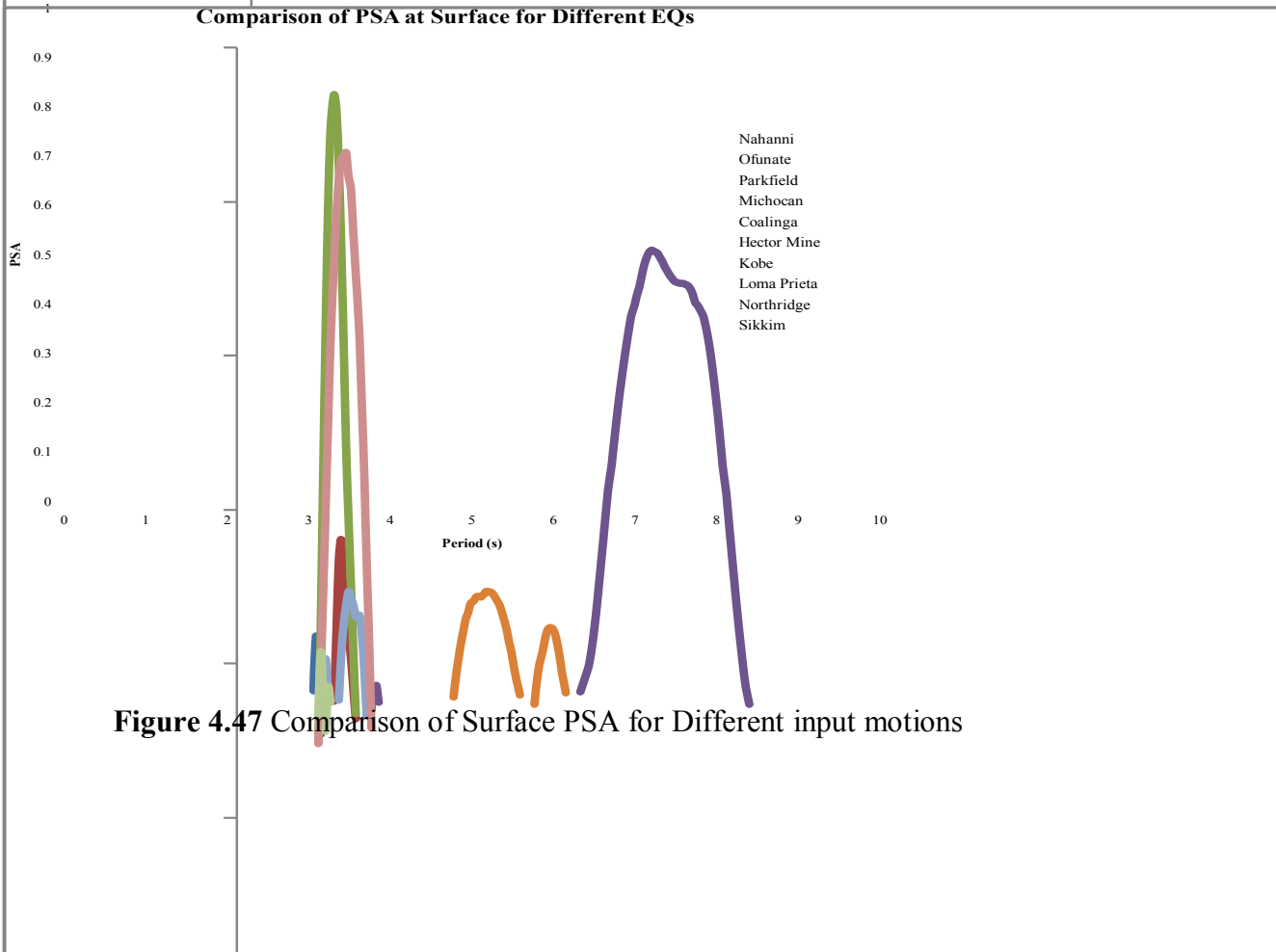

Figure 4.47 Comparison of Surface PSA for Different input motions

Figure 4.48 shows the comparison of Mean Input PSA and Mean Surface PSA produced for different input motions.

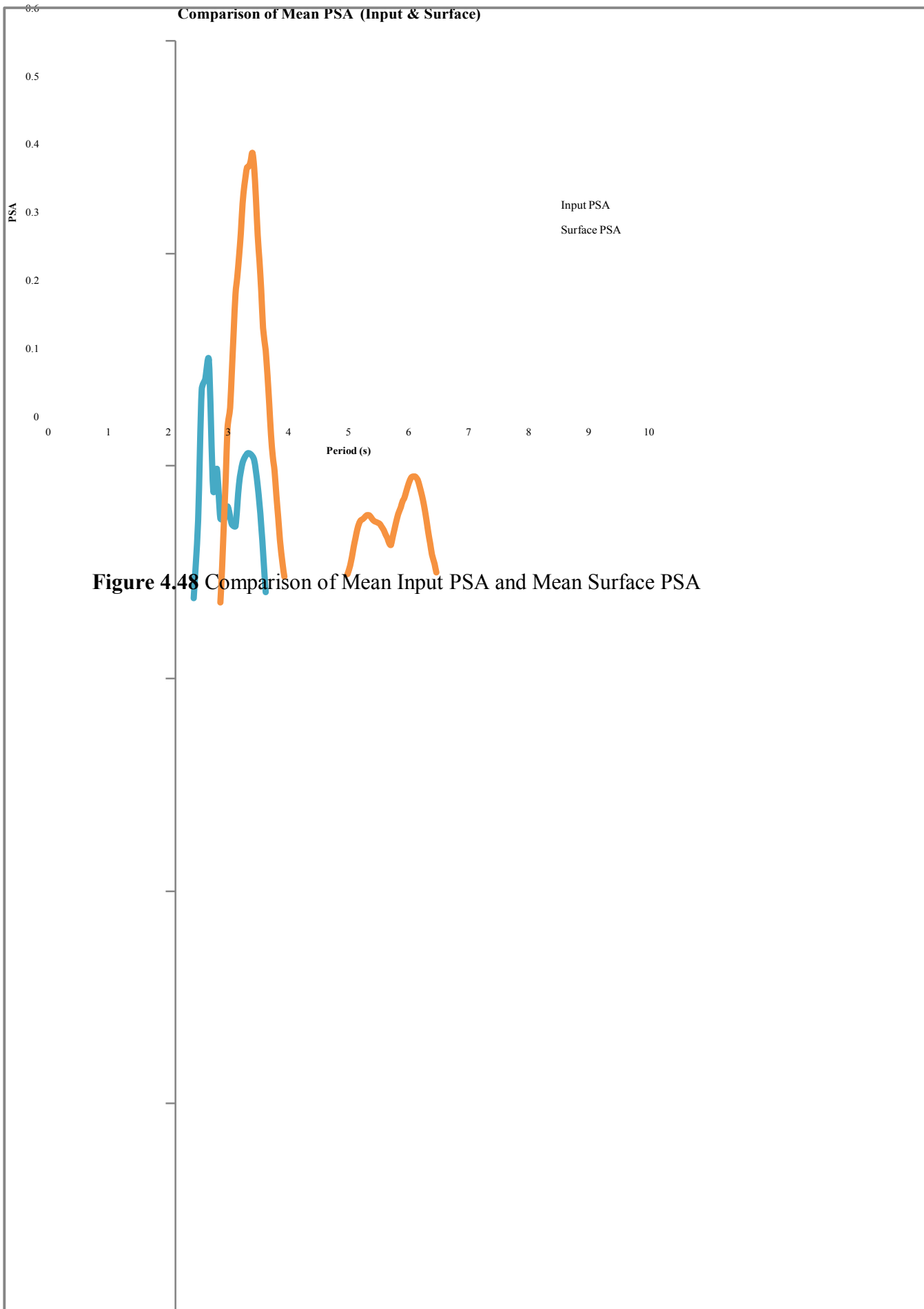

Figure 4.48 Comparison of Mean Input PSA and Mean Surface PSA

4.2.6 SITE: ASULIA

This site has been situated in north-western part of Dhaka city. Different geotechnical and geophysical test are conducted to characterize the site. Design soil profile is given in Figure 4.49 with average shear wave velocity for each layer. Average shear wave velocity for 30m layer (V_{30avg}) is

$$V_{30\,avg} = \frac{\sum_{i=1}^{N} h_i}{\sum_{i=1}^{N} \frac{h_i}{V_i}} = 140 \text{ m/s}$$

Where, h is the thickness of soil layer, and V is the respective shear wave velocity.

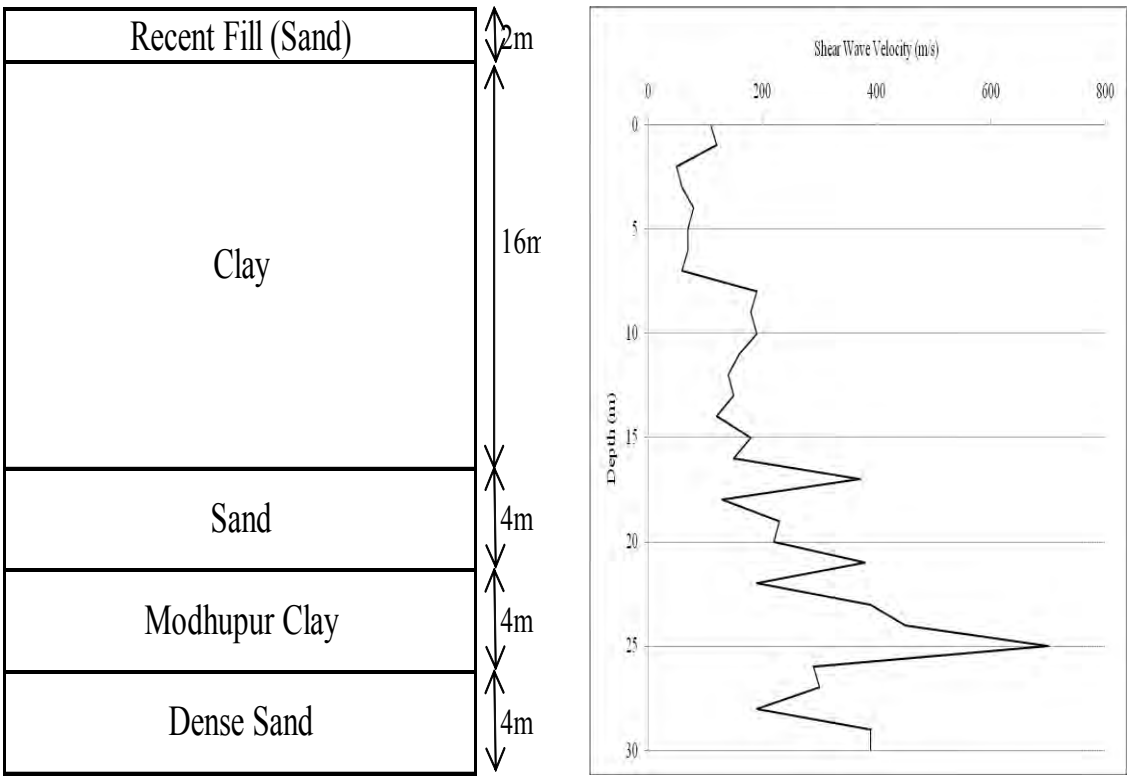

a) Design soil profile b) Shear wave velocity profile

Figure 4.49: Site Characterization

Response Spectra

Response spectra of four earthquakes are shown in Figure 4.50. Among the four earthquakes, Kobe earthquake produces highest (0.45g) peak spectral acceleration (PSA) for this site and Northridge earthquake produces lowest (0.0032g) peak spectral acceleration (PSA). It is observed that initially soil surface response is less than input response for all four earthquakes for this site. But gradually surface response increases.

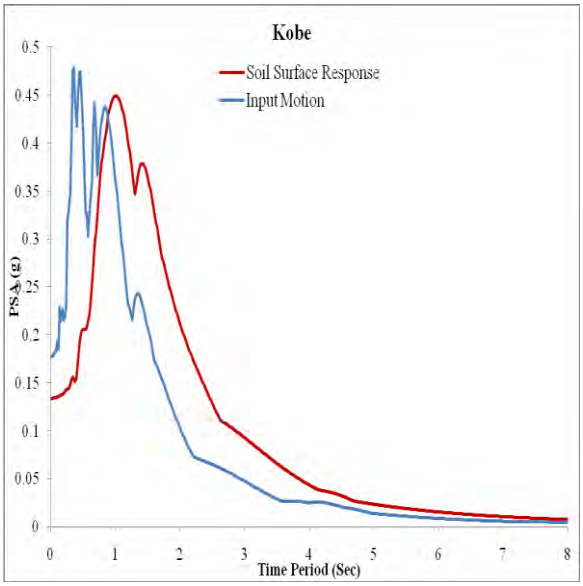

a) Kobe earthquake

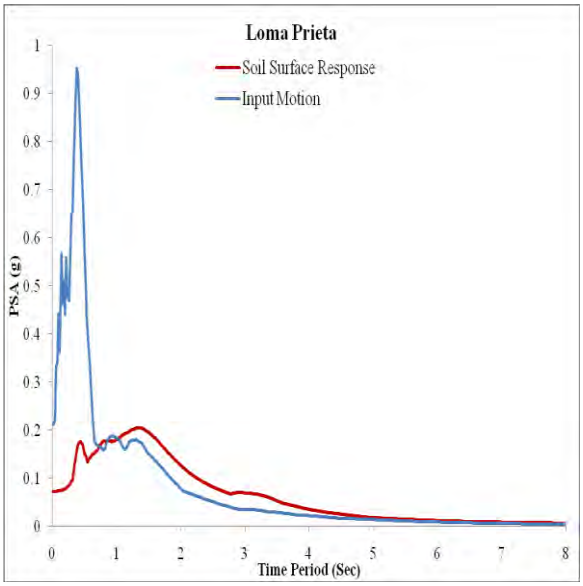

b) Loma prieta earthquake

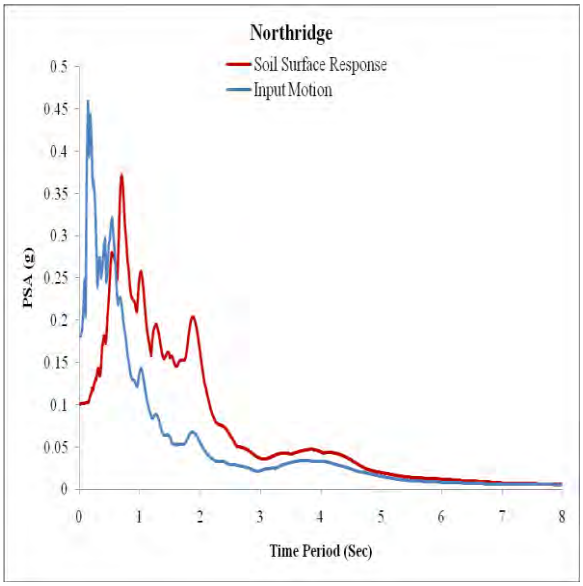

c) Nothridge earthquake

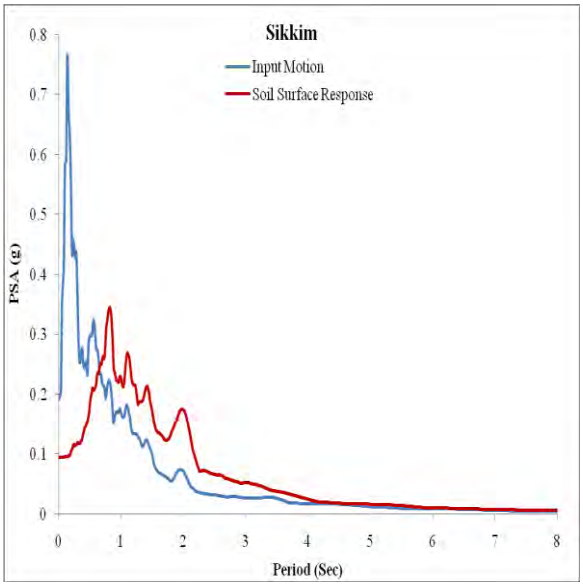

d) Sikkim earthquake

Figure 4.50: Response Spectra

Time Histories

The design soil profile is excited with input motion of four earthquakes to determine the dynamic response of local soil. Equivalent linear approach is used for site response analysis. As the seismic waves travel up and down, the soil vibrates. The acceleration of soil at the ground surface is shown in Figure 4.51. It is noted that the PGA and the ordinates of the response spectra increased.

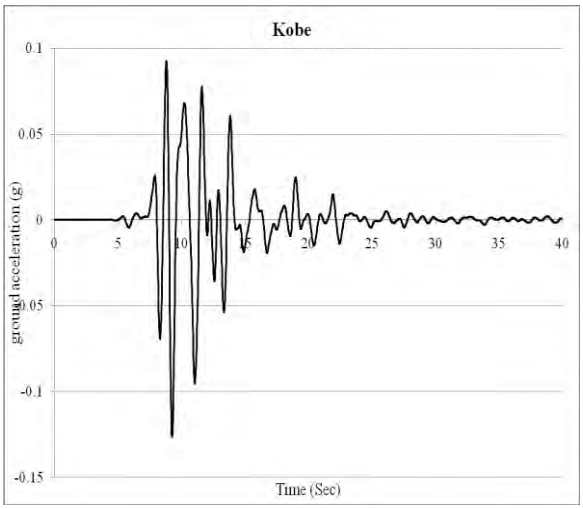

a) Kobe earthquake

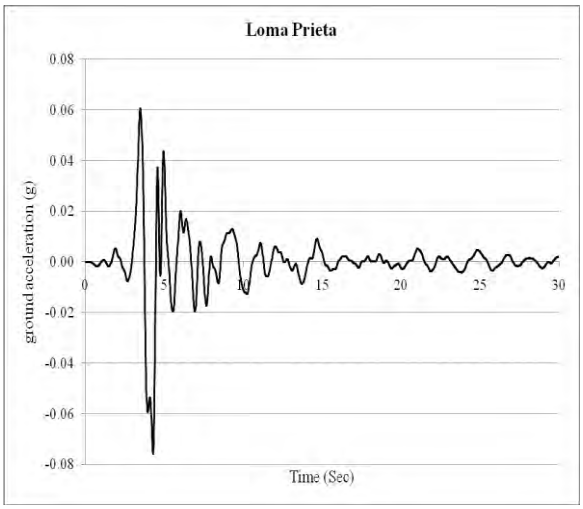

b) Loma prieta earthquake

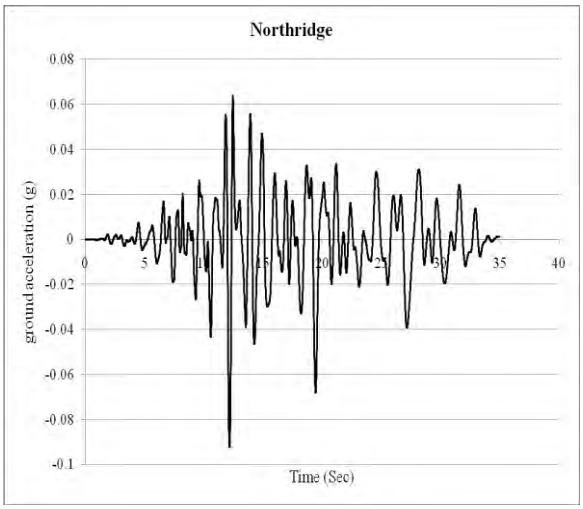

c) Nothridge earthquake

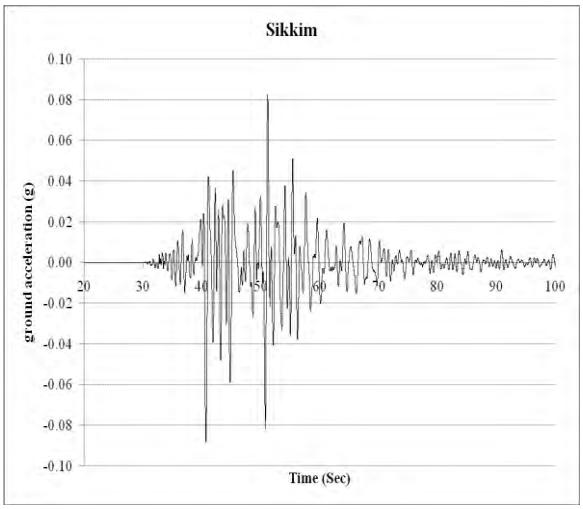

d) Sikkim earthquake

Figure 4.51: Time histories for local site effects

Maximum Peak Ground Acceleration (PGA)

Maximum Peak Ground Acceleration (PGA) at different depths of four earthquakes for this site is shown in figure 4.52. PGA at surface and that at bedrock is obtained from the analysis. The peak ground acceleration values at surface are observed to be in the range of 0.073g (Loma Prieta) to as high as 0.134g (Kobe) and that of the bedrock were observed to vary from 0.177g (Kobe) to 0.212g (Loma prieta). The impedance in the acceleration values can be observed. Such as, a sudden rise within few meters can cause considerable damage to the sub and super structure resulting in huge loss.

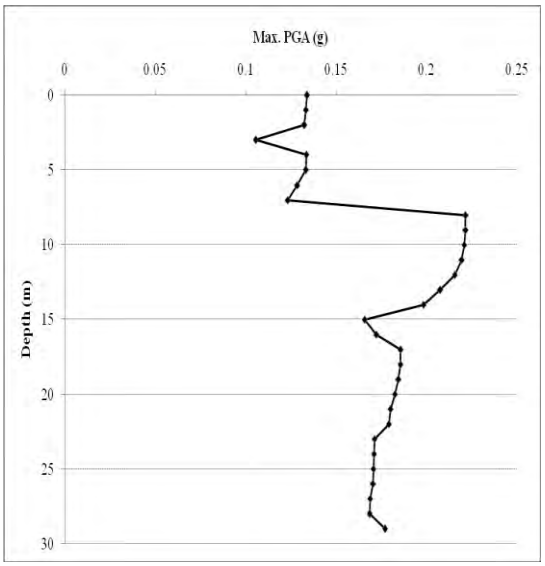

a) Kobe earthquake

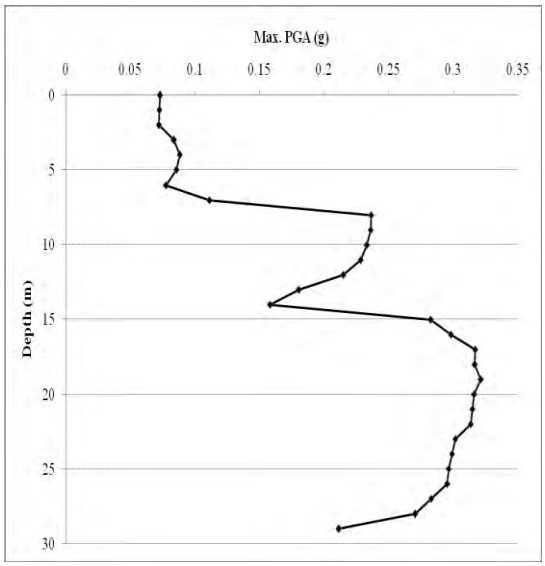

b) Loma prieta earthquake

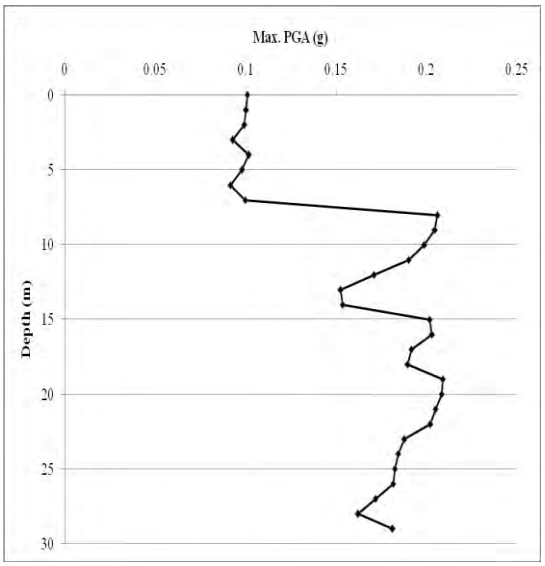

c) Nothridge earthquake

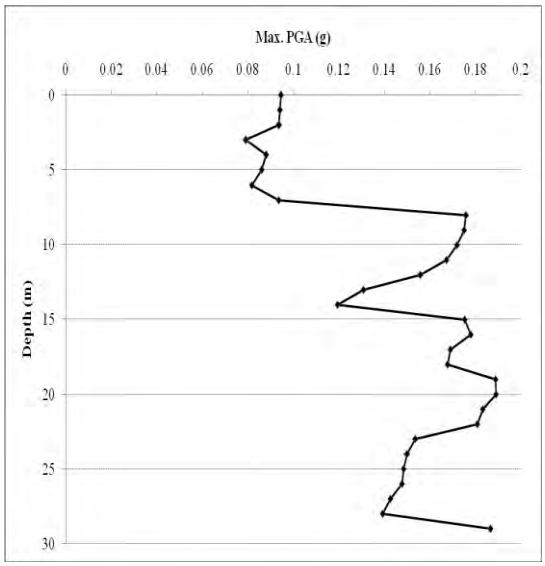

d) Sikkim earthquake

Figure 4.52: Maximum Peak Ground Acceleration for local site effects

Site amplification factors at sub surface layers are often used as one of the parameters for estimation of ground response. The amplification factor is the ratio of peak ground acceleration at surface to that of acceleration at hard rock. The amplification factors are determined as;

Amplification Factor = PGA recorded at ground surface / PGA recorded at hard rock
Amplification Factor (For Kobe earthquake) = 0.134/0.177 = 0.76
Amplification Factor (For Loma prieta earthquake) = 0.073/0.212 = 0.34
Amplification Factor (For Northridge earthquake) = 0.101/0.181 = 0.56
Amplification Factor (For Gangtok earthquake) = 0.095/0.187 = 0.51

Hence, the amplification factors have also been computed and it has been identified that similar to the peak ground acceleration values, the variation is within 0.34 (Loma prieta) to 0.76 (Kobe).

Maximum Stress Ratio

Maximum Stress Ratio at different depths of four earthquakes for this site is shown in figure 4.53. Maximum stress ratio at different depths of four earthquakes for this site is obtained from the analysis. The Maximum stress ratio values for Kobe earthquakes are observed to be in the range of 0.108 to as high as 0.294. The Maximum stress ratio values for Loma prieta earthquakes are observed to be in the range of 0.128 to as high as 0.209. The Maximum stress ratio values for Northridge earthquakes are observed to be in the range of 0.077 to as high as 0.221. The Maximum stress ratio values for Sikkim earthquakes are observed to be in the range of 0.108 to as high as 0.210.

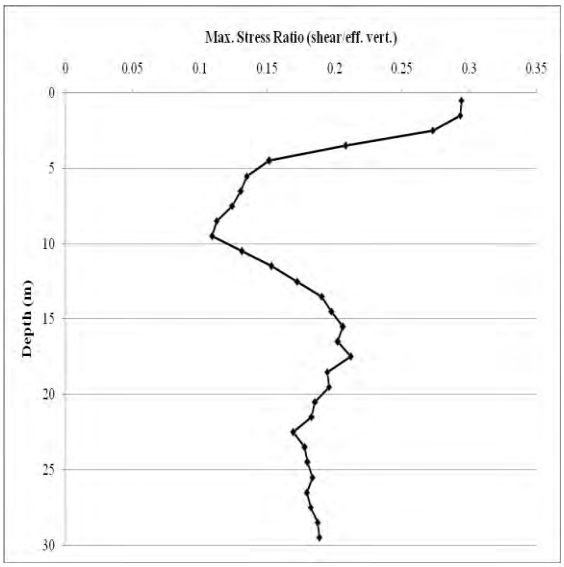

a) Kobe earthquake

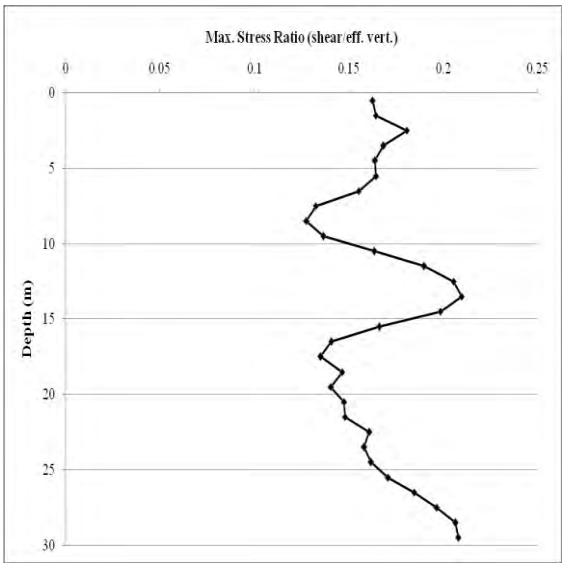

b) Loma prieta earthquake

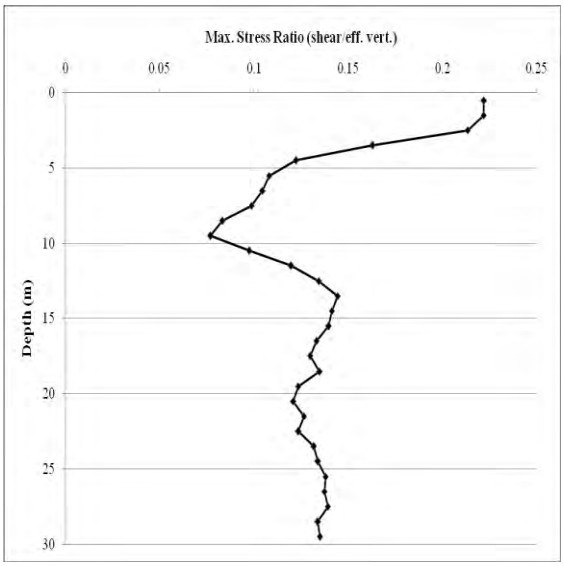

c) Nothridge earthquake

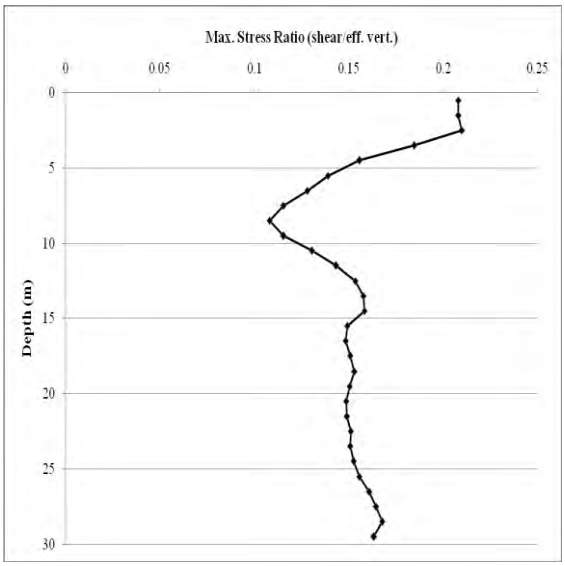

d) Sikkim earthquake

Figure 4.53: Maximum stress ratio for local site effects

Maximum Strain

Maximum Strain at different depths of four earthquakes for this site is shown in figure 4.54. Maximum strain values at different depths of four earthquakes for this site are obtained from the analysis. The Maximum strain values for Kobe earthquakes are observed to be in the range of 0.0049 to as high as 4.10. The Maximum strain values for Loma prieta earthquakes are observed to be in the range of 0.0033 to as high as 4.29. The Maximum strain values for Northridge earthquakes are observed to be in the range of 0.0035 to as high as 1.66. The Maximum strain values for Sikkim earthquakes are observed to be in the range of 0.0041 to as high as 2.44.

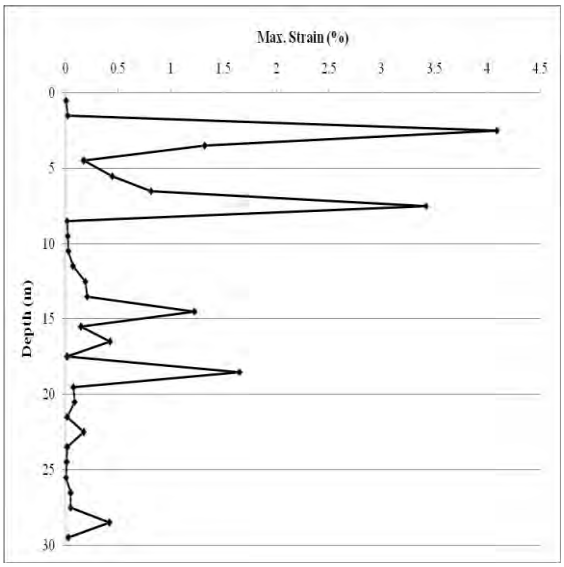

a) Kobe earthquake

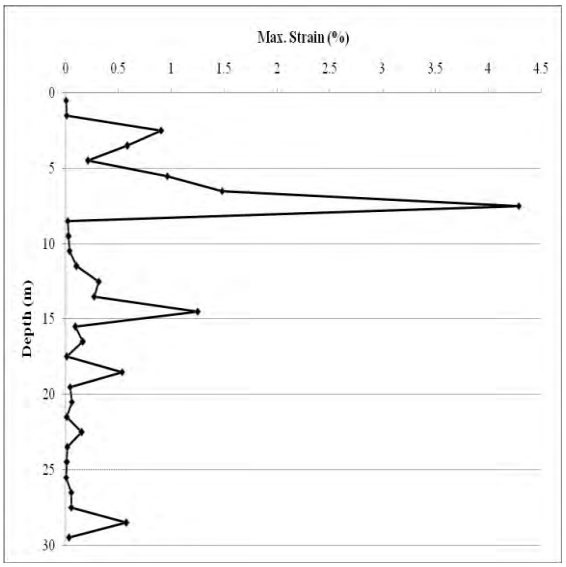

b) Loma prieta earthquake

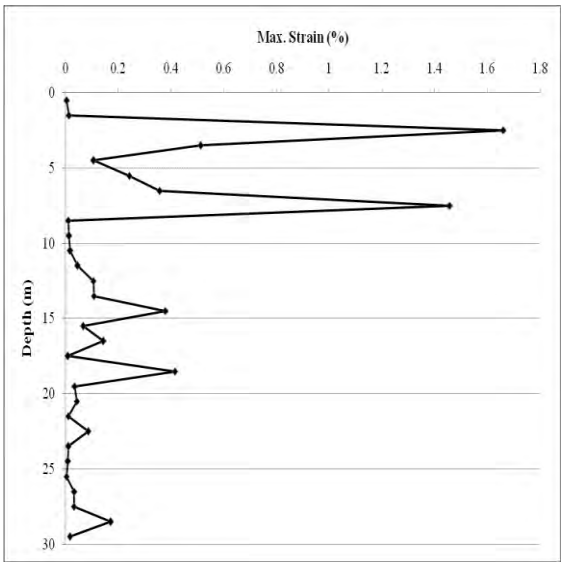

c) Nothridge earthquake

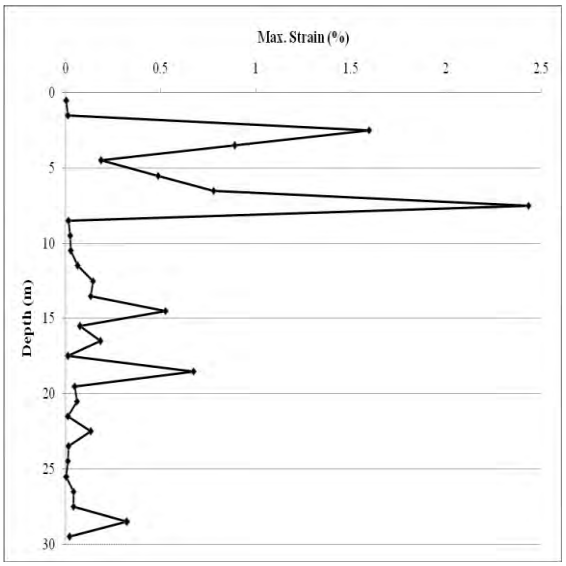

d) Sikkim earthquake

Figure 4.54: Maximum strain for local site effects

Figure 4.55 shows the comparison of Mean and Standard Deviation for surface PSA and Figure 4.56 shows the comparison of Surface PSA which are produced for different input motions.

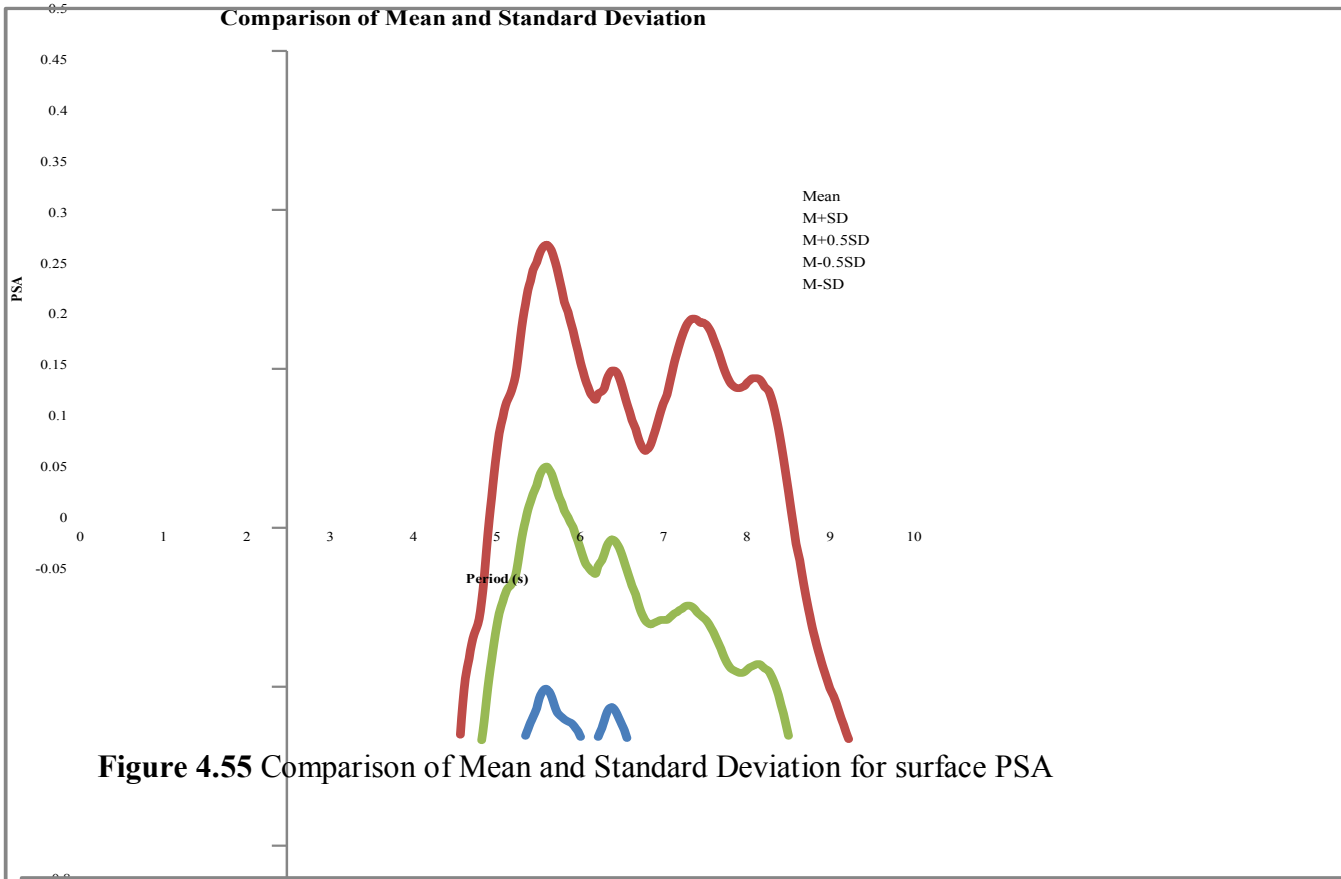

Figure 4.55 Comparison of Mean and Standard Deviation for surface PSA

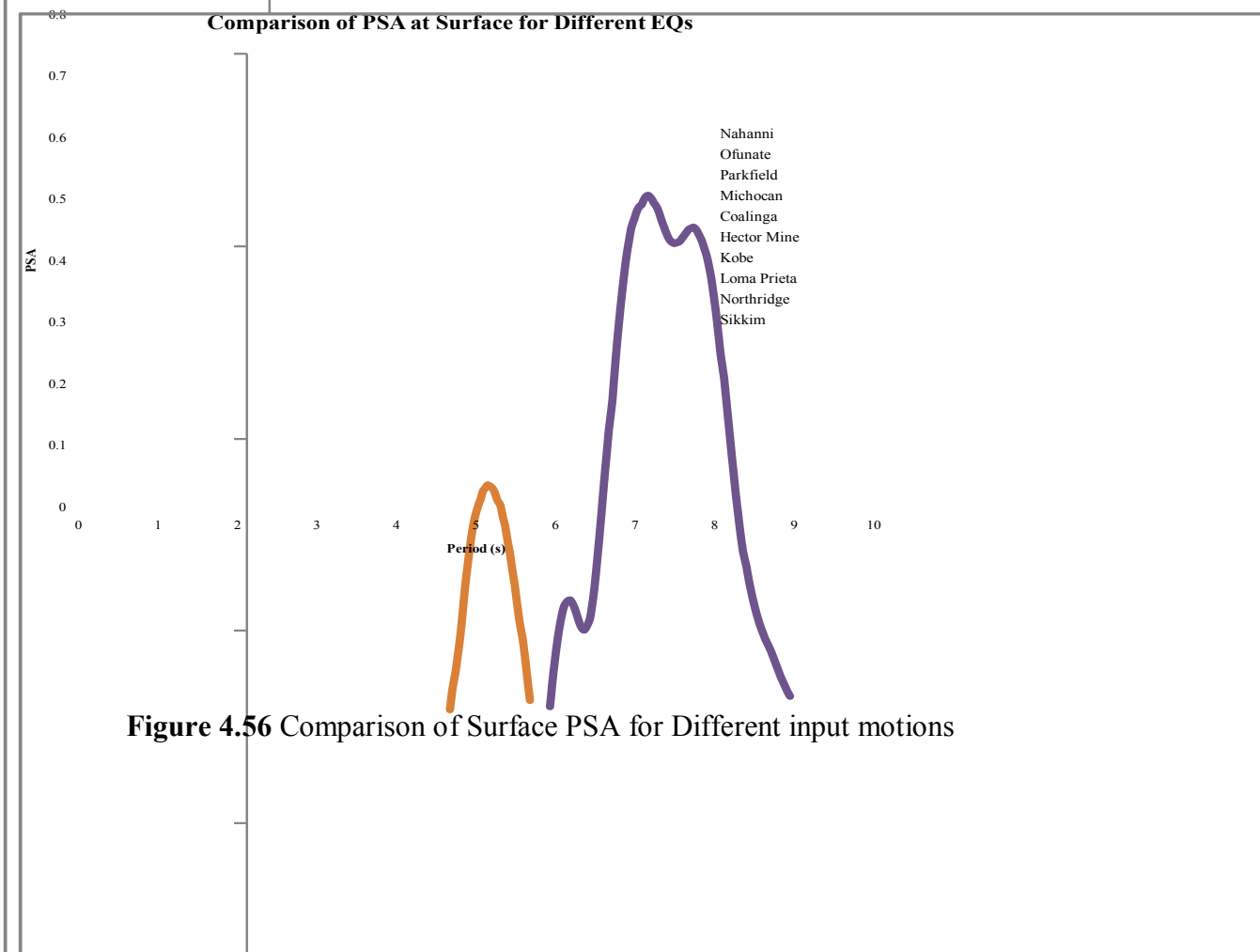

Figure 4.56 Comparison of Surface PSA for Different input motions

Figure 4.57 shows the comparison of Mean Input PSA and Mean Surface PSA produced for different input motions.

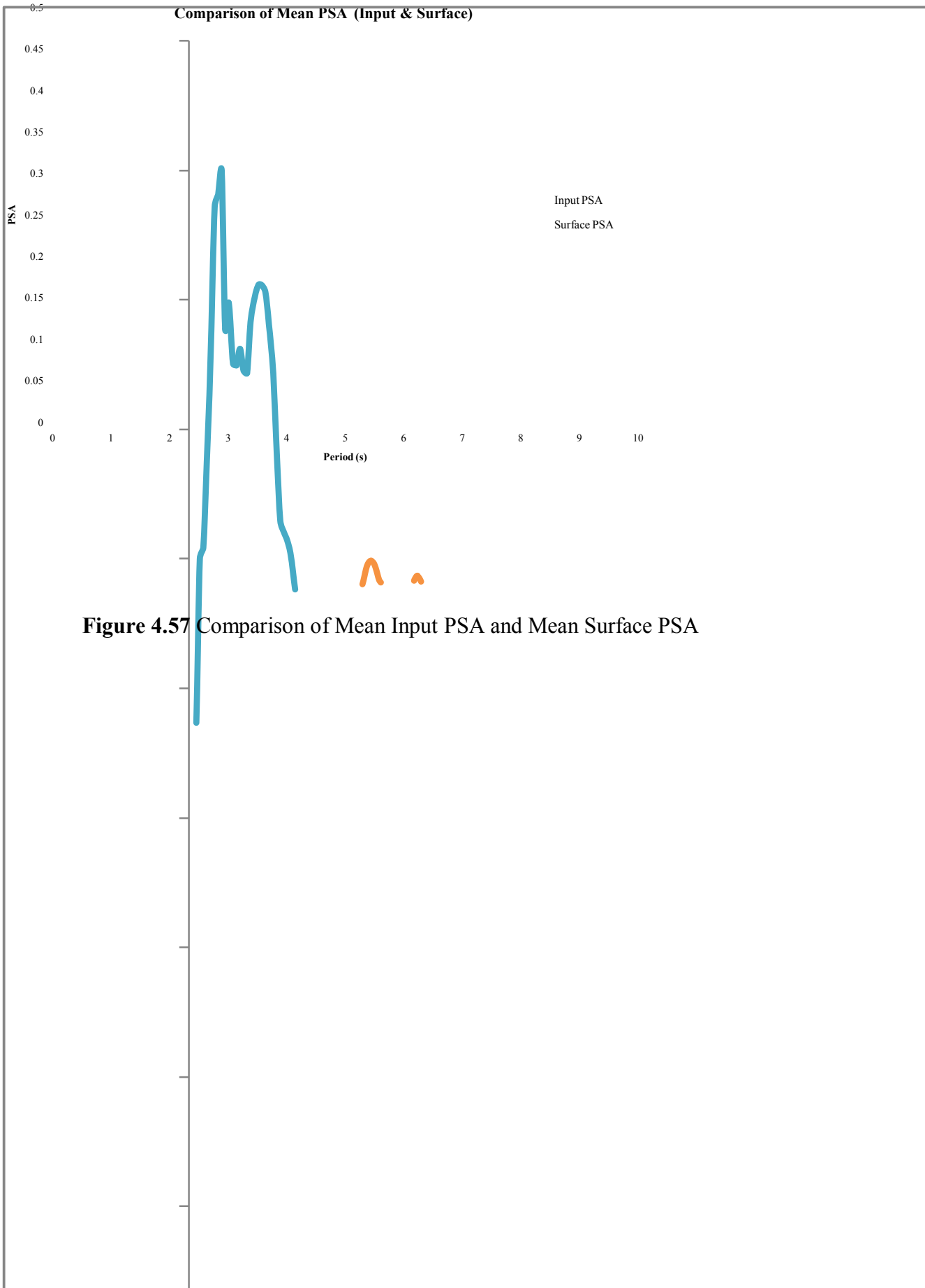

Figure 4.57 Comparison of Mean Input PSA and Mean Surface PSA

4.2.7 SITE: MIRPUR

This site has been situated in north-west part of Dhaka city. Different geotechnical and geophysical test are conducted to characterize the site. Design soil profile is given in Figure 4.58 with average shear wave velocity for each layer. Average shear wave velocity for 30m layer (V_{30avg}) is

$$V_{30\,avg} = \frac{\sum_{i=1}^{N} h_i}{\sum_{i=1}^{N} \frac{h_i}{V_i}} \quad = 320 \text{ m/s}$$

Where, h is the thickness of soil layer, and V is the respective shear wave velocity.

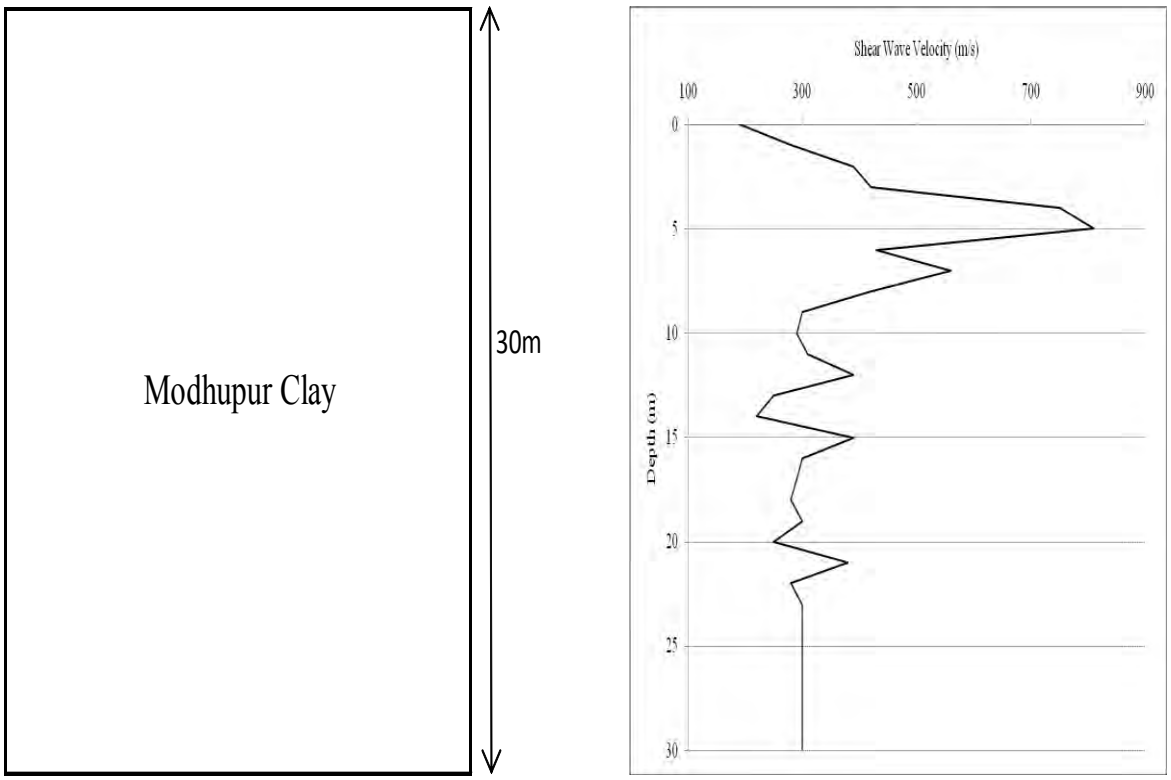

a) Design soil profile b) Shear wave velocity profile

Figure 4.58: Site Characterization

Response Spectra

Response spectra of four earthquakes are shown in Figure 4.59. Among the four earthquakes, Kobe earthquake produces highest (0.92g) peak spectral acceleration (PSA) for this site and Northridge earthquake produces lowest (0.0028g) peak spectral acceleration (PSA). It is observed that initially soil surface response is less than input response for all four earthquakes for this site. But gradually surface response increases.

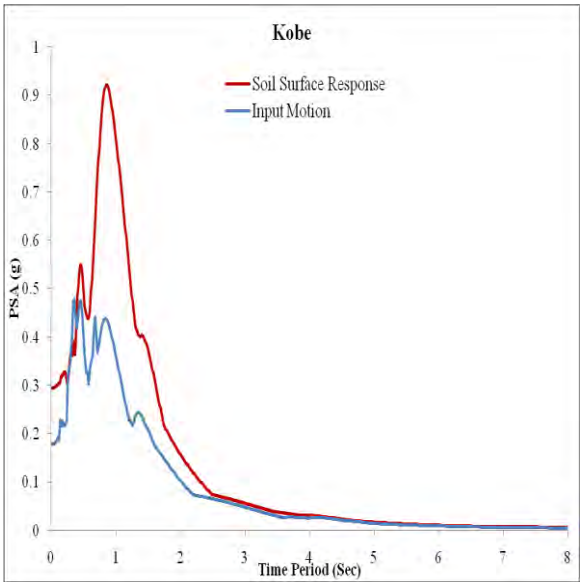

a) Kobe earthquake

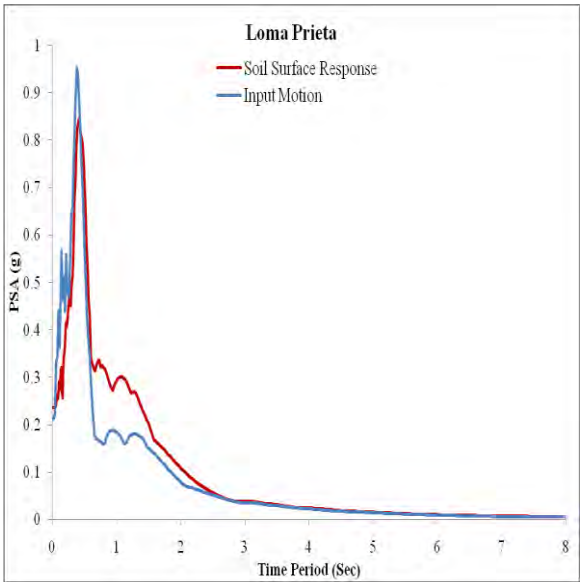

b) Loma prieta earthquake

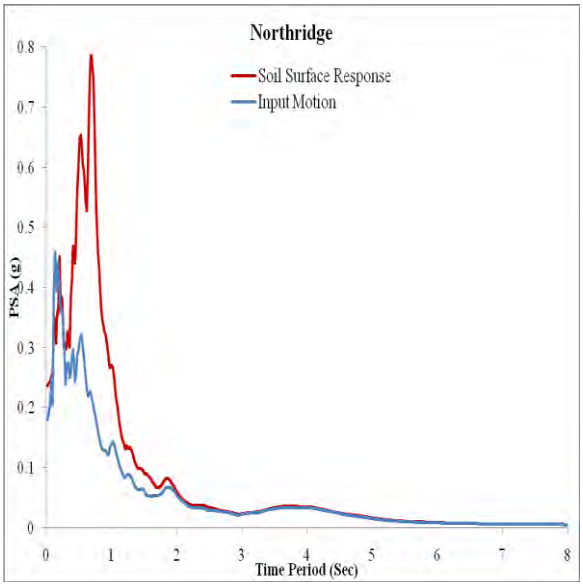

c) Nothridge earthquake

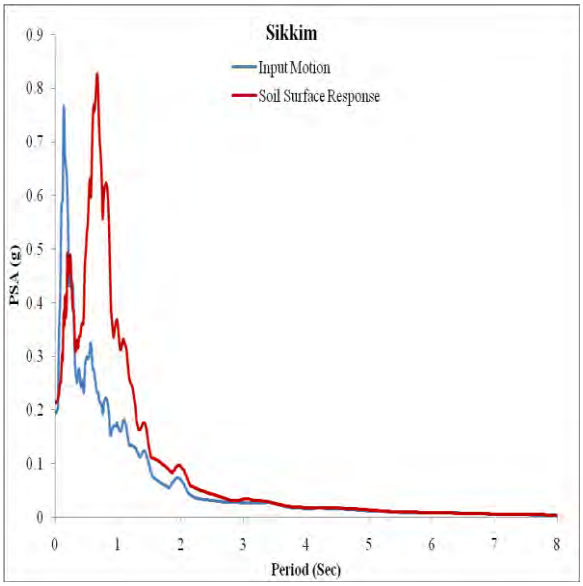

d) Sikkim earthquake

Figure 4.59: Response Spectra

Time Histories

The design soil profile is excited with input motion of four earthquakes to determine the dynamic response of local soil. Equivalent linear approach is used for site response analysis. As the seismic waves travel up and down, the soil vibrates. The acceleration of soil at the ground surface is shown in Figure 4.60 It is noted that the PGA and the ordinates of the response spectra increased.

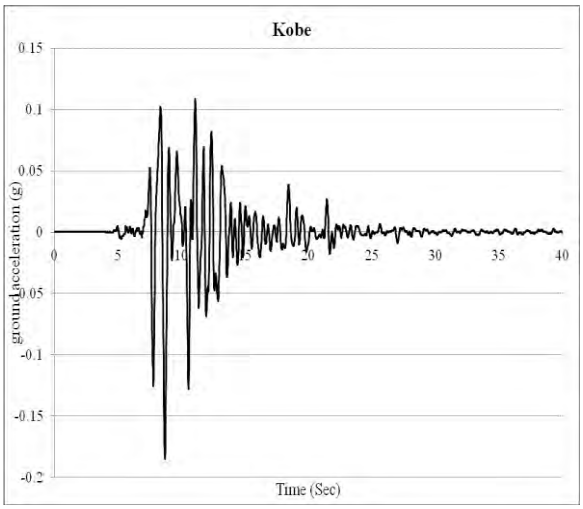

a) Kobe earthquake

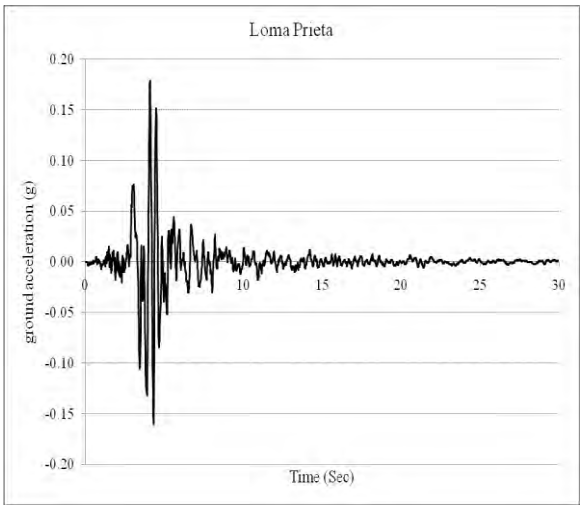

b) Loma prieta earthquake

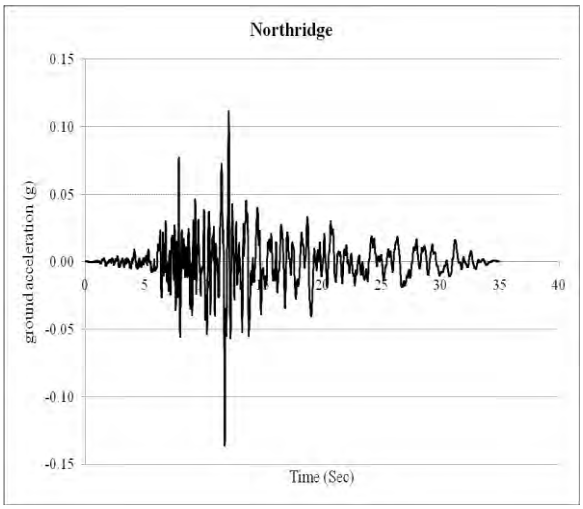

c) Nothridge earthquake

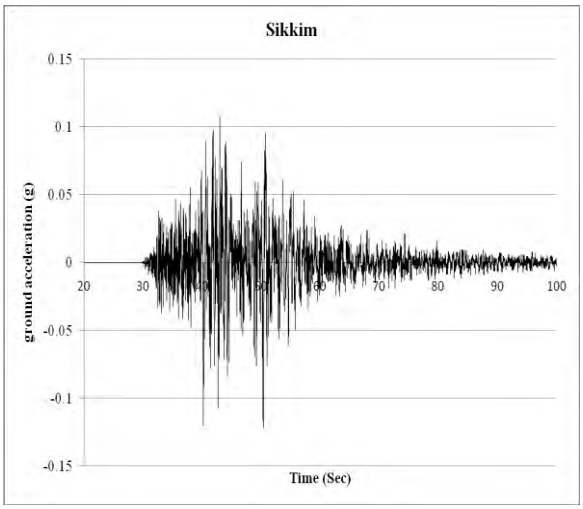

d) Sikkim earthquake

Figure 4.60: Time histories for local site effects

Maximum Peak Ground Acceleration (PGA)

Maximum Peak Ground Acceleration (PGA) at different depths of four earthquakes for this site are shown in figure 4.61. PGA at surface and that at bedrock is obtained from the analysis. The peak ground acceleration values at surface are observed to be in the range of 0.214g (Sikkim) to as high as 0.295g (Kobe) and that of the bedrock were observed to vary from 0.177g (Kobe) to 0.212g (Loma prieta). The impedance in the acceleration values can be observed. Such as, a sudden rise within few meters can cause considerable damage to the sub and super structure resulting in huge loss.

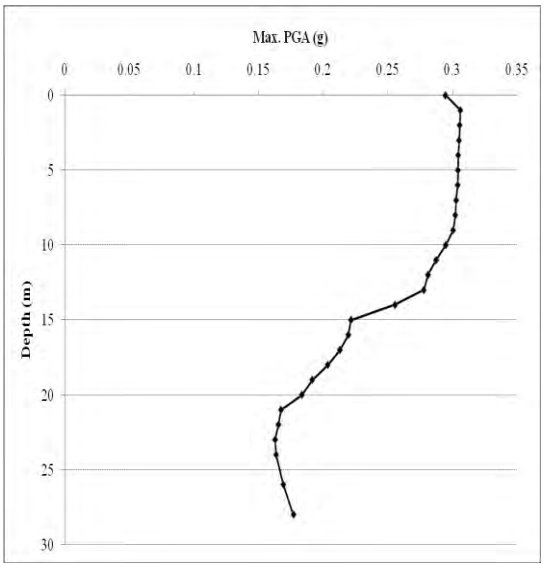

a) Kobe earthquake

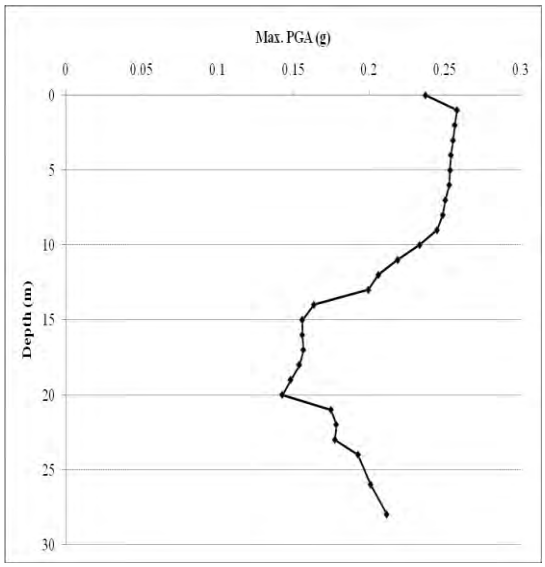

b) Loma prieta earthquake

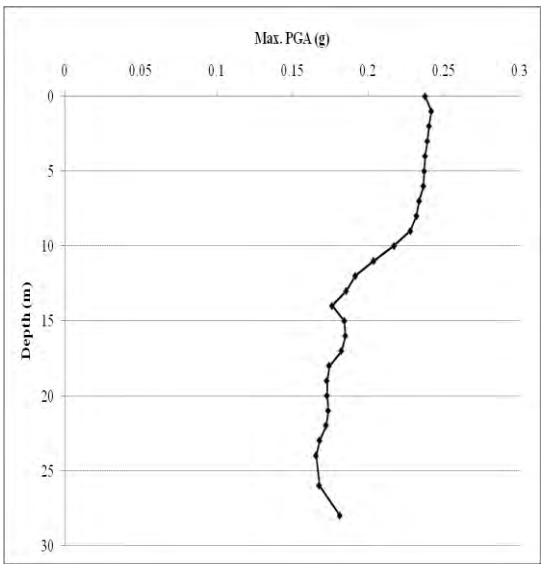

c) Nothridge earthquake

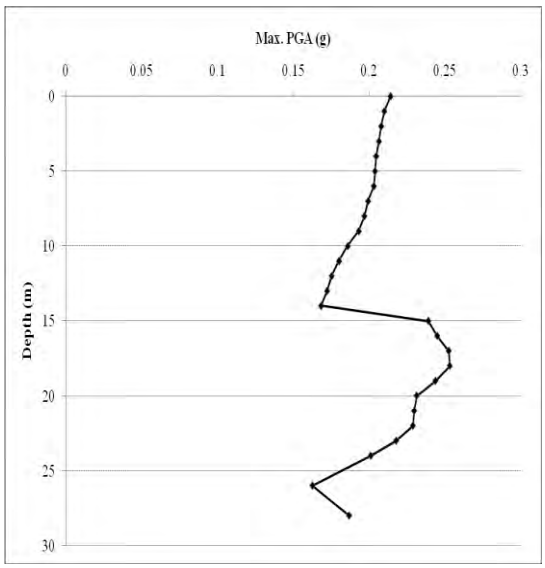

d) Sikkim earthquake

Figure 4.61: Maximum Peak Ground Acceleration for local site effects

Site amplification factors at sub surface layers are often used as one of the parameters for estimation of ground response. The amplification factor is the ratio of peak ground acceleration at surface to that of acceleration at hard rock. The amplification factors are determined as;

Amplification Factor = PGA recorded at ground surface / PGA recorded at hard rock
Amplification Factor (For Kobe earthquake) = 0.295/0.177 = 1.67
Amplification Factor (For Loma prieta earthquake) = 0.237/0.212 = 1.12
Amplification Factor (For Northridge earthquake) = 0.238/0.181 = 1.31
Amplification Factor (For Gangtok earthquake) = 0.214/0.187 = 1.14

Hence, the amplification factors have also been computed and it has been identified that similar to the peak ground acceleration values, the variation is within 1.12 (Loma prieta) to 1.67 (Kobe).

Maximum Stress Ratio

Maximum Stress Ratio at different depths of four earthquakes for this site is shown in figure 4.62. Maximum stress ratio at different depths of four earthquakes for this site is obtained from the analysis. The Maximum stress ratio values for Kobe earthquakes are observed to be in the range of 0.414 to as high as 0.647. The Maximum stress ratio values for Loma prieta earthquakes are observed to be in the range of 0.243 to as high as 0.520. The Maximum stress ratio values for Northridge earthquakes are observed to be in the range of 0.271 to as high as 0.517. The Maximum stress ratio values for Sikkim earthquakes are observed to be in the range of 0.306 to as high as 0.470.

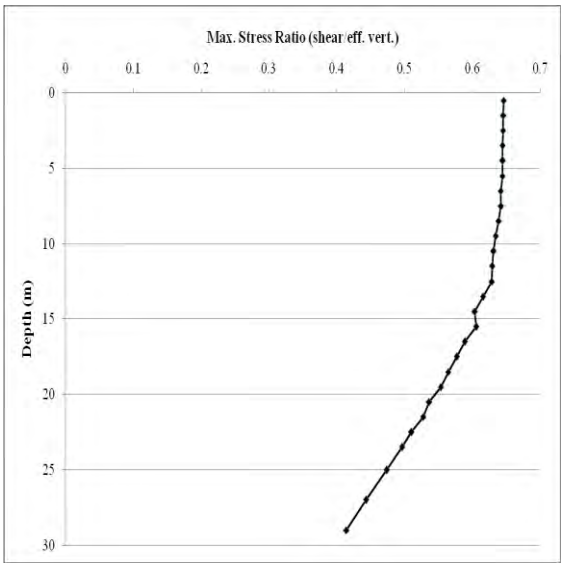

a) Kobe earthquake

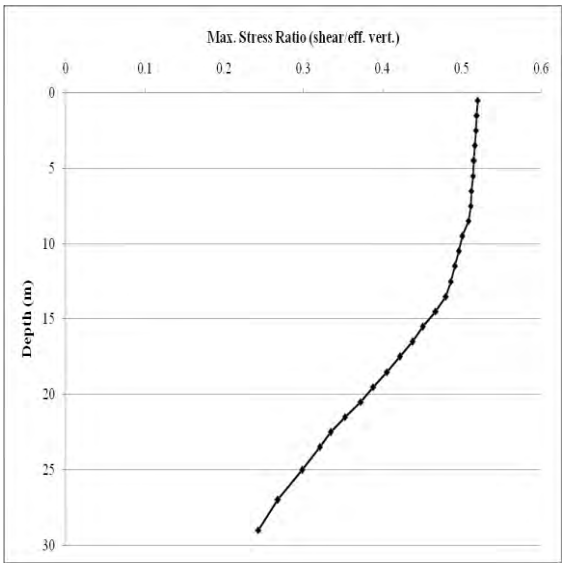

b) Loma prieta earthquake

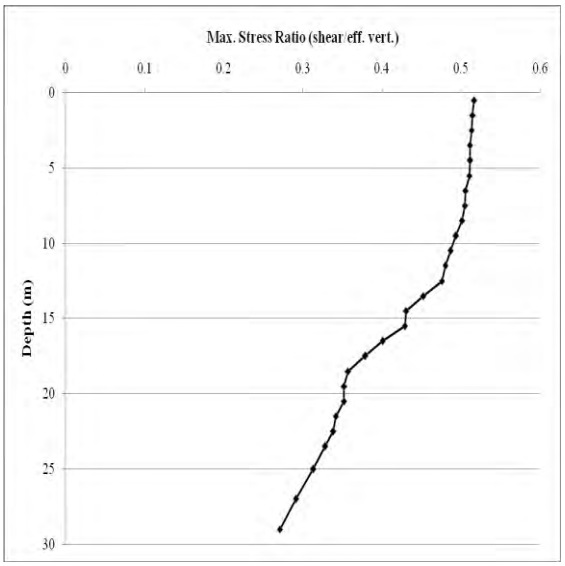

c) Nothridge earthquake

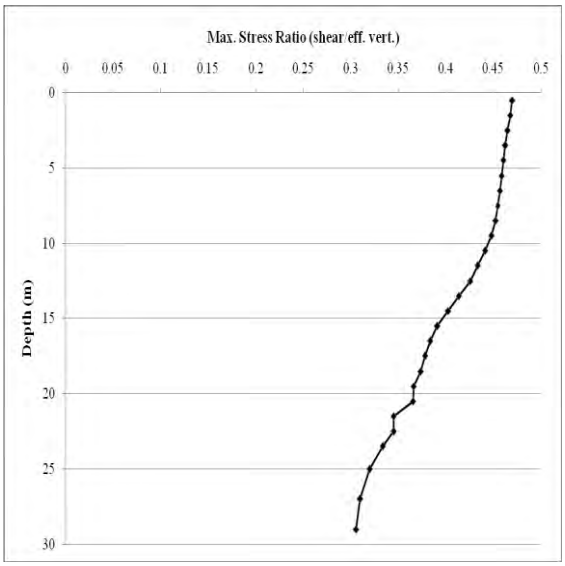

d) Sikkim earthquake

Figure 4.62: Maximum stress ratio for local site effects

Maximum Strain

Maximum Strain at different depths of four earthquakes for this site is shown in figure 4.63. Maximum strain values at different depths of four earthquakes for this site are obtained from the analysis. The Maximum strain values for Kobe earthquakes are observed to be in the range of 0.0025 to as high as 0.909. The Maximum strain values for Loma prieta earthquakes are observed to be in the range of 0.0020 to as high as 0.365. The Maximum strain values for Northridge earthquakes are observed to be in the range of 0.0019 to as high as 0.304. The Maximum strain values for Sikkim earthquakes are observed to be in the range of 0.0017 to as high as 0.238.

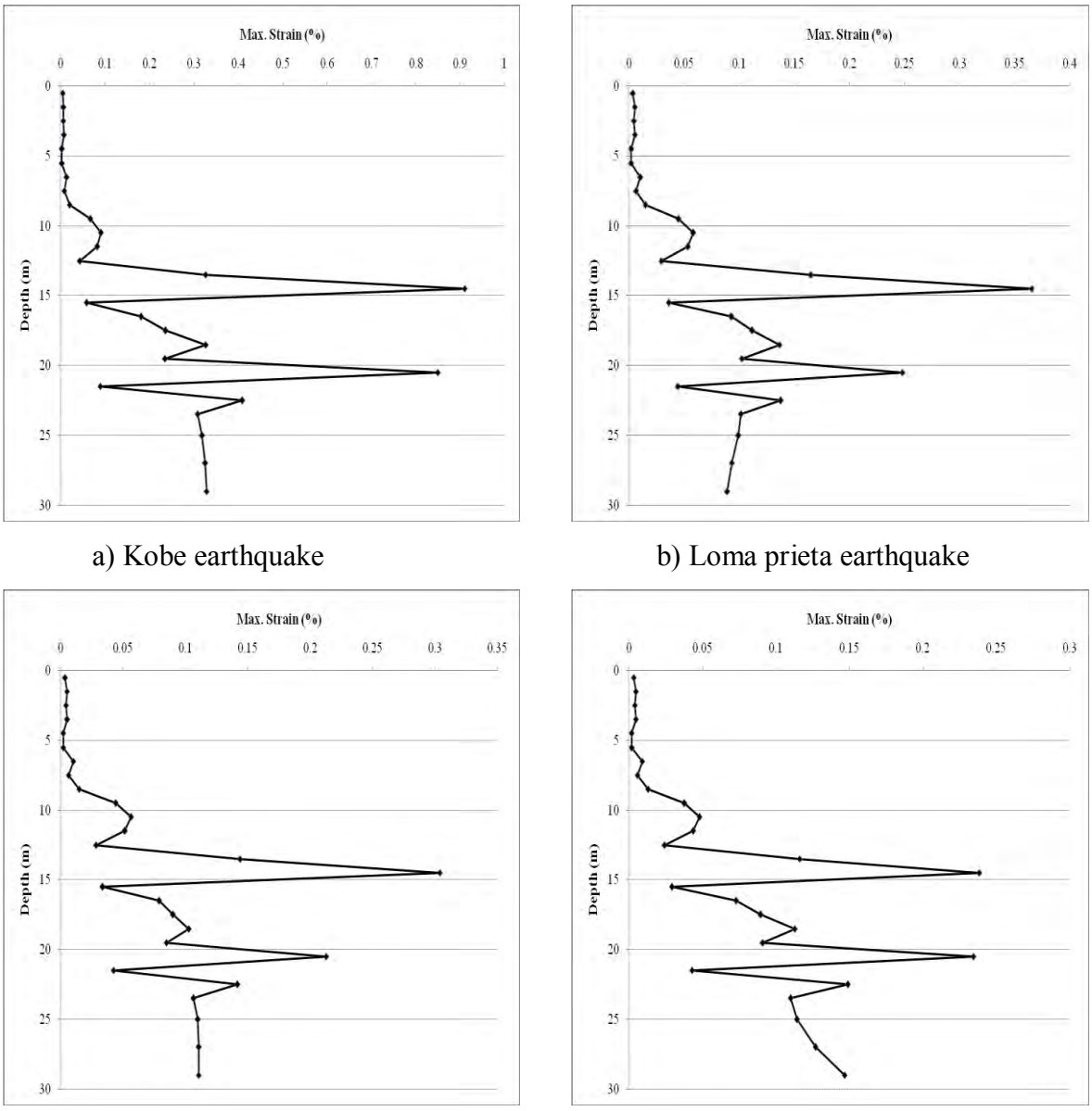

a) Kobe earthquake

b) Loma prieta earthquake

c) Nothridge earthquake

d) Sikkim earthquake

Figure 4.63: Maximum strain for local site effects

Figure 4.64 shows the comparison of Mean and Standard Deviation for surface PSA and Figure 4.65 shows the comparison of Surface PSA which are produced for different input motions.

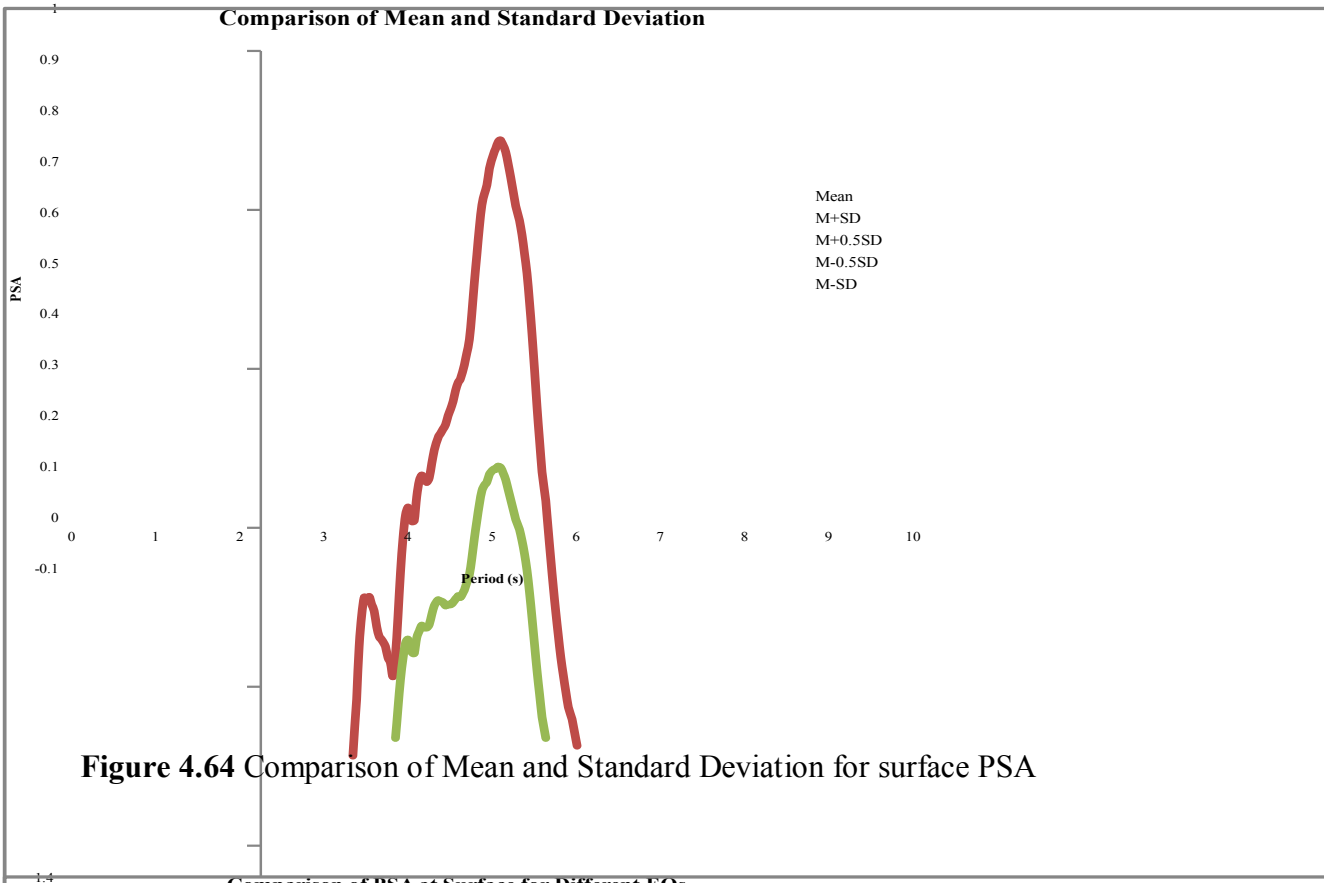

Figure 4.64 Comparison of Mean and Standard Deviation for surface PSA

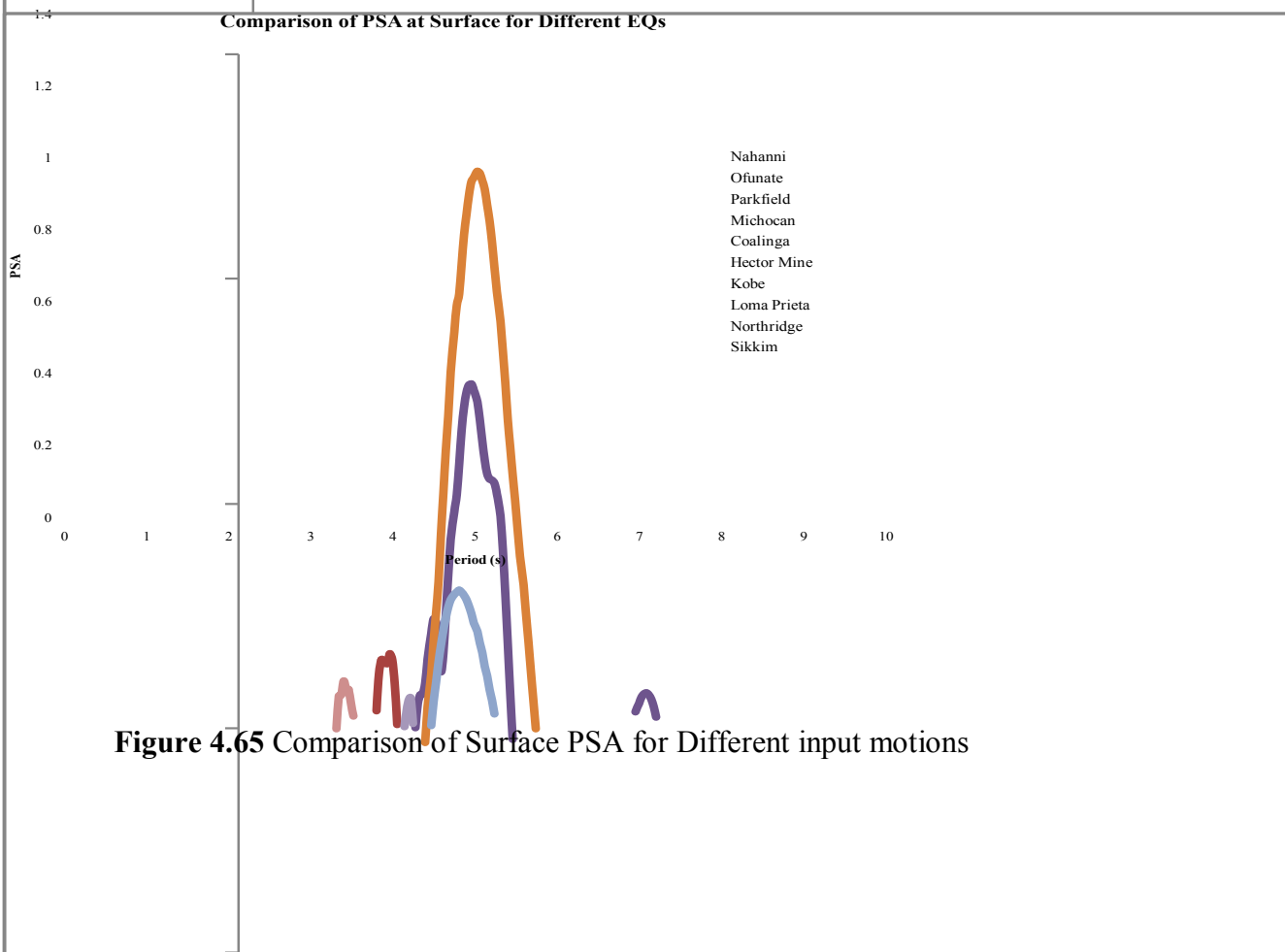

Figure 4.65 Comparison of Surface PSA for Different input motions

Figure 4.66 shows the comparison of Mean Input PSA and Mean Surface PSA produced for different input motions.

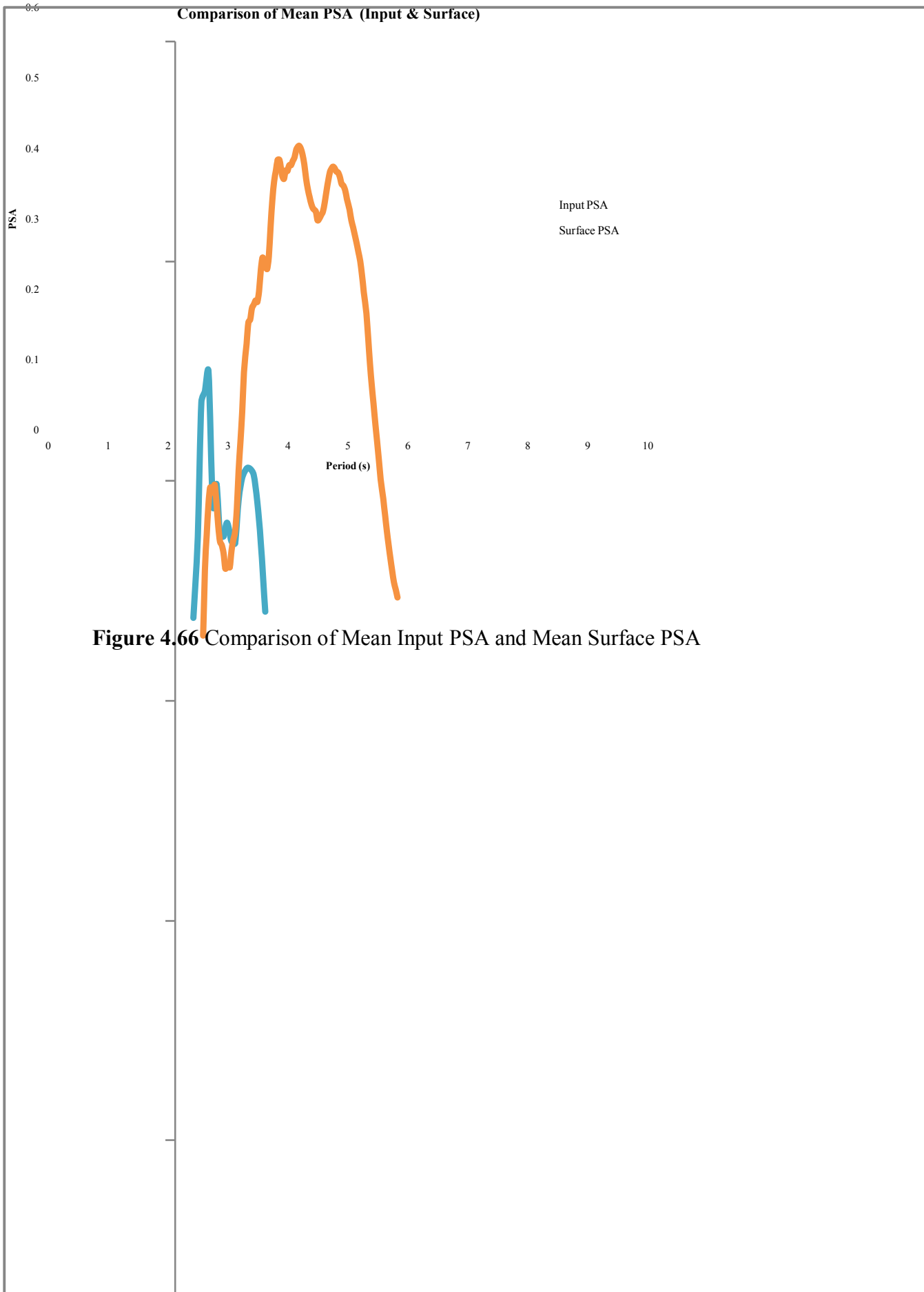

Figure 4.66 Comparison of Mean Input PSA and Mean Surface PSA

4.2.8 SITE: MOHAMMADPUR

This site has been situated in west part of Dhaka city. Different geotechnical and geophysical test are conducted to characterize the site. Design soil profile is given in Figure 4.67 with average shear wave velocity for each layer. Average shear wave velocity for 30m layer (V_{30avg}) is

$$V_{30\,avg} = \frac{\sum_{i=1}^{N} h_i}{\sum_{i=1}^{N} \frac{h_i}{V_i}} \quad = 195 \text{ m/s}$$

Where, h is the thickness of soil layer, and V is the respective shear wave velocity.

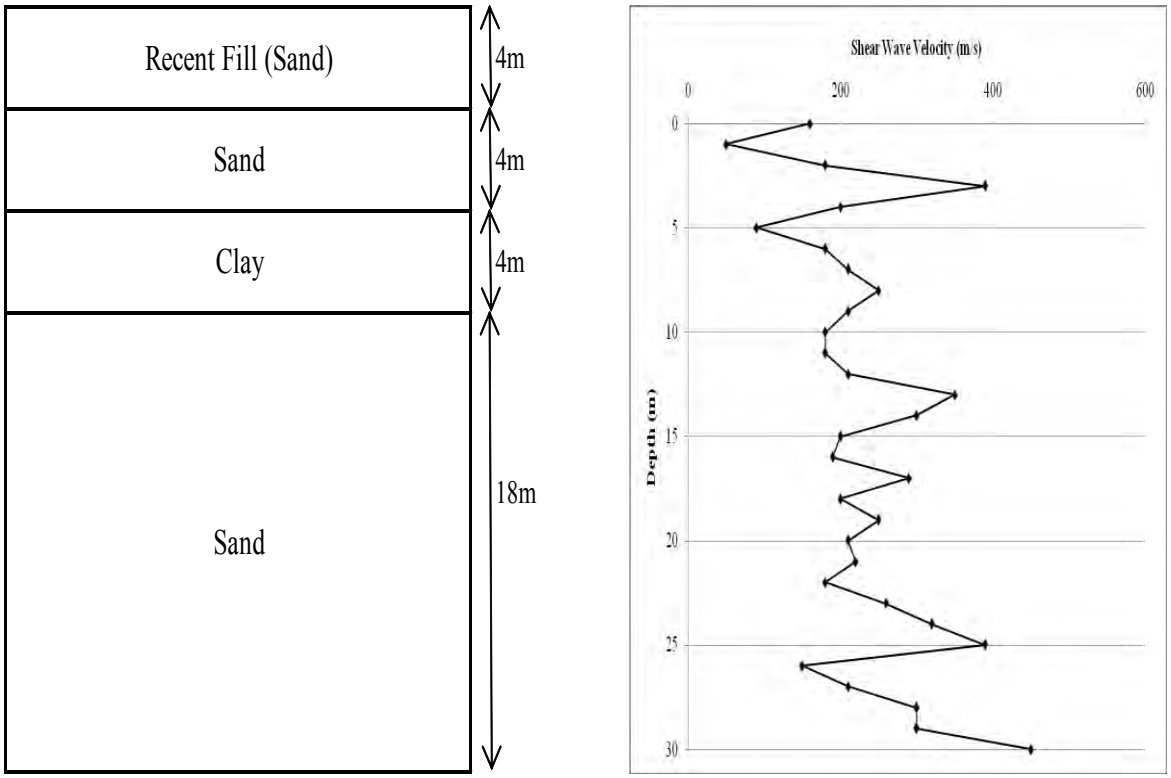

a) Design soil profile b) Shear wave velocity profile

Figure 4.67: Site Characterization

Response Spectra

Response spectra of four earthquakes are shown in Figure 4.68. Among the four earthquakes, Kobe earthquake produces highest (0.90g) peak spectral acceleration (PSA) for this site and Northridge earthquake produces lowest (0.0030g) peak spectral acceleration (PSA). It is observed that initially soil surface response is less than input response for all four earthquakes for this site. But gradually surface response increases.

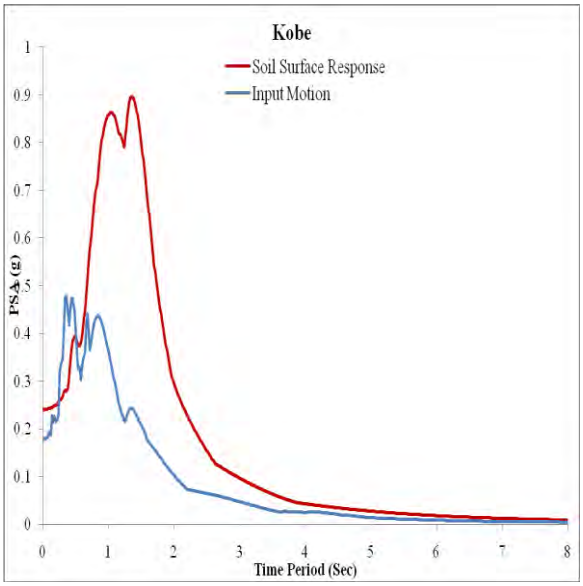

a) Kobe earthquake

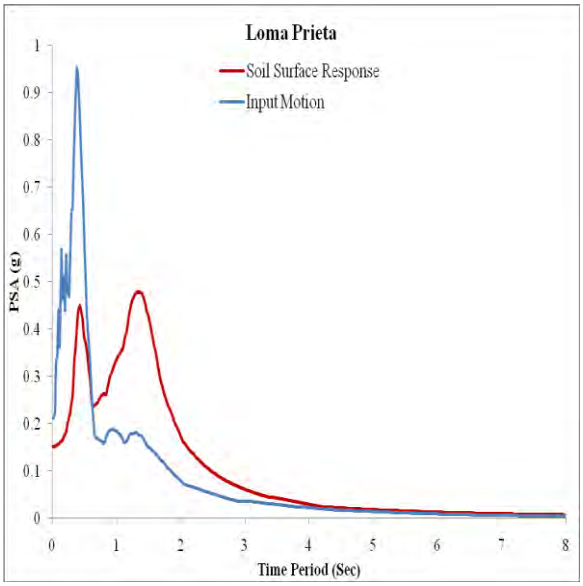

b) Loma prieta earthquake

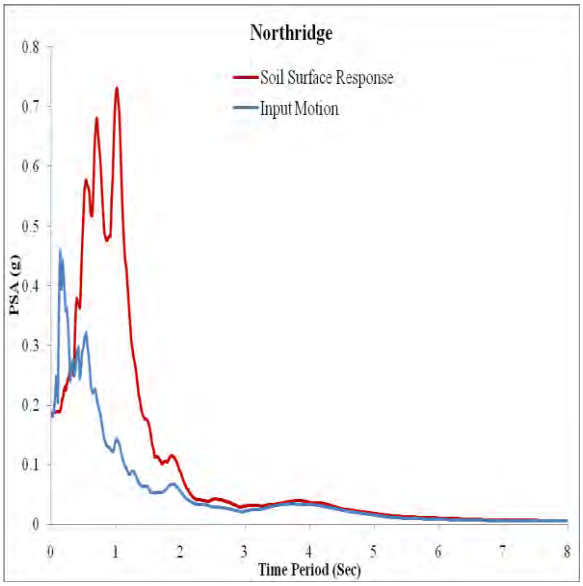

c) Nothridge earthquake

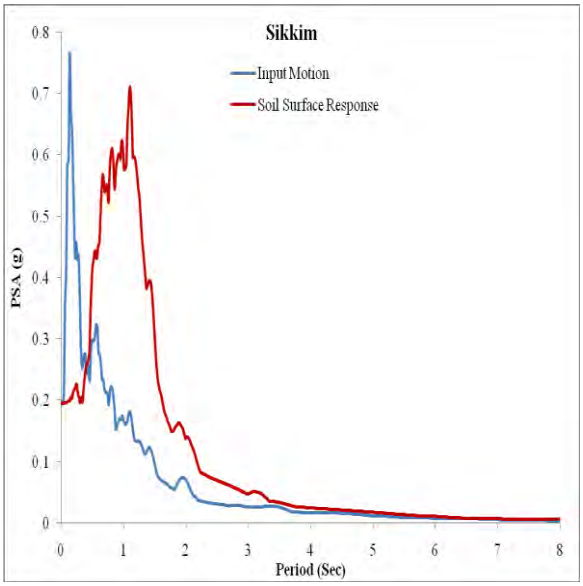

d) Sikkim earthquake

Figure 4.68: Response Spectra

Time Histories

The design soil profile is excited with input motion of four earthquakes to determine the dynamic response of local soil. Equivalent linear approach is used for site response analysis. As the seismic waves travel up and down, the soil vibrates. The acceleration of soil at the ground surface is shown in Figure 4.69. It is noted that the PGA and the ordinates of the response spectra increased.

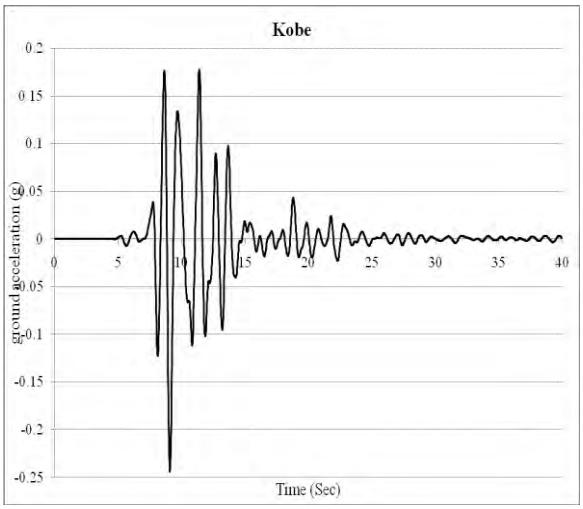

a) Kobe earthquake

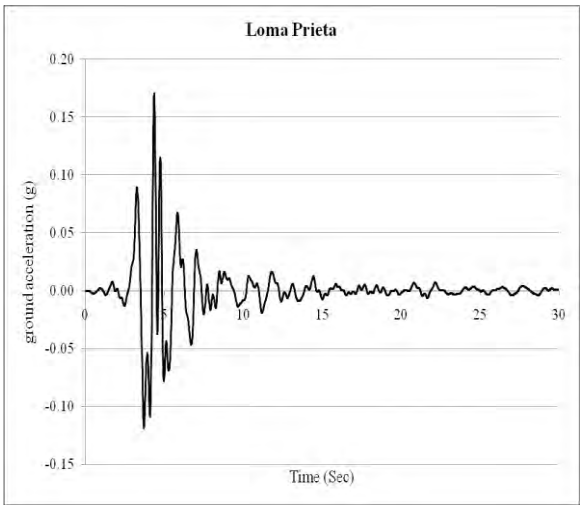

b) Loma prieta earthquake

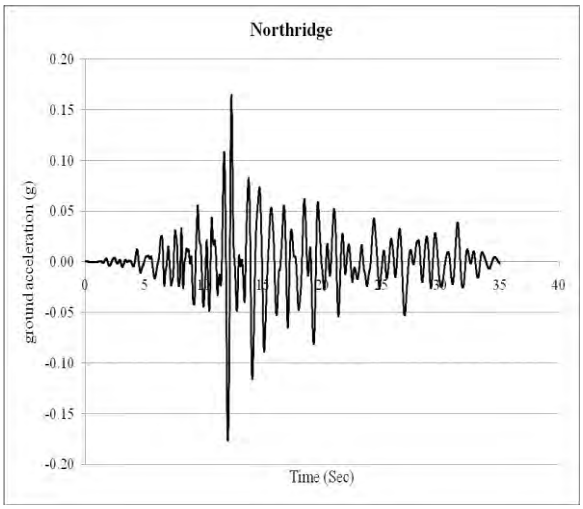

c) Nothridge earthquake

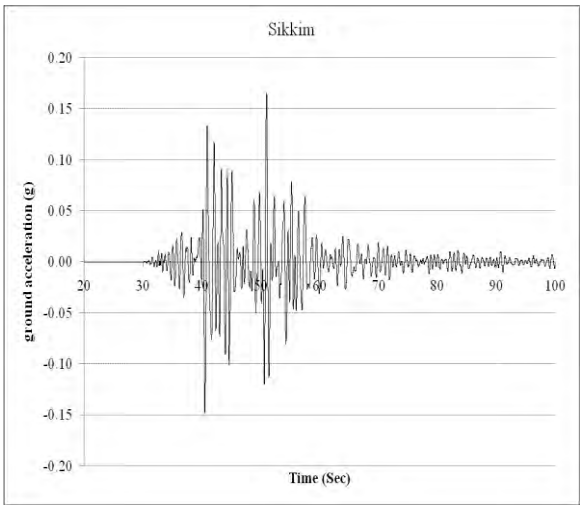

d) Sikkim earthquake

Figure 4.69: Time histories for local site effects

Maximum Peak Ground Acceleration (PGA)

Maximum Peak Ground Acceleration (PGA) at different depths of four earthquakes for this site are shown in figure 4.70. PGA at surface and that at bedrock is obtained from the analysis. The peak ground acceleration values at surface are observed to be in the range of 0.152g (Loma prieta) to as high as 0.241g (Kobe) and that of the bedrock were observed to vary from 0.177g (Kobe) to 0.212g (Loma prieta). The impedance in the acceleration values can be observed. Such as, a sudden rise within few meters can cause considerable damage to the sub and super structure resulting in huge loss.

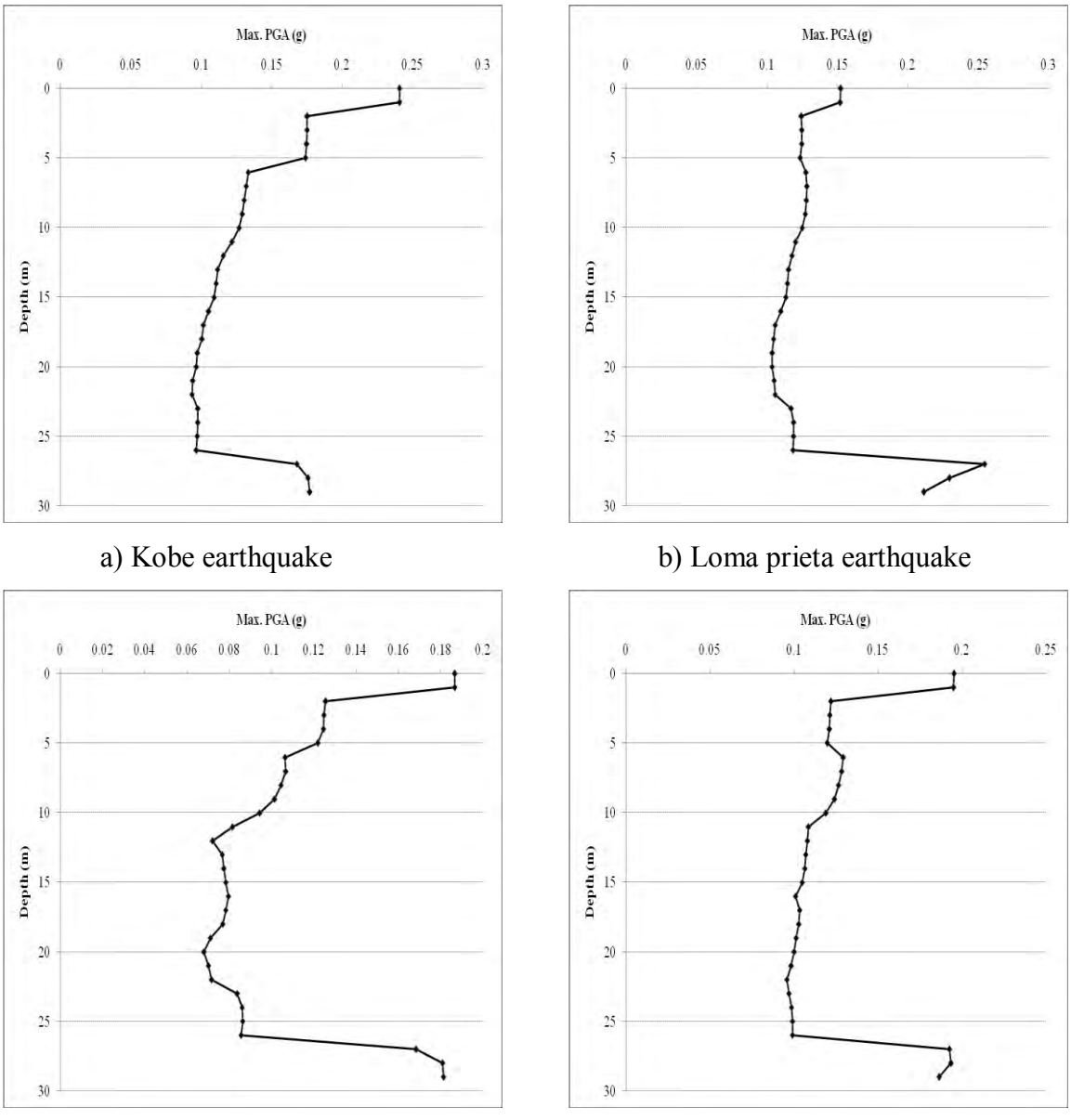

a) Kobe earthquake

b) Loma prieta earthquake

c) Nothridge earthquake

d) Sikkim earthquake

Figure 4.70: Maximum Peak Ground Acceleration for local site effects

Site amplification factors at sub surface layers are often used as one of the parameters for estimation of ground response. The amplification factor is the ratio of peak ground acceleration at surface to that of acceleration at hard rock. The amplification factors are determined as;

Amplification Factor = PGA recorded at ground surface / PGA recorded at hard rock
Amplification Factor (For Kobe earthquake) = 0.241/0.177 = 1.36
Amplification Factor (For Loma prieta earthquake) = 0.152/0.212 = 0.72
Amplification Factor (For Northridge earthquake) = 0.187/0.181 = 1.03
Amplification Factor (For Gangtok earthquake) = 0.195/0.187 = 1.04

Hence, the amplification factors have also been computed and it has been identified that similar to the peak ground acceleration values, the variation is within 0.72 (Loma prieta)to 1.36 (Kobe).

Maximum Stress Ratio

Maximum Stress Ratio at different depths of four earthquakes for this site is shown in figure 4.71. Maximum stress ratio at different depths of four earthquakes for this site is obtained from the analysis. The Maximum stress ratio values for Kobe earthquakes are observed to be in the range of 0.169 to as high as 0.527. The Maximum stress ratio values for Loma prieta earthquakes are observed to be in the range of 0.194 to as high as 0.329. The Maximum stress ratio values for Northridge earthquakes are observed to be in the range of 0.122 to as high as 0.410. The Maximum stress ratio values for Sikkim earthquakes are observed to be in the range of 0.144 to as high as 0.430.

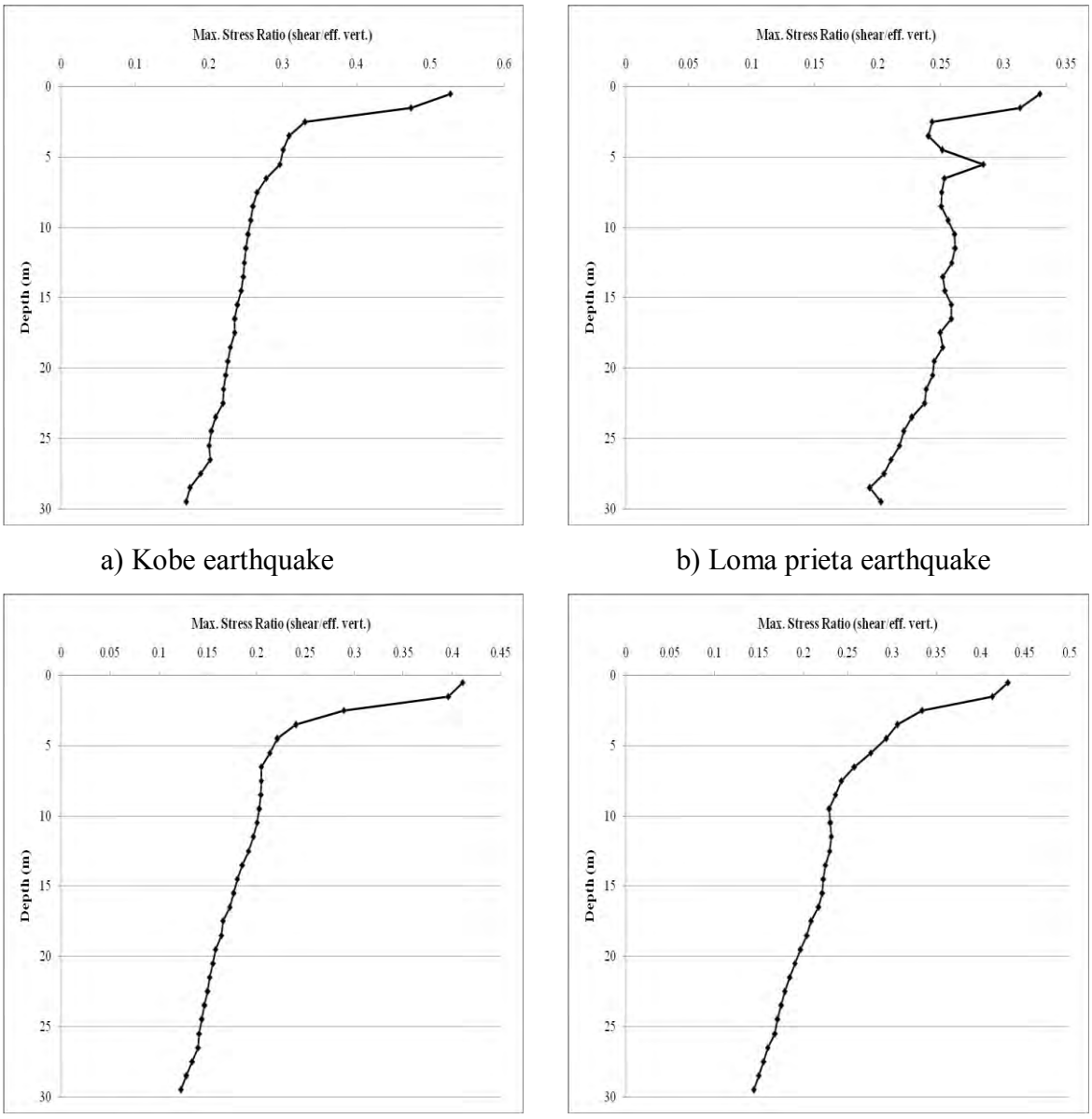

a) Kobe earthquake b) Loma prieta earthquake

c) Nothridge earthquake d) Sikkim earthquake

Figure 4.71: Maximum stress ratio for local site effects

Maximum Strain

Maximum Strain at different depths of four earthquakes for this site is shown in figure 4.72. Maximum strain values at different depths of four earthquakes for this site are obtained from the analysis. The Maximum strain values for Kobe earthquakes are observed to be in the range of 0.0035 to as high as 6.79. The Maximum strain values for Loma prieta earthquakes are observed to be in the range of 0.0027 to as high as 3.07. The Maximum strain values for Northridge earthquakes are observed to be in the range of 0.0027 to as high as 2.32. The Maximum strain values for Sikkim earthquakes are observed to be in the range of 0.0035 to as high as 3.03.

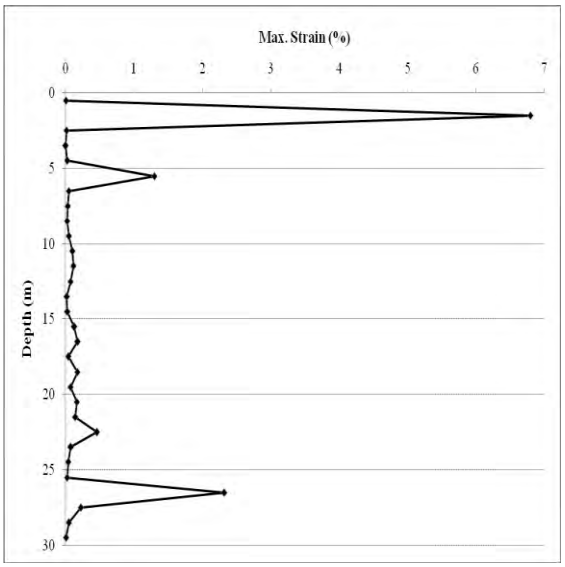

a) Kobe earthquake

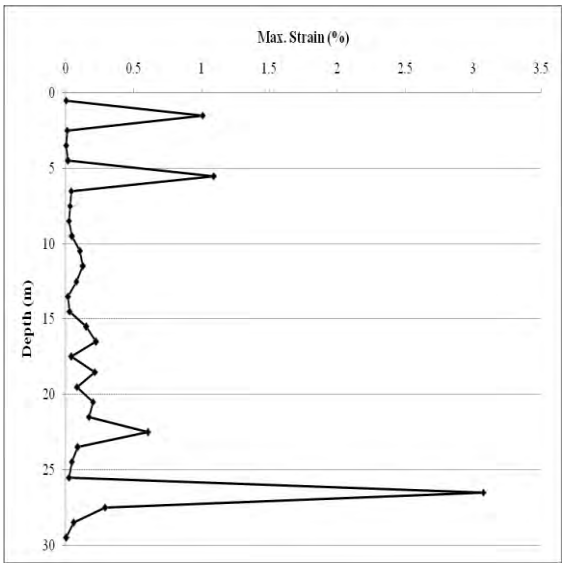

b) Loma prieta earthquake

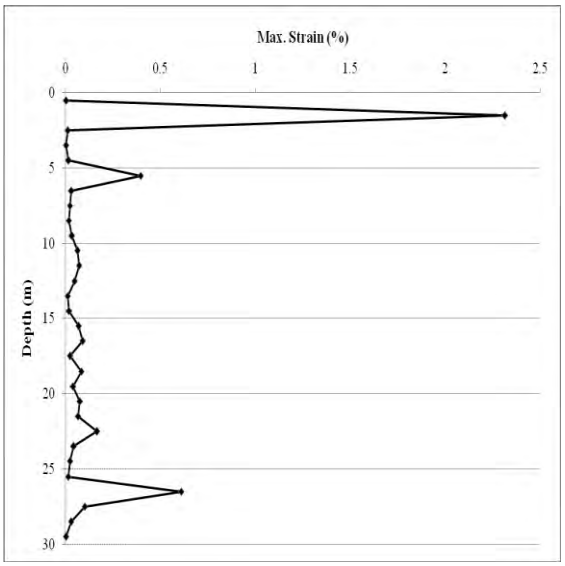

c) Nothridge earthquake

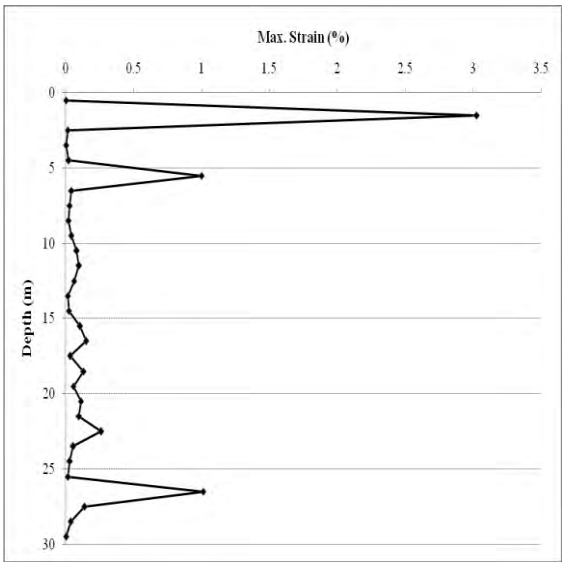

d) Sikkim earthquake

Figure 4.72: Maximum strain for local site effects

Figure 4.73 shows the comparison of Mean and Standard Deviation for surface PSA and Figure 4.74 shows the comparison of Surface PSA which are produced for different input motions.

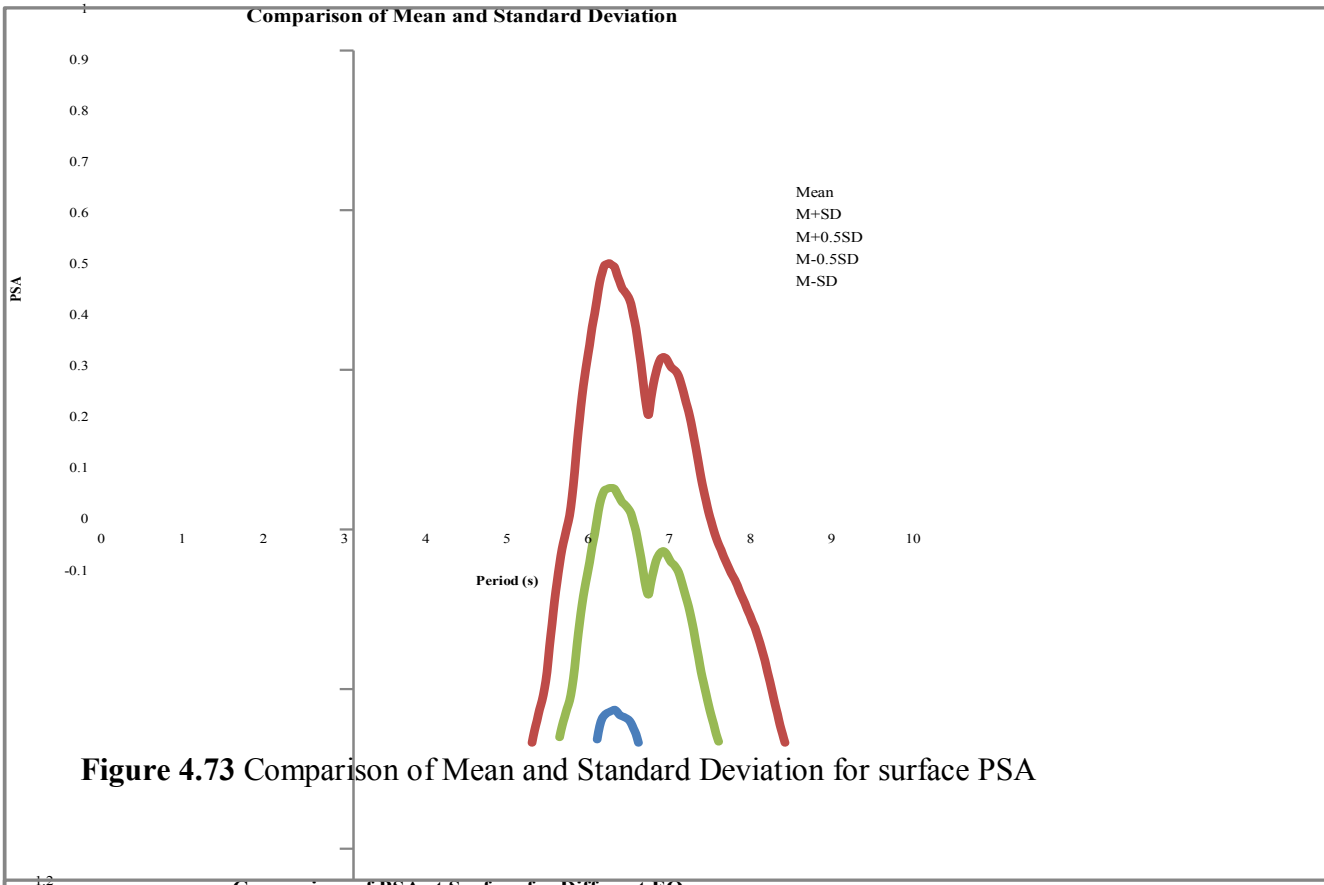

Figure 4.73 Comparison of Mean and Standard Deviation for surface PSA

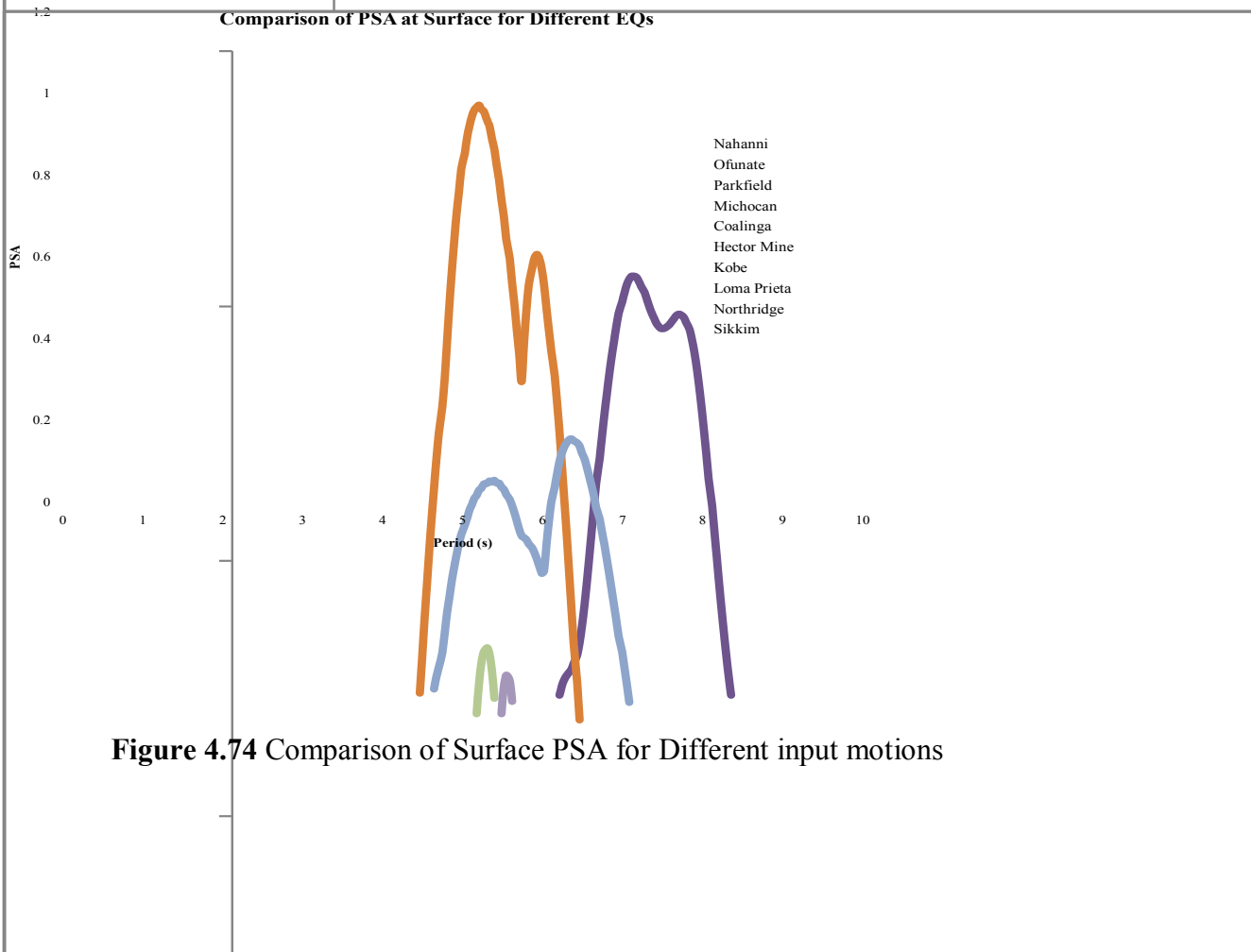

Figure 4.74 Comparison of Surface PSA for Different input motions

Figure 4.75 shows the comparison of Mean Input PSA and Mean Surface PSA produced for different input motions.

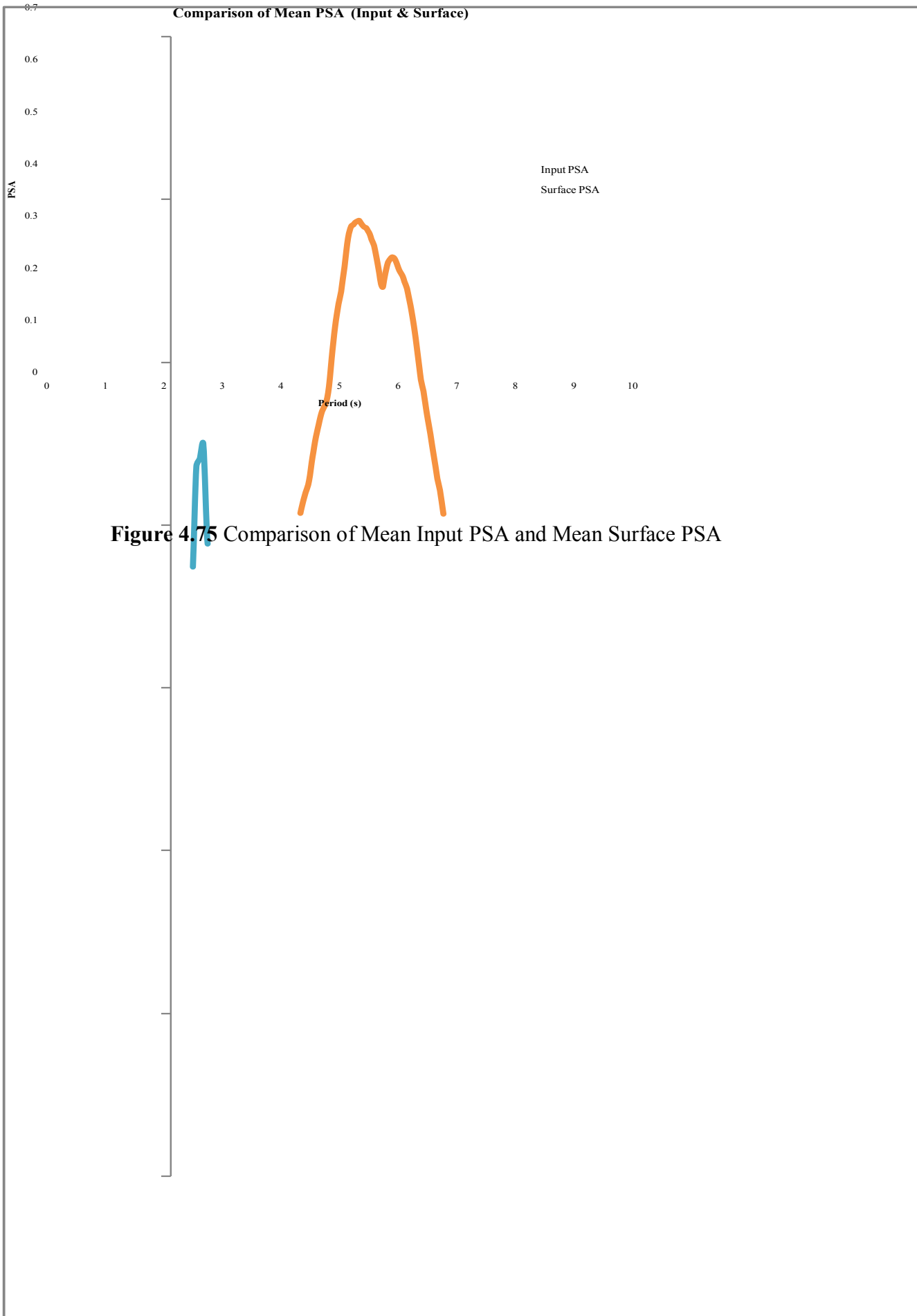

Figure 4.75 Comparison of Mean Input PSA and Mean Surface PSA

4.2.9 SITE: EAST NANDIPARA, MOTHERTEK

This site has been situated in Eastern part of Dhaka city. Different geotechnical and geophysical test are conducted to characterize the site. Design soil profile is given in Figure 4.76 with average shear wave velocity for each layer. Average shear wave velocity for 30m layer (V_{30avg}) is

$$V_{30\,avg} = \frac{\sum_{i=1}^{N} h_i}{\sum_{i=1}^{N} \frac{h_i}{V_i}} = 265 \text{ m/s}$$

Where, h is the thickness of soil layer, and V is the respective shear wave velocity.

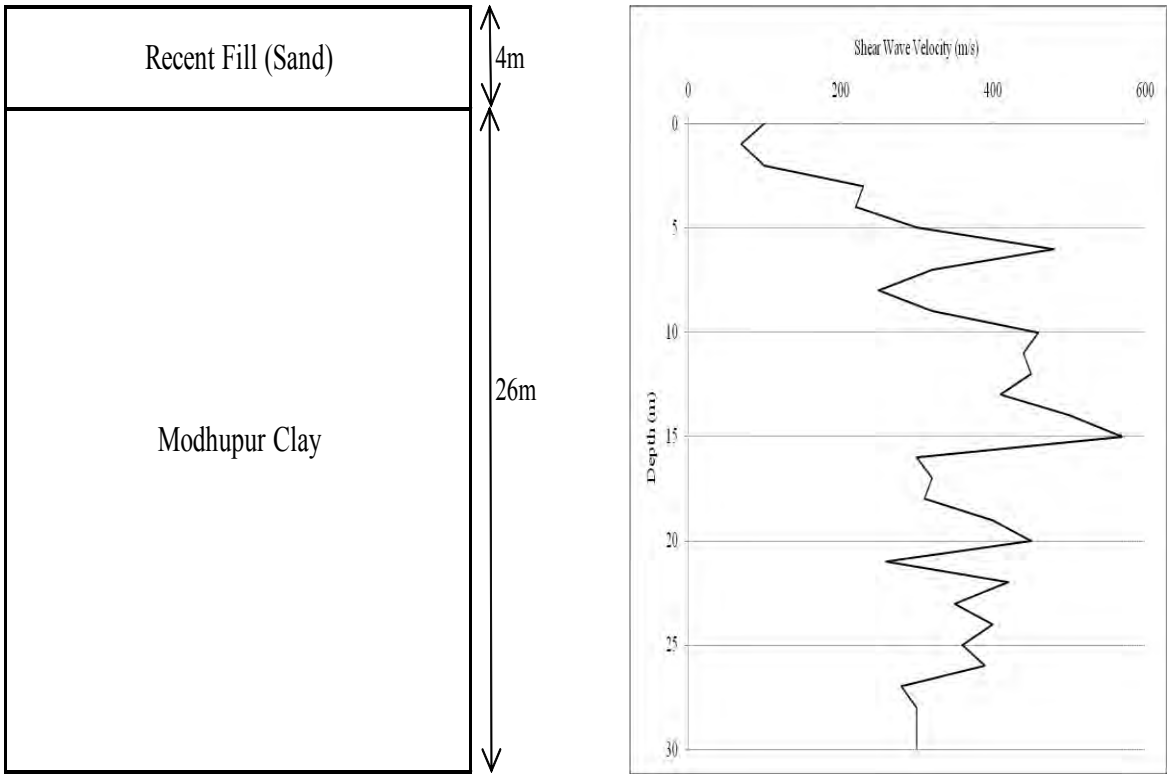

a) Design soil profile

b) Shear wave velocity profile

Figure 4.76: Site Characterization

Response Spectra

Response spectra of four earthquakes are shown in Figure 4.77. Among the four earthquakes, Loma prieta earthquake produces highest (1.67g) peak spectral acceleration (PSA) for this site and Northridge earthquake produces lowest (0.0029g) peak spectral acceleration (PSA). It is observed that initially soil surface response is less than input response for all four earthquakes for this site. But gradually surface response increases.

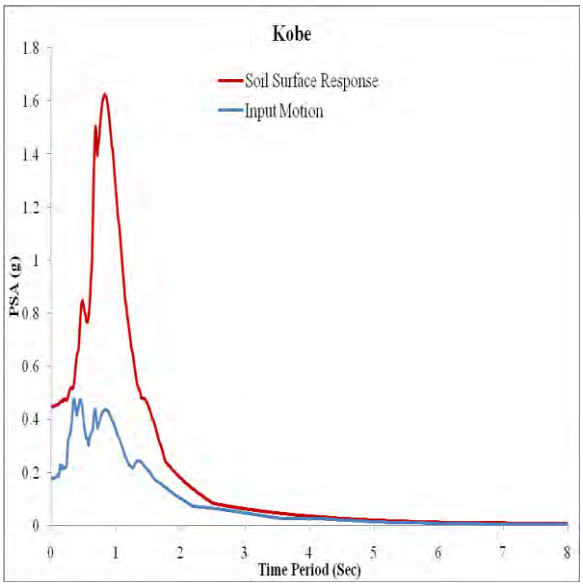

a) Kobe earthquake

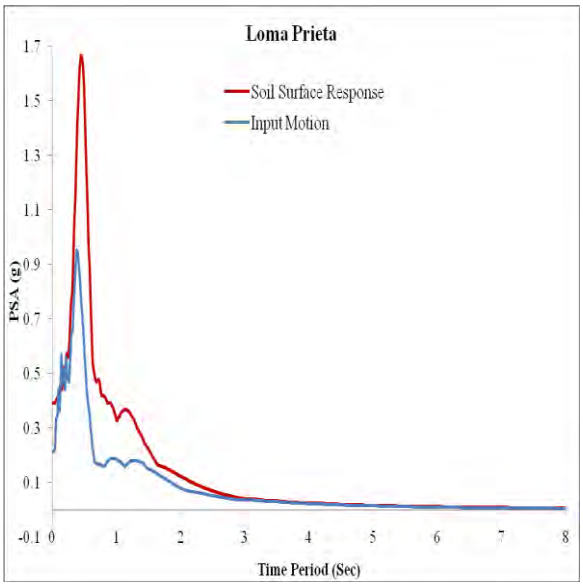

b) Loma prieta earthquake

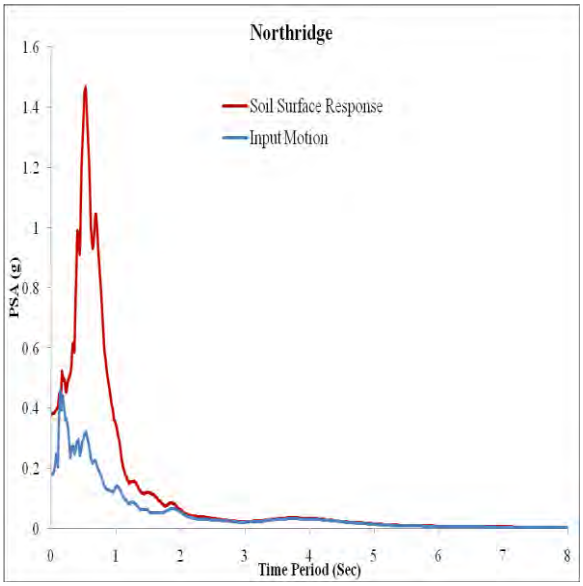

c) Nothridge earthquake

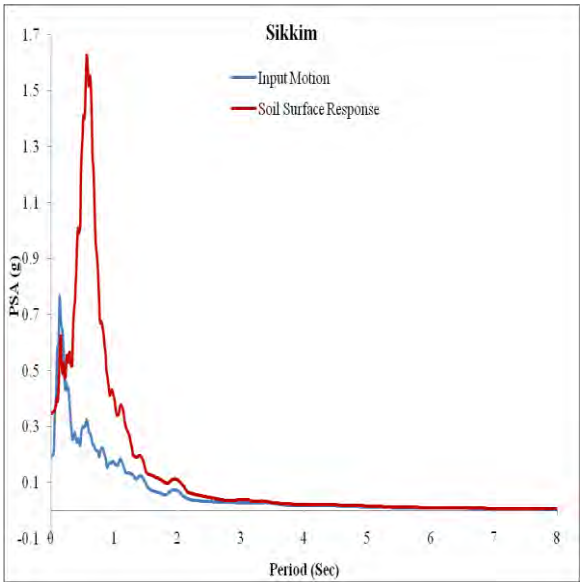

d) Sikkim earthquake

Figure 4.77: Response Spectra

Time Histories

The design soil profile is excited with input motion of four earthquakes to determine the dynamic response of local soil. Equivalent linear approach is used for site response analysis. As the seismic waves travel up and down, the soil vibrates. The acceleration of soil at the ground surface is shown in Figure 4.78. It is noted that the PGA and the ordinates of the response spectra increased.

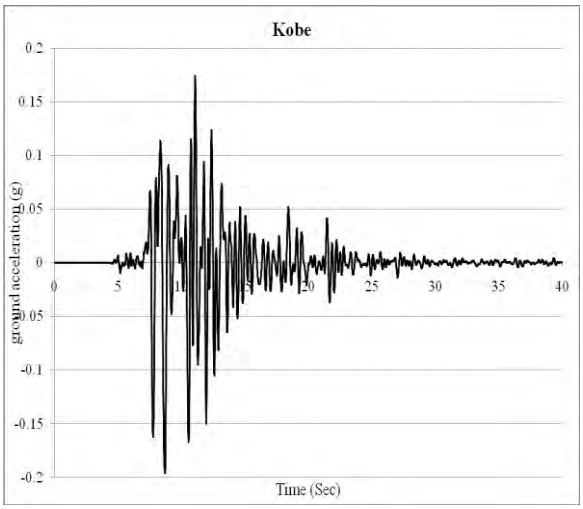

a) Kobe earthquake

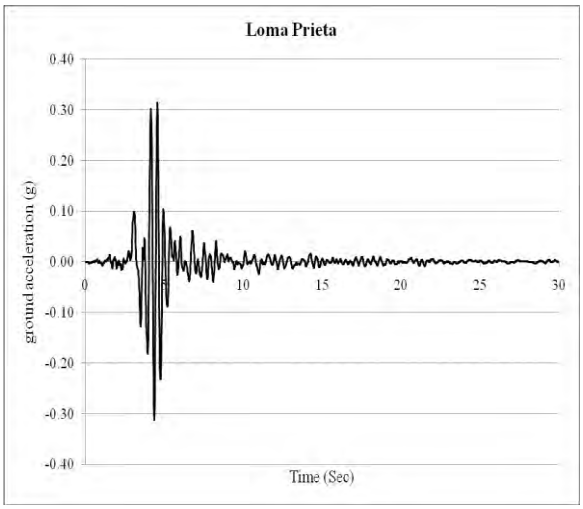

b) Loma prieta earthquake

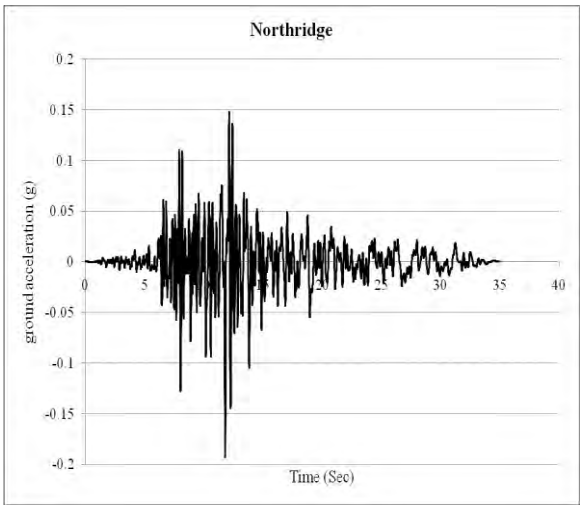

c) Nothridge earthquake

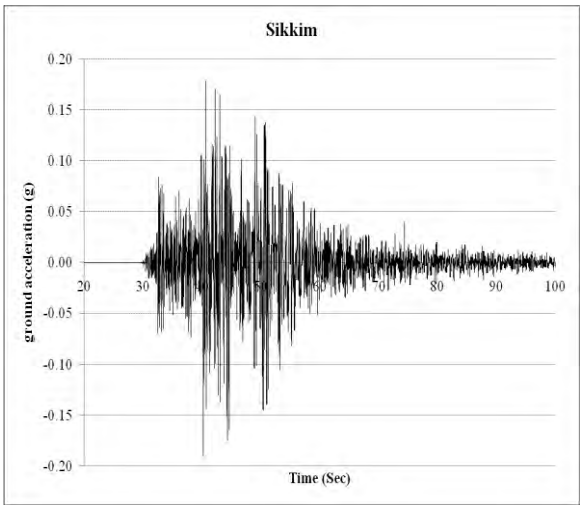

d) Sikkim earthquake

Figure 4.78: Time histories for local site effects

Maximum Peak Ground Acceleration (PGA)

Maximum Peak Ground Acceleration (PGA) at different depths of four earthquakes for this site are shown in figure 4.79. PGA at surface and that at bedrock is obtained from the analysis. The peak ground acceleration values at surface are observed to be in the range of 0.347g (Sikkim) to as high as 0.450g (Kobe) and that of the bedrock were observed to vary from 0.177g (Kobe) to 0.212g (Loma prieta). The impedance in the acceleration values can be observed. Such as, a sudden rise within few meters can cause considerable damage to the sub and super structure resulting in huge loss.

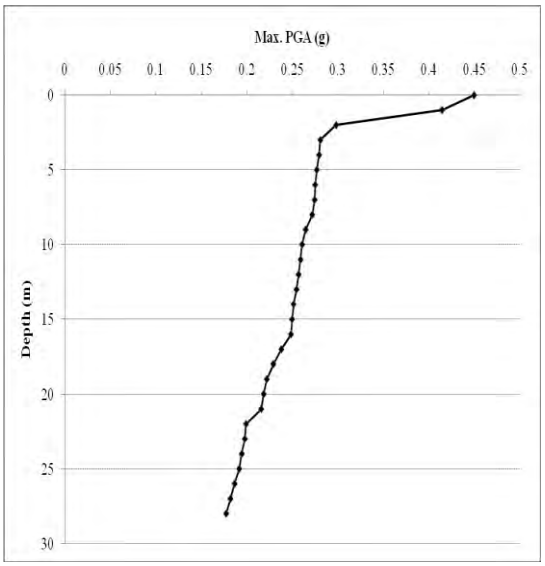

a) Kobe earthquake

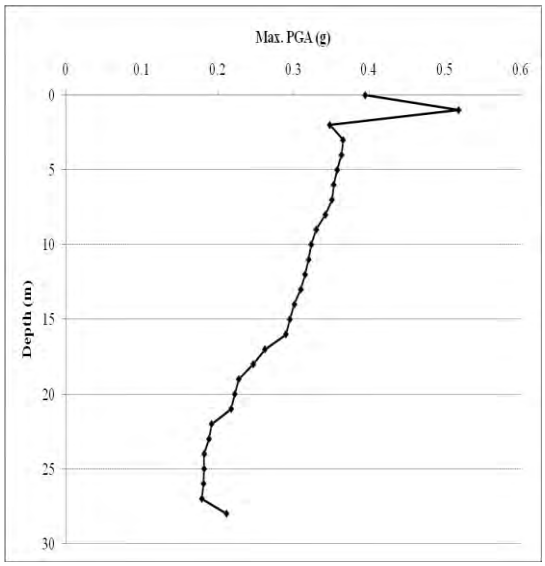

b) Loma prieta earthquake

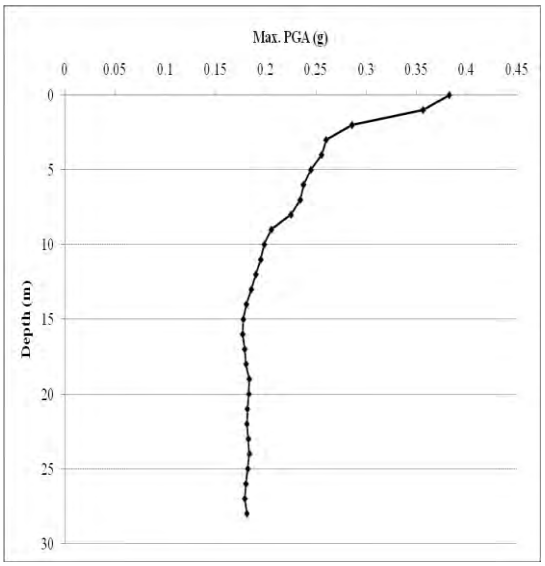

c) Nothridge earthquake

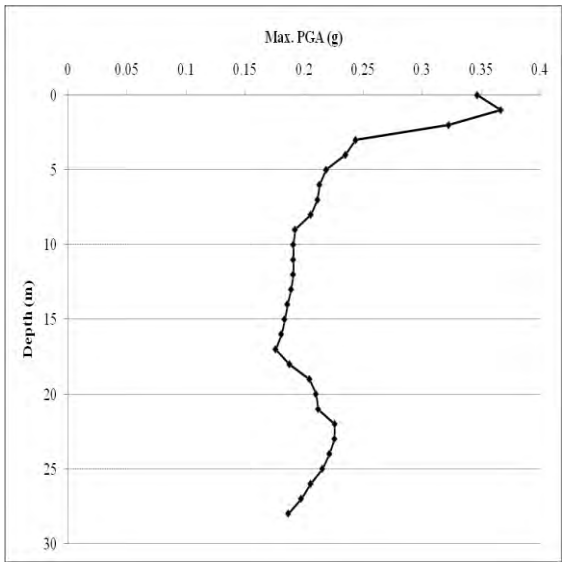

d) Sikkim earthquake

Figure 4.79: Maximum Peak Ground Acceleration for local site effects

Site amplification factors at sub surface layers are often used as one of the parameters for estimation of ground response. The amplification factor is the ratio of peak ground acceleration at surface to that of acceleration at hard rock. The amplification factors are determined as;

Amplification Factor = PGA recorded at ground surface / PGA recorded at hard rock
Amplification Factor (For Kobe earthquake) = 0.450/0.177 = 2.54
Amplification Factor (For Loma prieta earthquake) = 0.395/0.212 = 1.86
Amplification Factor (For Northridge earthquake) = 0.383/0.181 = 2.12
Amplification Factor (For Sikkim earthquake) = 0.347/0.187 = 1.85

Hence, the amplification factors have also been computed and it has been identified that similar to the peak ground acceleration values, the variation is within 1.85 (Sikkim) to 2.54 (Kobe).

Maximum Stress Ratio

Maximum Stress Ratio at different depths of four earthquakes for this site is shown in figure 4.80. Maximum stress ratio at different depths of four earthquakes for this site is obtained from the analysis. The Maximum stress ratio values for Kobe earthquakes are observed to be in the range of 0.478 to as high as 1.001. The Maximum stress ratio values for Loma prieta earthquakes are observed to be in the range of 0.359 to as high as 0.844. The Maximum stress ratio values for Northridge earthquakes are observed to be in the range of 0.317 to as high as 0.854. The Maximum stress ratio values for Sikkim earthquakes are observed to be in the range of 0.293 to as high as 0.740.

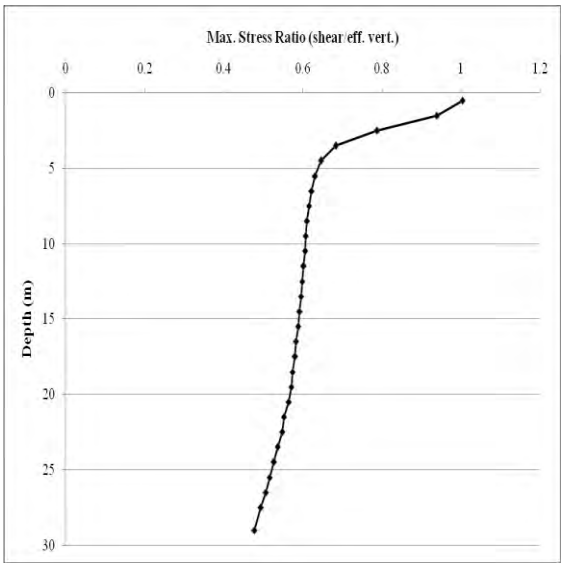

a) Kobe earthquake

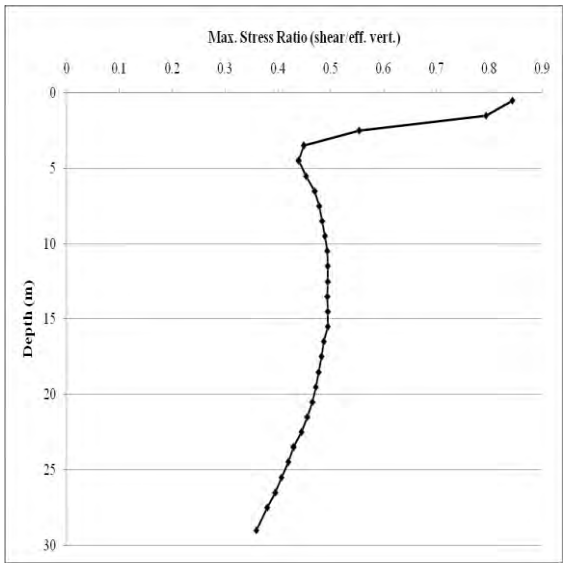

b) Loma prieta earthquake

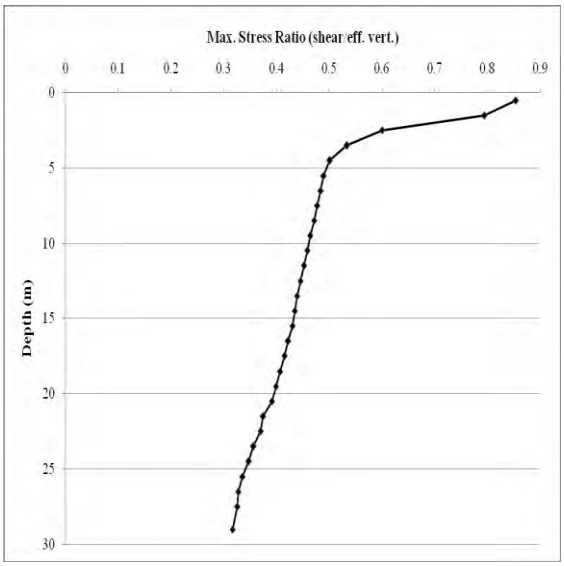

c) Nothridge earthquake

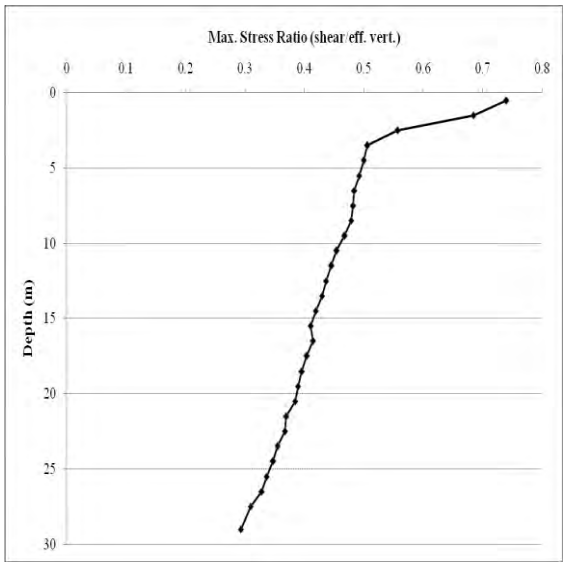

d) Sikkim earthquake

Figure 4.80: Maximum stress ratio for local site effects

Maximum Strain

Maximum Strain at different depths of four earthquakes for this site is shown in figure 4.81. Maximum strain values at different depths of four earthquakes for this site are obtained from the analysis. The Maximum strain values for Kobe earthquakes are observed to be in the range of 0.0099 to as high as 6.066. The Maximum strain values for Loma prieta earthquakes are observed to be in the range of 0.0070 to as high as 2.58. The Maximum strain values for Northridge earthquakes are observed to be in the range of 0.0073 to as high as 2.59. The Maximum strain values for Sikkim earthquakes are observed to be in the range of 0.0072 to as high as 1.59.

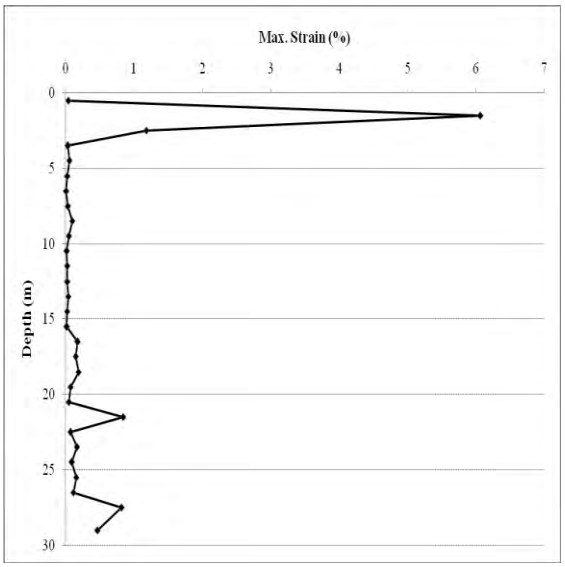

a) Kobe earthquake

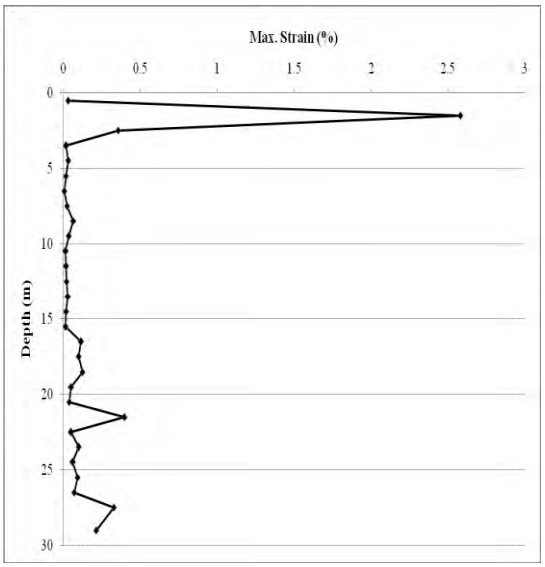

b) Loma prieta earthquake

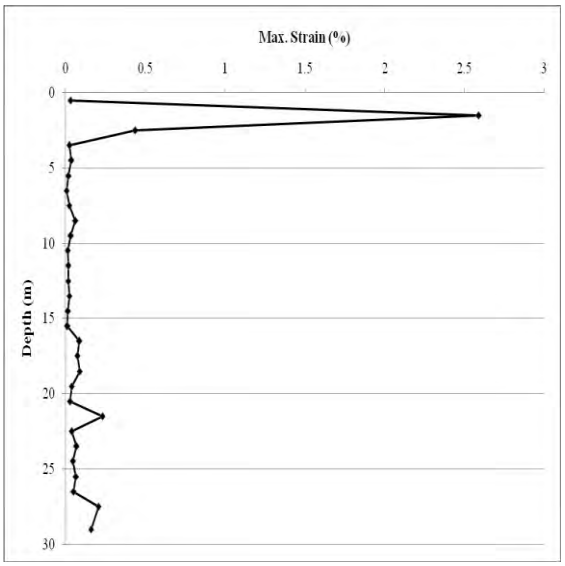

c) Nothridge earthquake

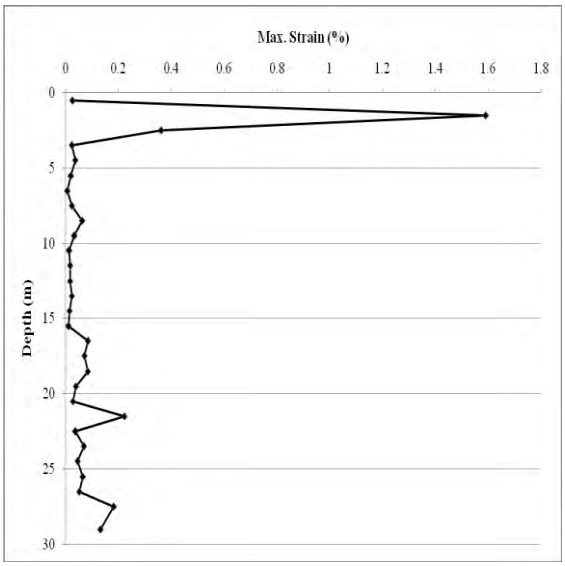

d) Sikkim earthquake

Figure 4.81: Maximum strain for local site effects

Figure 4.82 shows the comparison of Mean and Standard Deviation for surface PSA and Figure 4.83 shows the comparison of Surface PSA which are produced for different input motions.

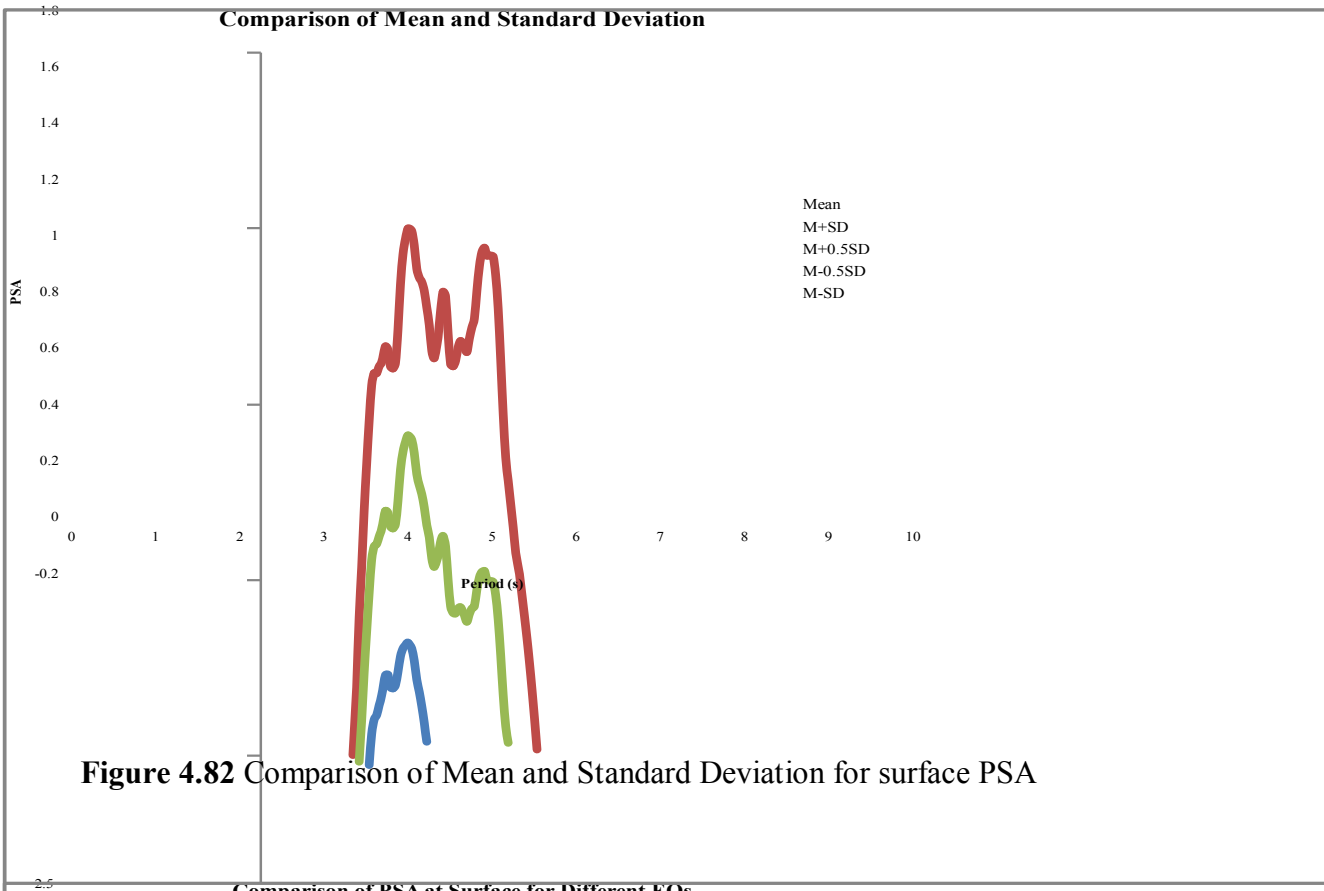

Figure 4.82 Comparison of Mean and Standard Deviation for surface PSA

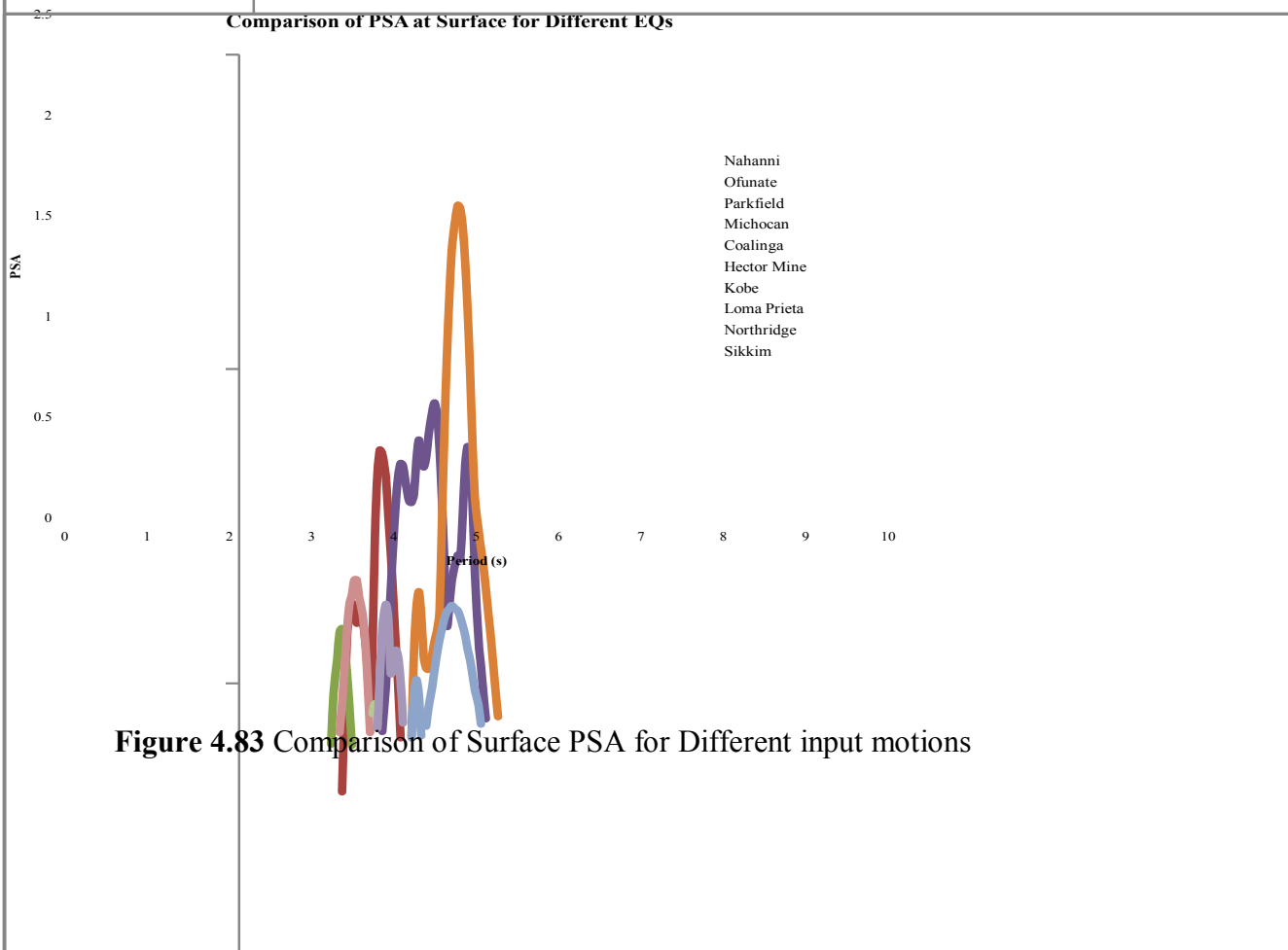

Figure 4.83 Comparison of Surface PSA for Different input motions

Figure 4.84 shows the comparison of Mean Input PSA and Mean Surface PSA produced for different input motions.

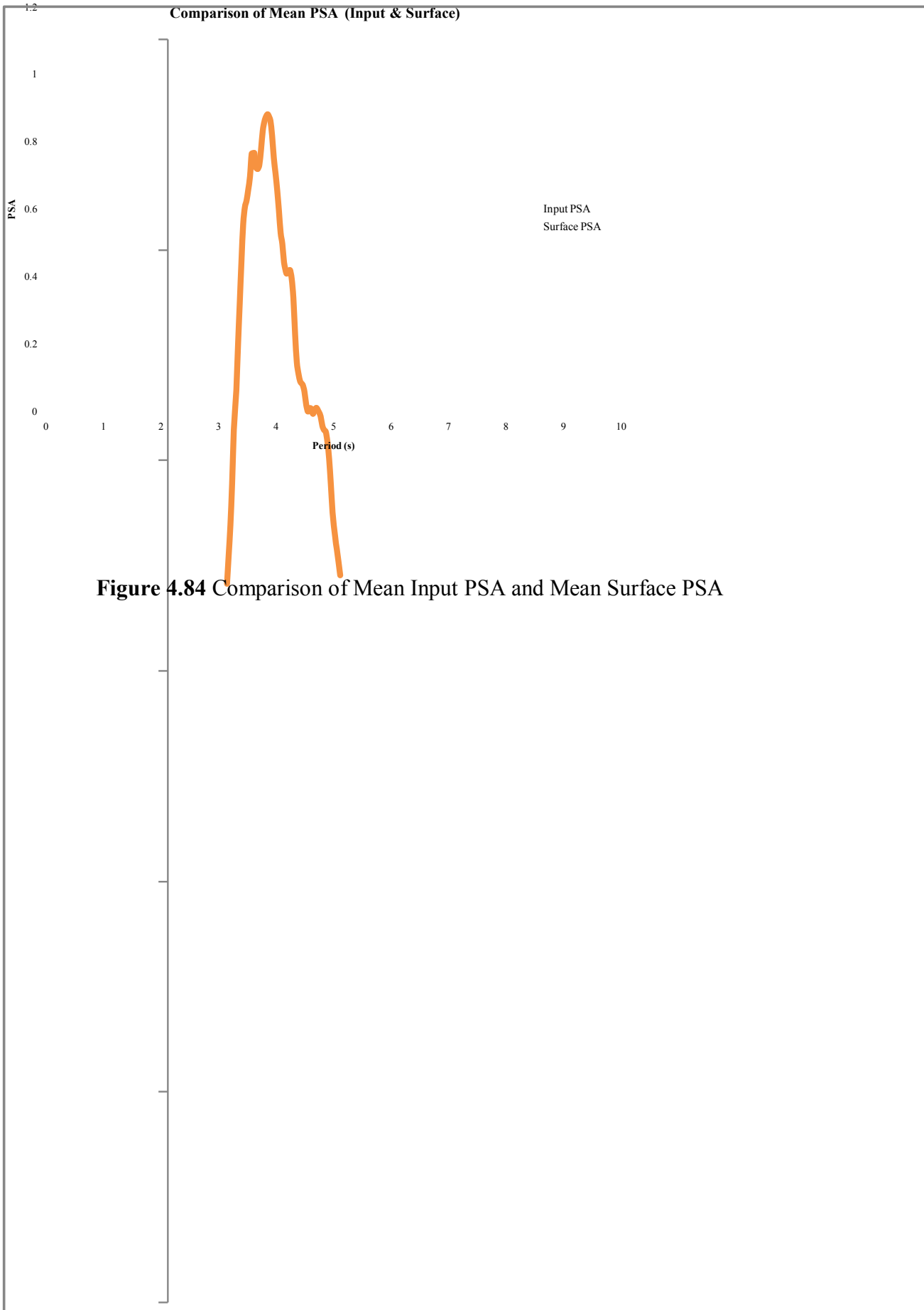

Figure 4.84 Comparison of Mean Input PSA and Mean Surface PSA

4.2.10 SITE: UNITED CITY PROJECT

This site has been situated in Eastern part of Dhaka city. Different geotechnical and geophysical test are conducted to characterize the site. Design soil profile is given in Figure 4.85 with average shear wave velocity for each layer. Average shear wave velocity for 30m layer (V_{30avg}) is

$$V_{30\,avg} = \frac{\sum_{i=1}^{N} h_i}{\sum_{i=1}^{N} \frac{h_i}{V_i}} = 162 \text{ m/s}$$

Where, h is the thickness of soil layer, and V is the respective shear wave velocity.

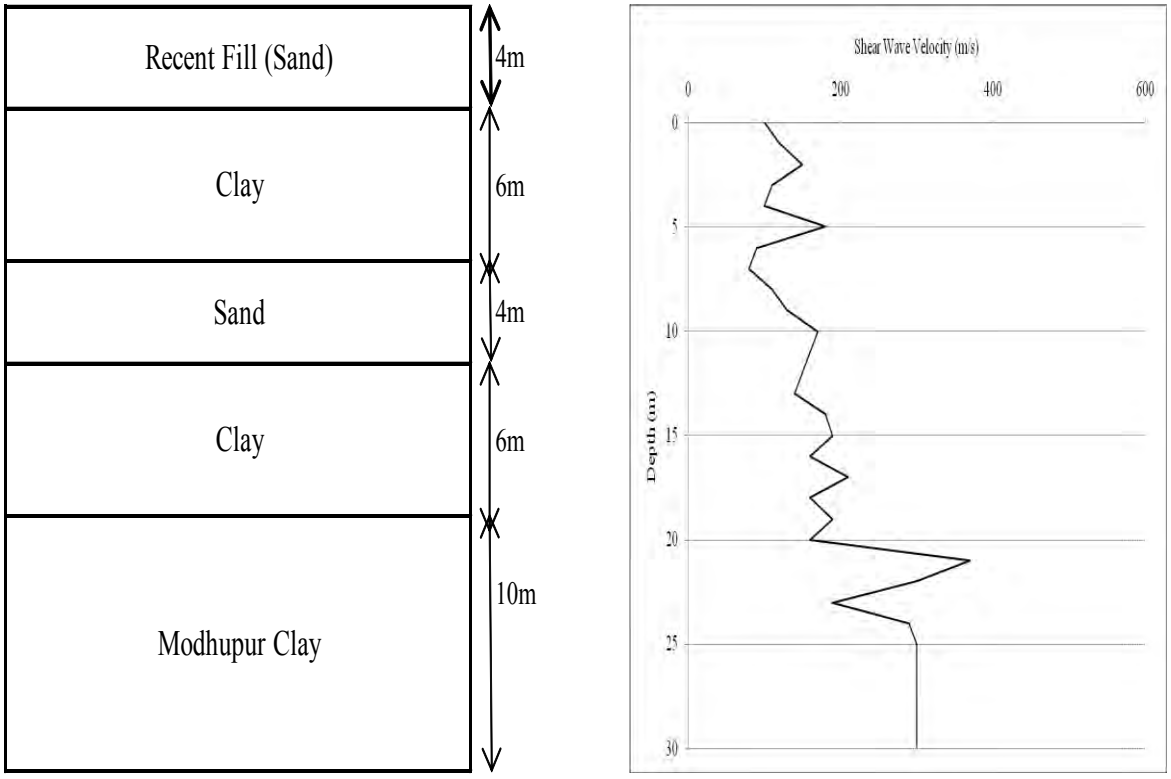

a) Design soil profile b) Shear wave velocity profile

Figure 4.85: Site Characterization

Response Spectra

Response spectra of four earthquakes are shown in Figure 4.86. Among the four earthquakes, Kobe earthquake produces highest (0.46g) peak spectral acceleration (PSA) for this site and Northridge earthquake produces lowest (0.0028g) peak spectral acceleration (PSA). It is observed that initially soil surface response is less than input response for all four earthquakes for this site. But gradually surface response increases.

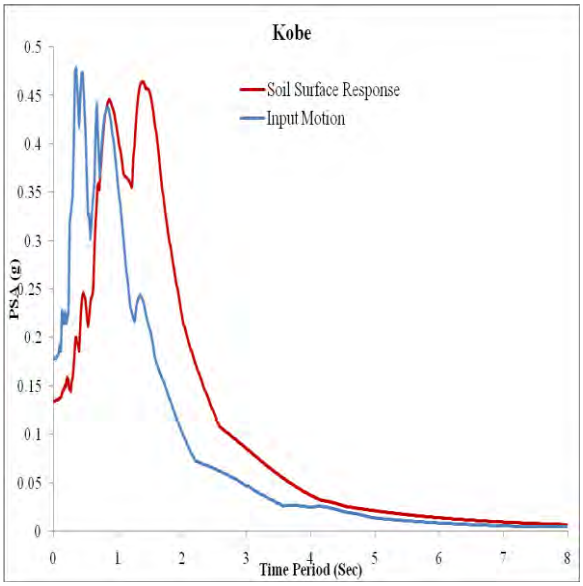

a) Kobe earthquake

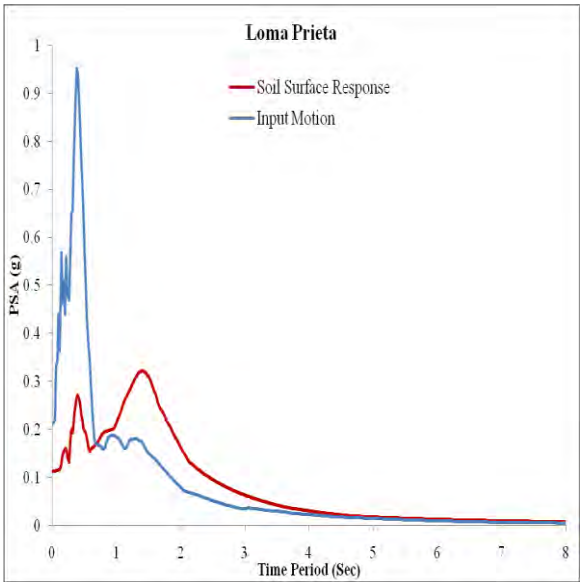

b) Loma prieta earthquake

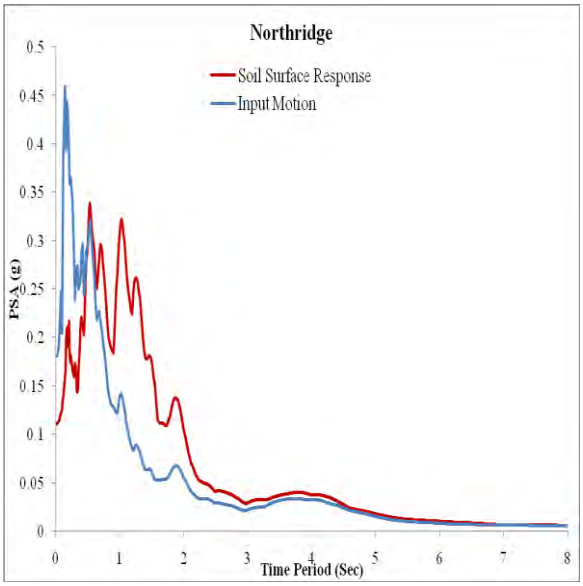

c) Nothridge earthquake

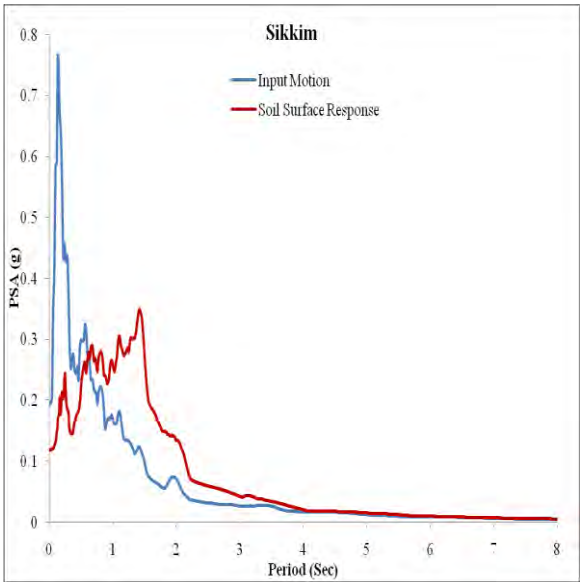

d) Sikkim earthquake

Figure 4.86: Response Spectra

Time Histories

The design soil profile is excited with input motion of four earthquakes to determine the dynamic response of local soil. Equivalent linear approach is used for site response analysis. As the seismic waves travel up and down, the soil vibrates. The acceleration of soil at the ground surface is shown in Figure 4.87. It is noted that the PGA and the ordinates of the response spectra increased.

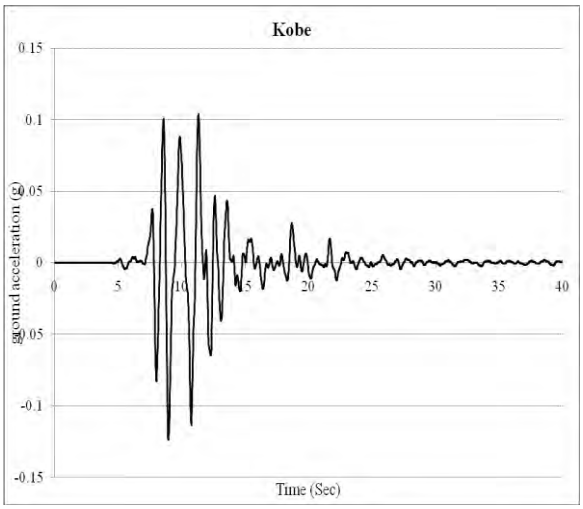

a) Kobe earthquake

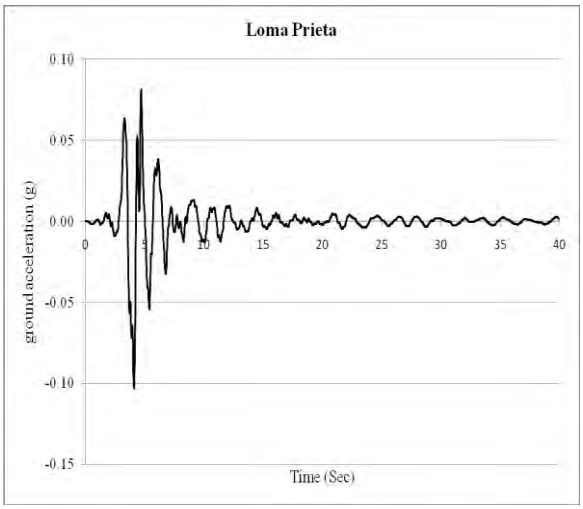

b) Loma prieta earthquake

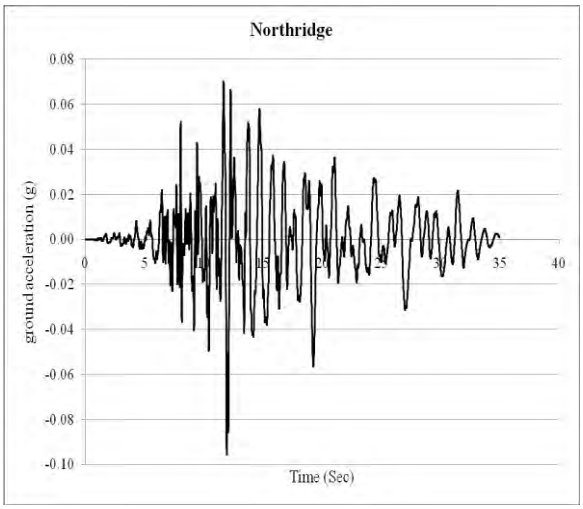

c) Nothridge earthquake

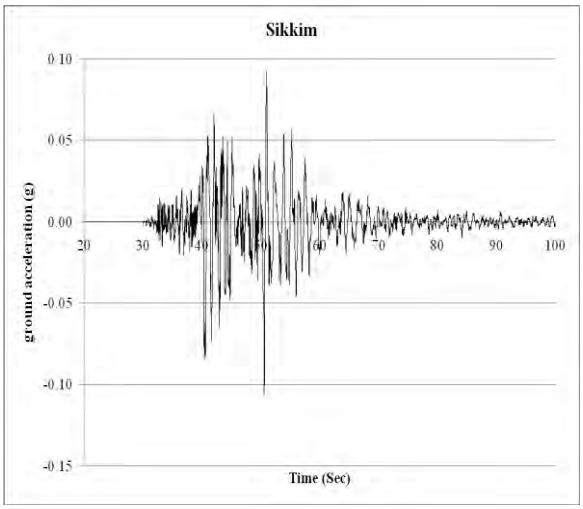

d) Sikkim earthquake

Figure 4.87: Time histories for local site effects

Maximum Peak Ground Acceleration (PGA)

Maximum Peak Ground Acceleration (PGA) at different depths of four earthquakes for this site are shown in figure 4.88. PGA at surface and that at bedrock is obtained from the analysis. The peak ground acceleration values at surface are observed to be in the range of 0.112g (Northridge) to as high as 0.135g (Kobe) and that of the bedrock were observed to vary from 0.177g (Kobe) to 0.212g (Loma prieta). The impedance in the acceleration values can be observed. Such as, a sudden rise within few meters can cause considerable damage to the sub and super structure resulting in huge loss.

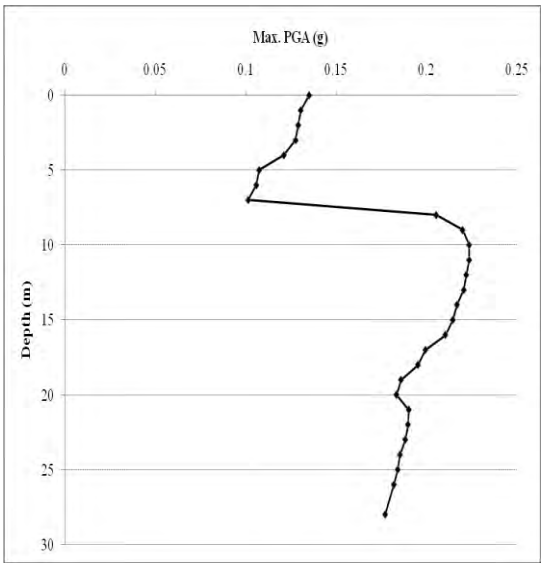

a) Kobe earthquake

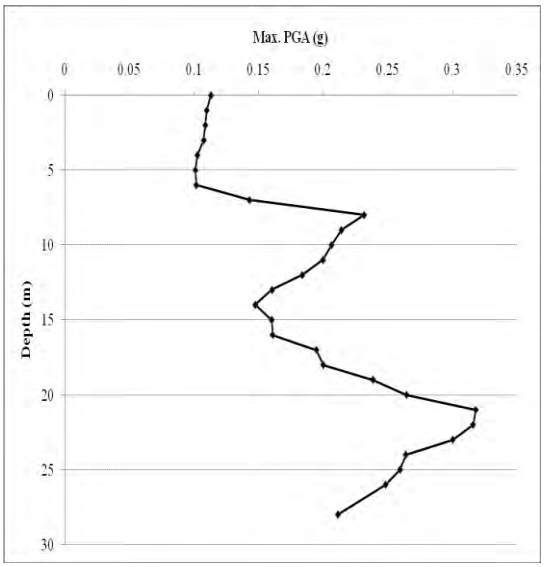

b) Loma prieta earthquake

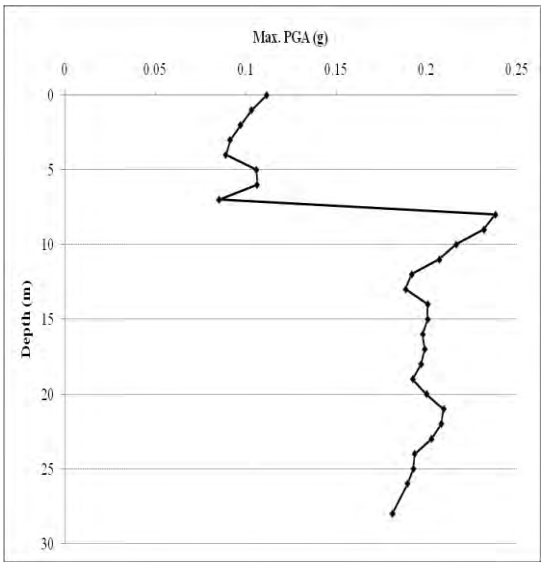

c) Nothridge earthquake

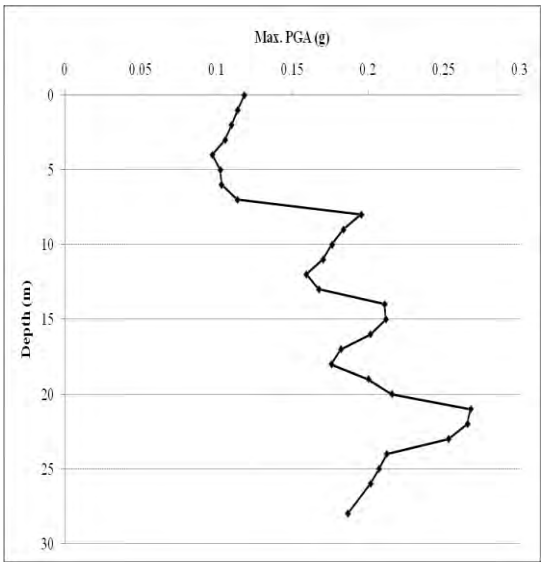

d) Sikkim earthquake

Figure 4.88: Maximum Peak Ground Acceleration for local site effects

Site amplification factors at sub surface layers are often used as one of the parameters for estimation of ground response. The amplification factor is the ratio of peak ground acceleration at surface to that of acceleration at hard rock. The amplification factors are determined as;

Amplification Factor = PGA recorded at ground surface / PGA recorded at hard rock
Amplification Factor (For Kobe earthquake) = 0.135/0.177 = 0.76
Amplification Factor (For Loma prieta earthquake) = 0.113/0.212 = 0.53
Amplification Factor (For Northridge earthquake) = 0.112/0.181 = 0.62
Amplification Factor (For Sikkim earthquake) = 0.118/0.187 = 0.63

Hence, the amplification factors have also been computed and it has been identified that similar to the peak ground acceleration values, the variation is within 0.53 (Loma Prieta) to 0.76 (Kobe).

Maximum Stress Ratio

Maximum Stress Ratio at different depths of four earthquakes for this site is shown in figure 4.89. Maximum stress ratio at different depths of four earthquakes for this site is obtained from the analysis. The Maximum stress ratio values for Kobe earthquakes are observed to be in the range of 0.188 to as high as 0.292. The Maximum stress ratio values for Loma prieta earthquakes are observed to be in the range of 0.178 to as high as 0.265. The Maximum stress ratio values for Northridge earthquakes are observed to be in the range of 0.111 to as high as 0.239. The Maximum stress ratio values for Sikkim earthquakes are observed to be in the range of 0.170 to as high as 0.263.

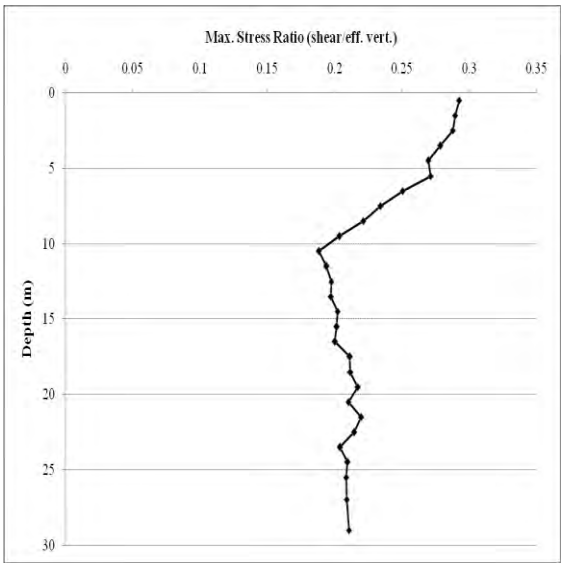

a) Kobe earthquake

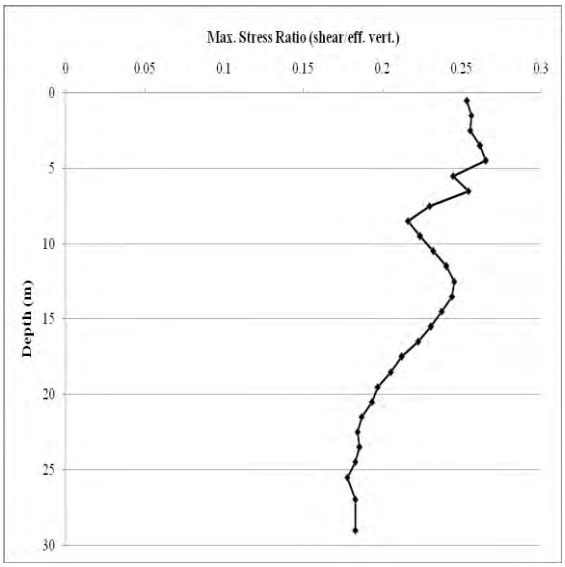

b) Loma prieta earthquake

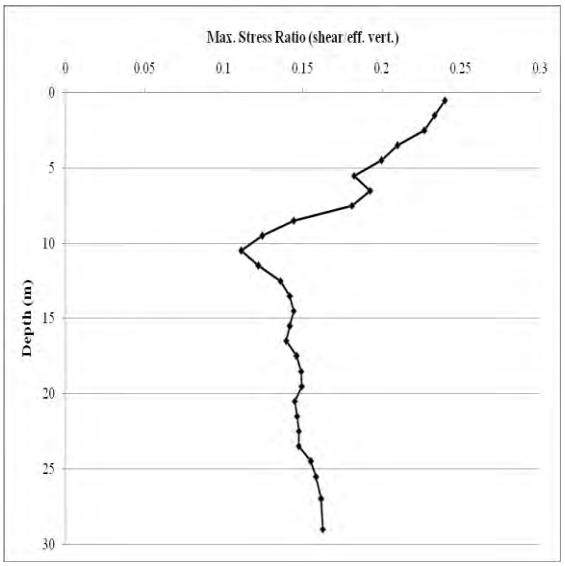

c) Nothridge earthquake

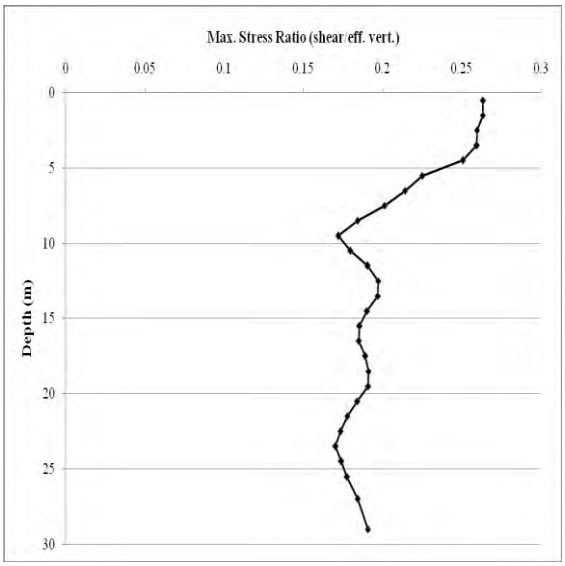

d) Sikkim earthquake

Figure 4.89: Maximum stress ratio for local site effects

Maximum Strain

Maximum Strain at different depths of four earthquakes for this site is shown in figure 4.90. Maximum strain values at different depths of four earthquakes for this site are obtained from the analysis. The Maximum strain values for Kobe earthquakes are observed to be in the range of 0.0079 to as high as 4.15. The Maximum strain values for Loma prieta earthquakes are observed to be in the range of 0.0067 to as high as 3.92. The Maximum strain values for Northridge earthquakes are observed to be in the range of 0.0063 to as high as 1.64. The Maximum strain values for Sikkim earthquakes are observed to be in the range of 0.0069 to as high as 2.25.

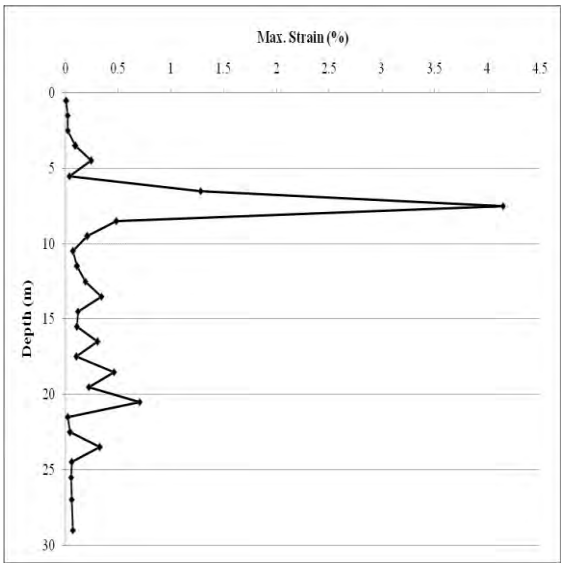

a) Kobe earthquake

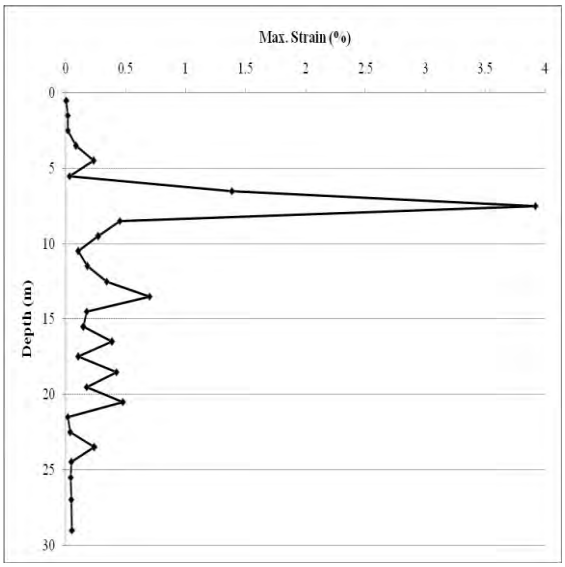

b) Loma prieta earthquake

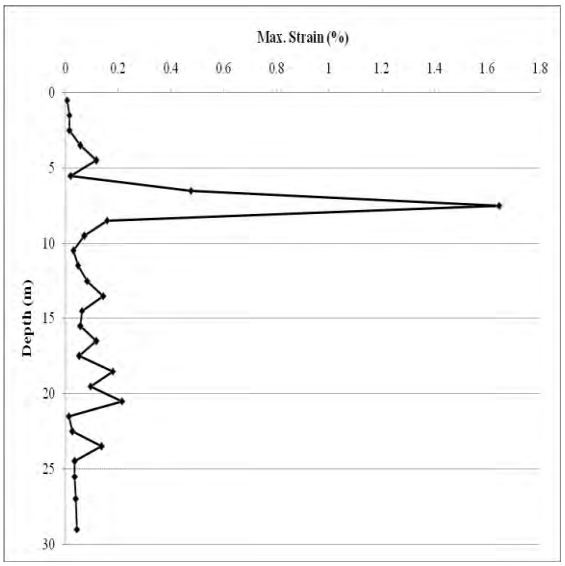

c) Nothridge earthquake

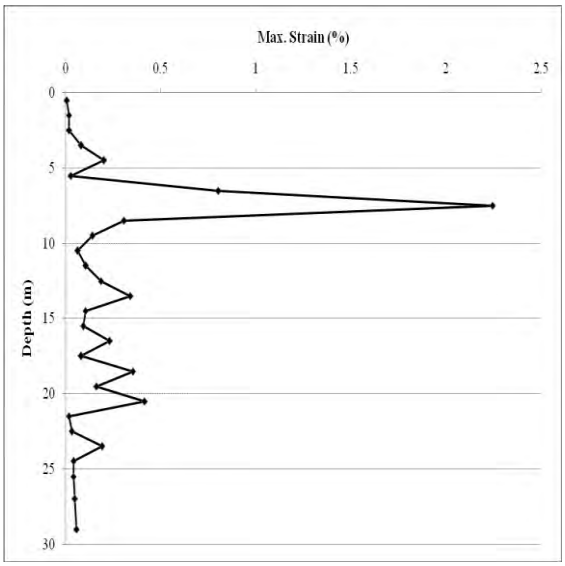

d) Sikkim earthquake

Figure 4.90: Maximum strain for local site effects

Figure 4.91 shows the comparison of Mean and Standard Deviation for surface PSA and Figure 4.92 shows the comparison of Surface PSA which are produced for different input motions.

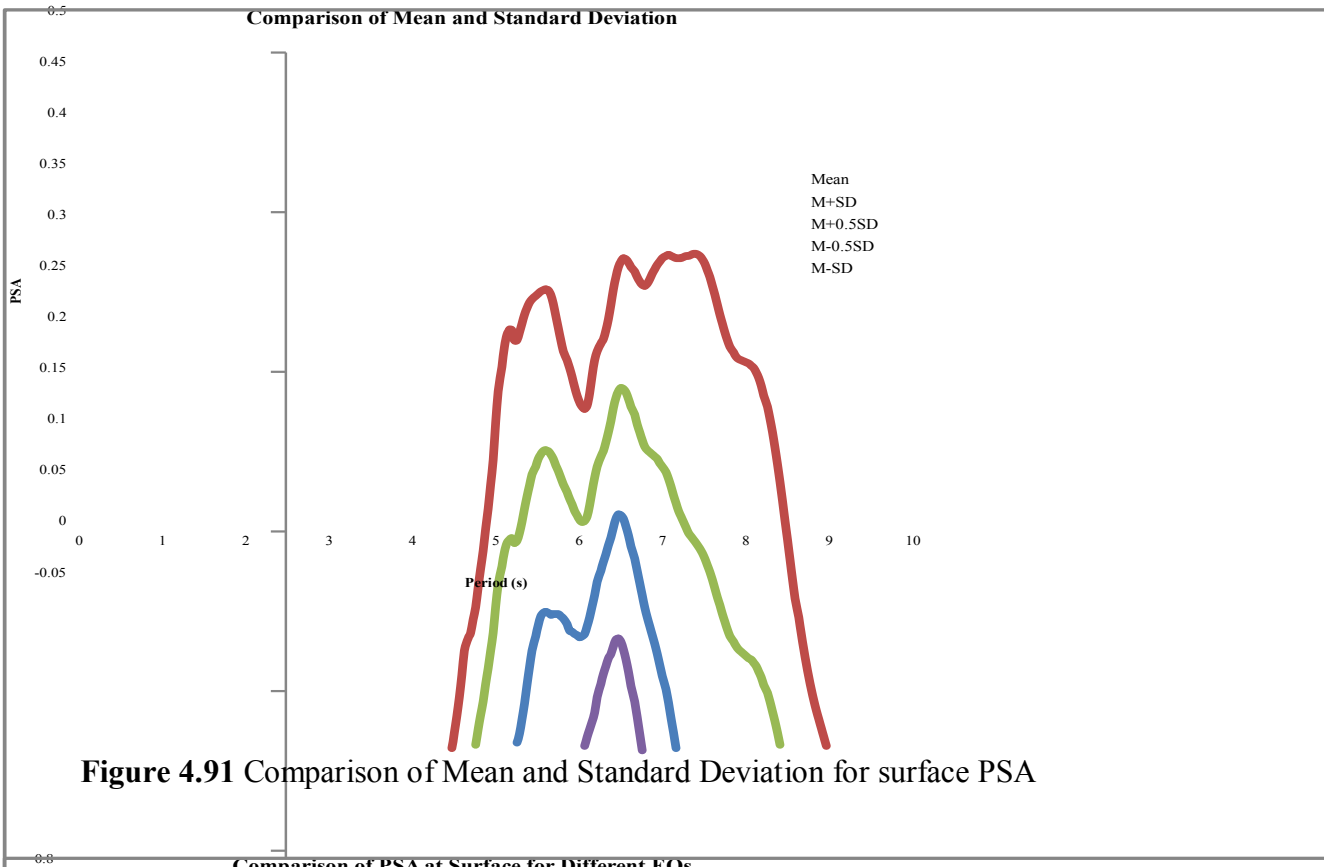

Figure 4.91 Comparison of Mean and Standard Deviation for surface PSA

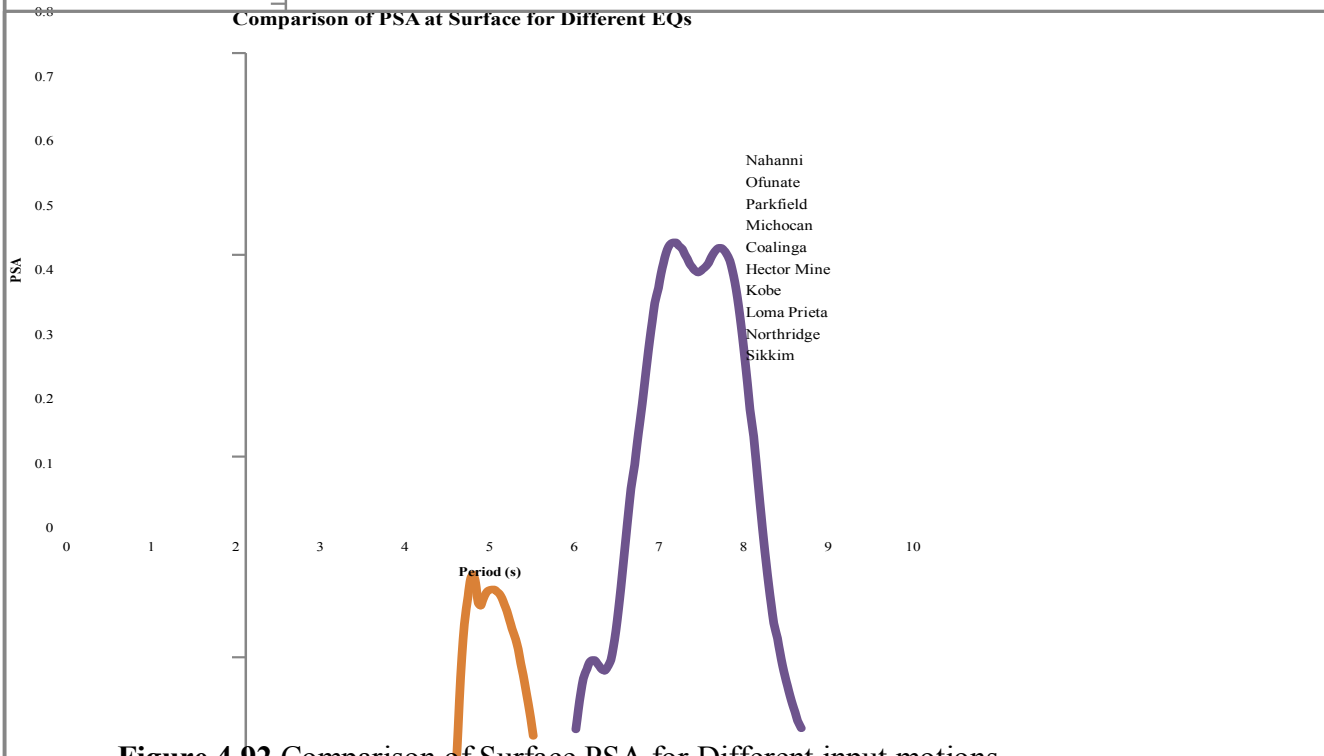

Figure 4.92 Comparison of Surface PSA for Different input motions

Figure 4.93 shows the comparison of Mean Input PSA and Mean Surface PSA produced for different input motions.

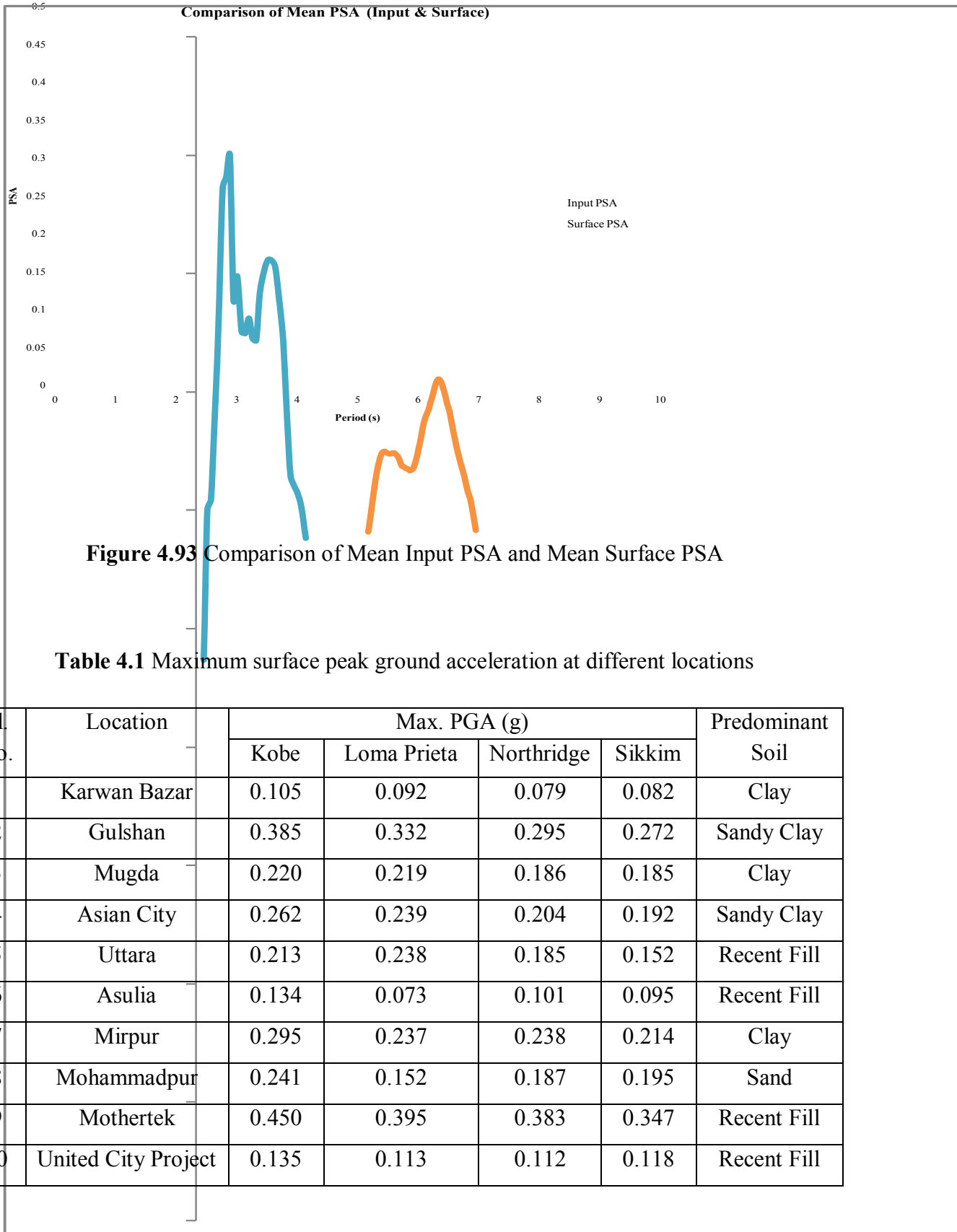

Figure 4.93 Comparison of Mean Input PSA and Mean Surface PSA

Table 4.1 Maximum surface peak ground acceleration at different locations

Sl. No.	Location	Max. PGA (g)				Predominant Soil
		Kobe	Loma Prieta	Northridge	Sikkim	
1	Karwan Bazar	0.105	0.092	0.079	0.082	Clay
2	Gulshan	0.385	0.332	0.295	0.272	Sandy Clay
3	Mugda	0.220	0.219	0.186	0.185	Clay
4	Asian City	0.262	0.239	0.204	0.192	Sandy Clay
5	Uttara	0.213	0.238	0.185	0.152	Recent Fill
6	Asulia	0.134	0.073	0.101	0.095	Recent Fill
7	Mirpur	0.295	0.237	0.238	0.214	Clay
8	Mohammadpur	0.241	0.152	0.187	0.195	Sand
9	Mothertek	0.450	0.395	0.383	0.347	Recent Fill
10	United City Project	0.135	0.113	0.112	0.118	Recent Fill

Table 4.2 Site amplification factor at different locations

Sl. No.	Location	Amplification Factors									
		Kobe	**Loma Prieta**	**Northridge**	**Sikkim**	**Coalinga**	**Hector Mine**	**Michocan**	**Nahanni**	**Ofunata**	**Parkfield**
1	Karwan Bazar	0.59	0.43	0.44	0.44	0.41	0.59	0.73	0.35	0.58	0.43
2	Gulshan	2.18	1.57	1.63	1.45	1.51	1.87	1.86	0.87	1.40	1.56
3	Mugda	1.24	1.03	1.03	0.99	1.13	1.31	1.58	0.74	1.07	0.98
4	Asian City	1.48	1.12	1.13	1.03	1.05	1.41	1.47	0.75	1.11	0.96
5	Uttara	1.20	1.12	1.02	0.81	0.74	1.02	1.21	0.60	1.12	1.17
6	Asulia	0.76	0.34	0.56	0.51	0.41	0.76	1.02	0.33	0.6	0.45
7	Mirpur	1.67	1.12	1.31	1.14	0.92	1.63	1.39	0.77	1.23	0.98
8	Mohammadpur	1.36	0.72	1.03	1.04	0.85	1.52	1.28	0.47	0.84	0.77
9	Mothertek	2.54	1.86	2.12	1.85	1.74	2.40	2.29	1.03	1.71	1.80
10	United City	0.76	0.53	0.62	0.63	0.49	0.80	0.96	0.40	0.85	0.63

Table 4.3 PSA based Surface-Input Ratio

Sl. No.	Location	Surface-Input Ratio
1	Karwan Bazar	0.61
2	Gulshan	1.67
3	Mugda	1.23
4	Asian City	1.22
5	Uttara	1.22
6	Asulia	0.66
7	Mirpur	1.23
8	Mohammadpur	1.30
9	Mothertek	2.51
10	United City	0.79

From the detailed site specific analysis, the PGA values at surface have been obtained in the range of 0.073g to 0.450g. The surface acceleration values have been very high (>0.2g) in the areas of Gulshan, Dakhin Khan, Mirpur and Mothertek. These areas have a water table depth of >4m and the predominant soil consist of sandy clays. Values of 0.1g to 0.2g were estimated in different locations like Mugda, Uttara, Asulia, M0hammadpur, and United City locations. Most of these locations had a water table depth ranging from 2m-4m. These locations are characterized by clayey sand and mixture of sand, silt and clay. Peak ground acceleration has been observed to be very low (<0.1g) in the area of Kawran Bazar. These locations have soils with layers of silty sand and silty clays.

4.3. Concluding Remarks

Ground response analysis is an important step in the seismic hazard assessment of any area. Response of a site to seismic shaking is required to evaluate and remediate geotechnical as well as structural hazards. Different methods of ground response analysis, material constitutive laws have been discussed in detail. Dhaka city has varied geological formations and has a very interesting geology. To evaluate the effects of alluvium and to estimate its dynamic effects, site specific ground response analysis has been carried out. For site specific ground response analysis, three basic input parameters that are essential are input ground motion, shear wave velocity profile and dynamic soil characteristics (e.g., strain dependent modulus reduction and damping behavior and cyclic strength curves). One dimensional soil response evaluation tool DEEPSOIL (Hashash,Y.M.A. et al., 2011), has been selected for the analysis. Equivalent linear analysis in frequency domain was the form of analysis selected to obtain free field response. Thickness (m), unit weight (kN/m^3) and shear velocity (m/sec) were the inputs given. Kobe earthquake (M_w 6.8), Loma Prieta earthquake (M_w 6.9), Northridge earthquake (M_w 6.7) and Sikkim earthquake (M_w 6.9) has been used as the input ground motion due to the absence of recorded data. Shear wave velocity was calculated using CPT machine. Applying fast fourier transform, equivalent linear analysis is performed. From the analysis it has been identified that most parts of the city have a peak acceleration of 0.138g to 0.244g. Very low PGA (<0.1g) was observed in one location. Highest PGA of about 0.450g was in the Mothertek.

CHAPTER FIVE
CONCLUSIONS AND RECOMMENDATIONS

5.1 General

The purpose of this research is to estimate the site amplification of some selected areas of Dhaka city based on shear wave velocity. This research includes field tests of such areas in order to estimate the site amplification. Field tests that include estimation of shear wave velocity at ten locations of Dhaka city have been conducted. The shear wave velocity is found out using CPT equipment.The depth of sand filling in areas varies from 2.0 to 6.0 m from existing ground level (EGL). The depth of clay layer varies from 4.0 m to 30.0 m. The depth of silty clay layer varies from 4.0 m to 6.0 m. The depth of clay layer varies from 4.0 m to 26.0 m. The depth of fine sand layer varies from 4.0 m to 20.0 m. The depth of dense sand layer varies from 4.0 m to 20.0 m from EGL. The maximum value of shear wave velocity varies from 300 m/s to 810 m/s. The minimum value of shear wave velocity varies from 50 m/s to 100 m/s. The average value of shear wave velocity varies from 164 m/s to 320 m/s. This chapter presents the summary and salient conclusions derived from this study.

5.2 Ground Response Analysis

The damage pattern in urban areas during an earthquake depends on the characteristics of the event and on the interaction between site response and vulnerability of the exposed structures. Most of the urban settlements have occurred with soft and young soil deposits which were prone to serious damage during earthquake. Dhaka city is located along the stream of Buriganga River and is covered by dominant amounts of silty clay with some amount of silty sands and sandy silts. Ground response analysis is useful for the prediction of local siteeffects and to estimate the dynamic behavior of the soil during seismic loading. Depending on the geometry and loading conditions

different analysis i.e, one, two and three dimensional can be used. For the detailed ground response analysis of Dhaka city, equivalent linear analysis has been considered. A computer program DEEPSOIL (Hashash, Y.M.A. et al., 2011), for equivalent linear approximation of layered soils has been used to compute the seismic response of horizontally layered soil deposits of the study area. For performing 1D equivalent linear analysis inputs such as number of layers of the profile, thickness of layer, shear wave velocity, shear modulus, % of damping and unit weight are required. For defining the soil properties, borehole data collected has been used. Standard Penetration Test (SPT) has been conducted in ten selected locations of Dhaka City. Shear wave velocities of each layer for ten selected locations of Dhaka city have been found out from the CPT Equipment. In this study, Kobe earthquake (Mb = 6.8), Loma Prieta earthquake (Mb = 6.9), Northridge earthquake (Mb = 6.7), Sikkim earthquake (Mb = 6.9), Coalinga earthquake, Hector Mine earthquake, Michocan earthquake, Nahanni earthquake, Ofunata earthquake and Parkfield earthquake, have been selected as the input ground motions.

5.2.1 Site: Kawran Bazar

Site amplification based on shear wave velocity data has been estimated.The average shear wave velocity of this site is 164 m/s. The maximum value of shear wave velocity is 300 m/s and the minimum value of shear wave velocity is 60 m/s.

- Kobe earthquake produces highest (0.35g) peak spectral acceleration (PSA) and Northridge earthquake produces lowest (0.0029g) peak spectral acceleration (PSA) for this site.
- The peak ground acceleration (PGA) values at surface are observed from 0.079g (Northridge) to 0.105g (Kobe) and that of the bedrock are observed from 0.177g (Kobe) to 0.212g (Loma prieta).
- Amplification factors varies from 0.43 (Loma prieta) to 0.59 (Kobe).
- The Maximum stress ratio for Kobe earthquakes are observed from 0.142 to 0.237, for Loma prieta earthquakes are observed from 0.177 to 0.351, for

Northridge earthquakes are observed from 0.083 to 0.181 and for Sikkim earthquakes are observed from 0.133 to 0.222 for this site.

- The Maximum strain values are observed from 0.0061 to 3.30 (Kobe), from 0.0054 to 3.77 (Loma prieta), from 0.0044 to1.49 (Northridge) and from 0.0047 to 2.26 (Sikkim).

5.2.2 Site: Gulshan

Site amplification based on shear wave velocity data has been estimated.The average shear wave velocity of this site is 234 m/s. The maximum value of shear wave velocity is 300 m/s and the minimum value of shear wave velocity is 100 m/s.

- Kobe earthquake produces highest (1.21g) peak spectral acceleration (PSA) and Northridge earthquake produces lowest (0.0028g) peak spectral acceleration (PSA) for this site.
- The peak ground acceleration (PGA) values at surface are observed from 0.272g (Sikkim) to 0.385g (Kobe) and that of the bedrock are observed from 0.177g (Kobe) to 0.212g (Loma prieta).
- Amplification factors varies from 1.45 (Sikkim) to 2.18 (Kobe).
- The Maximum stress ratio for Kobe earthquakes are observed from 0.351 to 0.853, for Loma prieta earthquakes are observed from 0.314 to 0.733, for Northridge earthquakes are observed from 0.212 to 0.648 and for Sikkim earthquakes are observed from 0.235 to 0.601 for this site.
- The Maximum strain values are observed from 0.0033 to 5.25 (Kobe), from 0.0028 to 2.89 (Loma prieta), from 0.0196 to 1.63 (Northridge) and from 0.0023 to as high as 1.20 (Sikkim).

5.2.3 Site: Mugda

Site amplification based on shear wave velocity data has been estimated.The average shear wave velocity of this siteis 220 m/s. The maximum value of shear wave velocity is 360 m/s and the minimum value ofshear wave velocity is 90 m/s.

- Kobe earthquake produces highest (0.66g) peak spectral acceleration (PSA) and Northridge earthquake produces lowest (0.0028g) peak spectral acceleration (PSA) for this site.
- The peak ground acceleration (PGA) values at surface are observed from 0.185g (Sikkim) to 0.220g (Kobe) and that of the bedrock are observed from 0.177g (Kobe) to 0.212g (Loma prieta).
- Amplification factors varies from 0.99 (Sikkim) to 1.24 (Kobe).
- The Maximum stress ratio for Kobe earthquakes are observed from 0.255 to 0.477, for Loma prieta earthquakes are observed from 0.263 to 0.473, for Northridge earthquakes are observed from 0.222 to 0.401and for Sikkim earthquakes are observed from 0.236 to 0.402 for this site.
- The Maximum strain values are observed from 0.014 to 6.43 (Kobe), from 0.015 to 3.68 (Loma prieta), from 0.011 to 2.33 (Northridge) and from 0.0136 to 1.99 (Sikkim).

5.2.4 Site: Dakhin Khan

Site amplification based on shear wave velocity data has been estimated.The average shear wave velocity of this site is 205 m/s. The maximum value of shear wave velocity is 520 m/s and the minimum value of shear wave velocity is 80 m/s.

- Kobe earthquake produces highest (0.76g) peak spectral acceleration (PSA) and Northridge earthquake produces lowest (0.0028g) peak spectral acceleration (PSA) for this site.

- The peak ground acceleration (PGA) values at surface are observed from 0.192g (Sikkim) to as high as 0.262g (Kobe) and that of the bedrock are observed from 0.177g (Kobe) to 0.212g (Loma prieta).
- Amplification factors varies from 1.03 (Sikkim) to 1.48 (Kobe).
- The Maximum stress ratio for Kobe earthquakes are observed from 0.283 to 0.572, for Loma prieta earthquakes are observed from 0.281 to 0.520, for Northridge earthquakes are observed from 0.184 to 0.438 and for Sikkim earthquakes are observed from 0.205 to 0.418for this site.
- The Maximum strain values are observed from 0.0165 to 5.03 (Kobe), from 0.0145 to 3.11 (Loma prieta), from 0.0117 to 1.45 (Northridge) and from 0.0112 to 1.24 (Sikkim).

5.2.5 Site: Uttara

Site amplification based on shear wave velocity data has been estimated.The average shear wave velocity of this site is 188 m/s. The maximum value of shear wave velocity is 500 m/s and the minimum value of shear wave velocity is 80 m/s.

- Loma prieta earthquake produces highest (0.93g) peak spectral acceleration (PSA) and Northridge earthquake produces lowest (0.0029g) peak spectral acceleration (PSA) for this site.
- The peak ground acceleration (PGA) values at surface are observed from 0.152g (Sikkim) to 0.238g (Loma prieta) and that of the bedrock are observed from 0.177g (Kobe) to 0.212g (Loma prieta).
- Amplification factors varies from 0.81 (Sikkim) to 1.20 (Kobe).
- The Maximum stress ratio for Kobe earthquakes are observed from 0.271 to 0.464, for Loma prieta earthquakes are observed from 0.297 to 0.525, for Northridge earthquakes are observed from 0.180 to 0.393 and for Sikkim earthquakes are observed from 0.215 to 0.341 for this site.
- The Maximum strain values are observed from 0.0107 to 2.21(Kobe), from 0.0120 to 2.14 (Loma prieta), from 0.0076 to 0.68 (Northridge) and from 0.0074 to 1.30 (Sikkim).

5.2.6 Site: Asulia

Site amplification based on shear wave velocity data has been estimated.The average shear wave velocity of this site is 139 m/s. The maximum value of shear wave velocity is 700 m/s and the minimum value of shear wave velocity is 50 m/s.

- Kobe earthquake produces highest (0.45g) peak spectral acceleration (PSA) and Northridge earthquake produces lowest (0.0032g) peak spectral acceleration (PSA) for this site.
- The peak ground acceleration (PGA) values at surface are observed from 0.073g (Loma Prieta) to 0.134g (Kobe) and that of the bedrock are observed from 0.177g (Kobe) to 0.212g (Loma prieta).
- Amplification factors varies from 0.34 (Loma prieta) to 0.76 (Kobe).
- The Maximum stress ratio for Kobe earthquakes are observed from 0.108 to 0.294, for Loma prieta earthquakes are observed from 0.128 to 0.209, for Northridge earthquakes are observed from 0.077 to 0.221 and for Sikkim earthquakes are observed from 0.108 to 0.210 for this site.
- The Maximum strain values are observed from 0.0049 to 4.10 (Kobe), from 0.0033 to 4.29 (Loma prieta), from 0.0035 to 1.66 (Northridge) and from 0.0041 to 2.44 (Sikkim).

5.2.7 Site: Mirpur

Site amplification based on shear wave velocity data has been estimated.The average shear wave velocity of this site is 320 m/s. The maximum value of shear wave velocity is 810 m/s and the minimum value of shear wave velocity is 190 m/s.

- Kobe earthquake produces highest (0.92g) peak spectral acceleration (PSA) and Northridge earthquake produces lowest (0.0028g) peak spectral acceleration (PSA) for this site.

- The peak ground acceleration (PGA) values at surface are observed from 0.214g (Sikkim) to 0.295g (Kobe) and that of the bedrock are observed from 0.177g (Kobe) to 0.212g (Loma prieta).
- Amplification factors varies from 1.12 (Loma prieta) to 1.67 (Kobe).
- The Maximum stress ratio for Kobe earthquakes are observed from 0.414 to 0.647, for Loma prieta earthquakes are observed from 0.243 to 0.520, for Northridge earthquakes are observed from 0.271 to 0.517 and for Sikkim earthquakes are observed from 0.306 to 0.470 for this site.
- The Maximum strain values are observed from 0.0025 to 0.91 (Kobe), from 0.0020 to 0.37 (Loma prieta), from 0.0019 to 0.31 (Northridge) and from 0.0017 to 0.24 (Sikkim).

5.2.8 Site: Mohammadpur

Site amplification based on shear wave velocity data has been estimated.The average shear wave velocity of this site is 194 m/s. The maximum value of shear wave velocity is 750 m/s and the minimum value of shear wave velocity is 50 m/s.

- Kobe earthquake produces highest (0.90g) peak spectral acceleration (PSA) and Northridge earthquake produces lowest (0.0030g) peak spectral acceleration (PSA) for this site.
- The peak ground acceleration (PGA) values at surface are observed from 0.152g (Loma prieta) to 0.241g (Kobe) and that of the bedrock are observed from 0.177g (Kobe) to 0.212g (Loma prieta).
- Amplification factors varies from 0.72 (Loma prieta) to 1.36 (Kobe).
- The Maximum stress ratio for Kobe earthquakes are observed from 0.169 to 0.527, for Loma prieta earthquakes are observed from 0.194 to 0.329, for Northridge earthquakes are observed from 0.122 to 0.410 and for Sikkim earthquakes are observed from 0.144 to 0.430 for this site.
- The Maximum strain values are observed from 0.0035 to 6.79 (Kobe), from 0.0027 to 3.07 (Loma prieta), from 0.0027 to 2.32 (Northridge) and from 0.0035 to 3.03 (Sikkim).

5.2.9 Site: Mothertek

Site amplification based on shear wave velocity data has been estimated.The average shear wave velocity of this site is 265 m/s. The maximum value of shear wave velocity is 570 m/s and the minimum value of shear wave velocity is 70 m/s.

- Loma prieta earthquake produces highest (1.67g) peak spectral acceleration (PSA) and Northridge earthquake produces lowest (0.0029g) peak spectral acceleration (PSA) for this site.
- The peak ground acceleration (PGA) values at surface are observed from 0.347g (Sikkim) to as high as 0.450g (Kobe) and that of the bedrock are observed from 0.177g (Kobe) to 0.212g (Loma prieta).
- Amplification factors varies from 1.85 (Sikkim) to 2.54 (Kobe).
- The Maximum stress ratio for Kobe earthquakes are observed from 0.478 to 1.001, for Loma prieta earthquakes are observed from 0.359 to 0.844, for Northridge earthquakes are observed from 0.317 to 0.854 and for Sikkim earthquakes are observed from 0.293 to 0.740 for this site.
- The Maximum strain values are observed from0.0099 to 6.06 (Kobe), from 0.0070 to 2.58 (Loma prieta), from 0.0073 to 2.59 (Northridge) and from 0.0072 to 1.59 (Sikkim).

5.2.10 Site: United City

Site amplification based on shear wave velocity data has been estimated.The average shear wave velocity of this site is 161 m/s. The maximum value of shear wave velocity is 370 m/s and the minimum value of shear wave velocity is 80 m/s.

- Kobe earthquake produces highest (0.46g) peak spectral acceleration (PSA) and Northridge earthquake produces lowest (0.0028g) peak spectral acceleration (PSA) for this site.

- The peak ground acceleration (PGA) values at surface are observed from 0.112g (Northridge) to 0.135g (Kobe) and that of the bedrock are observed from 0.177g (Kobe) to 0.212g (Loma prieta).
- Amplification factors varies from 0.53 (Loma Prieta) to 0.76 (Kobe).
- The Maximum stress ratio for Kobe earthquakes are observed from 0.188 to 0.292, for Loma prieta earthquakes are observed from 0.178 to 0.265, for Northridge earthquakes are observed from 0.111 to 0.239 and for Sikkim earthquakes are observed from 0.170 to 0.263 for this site.
- The Maximum strain values are observed from 0.0079 to 4.15 (Kobe), from 0.0067 to 3.92 (Loma prieta), from 0.0063 to 1.64 (Northridge) and from 0.0069 to 2.25 (Sikkim).

5.3 Summary

From the detailed site specific analysis, the PGA values at surface have been obtained in the range of 0.073g to 0.450g. The surface acceleration values have been very high (>0.2g) in the areas of Gulshan, Dakhin Khan, Mirpur and Mothertek. These areas have the predominant soil consist of sandy clays. Values of 0.1g to 0.2g were estimated in different locations like Mugda, Uttara, Asulia, Mohammadpur, and United City locations. These locations are characterized by clayey sand and mixture of sand, silt and clay. Peak ground acceleration has been observed to be very low (<0.1g) in the area of Kawran Bazar. This location has soils with layers of clay and finds sand.

5.4 Limitations and Suggestions

The detailed ground response analysis of the Dhaka city has been carried out by conducting equivalent linear analysis and CPT equipment tests. Limitations of the study have been listed and can be considered in cases of future study.

Few limitations of the study are as follows:

1. Geotechnical characterization of Dhaka city was carried out based on the collected borehole data from different organizations. This data was only upto 30m on an average. Deep boreholes can be drilled and the depth of bedrock and its profile can be identified.
   This would also be useful to check the accuracy of the collected data.

2. Shear wave velocity was found out from CPT machine test.This can be used for the site characterization by geophysical testing.

3. Kobe earthquake (Mb = 6.8), Loma Prieta earthquake (Mb = 6.9), Northridge earthquake (Mb = 6.7), and Sikkim earthquake (Mb = 6.9) ground motion was used as an input for the calculation of PGA of Dhaka city due to unavailability of any recorded seismic data in the area. Artificial accelerogram could be generated forcould be generated for the soil conditions in the city and can be analyzed.

5.5 Scopes for Future Research

The research conducted in testing program and empirical analysis has led to many questions and subsequent future research interests. The areas of future research have been listed below followed by brief comments:

a) Study may be conducted to prepare guidelines for reclamation procedure to reduce seismic hazards of reclaimed areas.
b) Study may be conducted to determine the suitable ground improvement techniques for such areas.
c) It is observed that the shear wave velocity determined by various methods varies significantly. Research may be conducted to determine shear wave velocity more accurately.
d) Ground response analysis may be performed of selected reclaimed Areas of Bangladesh based on Cone Penetration Test and other methods.
e) Study may be conducted to make a GIS Map of Bangladesh based on shear wave velocity.
f) Study may be conducted to develop a surface PGA map of Bangladesh based on shear wave velocity.

REFERENCES

1. Rashid, A. (2000), "Seismic Microzonation of Dhaka City based on site amplification and liquefaction", M. Engg. Thesis, Department of Civil Engineering, BUET, Dhaka, Bangladesh.
2. Islam, M. R (2005). "Seismic Loss Estimation for Sylhet City, MSc. Engg. Thesis, Department of Civil Engineering, BUET, Dhaka, Bangladesh.
3. Masud, M. A. (2007), "Earthquake Risk Analysis for Chittagong", M. Engg. Thesis, Department of Civil Engineering, BUET, Dhaka, Bangladesh.
4. Schnabel, P.B., J. Lysmer and H.B. Seed (1972). SHAKE: a computer program for earthquake response analysis of horizontally layered sites, Report no. EERC 72-12. Earthquake Engineering Research Center, Berkeley, California, 1972
5. Kanai, K. (1951). Relation between the Nature of Surface Layer and the Amplitude of Earthquake Motions, Bulletin Tokyo Earthquake Research Institute.
6. Idriss, I. M. and Seed, H.B. (1968). Seismic Response of Horizontal Soil Layers, Journal of the Soil Mechanics and Foundations Division, ASCE, Vol. 94, No. SM4. July, PP. 1003-1031
7. Seed, H. B. and Idriss, I. M. (1970). Soil Moduli and Damping Factors for Dynamic Response Analysis, Report no. EERC 70-10.University of California, Berkeley.
8. Manne, A. (2013). "Site Characterization and Ground Response Analysis for Vijayawada urban", MSc. Engg. Thesis, Earthquake Engineering Research Centre, International Institute of Information Technology Hyderabad, India.
9. Hashash, Y.M.A, Groholski, D.R., Phillips, C. A., Park, D and Musgrove, M. (2011) DEEPSOIL 4.0, User Manual and Tutorial. 98 p.
10. Mueller, C. S. (1986). The influence of site conditions on near-source high-frequency ground motion: case studies from earthquakes in Imperial Valley, Ca., Coalinga, Ca., and Miramichi, Canada, Ph.D.Thesis, Stanford University, Stanford, California.
11. Kramer, S.L. (1996), Geotechnical Earthquake Engineering, Upper Saddle River, New Jersey, USA.
12. Aki, K., (1993), Local site effects on weak and strong ground motion, Tectonophysics. (218). 93-111.
13. Towhata, I. (2008). Geotechnical Earthquake Engineering. Springer Verlag-Berlin Heidelberg.

14. Silva, W. J., Turcotte, T., and Moriwaki, Y. (1988). Soil Response to Earthquake Ground Motion. Electric Power Research Institute, RP-2556-07.
15. Faccioli, E. and Pessina, V. (2003). WP2-Basis of an handbook of earthquake ground motion scenarios. Risk-UE Project An advanced approach to earthquake risk scenarios with applications.
16. Idriss, I.M. (1990). Response of Soft Soil Sites During Earthquakes. Proc.Memorial Symposium to Honor Professor H. B. Seed, Berkeley, California.
17. EPRI (1993). Guidelines for Determining Design Basis Ground Motions. Electric Power Research Institute, EPRI TR-012293s, Palo Alto, CA.
18. Vucetic, M. and Dobry, R. (1991) Effect of Soil Plasticity on Cyclic Response, Journal of the Geotechnical Engineering Division, ASCE, Vol. 111, No. 1, January, pp. 89-107.
19. Seed, H. B., and Sun, J. I. (1989). Implications of site effects in the Mexico City earthquake of Sept. 19, 1985 for earthquake-resistant design criteria in the San Francisco Bay Area of California (Vol. 89, No. 3). Earthquake Engineering Research Center, University of California.
20. Seed, H. B. , Wong, R. T. , Idriss, I. M. , and Tokimatsu, K. (1986). ―Moduli and damping factors for dynamic analyses of cohesionless soils.‖ J. Geotech. Engrg. , ASCE, 112 (11), 1016–1032.8zn J. Geotech. Engrg.
21. Seed, H. B., and Idriss, I. M. (1970). Soil Moduli and Damping Factors for Dynamic Response Analyses, Report No. EERC 70-10, Earthquake Engineering Research Center, University of California, Berkeley, California.
22. Hardin, B. O., and Drnevich, V. P. (1972a). Shear modulus and damping in soils: measurements and parameter effects. Journal of Soil Mechanics and Foundation Engineering Division, ASCE 98(SM6) 603-624.
23. Park, D., and Hashash, Y.M.A. (2004). Estimation of non-linear seismic site effects for deep deposits of the Mississippi Embayment
24. Bielak, J., Xu, J., and Ghattas, O. (1999). Earthquake ground motion and structural response in alluvial valleys. Journal of Geotechnical and Geoenvironmental Engineering, 125(5), 413-423.
25. Law, H. K., and Lam, I. P. (1999). Seismic Performance of the Yerba Buena Island Tunnel. In Geo-Engineering for Underground Facilities.ASCE. (659-670).
26. Govindarajulu, L., Ramana, G.V., HanumanthaRao, C., and Sitharam, T.G. (2004). Site specific zground response analysis. Curr. Sci., 87(10), 1354-1362

27. Schnabel, P.B., Lysmer, J. and Seed, H.B. (1972). SHAKE – A Computer Program for Earthquake Response Analysis of Horizontally Layered Sites, Report No. EERC 72-12, University of California Berkeley.
28. Sugito, M., Goda, H., and Masuda, T. (1994). Frequency dependent equi-linearized technique for seismic response analysis of multi-layered ground. Proc JSCE 493/III- 27:49–58 (in Japanese).
29. Assimaki, D., Kausel, E., and Whittle, A. (2000). Model for dynamic shear modulus and damping for granular soils. Journal of geotechnical and geo-environmental engineering, 126(10), 859-869.
30. Toro, G. R., Abrahamson, N. A., and Schneider, J. F. (1997). Model of strong ground motions from earthquakes in central and eastern North America: best estimates and uncertainties. Seismological Research Letters, 68(1), 41-57.
31. Hashash, Y.M.A, Groholski, D.R., Phillips, C. A., Park, D and Musgrove, M. (2011) DEEPSOIL 4.0, User Manual and Tutorial. 98 p.
32. Schnabel, P.B., Lysmer, J. and Seed, H.B. (1972). SHAKE – A Computer Program for Earthquake Response Analysis of Horizontally Layered Sites, Report No. EERC 72-12, University of California Berkeley.
33. Cramer, C. H., and Real, C. R. (1992). A statistical analysis of submitted site-effects predictions for the weak-motion blind prediction test conducted at the Turkey Flat, USA, site effects test area near Parkfield, California. InProceedings of the International Symposium on the Effects of Surface Geology on Seismic Motion, March, 1992, Odawara, Japan.Vol. 2, 15-20).
34. Finn, W.D.L., Iai, S., Matsunaga, Y. (1995). The effects of site conditions on ground motions. In Proc. Of 10th ECEE, 2607-2612.
35. Martin, G.R., Dobry R. Earthquake site response and seismic code provisions. NCEER Bull. 1994, 8(4): 1-6.
36. Durward, J.A., Boore, D.M., Joyner, W.B.(1996) The Amplitude Dependence of High- Frequency Spectral Decay: Constraint on Soil Non-Linearity. Int.Workshop on Site Response, Yokosuka Japan, 82-103.
37. Dobry, R., Borchert R.D., Crouse C.B., Idriss, I.M., Joyner, W.N., Martin, G.R., Power, M.S., Rinne, E.E., Seed, R.B. (2000) New Site coefficients and site classification system used in recent building seismic code provisions. Earthquake Spectra, 16(1): 41-67.

38. Dickenson, S. E., Seed, R. B. Nonlinear dynamic response of soft and deep cohesive soil deposits, Proc. of Int. Workshop on Site Response, 1995, Yokosuka, Japan, 2: 67-81.
39. Aki, K. and Irikura, I. (1991). Characterization and mapping of earthquake shaking for seismic zonation, Proc. of the 4th International Conf. on Seismic Zonation. Stanford. California. Vol. 1, 61–110.
40. Finn,W.D.L.(1991). Geotechnical engineering aspects of microzonation. Proc. 4th International Conference on Seismic Zonation, Vol.1, 199-259.
41. Ansal, A., Erdik, M., Studer, J., Springman, S., Laue, J., Buchheister, J., Giardini, D.,Faeh,. D. and Koksal, D. (2004). Seismic Microzonation for Earthquake Risk Mitigation in Turkey. Proc. 13th World Conf. Earthquake Eng.Vancouver.CD. Paper Number: 1428.
42. Faccioli, E. and Pessina, V. (2003). WP2-Basis of an handbook of earthquake ground motion scenarios. Risk-UE Project An advanced approach to earthquake risk scenarios with applications.
43. Midorikawa, S. (1987). Prediction of Isoseismal map in the Kanto Plain due to hypothetical Earthquake.
44. Rodriguez-Marek,A. (2000), Near-Fault Seismic Site Response, Doctoral Theisis, University of California, Berkeley.
45. Abrahamson, N.A. and Shedlock, K.M. (1997). Overview. Seismological Research Letters, 68(1): pp. 9-23.
46. Kanno, T., Narita, A., Morikawa,N.,Fujiwara, H., and Fukushima, Y.(2006). A New Attenuation Relation for Strong Ground Motion in Japan Based on Recorded Data. Bulletin of the Seismological Society of America, June 2006 v. 96 no. 3 p. 879-897.
47. Campbell, K. W. and Bozorgnia, Y. (2006). Next generation attenuation (NGA) empirical ground motion models: can they be used in Europe? First European Conference on Earthquake Engineering and Seismology, Switzerland.
48. Abrahamson, N. A. and Silva, W. J. (1997). Empirical Response Spectral Attenuation Relationships for Shallow Crustal Earthquakes. Seismological Research Letters, Vol. 68(1), 94-127.
49. Youngs, R. R. (1993). Soil amplification and vertical and horizontal ratios for analysis of strong motion data from active tectonic regions, Appendix 2C in Guidelines for Determining Design Basis Ground Motions.

50. Boore, D. M., Joyner, W. B. and Fumal, T. E.(1997). Equations for Estimating Horizontal Response Spectra and Peak Acceleration from Western North American Earthquakes: A Summary of Recent Work. Seismological Research Letters. Vol. 68(1), 128-153.
51. Campbell, K. W. (1997).Empirical Near-Source Attenuation Relationships for Horizontal and Vertical Components of Peak Ground Acceleration, Peak Ground Velocity, and Pseudo-Absolute Acceleration Response Spectra. Seismological Research Letters, Vol. 68(1).154-179.
52. Sadigh, K., Chang, C. Y., Egan, J. A., Makdisi, F., and Youngs, R. R. (1997).Attenuation relationships for shallow crustal earthquakes based on California strong motion data. Seismological Research Letters, Vol. 68(1), 180-189.
53. Spudich, P., Fletcher, J. B., Hellwev, M., Boatwright, J., Sullivan, C., Joyner, W.B., Hanks, T. C., Boore, D. M., McGarr, A., Baker, L. M., and Lindh, A. G. (1997). SEA96 – A new predictive relation for earthquake ground motions in extensional tectonic regimes. Seismological Research Letters, Vol. 68(1), 190-198.
54. Borcherdt, R. D. (1992). Simplified site classes and empirical amplification factors for site dependent code provisions Proc. NCEER, SEAOC, BSSC Workshop on Site Response during Earthquakes and Seismic Code Provisions. November 18-20. University of Southern California.Los Angeles. California.
55. Anderson, J. G., Lee, Y., Zeng, Y. and Day, S. (1996). Control of Strong Motion by the Upper 30 Meters, Bull. Seism. Soc. Am., Vol. 86, 1749-1759.
56. Pitilakis, K., Gazepis, C., Anastasiadis, A. (2004).Design Response Spectra and Soil Classification for Seismic Code Provisions. 13th World Conference on Earthquake Engineering Vancouver, B.C., Canada, Paper No. 2904.